NATURAL ATTENUATION OF ORGANIC CONTAMINANTS IN GROUNDWATER: BIODEGRADATION OF HIGH PHENOL CONCENTRATIONS UNDER SULPHATE-REDUCING CONDITIONS AND ANAEROBIC OXIDATION OF VINYL CHLORIDE

Nadeem Wasif Shah

Submitted for the degree of Doctor of Philosophy

Department of Civil and Structural Engineering
University of Sheffield

September 2003

ACKNOWLEDGEMENTS

I would like to thank my supervisors Prof. Steven A. Banwart, Prof. Philip Morgan and Dr. Daniel J. Gilmour for expert advice, guidance and assistance throughout this project.

I appreciate the assistance of colleagues at the GPRG, particularly Dr Steve Thornton for answering the numerous questions put to him over the last few years. I also gained from the advice of Prof Robert J. Watkinson in the early stages of the work.

The laboratory work owes a great deal to the skill of the technical staff, special thanks to Mr Paul Dewsbury whose chromatographic expertise is legendary.

Sincere thanks to Prof Christof Holliger for hosting me at the IGE/LBE Laboratory for Environmental Biotechnology, Swiss Institute of Technology, Lausanne. The stay was beneficial for my development as a researcher but was also a great life experience. Thanks also to Katia Szynalski for teaching me valuable molecular and microbiological techniques, and Christophe Collet for showing me the beautiful country.

Many thanks to Judith Watson of the graduate research office for her valuable advice over the last few months.

I am extremely grateful for the friendship and assistance, above and beyond the call of duty, of Dr Michael J. Spence. He provided masterful assistance with all manner of enquiries, and was a constant purveyor of rare knowledge and chemistry expertise.

I am especially thankful for the love and prayers of my parents and family.

Special thanks go to Lyn Wilson for more than can be mentioned throughout the course of this research. The project would not even have begun without her love and friendship.

I am grateful to the many people who have provided friendship, distractions and strength-giving soup during my time in Sheffield, especially my brother Zahid Jaffa Ahmed for the many meaningful discussions and making me laugh.

Finally I would like to thank Allah for giving me the strength to complete this endeavour under difficult circumstances.

ABSTRACT

A plume of phenolic compounds (phenols, cresols, xylenols) with a total organic compound concentration of 24,800mg/L (in the core of the plume), including 12,500mg/L phenol, was found at a site (four-ashes) that has been used in the production of chemicals since 1950. Phenol biodegradation studies of microcosms with four-ashes inoculum demonstrated that phenol degraded readily, with concurrent SO_4^{2-}-reduction, at initial concentrations of $\leq$ 235 mg/L, at 770 mg/L phenol and also at ~ 900 mg/L phenol. Oxidation of phenol at such high concentrations, under sulphidogenic conditions, has not been reported in bacteria from sediment or groundwater systems. Previous studies have shown phenol to be inhibitory or toxic at concentrations between 200 mg/L and 600 mg/L, to sulphate-reducing bacteria and also to bacteria utilising alternative electron acceptors under anaerobic conditions.

Phenol biodegradation curves obtained from the Monod model correlate well with the experimental data, as do predicted biomass concentrations at the conclusion of the experiment. Values for k_{max} (maximum phenol utilisation rate) are between 4.90×10^{-8}/s and 3.74×10^{-6}/s. Half-saturation constants K_P (phenol) and K_{SO4} (sulphate) were determined to be 2.0×10^{-4} mol/L and 3.7×10^{-4}, respectively. These values are of the same order of magnitude but higher than those reported in the literature. Half-life calculations suggest that concentrations of up to 575 mg/L phenol may be remediated within 6 years, if environmental conditions were suitable.

VC concentrations were accurately determined in microcosms investigating VC oxidation under SO_4^{2-}-reducing conditions, using SPME/direct headspace sampling coupled with GC-MS. Initial experimentation suggested that VC oxidation may have occurred, however this could not be confirmed in subsequent experiments. Cometabolic VC degradation did not occur under SO_4^{2-}-reducing conditions. The methodology presented in these experiments is suitable for long-term VC microcosm experiments, and forms a sound basis for future studies of VC degradation.

CONTENTS

LIST OF FIGURES

LIST OF TABLES

ABBREVIATIONS

DCE	- Dichloroethene
GC	- Gas chromatography
GC-MS	- Gas chromatography mass spectrometry
HPLC	- High pressure liquid chromatography
IC	- Ion chromatography
ICP-AES	- Inductively coupled plasma atomic emission spectroscopy
KC	- Killed controls
k_{max}	- maximum substrate utilisation rate
K_P	- Half saturation constant with respect to phenol
K_{SO4}	- Half saturation constant with respect to sulphate
MNA	- Monitored natural attenuation
NA	- Natural attenuation
N/A	- Not applicable
ND	- No data
PCE	- Tetrachloroethene
SG	- Synthetic groundwater prepared to grow four-ashes bacteria
SG-SO_4^{2-}	- Synthetic groundwater prepared for phenol biodegradation experiment
SPME	- Solid phase microextraction
SRB	- Sulphate-reducing bacteria
TCE	- Trichloroethene
TEA	- Terminal electron acceptor
UST	- Underground storage tank
VC	- Vinyl chloride

1. INTRODUCTION AND RESEARCH BACKGROUND

1.1 Groundwater Contamination

In the entire water-pollution problem, there is probably nothing more disturbing than the threat of widespread contamination of groundwater. (Silent Spring, Rachel Carson, 1962)

Groundwater is an integral component of the Hydrological Cycle (Figure 1.1).

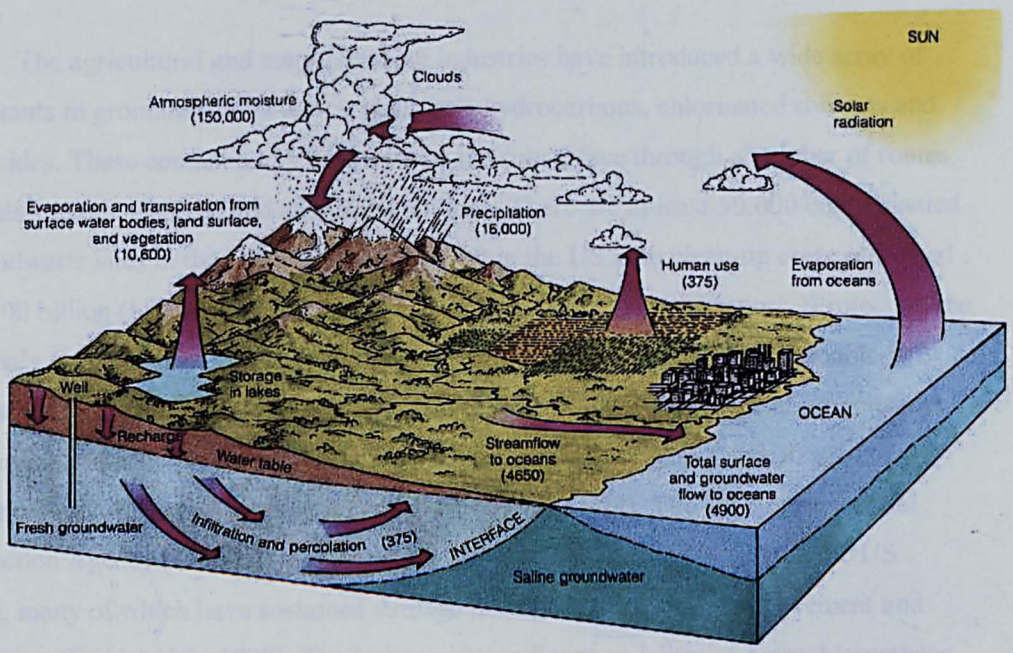

Figure 1.1 The Hydrological Cycle.

It makes up 0.61% of the worlds total water supply, exceeded only by saline waters in oceans (97.2%) and water stored in ice caps and glaciers (2.14%) (Fetter, 1994). Therefore, only a few percent of the earth's total water is freshwater and available for drinking. The immense importance of groundwater can be appreciated when we consider that it constitutes 98% of the total fresh water supply (ibid.), and is widely utilised throughout the world. The significance of this underground store is obvious in drought-ridden, poorer and under-developed areas of the world, but it is also extensively

exploited in developed countries. Groundwater accounts for 33% of all drinking water used in the UK (Price, 1996) 53% in the USA and is as high as 70% in Germany (Trauth and Xanthopoulos, 1997). Maintaining the purity and protecting this precious resource is therefore essential. However, many groundwater aquifers have been polluted by years of environmental mismanagement since the Industrial Revolution. The improvement of Newcomen's atmospheric engine in the late 18th Century by James Watt, in turn led to the use of petroleum and then electricity during the 19th and 20th Centuries. Watts' invention had triggered an exponential increase in human energy usage which, coupled with a rising population, rose slowly through the 19th and early 20th centuries but increased drastically post-World War II (Parker, 1980). Increased energy usage led to a corresponding rise in anthropogenic wastes that, without suitable procedures for disposal, consequently made their way into groundwater aquifers.

The agricultural and manufacturing industries have introduced a wide array of pollutants to groundwater including petroleum hydrocarbons, chlorinated solvents and pesticides. These contaminants have entered the subsurface through a number of routes including waste disposal and accidental spillage. There are at least 50,000 contaminated groundwater sites in the UK alone and 400,000 in the US with clean-up costs estimated at $500 billion (Lerner et al., 2000; Spence et al., 2001b). A 1984 report, 'Protecting the Nation's Groundwater from Contamination', produced by the Office of Technology Assessment (OTA) of the US congress, listed over 30 different sources of groundwater contamination including landfills, agricultural activity, septic tanks and, most commonly, underground storage tanks (UST) (Fetter, 1999). The US Environmental Protection Agency (USEPA) estimates that 200,000 leaking UST's exist in the US alone, many of which have sustained damage through settling, ground movement and corrosion (Eweis et al., 1998). The leakage is significant as 1 litre of Tetrachloroethene (TCE) has the potential to contaminate 347 million litres of water (Eweis et al., 1998).

Remediating the contaminated aquifers has become increasingly important due to heightened awareness of the environmental impact and implementation of more stringent regulation regulatory controls. Governmental environment agencies have become concerned about the pollution, especially when it has the potential to impact on a drinking water well. Fortunately, groundwater contamination is, in many cases, reversible and numerous man-made techniques have been developed to remediate contaminated aquifers. However, the most exciting developments have come over the last 20-30 years, with the realisation that natural processes have the ability to reduce the concentrations of, and even remove contaminants from groundwater.

1.2 Natural Attenuation of Contaminated Groundwater

1.2.1 Monitored Natural Attenuation (MNA)

Natural attenuation (NA), also referred to as intrinsic bioremediation, in groundwater is defined by the UK Environment Agency (UKEA) as:

'The effect of naturally occurring physical, chemical and biological processes, or any combination of those processes to reduce the load, concentration, flux or toxicity of polluting substances in groundwater. For natural attenuation to be effective as a remedial action, the rate at which these processes occur must be sufficient to prevent polluting substances entering identified receptors and to minimise expansion of pollutant plumes into currently unpolluted groundwater. Dilution within a receptor, such as in a river or borehole, is not natural attenuation' (Carey et al., 2000).

Natural attenuation processes include dilution, dispersion, sorption, mechanical filtration, volatilisation, abiotic degradation and biodegradation (Fetter, 1994; Suthersan, 1997). However, most of these processes only reduce the contaminant concentration without affecting the total mass present in the aquifer. Removal is primarily carried out by biodegradation processes (Figure 1.2) and although abiotic degradation is also destructive (e.g hydrolysis), it is slow and usually less significant relative to biodegradation for most contaminants (Wiedemeier et al., 1999).

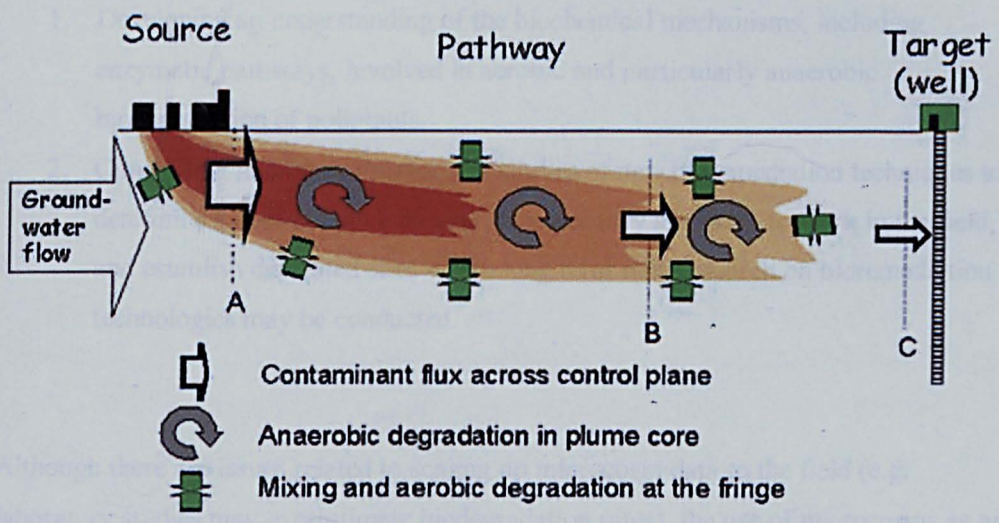

Figure 1.2 Conceptual model for NA processes of biodegradable contaminants in groundwater. Fluxes are reduced during flow from source to receptor.

Where NA is to be implemented, it is important to quantitatively monitor the processes to ensure remediation objectives will be achieved within a reasonable time-frame (Carey et al., 2000; Wiedemeier et al., 1999). This remedial approach is termed Monitored Natural Attenuation (MNA). MNA has become increasingly popular as a groundwater remediation technology as other methods have proven to be ineffective and costly. One of the most popular remediation technologies of recent times has been pump-and-treat. Between 1982 and 1992, 73% of groundwater clean-up agreements for US superfund sites specified the use of pump-and-treat technology (Suthersan, 1997). However, a study of pump-and-treat efficiency showed that, where contamination was below 1000μg/L, less than 90% removal could be accomplished which, in most cases, would not reduce the contaminant to the level required (Fetter, 1994).

Other than the capability to completely degrade pollutants to harmless by-products, MNA also prevents transference of the pollutants elsewhere. It is non-intrusive and can be, in most cases, more cost-effective (Carey et al., 2000; Wiedemeier et al., 1999). Moreover, NA is favourable from an environmental perspective as it utilises naturally occurring processes and is therefore energy efficient unlike other groundwater remediation technologies (Carey et al., 2000). These benefits mean that government agencies and environmental regulatory bodies became increasingly interested in intrinsic bioremediation. In 1995, the National Science and Technology Council's (NSTC) biotechnology research committee reported several priorities for research in bioremediation (Shah, 1999). These included:

1. Developing an understanding of the biochemical mechanisms, including enzymatic pathways, involved in aerobic and particularly anaerobic biodegradation of pollutants.
2. Conducting microcosm/mesocosm studies of new bioremediation techniques to determine a cost-effective manner, whether they are likely to work in the field, and establish dedicated sites where long term field research on bioremediation technologies may be conducted.

Although there are issues related to scaling up microcosm data to the field (e.g. laboratory studies may overestimate biodegradation rates), the use of microcosms as an integral part of the MNA process was acknowledged and incorporated into both the USEPA and UKEPA's guidance documents on MNA. They both advocate the 3 lines of

evidence approach to demonstrate NA of a contaminated site (Carey et al., 2000; Wiedemeier et al., 1998). These include:

1. The use of historical data to demonstrate reduced contaminant mass down-gradient of the source
2. Chemical and geochemical data showing decrease in parent contaminant, depletion of electron acceptors/donors, increase in breakdown products or data demonstrating that the plum is shrinking, stable or expanding slower than predicted by conservative groundwater velocity calculations.
3. Data from microbiological microcosm studies showing biodegradation occurrence and capability of indigenous bacteria.

This study corresponds to the 3rd or tertiary line of evidence for NA that is often required when the 1st two lines of evidence and the field data are inconclusive.

1.2.2 Natural Attenuation by Biodegradation

Intrinsic bioremediation occurs through biological degradation of contaminants by naturally occurring microbial populations. It has been known since the early 1900's that bacteria were metabolising in groundwater contaminated by petroleum deposits (Chapelle, 2000) but it was thought that only the topsoil contained significant numbers of microorganisms (Bone and Balkwill, 1988). More recent studies, as a result of improved aseptic sampling and microbiological identification methods (Ghiorse and Wilson, 1988), have shown there are significant numbers of microorganisms able to degrade contaminants in subsurface soil and groundwater (Bone and Balkwill, 1988; Ehrlich et al., 1983; Godsy et al., 1983; Pedersen and Ekendahl, 1990).

Most microorganisms require energy for growth and activity. In groundwater environments, this is obtained by collecting chemical energy produced by oxidation-reduction (REDOX) half-reactions reactions that involve a transfer of electrons from an electron donor to an electron acceptor. (Wiedemeier et al., 1999). These REDOX reactions are biologically mediated in most natural environments, although some can proceed abiotically (Suthersan, 2002). In most biodegradation reactions the microorganisms utilise organic contaminants as an electron donor or primary energy source and this results in the loss of electrons (oxidation). These electrons are gained by a suitable electron acceptor (reduction) such as oxygen, nitrate, Fe (III), sulphate or

carbon dioxide. This process, ideally, results in a release of energy and microbial growth as shown by the simplified reaction below:

Microorganisms + Electron Donor (carbon source) + Electron Acceptor + Nutrients

⇓

Oxidised by-products + Growth (microorganisms) + Energy + Reduced Electron Acceptor

Figure 1.3 Simplified schematic of biodegradation process.

The dominant electron accepting process at any time is termed the Terminal Electron Accepting Process (TEAP). The standard reduction potential (E°_{h}) gives an indication of the ease with which electrons are donated or accepted and, given that these REDOX reactions are mediated by microorganisms, the reduction potential is both determined by, and influences the microbial processes (Schwarzenbach et al., 2003). The energy produced by a redox reaction is termed the Gibbs free energy, ΔG°_{r}, of the reaction. This defines the maximum useful energy change for a chemical reaction at standard temperature and pressure, and can be deduced from the sum of the free energies of the products minus the sum of the free energies of the reactants (Fetter, 1999; Wiedemeier et al., 1999):

$$\mathbf{aA + bB \Leftrightarrow cC + dD} \qquad \mathbf{(1.1)}$$

For (1.1) above, ΔG°_{r}, can be deduced from:

$$\mathbf{\Delta G^{\circ}_{r} = c\Delta G^{\circ}_{c} + d\Delta G^{\circ}_{d} - a\Delta G^{\circ}_{a} - b\Delta G^{\circ}_{b}} \qquad \mathbf{(1.2)}$$

A negative value for ΔG°_{r} indicates that the reaction is exothermic and will produce energy as it proceeds from left to right, whereas a positive value indicates that the

reaction is endothermic and requires an input of energy to proceed from left to right. The standard reduction potential (E_h) is directly proportional to the energy released (ΔG°_r) and is given by the following relationship:

$$E^\circ_h = \frac{\Delta G^\circ_r}{nF} \qquad \textbf{(1.3)}$$

E°_h = Standard reduction potential (V)

ΔG°_r = Gibbs free energy of the reaction (kcal/mol)

n = number of electrons transferred in half-reaction

F = Faraday constant (23.06Kcal/V)

Table 1.1 shows some important electron acceptor and electron donor half-cell reactions and calculated ΔG°_r's.

Table 1.1 Standard reduction potentials and calculated free energies of reaction for various electron acceptor and electron donor half-reactions. The electron acceptor half-reactions are written in the conventional fashion, as reductions, whilst the donor reactions are presented as oxidations (adapted from Wiedemeier *et al.*, 1999).

Half reaction	E^{o}_{h} (V)	ΔG^{o}_{r} (kcal/mol)
Oxidised species Reduced species		
O_2 (g) + $4H^+$ + $4e^-$ ⇒ $2H_2O$ *Aerobic respiration*	+0.80	-18.5
2 NO_3^- + $12H^+$ + $10e^-$ ⇒ N_2 (g) + $6H_20$ *Denitrification*	+0.73	-16.9
MnO_2 (s) + $4H^+$ + $2e^-$ ⇒ Mn^{2+} + $2H_2O$ *Pyrolusite reduction/dissolution*	+0.37	-8.6
MnOOH (s) + CO_2 + H^+ + e^- ⇒ $MnCO_3$ (s) + H_2O *Pyrolusite reduction/carbonation*	+0.5	-13.3
MnO_2 (s) + H^+ + e^- ⇒ MnOOH (s) *Pyrolusite reduction/hydrolysis*	+0.53	-12.2
Fe^{3+} + e^- ⇒ Fe^{2+} *Iron(III) reduction*	+0.77	-17.8
SO_4^{2-} + $9.5H^+$ + $8e^-$ ⇒ $0.5HS^-$ + 0.5 H_2S + $4H_2O$ *Sulphate reduction*	-0.23	+5.3
CO_2 (g) + $8H^+$ + $8e^-$ ⇒ CH_4 (g) $2H_2O$ *Methanogenesis*	-0.26	+5.9
H_2 ⇒ H^+ + e^- *Hydrogen oxidation*	+0.43	-9.9
C_6H_6 + $12H_2O$ ⇒ $6CO_2$ + $30H^+$ + $30e^-$ *Benzene oxidation*	+0.31	-7.0
C_2H_3Cl + $4H_2O$ ⇒ $2CO_2$ + Cl^- + $11H^+$ + $10e^-$ *Vinyl chloride oxidation*	+0.5	-11.4

Microorganisms will not perform reactions that require more net energy than is produced as, like all living things, they are constrained by the laws of thermodynamics and can carry out only those REDOX reactions that are thermodynamically possible (Wiedemeier et al., 1999). Subsequently, the coupled REDOX reaction consists of both an endothermic and exothermic reaction that produces energy for growth. The

microorganisms will preferentially utilise the electron acceptors on the basis of energy yield with the order of utilisation generally given as, $O_2 > NO_3^- > MnO_2 > Fe^{3+} > SO_4^{2-} >$ methanogenesis (Kennedy et al., 1999). It's worth noting, however, that under certain conditions the order of use can change. At high sulphate-reduction, the Sulphate-Reducing Bacteria (SRB) may out-compete iron-reducing bacteria even though the iron-reducers have a greater affinity for the carbon source. This increased affinity may not be sufficient to render iron-reduction as the TEAP when, as is quite common in marine and other highly reduced environments, SRB are present in greater numbers (Coates et al., 1996a).

1.2.3 Sulphate-reduction and Sulphate-reducing Bacteria

Sulphur is an essential component of the biosphere as most global sulphur cycling is biologically controlled (Parker, 1980). In fact, approximately 1% of living organisms' dry mass is sulphur and many living organisms such as higher plants and bacteria use sulphate as a sulphur source for biosynthesis (Hao et al., 1996). However, the ability to generate energy using sulphate as an electron acceptor is unique to sulphate-reducing bacteria (SRB). SRB were isolated from a Dutch canal in 1895 by Biejerinck (LeGall and Xavier, 1996) but their true importance and role in the global cycling of sulphur has only been realised relatively recently. The combined action of sulphate-reducers and sulphate-oxidisers in the environment constitutes the biological sulphur cycle (Fauque, 1995) as shown in Figure 1.4.

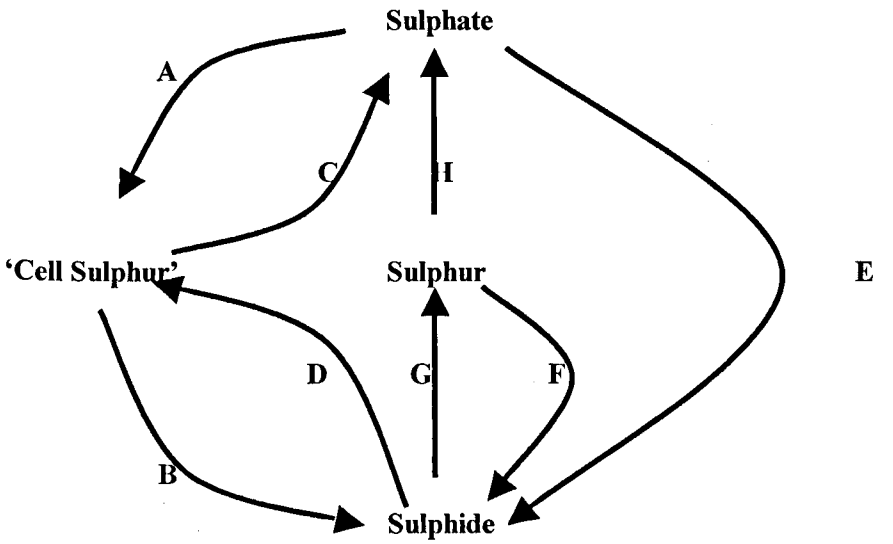

Figure 1.4 The biological sulphur cycle. 'Cell sulphur' includes sulphur bound in bacteria, fungi, animals and plants. (A) Assimilatory sulphate-reduction by bacteria, plants and fungi. (B) Death and decomposition by bacteria and fungi. (C) Sulphate excretion by animals. (D) Sulphide assimilation by bacteria (and some plants). (E) Dissimilatory sulphate-reduction. (F) Dissimilatory elemental sulphur reduction. (G) Chemotrophic and phototrophic sulphide oxidation. (H) Chemotrophic and phototrophic sulphur oxidation. (Adapted from (Fauque, 1995).

The SRB mediate dissimilatory sulphate-reduction (Figure 1-4, E), where the sulphate ion acts as an oxidising agent for the dissimilation of carbon with the production of sulphide. The process occurs in many anoxic, reduced environments (E_h of ~ -150 to -200mV) including groundwater aquifers, marine sediments, soils, hot springs and oil wells (Bolliger et al., 2001; Kleikemper et al., 2002; Postgate, 1984) Although sulphate concentrations in freshwater environments can be low, they are often augmented by dissolution of gypsum, pyrite oxidation, seawater/freshwater mixing, acid rain and fertiliser leachate (Appelo and Postma, 1999). This combined with the fact that SRB are present in many subsurface environments indicates that sulphate-reduction can be an important electron accepting process.

Following the initial discovery that SRB could oxidise acetate (Postgate, 1984), numerous studies have shown that indigenous SRB in subsurface environments can mediate the biodegradation of many organic contaminants. These include phenol (Lin and Lee, 2001; Mort and Deanross, 1994; Thornton et al., 2001b), halogenated phenols

(Haggblom and Young, 1995), o-, m- and p-cresol (Londry et al., 1997; Mort and Deanross, 1994; Ramanand and Suflita, 1991; Suflita et al., 1989), naphthalene (Coates et al., 1996b) long-chain n-alkanes (Caldwell et al., 1998), nitroaromatics (Boopathy et al., 1998) toluene (Beller et al., 1992a; Bolliger et al., 2001), benzene (Coates et al., 1996b; Lovley et al., 1995), o-xylene (Davis et al., 1999), p-xylene (Edwards et al., 1992a), carbon tetrachloride (Devlin and Muller, 1999), and the chlorinated solvents cis-1,2-dichloroethene (cis-DCE) and vinyl chloride (VC) (Davis et al., 2002). Although sulphate-reduction is not energetically favourable in the presence of O_2, NO^{3-} and Fe^{3+} (Albrechtsen and Christensen, 1994), overwhelming carbon loading of natural environments, as often happens with groundwater contamination, leads to a hierarchal, sequential depletion of the most energetically favourable electron acceptors. This in turn leads to highly reduced conditions suitable for sulphate-reduction. Moreover, the order of electron acceptor utilisation is altered under certain conditions, and sulphate-reduction has been known to out-compete thermodynamically favourable processes, for example when Fe^{3+}-reduction is limited by the low bio-availability of Fe-oxides (Ludvigsen et al., 1998).

1.3 Phenol Contamination and Biodegradation in Groundwater

1.3.1 Biodegradation of Phenol

Phenol is colourless with a strong, irritating odour and consists of a hydroxyl group bonded to a benzene ring (Figure 1.6). It occurs naturally in soil and groundwater, associated with animal wastes and decomposing organic matter. However, natural concentrations are insignificant in comparison to the huge amounts of anthropogenic phenol introduced to the environment (Shah, 1999).

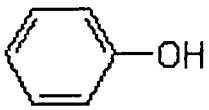

Phenol

Figure 1.5 Chemical structure of phenol (C_6H_60).

Phenol is used in many industrial processes and is, consequently, a common groundwater contaminant listed as a priority pollutant by the USEPA (Thomas et al., 2002). Common sources of contamination to groundwater include synthetic chemical industries, textile factories, wood treatment plants, coal-gasification works, petrochemical plants and waste disposal sites (Daun et al., 1998; Eweis et al., 1998; Lay and Cheng, 1998; Lerner et al., 2000; Lovley et al., 1998; Spence et al., 2001b; Thomas et al., 2002). Ecotoxicological studies have shown that phenol is highly toxic (Thomas et al., 2002) and ingestion can cause diarrhoea, muscle aches, dark urine, and even serious liver and tissue damage (U.S. Department of Health and Human Services, 1997) The EU recommends that concentration in water supplies should not exceed 0.5µg/L (EEC, 1988).

Biodegradation of phenol has been documented in studies looking into waste-water treatment for many years (Yang and Humphrey, 1975). However, degradation in groundwater received less attention with the exception of studies involving low level contamination of shallow sand and gravel aquifers (Lerner et al., 2000; Spence et al.,

2001b). Phenol degrades under a range of conditions including aerobic respiration (Ambujom and Manilal, 1995; Higgo et al., 1996; Kuhlmann and Schottler, 1996), nitrate-reducing (Broholm and Arvin, 2001; Broholm and Arvin, 2000; Broholm et al., 2000; Flyvbjerg et al., 1993; Spence et al., 2001a), Iron (III)-reducing (Lovley and Lonergan, 1990; Monserrate and Haggblom, 1997) and sulphate-reducing (Boopathy, 1997; Haggblom and Young, 1995; Kazumi et al., 1995; Mort and Deanross, 1994). There are various pathways for anaerobic phenol degradation to inorganic products such as CO_2 and CH_4. One such pathway (Figure 1.6), involves formation of the intermediates 4-Hydroxybenzoate and, subsequently, Benzoate which can undergo further biodegradation via Acetyl-CoA and ultimately to CO_2.

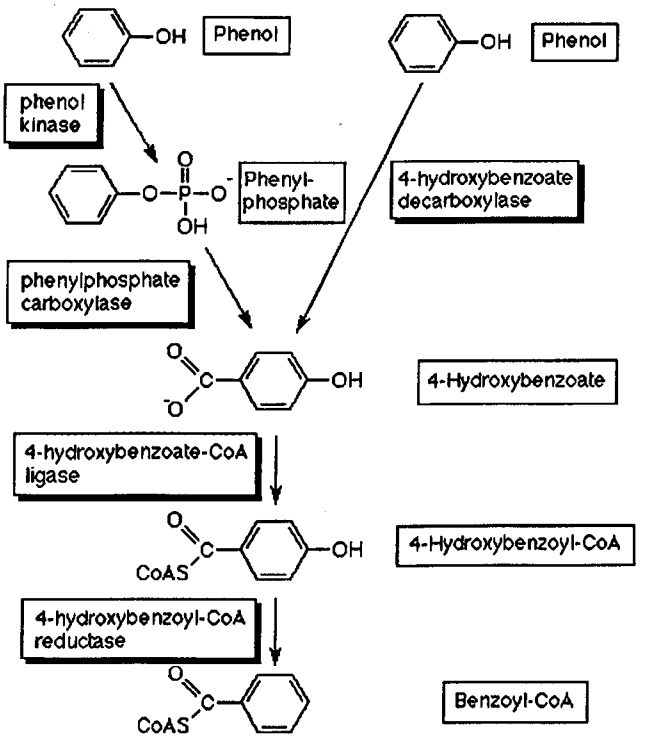

Figure 1.6 Anaerobic phenol degradation pathway (Biodegradation and Biocatalysis database, 2003).

1.3.2 Phenol Contamination and the Potential for Intrinsic Biodegradation by Bacterial Sulphate-reduction at a Highly Contaminated Field Site.

The sampling site for this study, known as four-ashes, was formerly a coal-tar distillery that now uses feedstocks brought in from other chemical plants and has been involved in chemical production since 1950. It is located near Wolverhampton, England and overlies the second most important aquifer in the UK, the Permo-Triassic Sherwood Sandstone which, in the environs of the site, is 250m thick with the water table at less than 5 metres below ground level (mbgl) (Thornton et al., 2001a). Locally the aquifer is a fluviatile red-bed quartzo-feldspathic sandstone with a porosity of about 26%, is abundant in Fe and Mn oxides as grain coatings. Regionally, the aquifer comprises aerobic groundwater flowing westward at 4-11 m/year and background NO_3^- and SO_4^{2-} concentrations are at 110 mg/L and 70mg/L, respectively (Lerner et al., 2000; Spence et al., 2001b; Thornton et al., 2001a). A plume of phenolic compounds (phenols, cresols, xylenols) with a total organic compound concentration of 24,800mg/L (in the core of the plume), including 12,500mg/L phenol, was found under the site in 1987. Contamination with SO_4^{2-} and NaOH has also taken place due to spillage of mineral acids and alkali and there is also Cl^- from the use of de-icers (Thornton et al., 2001a). Pollution of the aquifer began soon after the plant started operation in 1950 and the plume is now 500m long and 50m deep. The only receptor at risk is a public water supply borehole, 2km West of the site (Figure 1.7).

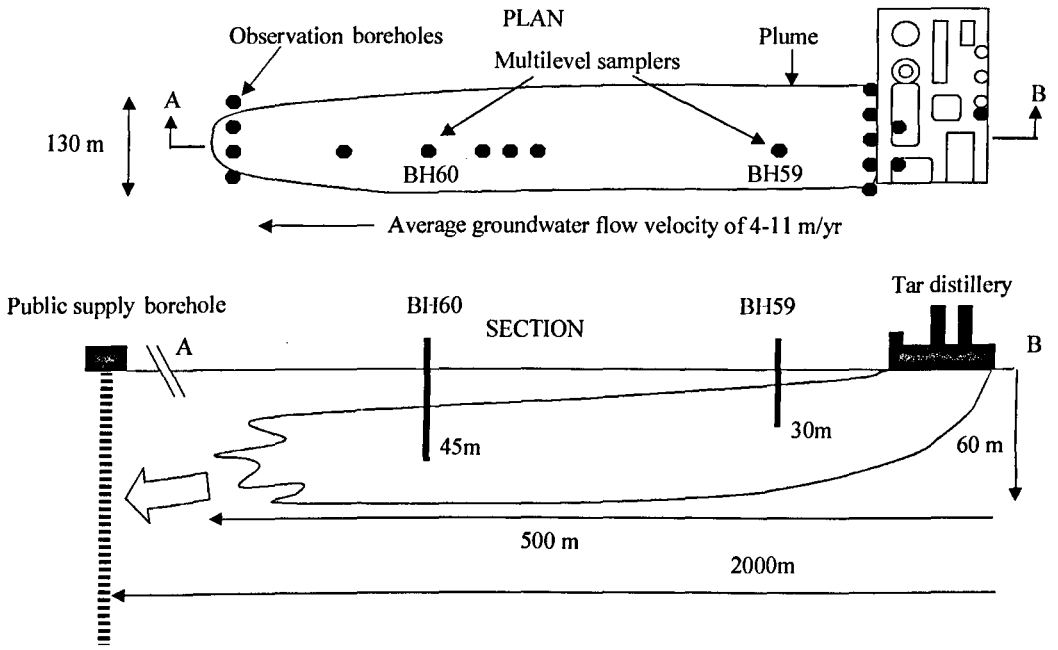

Figure 1.7 Schematic plan and section of the Four Ashes site, showing general observation wells, multilevel samplers, and approximate locations of plume (taken from Lerner et al., 2000).

Laboratory and field studies have been carried out at the site using groundwater and core samples taken from the multi-level samplers (MLS), BH59 (30m depth) and BH60 (45m depth) in Figure 1.8, installed 150m and 350m from the source, respectively. Analysis of samples from the MLS has shown that degradation of the phenolics occurs under various TEAP conditions; aerobic respiration, nitrate-reduction, Mn(IV)-/Fe(III)-reduction, sulphate-reduction, methanogenesis and fermentation (Thornton et al., 2001b). Table 1.2 shows that O_2, $NO3^-$, and MnO_2 are thermodynamically favourable electron acceptors as they yield the most free energy (ΔG°_r) and theoretically they should be utilised as the TEA's before Fe(III), SO_4^{2-} and CH_4.

Table 1.2 Gibbs free energy of reaction (ΔG°_r) for phenol oxidation under different electron accepting conditions (taken from Thornton *et al.*, 2001b)

Reaction stoichiometry	TEAP	ΔG°_r (kcal/equiv)
$C_6H_6O + 7O_2 \Rightarrow 6CO_2 + 3H_2O$	Aerobic Respiration	-25.85
$5C_6H_6O + 28NO_3^- + 28H^+ \Rightarrow 6CO_2 + 14N_2 + 29H_2O$	Denitrification	-26.18
$C_6H_6O + 14MnO_2 + 28H^+ \Rightarrow 6CO_2 + 14Mn^{2+} + 17H_2O$	Mn-reduction	-25.84
$C_6H_6O + 28FeOOH + 56H^+ \Rightarrow 6CO_2 + 28Fe^{2+} + 45H_2O$	Fe-reduction	-12.93
$2C_6H_6O + 7SO_4^{2-} \Rightarrow 12CO_2 + 7S^{2-} + 6H_2O$	SO_4-reduction	-1.03
$2C_6H_6O + 8H_2O \Rightarrow 7CH_4 + 5CO_2$	Methanogenesis	-1.4

ΔG°_r calculated for 25°C using thermodynamic data from Stumm and Morgan, 1996.

However, in certain areas of the plume where Fe (III) is theoretically energetically favourable, SO_4^{2-}-reduction is the TEAP (Spence et al., 2001b). This could occur if Fe(III) is less bioavailable (Thornton et al., 2001b) or when SRB are present in greater numbers in comparison to Fe-reducing bacteria (Coates et al., 1996b). Moreover, SO_4^{2-}-reduction does not always take place exclusively of Fe(III)-reduction, the processes can take place simultaneously (Kennedy et al., 1999). Profiles of SO_4^{2-} and S^{2-} concentration from BH59 (Figure 1.8) indicate a SO_4^{2}-reducing zone between ~9.5 and 14mbgl.

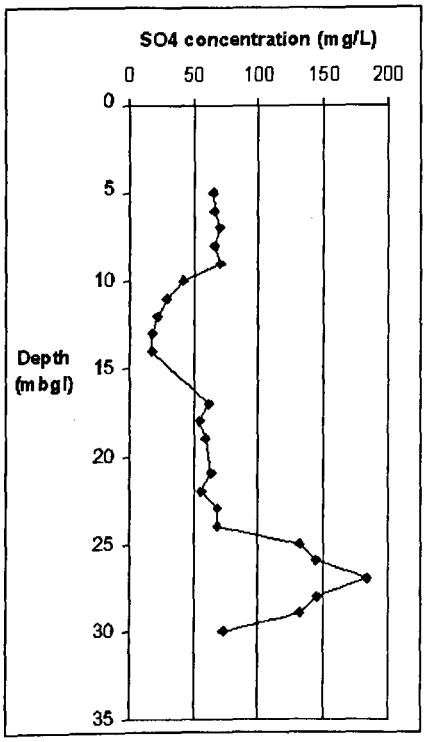

(a)

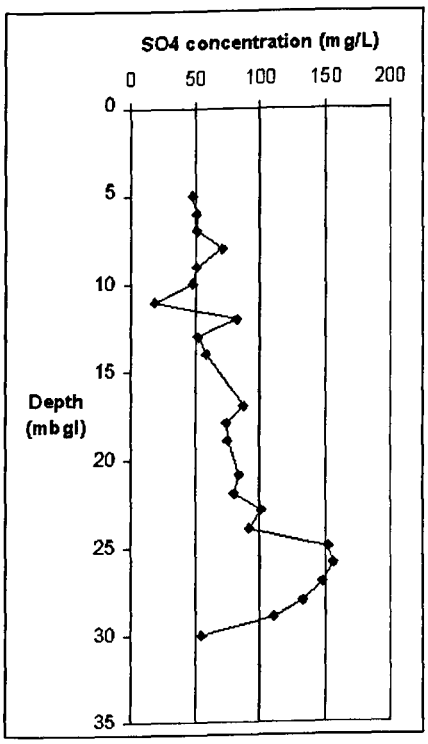

(b)

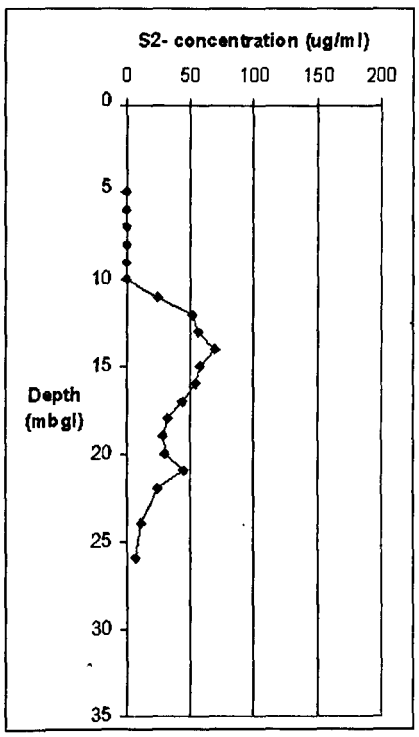

(c)

Figure 1.8 Variation in SO_4^{2-} and S_2^- concentrations with depth, in BH59. Data from 1998 (a) and 1999, (b), (c). No S_2^- analysis carried out in 1998.

Stable sulphur isotope modelling of BH59 groundwater samples has shown that phenol mineralisation has taken place up to a depth of 12m and that total phenol loss due to SO_4^{2-}-reduction accounts for only 0.05% of the total phenolic concentration (Spence et al., 2001b). The isotopic modelling also indicates that phenol toxicity renders sulphate-reduction insignificant at a total phenolics concentration greater than 2000mg/L (1000mg/L phenol) (Spence et al., 2001b; Thornton et al., 2001b) but this gives no conclusive evidence as to the phenol biodegradation potential of the SRB. A reduction of the total phenolics concentration, e.g. by a pump-and-treat system, to below 2000mg/L could instigate biodegradation by sulphate-reduction. Alternatively, sulphate addition to the aquifer may be sufficient to initiate biodegradation (Spence et al., 2001b) and, perhaps, result in considerable phenol removal.

Thus far biodegradation of phenol in groundwater has only been documented at field sites contaminated with relatively low phenol concentrations (~ 500mg/L or less). Intrinsic bioremediation of high concentrations of phenol >1000mg/L has only been recently investigated at one contaminated site (four-ashes, UK). Moreover, the potential of SRB to mediate the removal of high phenol concentrations has not been conclusively documented and, therefore, naturally occurring bacteria capable of degrading such high concentrations have not been identified.

1.4 Vinyl Chloride Contamination and Direct Microbial Oxidation in Groundwater

1.4.1 Vinyl Chloride

Vinyl chloride (VC), frequently called chloroethene or chloroethylene, is a colourless, flammable gas with a faint sweet odour. It was discovered in 1835 when Regnault produced the VC monomer (Figure 1.9), which was later found to polymerise to polyvinyl chloride (PVC). Commercial PVC production began in both the USA and Germany in the early 1930's (ECVM, 1999).

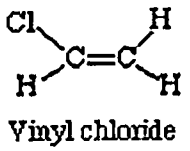

Figure 1.9 Chemical structure of vinyl chloride (C_2H_3Cl).

Until recently VC was considered purely anthropogenic however, recent studies have shown that VC can be produced naturally during oxidative degradation of organic matter in soil (Keppler et al., 2002). Over 95% of total VC synthesised is used in the PVC production process and it is estimated that that over 7 million tons per year are produced in the United States alone (Deng et al., 1999).

VC occurs in groundwater due accidental releases, un-educated disposal and due to the biological reductive dechlorination of other chlorinated solvents, such as tetrachloroethene (PCE), trichloroethene (TCE) and dichloroethene (DCE) which are more common groundwater contaminants (Deng et al., 1999; Rosner et al., 1997). VC is highly toxic and has a US maximum concentration level (MCL) of only 2μg/L (McCarty and Semprini, 1994). It is classified as a priority pollutant and Group A human carcinogen by the USEPA (Hartmans and Debont, 1992; USEPA, 1993) and ingestion can lead to liver damage as well as cancer of the liver, digestive tract and brain (ATSDR, 1990; ATSDR, 1993; Calabrese and Kenyon, 1991). The toxicity combined with the environmental concerns suggests that an understanding of the processes by which VC contaminated groundwater may be remediated is of great importance.

1.4.2 Natural Attenuation of Chlorinated Solvents: Direct Biological Oxidation of Vinyl Chloride.

Chlorinated solvents and their natural transformation products are amongst the most prevalent groundwater contaminants (McCarty and Semprini, 1994; Vogel, 1994). Until just over a decade ago, chlorinated solvents were considered to be recalcitrant but since then many studies have shown that microorganisms have the ability to take part, directly and indirectly, in the degradation of chlorinated ethenes. Biodegradation of chlorinated solvents can take place through halorespiration (utilisation of the solvents as respiratory substrates), reductive dechlorination (anaerobic cometabolic degradation) and aerobic/anaerobic oxidation reactions (utilisation of the compounds as carbon and energy sources) (Wiedemeier et al., 1999). Although chlorinated solvents can be subject to both substitution and elimination reactions, the most prevalent microbially-mediated reactions involve the gain or removal of electrons from the solvent and are usually either oxidations (quicker with the less halogenated compounds) or reductions (quicker with highly halogenated compounds), which usually involve dehalogenation of the solvents (McCarty and Semprini, 1994; Vogel, 1994). During reductive dechlorination, the chlorinated solvent acts as an electron acceptor causing it to be reduced with a chloride atom substituted by a hydrogen atom. Reductive dechlorination is quicker with the highly chlorinated solvents because they are more oxidised but VC is the least oxidised chlorinated solvent and, therefore, less susceptible to reductive dechlorination. This causes VC to accumulate at some contaminated sites with chlorinated solvent contaminated plumes that are undergoing reductive dechlorination. Transformation of PCE, TCE and DCE by reductive dechlorination has received a lot of attention over the last 2 decades or so (Ballapragada et al., 1997; Borch et al., 2003; Gerritse et al., 1995; Maymo-Gatell et al., 1999; McCarty and Semprini, 1994; Vogel, 1994; Wilson et al., 1990) and, in general, anaerobic dechlorination occurs according to the pathway shown in Figure 1.10.

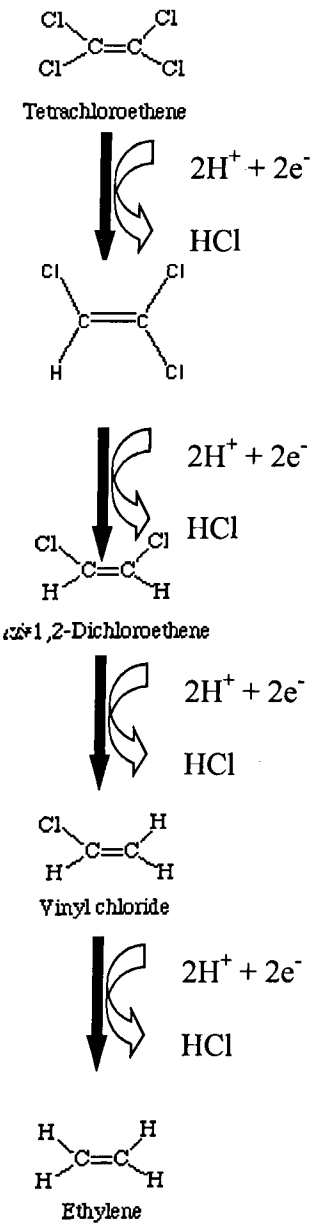

Figure 1.10 Production of VC, by anaerobic dechlorination of PCE and TCE (Ellis, 2000)

Cometabolic transformation of chlorinated solvents, where the chlorinated hydrocarbon is fortuitously oxidised by enzymes released from the oxidation of another primary carbon source, has also been documented (Alvarez-Cohen and Speitel, 2001; Chang and AlvarezCohen, 1997; Gao and Skeen, 1999; Hopkins et al., 1993a; Landmeyer et al., 1998; Lee et al., 2000; Lerner et al., 2000; Mousavi and Sarlack, 1997; Semprini et al., 1992). The process has mainly been documented in reductive dechlorination studies with stimulation by dissolved O_2 (aerobic) (Alvarez-Cohen and Speitel, 2001; Hopkins et al., 1993b) although cometabolic degradation can take place anaerobically (Lee et al., 2000; McCarty and Semprini, 1994; Wiedemeier et al., 1998). Anaerobic co-metabolism of non-chlorinated organic pollutants has previously been documented in biodegradation studies, including under SO_4^{2-}-reducing conditions (Annweiler et al., 2001; Daun et al., 1998). The rate of cometabolic activity increases as the degree of dechlorination decreases (McCarty and Semprini, 1994; Vogel, 1994), therefore VC would potentially be more susceptible to cometabolic biodegradation than its parent compounds. The possibility of anaerobic cometabolism as a mechanism for VC biodegradation requires investigation, McCarty and Semprini (1994) suggest that VC has some potential to undergo anaerobic cometabolism but there is a dearth of research on this subject. VC oxidation to CO_2 has been shown to occur via acetate, which is produced through oxidative acetogenesis (Bradley and Chapelle, 2000a). As acetate can be a product of anaerobic degradation of phenol, it is possible that the enzymes produced during this process may also fortuitously degrade VC to acetate and then to CO_2.

Given that VC is sometimes less susceptible to reductive dechlorination in the natural environment and that propensity to oxidise increases with fewer chlorine atoms, direct biological oxidation could play an important role in its removal from groundwater (Bradley, 2000; Bradley and Chapelle, 2000a; Bradley and Chapelle, 2000b; Bradley et al., 1998a). During direct microbial transformation, the VC acts as the carbon source or electron donor and loses electrons (i.e. is oxidised). A suitable electron acceptor, e.g. O_2, SO_4^{2-}, gains the electrons and energy is provided for microbial growth and metabolism. VC has been utilised as the sole carbon an energy source by *Mycobacterium aurum* L1, and various studies have reported the direct transformation of VC under aerobic conditions (Bradley and Chapelle, 1998a; Bradley and Chapelle, 1998b; Bradley and Chapelle, 1998c; Bradley et al., 1998a; Bradley et al., 1998b; Bradley et al., 1998c; Davis and Carpenter, 1990; Hartmans and Debont, 1992; Hartmans et al., 1985; Klecka et al., 1990; Landmeyer et al., 1998). Aerobic degradation of VC may be fruitful at sites where direct VC pollution has occurred at industrial processing plants (e.g. PVC

production). However, VC generally occurs in groundwater following anaerobic dechlorination of PCE or TCE and since addition of oxygen to an anaerobic aquifer may be unfeasible or expensive, utilisation of alternative electron acceptors (Fe(III), SO_4^{2-}) can be a central mechanism for VC oxidation (Bradley, 2000; Bradley and Chapelle, 2000a; Bradley and Chapelle, 2000b; Bradley et al., 1998a). Anaerobic oxidation of VC to CO_2 was first described under Fe(III)-reducing conditions (Bradley and Chapelle, 1996; Chapelle et al., 1996; Vroblesky et al., 1996). Fe(III) was provided as Fe-EDTA and mineralisation rates were comparable to those seen in aerobic degradation (Bradley and Chapelle, 1996; Chapelle et al., 1996; Vroblesky et al., 1996). Subsequent studies have shown that as well as Fe(III) (Bradley and Chapelle, 1998a; Bradley and Chapelle, 1998b; Bradley and Chapelle, 1998c; Bradley et al., 1998a; Bradley et al., 1998b; Bradley et al., 1998c; Landmeyer et al., 1998), alternative electron acceptors can participate in VC oxidation including SO_4^{2-} (Bradley and Chapelle, 1998a; Bradley and Chapelle, 1998b; Bradley and Chapelle, 1998c; Bradley et al., 1998a; Bradley et al., 1998b; Bradley et al., 1998c; Landmeyer et al., 1998), CO_2 (Bradley and Chapelle, 1997; Landmeyer et al., 1998; Vroblesky et al., 1997) and humic acids (Bradley and Chapelle, 1998a; Bradley and Chapelle, 1998b; Bradley and Chapelle, 1998c; Bradley et al., 1998a; Bradley et al., 1998b; Bradley et al., 1998c; Landmeyer et al., 1998). The degree of mineralisation decreases as conditions become more reducing but this lower mineralisation rate is significant even under methanogenic conditions provided electron acceptors are present (Bradley and Chapelle, 1998a; Bradley and Chapelle, 1998b; Bradley and Chapelle, 1998c; Bradley et al., 1998a; Bradley et al., 1998b; Bradley et al., 1998c; Landmeyer et al., 1998). These studies have shown that direct VC oxidation has the potential to play a considerable and, perhaps, crucial role in remediating chlorinated solvent sites to completion.

The high toxicity and volatility of VC mean that laboratory investigations can be problematic. Most VC oxidation studies have been conducted over short time scales (< 90 days) even when complete mineralisation has not occurred. It would be beneficial to conduct a long term VC oxidation microcosm study, especially since degradation rates may be slow under certain electron-accepting conditions (SO_4^{2-}-reducing, methanogenesis). Moreover, in order to utilise naturally occurring microorganisms for effective, cost-efficient groundwater remediation, we have to improve our understanding of the biological processes. It is important to investigate the potential of each TEAP (e.g. SO_4^{2-}) in VC mineralisation and also the extent which anaerobic reductive dechlorination and direct anaerobic oxidation co-occur (Bradley, 2000; Bradley and Chapelle, 2000a; Bradley and Chapelle, 2000b; Bradley et al., 1998a). Furthermore,

research is required to try and identify the anaerobic microorganisms responsible for direct oxidation of VC. We need to understand the microbial populations in terms of what they are, their numbers and potential, as well as how they are effected by varying environmental parameters. Moreover, there is a lack of research into the transfer of these observations from the controlled to the natural environment (McCarty and Semprini, 1994; Vogel, 1994).

1.5 Rationale and Objectives

1.5.1 Summary of Rationale

Groundwater contamination has occurred since the industrial revolution with many aquifers contaminated all over the world. MNA has been accepted as a valuable treatment process because it has the capability to completely degrade pollutants to harmless by-products. MNA is environmentally friendly as it involves naturally occurring processes and also prevents transference of the pollutants elsewhere. It's also non-intrusive and can be, in many cases, more cost-effective, therefore it is essential to investigate the processes by which intrinsic bioremediation progresses at field and laboratory scale. It is recommended that laboratory investigations incorporate a microcosm study as stipulated in the 3 lines of evidence approach, which is accepted by both the US and UKEA as the strategy to demonstrate NA.

An important Triassic sandstone aquifer in the UK has been heavily polluted by phenolics, including phenol, compounds. Field and lab investigations show that phenol is degrading under aerobic and anaerobic (NO_3^--reduction, Mn(IV)-/Fe(III)-reduction, SO_4^{2-}-reduction, methanogenesis and fermentation) conditions. In certain areas of the plume where Fe(III) is energetically favourable, SO_4^{2-}-reduction is the TEAP but the potential of SO_4^{2-} and the other electron acceptors to remove high concentrations of phenol has not been quantified and previous studies show that phenol has an inhibitory effect on anaerobic bacteria at ~ 200 mg/L and above (Broholm and Arvin, 2000; Harrison et al., 2001; Tschech and Fuchs, 1987). Degradation is retarded in the core, most probably due to phenol toxicity, however the toxicity threshold of phenol to the field SRB is not known. Quantification of this threshold would aid our understanding of the intrinsic biodegradation capability and potentially contribute to an enhanced NA strategy.

Chlorinated solvents are common contaminants in groundwater. The highly toxic and volatile VC may accumulate in aquifers following reductive dehalogenation of more chlorinated compounds such as PCE and TCE. Other than reductive dehalogenation, chloroethenes can undergo cometabolic oxidation or direct microbial oxidation. Cometabolic degradation has mainly been documented in aerobically stimulated reductive chlorination studies. Anaerobic cometabolic degradation may also be successful, especially with less chlorinated compounds such as VC. Direct oxidation of VC has recently been shown to occur both aerobically and anaerobically. Anoxically, VC degradation has been shown under a range of conditions including SO_4^{2-}-reducing and methanogenic. However, VC oxidation under SO_4^{2-}-reducing conditions has only been documented in one relatively short-term study (50 days) in small microcosms (20ml) and the potential of this TEAP to degrade VC to CO_2 requires further investigation. It would be beneficial to perform a long-term microcosm study on larger microcosms that can be sequentially sampled for reactants and products, and gain further information on the degradation potential and the processes taking place. Furthermore, it is imperative to try and identify the anaerobic microorganisms responsible for direct oxidation and understand their potential capabilities and limitations as well as how they are affected by varying environmental conditions.

1.5.2 Aims and Objectives

1. To develop and run a long-term microcosm experiment, inoculated with bacteria indigenous to a highly contaminated phenolic field site, investigating phenol biodegradation, coupled to SO_4^{2-}-reduction.

2. To determine the toxicity threshold of phenol on bacteria sampled from a field site highly contaminated in phenolics, drawing conclusions as to the biodegradation potential of the microorganisms, isolating and identifying the bacterial culture responsible by DNA sequencing and highlighting possible implications for MNA.

3. To fit phenol biodegradation data obtained from laboratory microcosms to a Monod kinetic model and to compare kinetic degradation parameters with literature values.

4. To develop and utilise an analytical method coupled with a long-term microcosm experiment investigating direct microbial transformation of VC under SO_4^{2-}-reducing conditions.

5. To explore the possibility of cometabolic mineralisation of VC by SRB, using phenol as the primary growth substrate.

1.6 Thesis Layout

The thesis consists of 6 chapters:

- Chapter 1- Introduction and research background. This chapter sets the scene and explains the rationale for the study.

- Chapter 2 - Overview of experimental methods. Gives an overview of the material and methods utilised during the course of the research project.

- Chapter 3 - Presents and discusses results from the long-term microcosm experiment investigating whether high phenol concentrations are biodegradable under SO_4^{2-}-reducing conditions and the toxicity threshold of phenol for the field bacteria. Also presents the results of DNA sequencing analysis carried out on the phenol degrading culture

- Chapter 4 - Shows and discusses results of the kinetic modelling performed on the data obtained from the phenol microcosm experiment.

- Chapter 5 - Describes the methodological development of an analytical technique to investigate VC degradation in microcosms. Also presents and discusses the results of direct microbial VC oxidation under SO_4^{2-}-reducing conditions and the cometabolic oxidation experiment.

- Chapter 6 - Draws conclusions from the experiments and makes suggestions for application of MNA at field sites. Recommendations are made for further research.

- Appendices - Shows raw data, calibration graphs and associated information of the experimental work

2. MATERIALS AND METHODS

2.1 Sample Collection, Handling and Storage

A core of aquifer material was collected from the phenolic contaminated field using a rotary diamond drill. The sampling point was 140 m from the plume source and 10 m downstream from the multi-level sampler, BH59 (Figure 2.1)

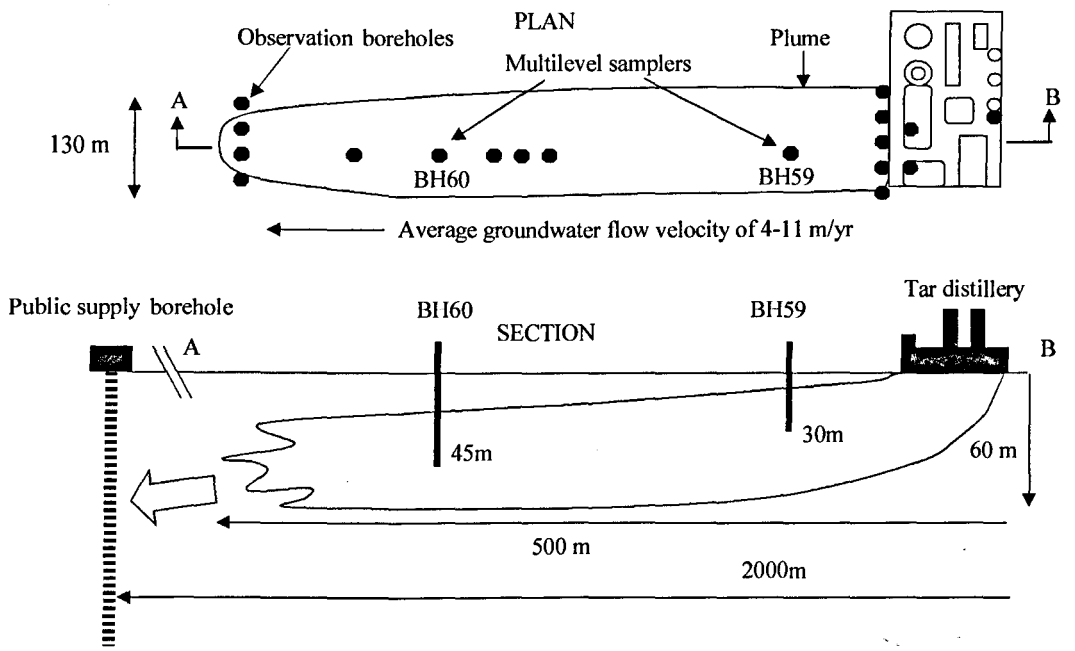

Figure 2.1 Schematic plan and section of the Four Ashes site, showing general observation wells, multilevel samplers, and approximate locations of plume (taken from Lerner et al., 2000).

The plume location at this point extends from 10 to 30 m depth so 28.5 m of core material from 7 to 35.5 mbgl gave sufficient samples of contaminated rock and pristine aquifer material bracketing the plume. It was imperative to maintain anaerobic conditions as exposure to oxygen could have affected the microbial consortia and unstable, reactive mineral phases. Therefore sampling was carried out with the apparatus shown in Figure 2.2 with the re-circulation tanks flushed with N_2 gas through porous silica diffusing bars during sampling.

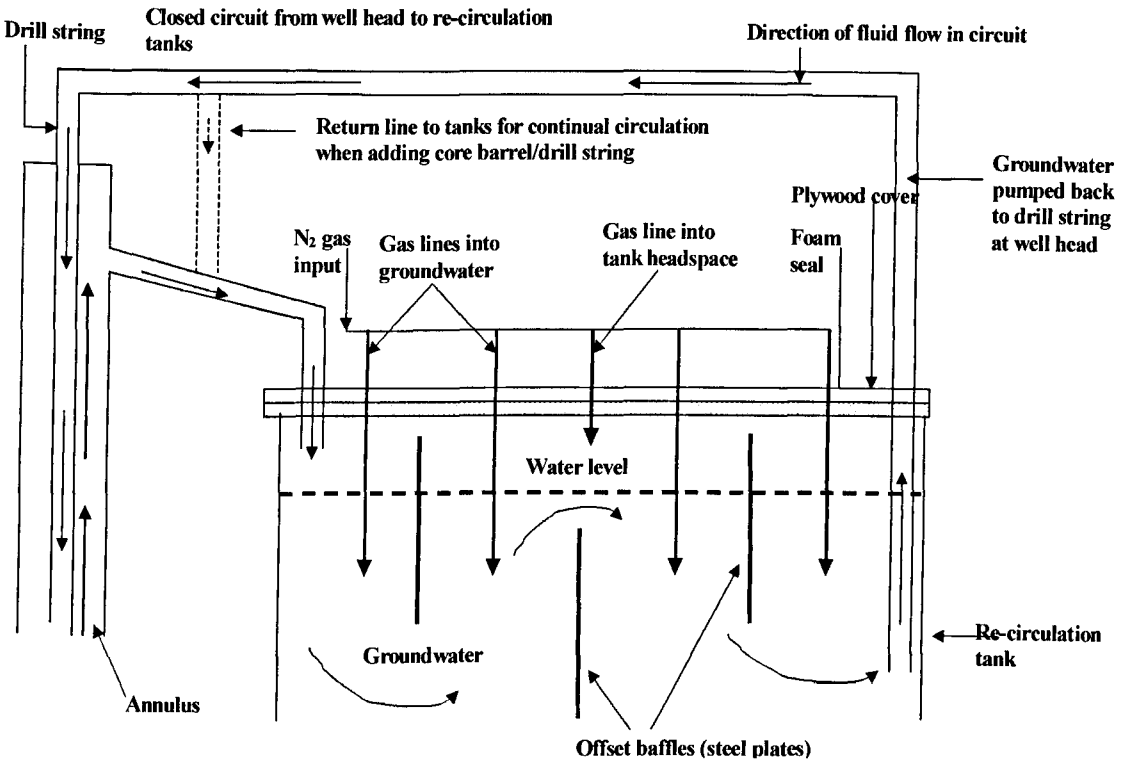

Figure 2.2 Section view of re-circulation tanks set-up for anerobic coring operation (Courtesy of Thornton, S. F.).

The cores, 3 m long and 10.6 cm in diameter, were recovered in an acrylic core liner within the core barrel to prevent atmospheric contamination. Upon removal from the barrel, the core liner was fitted with a N_2 line and flushed continuously whilst the samples were cut by a masonry disc saw (Spence, 2001; Spence et al., 2001a; Spence et al., 2001b; Thornton et al., 2001b). Samples were stored at the field site under N_2 at -10°C before being transported to the lab where they were stored at 4°C under a N_2 atmosphere.

The section of four-ashes core sample to be used for the phenol microcosm experiment was taken from 10 to 13.5 mbgl. This section was chosen, as sulphate and sulphide analysis indicated that this was a sulphate-reducing zone within the plume (Figure 1.8). Clean, uncontaminated sediment material was taken from the same depth as the contaminated aquifer core from a quarry adjacent to the contaminated site, and used in phenol and VC microcosm experiments.

2.2 Microcosm Study to Identify Toxicity Thresholds for Phenol Biodegradation Processes at a Heavily Contaminated Field Site

2.2.1 Design and Construction of Microcosms

Eight microcosms were prepared for a long-term biodegradation study using 500 ml glass bottles. Prior to construction, all bottles and fittings were chemically cleaned and rinsed with Ultra High Quality (UHQ) water with a specific resistance > 18 MΩ/cm. Each microcosm was fitted with a PTFE cap which had 3 threaded holes. To facilitate gas and liquid sampling, PTFE tubing (0.5 mm) was passed through 2 of the holes to different depths in the microcosm, whilst the 3rd hole was permanently sealed. Two-way, PEEK shut-off valves (Supelco, USA) were attached to the external section of the tubing and these were used to take samples or make any amendments to the microcosms. PTFE filters (0.2 μ) were attached to the valves to prevent bacterial contamination via the sampling ports. Figure 2.3 shows the microcosm set-up.

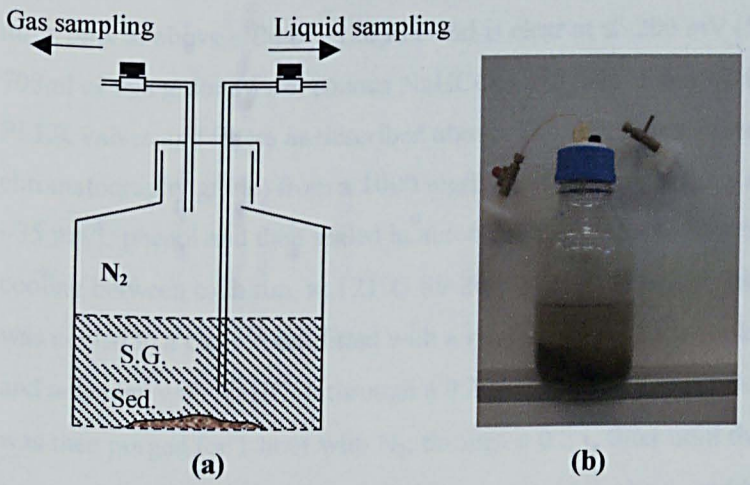

Figure 2.3 (a) Schematic of microcosm set-up for phenol biodegradation studies, and (b) image of complete microcosm.

2.2.2 Preparation of Four-Ashes Core Sample used as Inoculum

Great care had to be taken to preserve the microbial consortia in the four-ashes field core material. If the core was stored too long, it may have become contaminated with O_2 and, subsequently, altered or adversely affected the microbial consortia. Therefore, it was decided to grow the bacteria from the core in a batch reactor (termed the field inoculum) and utilise this as the inoculum for the experimental microcosms. This technique also meant that inoculation of the experimental microcosms was less problematic as the inoculum could be transferred by sterile, gastight syringe rather than transferring the core to each microcosm separately thereby exposing it to another atmosphere for longer, thus increasing the chance of contamination.

A stock of synthetic groundwater (SG) was prepared, using BDH ANALAR grade salts, with concentrations for most ions similar to background concentrations in uncontaminated groundwater sampled from the field site (Table A1.1, Appendix A1). Some alterations were made to promote SO_4^{2-}-reduction as the TEAP. Excess SO_4^{2-} was added as Na_2SO_4, NO_3^- was replaced by NH_4^+ as the Nitrogen source and $NaHCO_3$ was used for its buffering capacity and to bring the pH to 7.0. The redox indicator, Resazurin was added to the SG at ~ 1 mg/L. The indicator is purple when highly oxygenated but turns pink at above -100 to –120 mV and is clear at ≤ -200 mV (Salanitro et al., 1997). 700ml of this groundwater (minus $NaHCO_3$) was placed in a 1L bottle fitted with tubing, PEEK valves and filters as described above. The bottle was amended with phenol (BDH, chromatography grade) from a 1000 mg/L stock solution to give a final concentration of ~35 mg/L phenol and then sealed in autoclave bags before being sterilised 3 times, cooling between each run, at 121°C for 20 min. Following sterilisation the batch reactor was cooled in a clean room fitted with a High Efficiency Particulate Air (HEPA) filter, and amended with $NaHCO_3$ through a 0.2 μ filter around a Bunsen flame. The reactor was then purged for 1 hour with N_2, through a 0.2 μ filter until the resazurin indicator turned pink, before being transferred to an anaerobic glove chamber along with the field core material from 10.5 to 13 mbgl. To minimise contamination and alteration to the core it was kept sealed until it was in the chamber and ready for transfer to the reactor. The sealed core was eventually opened and within a few minutes ~ 50 g were transferred to the bottle which was quickly sealed. The batch reactor was removed from the chamber, mixed, stored in the dark at 20°C and sampled regularly for phenol analysis by HPLC. A plot of the phenol concentration over time is shown in Figure 2.4. It is clear

that the microbial populations in the field core material had the ability to degrade phenol.

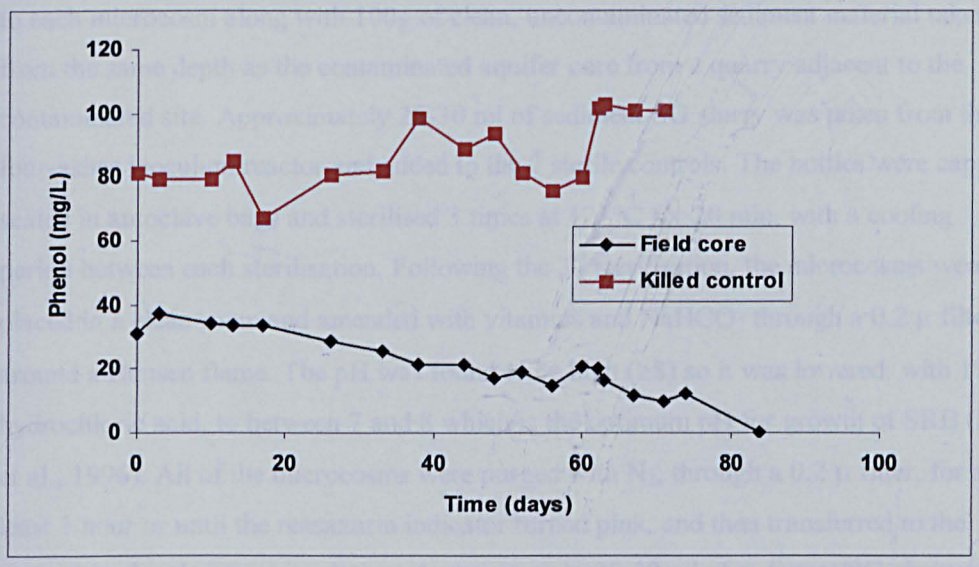

Figure 2.4 Phenol removal in batch reactors and sterile control containing field rock material and synthetic groundwater.

2.2.3 Preparation of Phenol Biodegradation Microcosms

To encourage dominance of SRB, the SG from Section 2.1.2 was altered slightly according to growth mediums previously used in biodegradation studies under sulphate-reducing conditions (Beller et al., 1992b; Edwards et al., 1992b) and contained the following (g/l Ultra High Quality [UHQ] water at 18 MΩ/cm): NH_4Cl (1.0), NaH_2PO_4 (0.50), NaCl (0.09), KCl (0.09), $CaCl_2.6H_2O$ (0.15), $MgCl_2.6H_2O$ (0.10), $MgSO_4.7H_2O$ (0.10), $MnCl_2.4H_2O$ (0.005), Na_2SO_4 (1.6), Resazurin redox indicator (0.001). This mixture will subsequently be referred to as SG-SO_4^{2-} (Table A1.1, Appendix A1). Additional solutions were prepared separately and added depending on the volume of the aqueous phase. These included (g/l UHQ): $NaHCO_3$ solution (2.52), vitamin solution consisting of d-Biotin (0.02), Folic acid (0.02), Pyridoxine HCl (0.1), Riboflavin (0.05), Thiamine HCl (0.05), Nicotinic acid (0.05), D-Pantothenic acid (0.05), p-aminobenzoate (0.05), Cyanocobalamin (0.05) (Edwards et al., 1992).

Eight bottles were prepared with varying initial phenol concentrations. There were 2 killed, sterile controls (1A and 1B) and 6 'live' varying only in their initial phenol concentrations. There were 2 at ~125 mg/L (2A and 2B), 2 at ~175 mg/L (3A and 3B) and another 2 at ~225 mg/L (4A and 4B). An addition of 450 ml of SG-SO_4^{2-} was made to each microcosm along with 100g of clean, uncontaminated sediment material taken from the same depth as the contaminated aquifer core from a quarry adjacent to the contaminated site. Approximately 25-30 ml of sediment/SG slurry was taken from the four-ashes inoculum reactor and added to the 2 sterile controls. The bottles were capped, sealed in autoclave bags and sterilised 3 times at 121°C for 20 min, with a cooling period between each sterilisation. Following the 3rd sterilisation, the microcosms were placed in a clean room and amended with vitamins and $NaHCO_3$ through a 0.2 μ filter around a Bunsen flame. The pH was found to be high (≥8) so it was lowered, with 1% hydrochloric acid, to between 7 and 8 which is the optimum pH for growth of SRB (Hao et al., 1996). All of the microcosms were purged with N_2, through a 0.2 μ filter, for at least 1 hour or until the reasazurin indicator turned pink, and then transferred to the anaerobic chamber for inoculation. Approximately 25-30 ml of sediment/SG slurry was taken from the four-ashes core batch reactor in a sterile gastight syringe and added to each of the six 'live' microcosms. The microcosms were mixed, covered in foil to exclude light and sampled. They were subsequently stored in a dark, temperature-controlled box at 20°C with a N_2 atmosphere. A slight positive pressure was maintained throughout the course of the experiment to prevent any incursions to the reactors. Samples were taken regularly and any amendments (e.g. phenol or SO_4^{2-} additions) were made through 0.2 μ filters in an anaerobic chamber. Microcosm headspaces were generally purged following any amendments to remove toxic H_2S gas produced during SO_4^{2-}-reduction. The microcosm set-up and phenol/sulphate amendments are summarised in Table 2.1 and 2.2, respectively.

Table 2.1 Summary of experimental microcosms prepared for phenol biodegradation experiment. SG-SO_4^{2-} (450ml) and clean sediment (100g) were added to all microcosms.

Microcosm	Inoculum	Environmental Conditions	Initial Phenol[α]
1A (killed, sterile control)	25-30 ml aliquot of four-ashes inoculum	20°C pH 8.5	~ 90 mg/L
1B (killed, sterile control)	25-30 ml aliquot of four-ashes inoculum	20°C pH 8.1	~ 90 mg/L
2A (live)	25-30 ml aliquot of four-ashes inoculum	20°C pH 7.6	~ 125 mg/L
2B (live)	25-30ml aliquot of four-ashes inoculum	20°C pH 7.6	~ 125 mg/L
3A (live)	25-30 ml aliquot of four-ashes inoculum	20°C pH 7.5	~ 175 mg/L
3B (live)	25-30 ml aliquot of four-ashes inoculum	20°C pH 7.5	~ 175 mg/L
4A (live)	25-30 ml aliquot of four-ashes inoculum	20°C pH 7.6	~ 225 mg/L
4B (live)	25-30 ml aliquot of four-ashes inoculum	20°C pH 7.6	~ 225 mg/L

[α] Initial phenol concentrations are approximate as additions were made in an anaerobic glovebox, which made exact transfer difficult. There was also some transfer from the inoculum that was grown on phenol.

Table 2.2 Sulphate and Phenol amendments made to microcosms. Phenol and sulphate added at the beginning of the experiment are termed the 1st addition. Microcosms where no 3rd addition was made are denoted by n/a.

Microcosm	2nd phenol addition	3rd phenol addition	2nd sulphate addition	3rd sulphate addition
2A	Day 175	Day 503	Day 175	Day 535
2B	Day 105	Day 503	Day 175	Day 535
3A	Day 105	Day 503	Day 175	n/a
3B	Day 503	n/a	Day 175	Day 678
4A	Day 313	n/a	Day 175	n/a
4B	Day 313	n/a	Day 175	n/a

2.3 Sampling and Chemical Analysis of Phenol Biodegradation Microcosms.

2.3.1 Microcosm Sampling Procedure

All microcosms were gently stirred on the morning of each sampling day to guarantee a representative sample and ensure that the sediment particulates had time to settle preventing filter blockage. Gases (CO_2, CH_4 and H_2) were sampled directly from the microcosm headspace by attaching a gas-tight syringe to the 0.2 μ filter on the gas port. Analysis of CO_2 and CH_4 was carried out by Gas Chromatography (GC) and H_2 analysis was carried out on a Trace Analytical RGA3 reduction gas analyser (Section 2.3.3). Aqueous samples were taken in the clean room around a bunsen flame. Approximately 5-10 ml of sample was removed using a sterile syringe. 1 ml was transferred through a 0.2 μ filter to a sterile glass HPLC vial for phenol analysis by High Pressure Liquid Chromatography, HPLC (Section 2.3.2) and the remainder was used for dissolved ion determination by Ion Chromatography (IC) (Section 2.3.4) and total elemental analysis by Inductively-Coupled Plasma Atomic Emission Spectroscopy (ICP-AES), (Section 2.3.5). The samples were stored frozen at -20°C if they could not be analysed immediately.

A flow cell capable of anaerobic sampling was constructed to measure the pH without exposing the sample to O_2. The sealed flow cell was attached to the aqueous sampling port and ~ 5 ml of sample was pulled through using a syringe. The pH and H_2

analysis was carried out less regularly as the volume of sample required was not conducive to running a long-term experiment. Aqueous samples for molecular and microbiological manipulation were used without filtration as described in Section 2.4.

2.3.2 Analysis of Phenol by High Pressure Liquid Chromatography (HPLC)

Aqueous samples taken from microcosms were analysed by HPLC on the day of sampling, if possible. Samples taken from storage at -20°C were defrosted and mixed thoroughly before analysis. The HPLC analysis was carried out on a Gilson HPLC modular system equipped with a Jones Genesis C-18 reverse-phase column (250 mm x 4 μm) and a Jones Genesis C-18, 4 μm guard column. The eluent was de-aerated, HPLC grade methanol in UHQ water with a methanol:water ratio of 60:40 (vol/vol). The eluent flow-rate was set at 1.0 ml/min and the sample injection loop was 5 μl. Detection was by a Pye-Unicam 4020 UV absorbance detector at 266 nm. The instrument was calibrated prior to each analysis using standards prepared in UHQ water from chromatography grade phenol at 99% purity (BDH) and a plot of the calibration curve always gave an r^2 value of at least 0.995. Independent analytical quality controls (AQC's) were run after every 10 samples.

2.3.3 Analysis of Carbon Dioxide, Methane and Hydrogen

CO_2 and CH_4 were sampled with more regularity than H_2 as only 0.5 ml of headspace sample was required for combined CO_2 and CH_4 analysis whereas at least 3 ml were required for H_2 analysis. Also, frequent sampling of H_2 was potentially disruptive to the microcosms. Samples for CO_2 and CH_4 analysis were taken directly from the microcosms gas sampling port and injected into a Varian 3400 GC equipped with a Flame Ionisation Detector (FID) with a valco valve loop injector (0.5 ml). The injector temperature was set at 340°C, the flow rate of the carrier gas, N_2, was at 40 ml/min and the FID detector was at 250°C. The sample was injected directly into a phase-separation sphericarb packed column (6 ft x 0.25 in) and a varian methaniser column, which allowed analysis of both gases on a single injection. The column was also suitable for simultaneous C_2H_4 analysis, which was carried out for the VC oxidation experiments. The GC was calibrated prior to each analytical run using standard calibration gases (Scientific and Technical Gases Ltd, UK) and AQC's were run every 10 samples.

Where H_2 was analysed, samples were taken at the same time as for CO_2 and CH_4 and injected into a Trace Analytical RGA3 Reduction Gas Analyser. H_2 was analysed at 105°C on 60/80 Spherocarb in a stainless steel column (0.92 m x 3.2 mm), utilising N_2 as the carrier gas at 30ml/min and with the reduction gas detector at 265°C. The analyser was calibrated prior to each analysis using a certified calibration gas (Scientific and Technical Gases Ltd, UK)

The pressure in the microcosms was measured just prior to gas sampling by a calibrated pressure transducer (Figure A1.1, Appendix A1) and this measurement was used in the following equation to calculate the headspace concentration in ppm:

$$C_m = \frac{P_m * T * C}{T_m * P_0} \qquad \textbf{(2.1)}$$

C_m = Concentration in microcosm headspace (ppm)
P_m = Headspace pressure of microcosm (kPa)
T = Standard temperature (273 K)
C = Concentration from GC analysis (ppm)
T_m = Temperature of microcosm (K)
P_0 = Atmospheric pressure (101.33 kPa)

The headspace concentration was converted from ppm to moles/L using the following equation:

$$C_m = \frac{P_m * T * C * V}{T_m * P_0 * 10^6 * V_{ig}} \qquad \textbf{(2.2)}$$

C_m = Concentration in microcosm headspace (mol/L)
P_m = Headspace pressure of microcosm (kPa)
T = Standard temperature (273 K)
C = Concentration from GC analysis (ppm)
V = Headspace volume
T_m = Temperature of microcosm (K)
P_0 = Atmospheric pressure (101.33 kPa)
V_{ig} = Molar volume of an ideal gas at standard temperature and pressure (22.4 L)

2.3.4 Analysis of Dissolved Ions by Ion Chromatography (IC).

Dissolved ions including SO_4^{2-}, NO_3^-, NO_2^-, PO_4, NH_4^+ and K^+ were analysed by IC. The technique is widely used to separate small anions and cations on the basis of their size and charge. The larger, highly charged molecules having a stronger affinity for the column packing material, which consists of ion exchange resins with a surface of resin beads.

The aqueous samples were diluted 1:10 with UHQ water using an auto-dilutor (Hamilton – Microlab 500 series), to ensure ions such as SO_4^{2-} were within the range of the detector. Samples were analysed on a Dionex Corporation DX120 system that incorporated both cation and anion modules for simultaneous detection. Anions were analysed on an AS14 column with an AG 14 guard column (Dionex Corporation), whilst cations were separated on a CS12 column with a CG12 guard column (Dionex Corporation). Analyses were isocratic with both the anion eluent, 3.5 mM Na_2CO_3 + 1.0 mM NaHCO3, and the cation eluent, 20mM methanesulphonic acid, flowing at 1.4 ml/min. Both modules incorporated self-generating suppressors. The IC was calibrated prior to each analysis using High Purity Reagent (HPR) standard metal solutions (Fisher Scientific) and independent AQC's were analysed after every 10 samples.

2.3.5 Total Elemental Analysis by Inductively Coupled Plasma Atomic Emission Spectroscopy (ICP-AES).

ICP-AES is highly effective analytical technique for elemental analysis with detection limits routinely down at the ppb level. The filtered aqueous microcosm samples were diluted 1:10 in 1% HNO_3 (Nitric acid) and transferred to the Sheffield Assay Office, Sheffield, UK for analysis of dissolved elements including S, Fe, Mn, K, and P. The standards, samples and quality controls were run on a Perkin Elmer Optima 3300 RL (Radial Torch) instrument with ICP power at 1300 Watts. Argon flow through the nebulizer was 0.8 L/min, coolant flow was at 15 L/min, plasma flow a 0.5 L/min and the solution was pumped at 2.5 ml/min. The detector was a solid state device and all element emission wavelengths were measured simultaneously.

2.4 Molecular and Microbiological Analysis of Phenol Microcosms

2.4.1 Growth of Phenol Degraders on Sulphate-Reducing Agar Plates and Slopes

Sulphate-reducing agar containing 50 mg/L phenol was prepared by mixing 15 g/L of Agar No. 3 with the SG-SO_4^{2-}, including the redox indicator, described in 2.2.3. The agar was autoclaved at 121°C for 30 minutes, cooled to 50°C whilst being flushed with N_2 through a 0.2 μ filter, and then poured into sterile petri dishes under a stream of filtered N_2. The plates were allowed to set overnight in an anaerobic storage jar under a N_2 atmosphere at room temperature. The following day (day 622 of the phenol experiment) 0.3 ml of aqueous/sediment slurry was removed from the microcosms, placed directly onto the agar plates and spread over the plates with a sterile glass spreader. These actions were carried out around a Bunsen burner and under a constant stream of filtered N_2. The plates were sealed in the anaerobic jar, flushed with sterile N_2 and incubated at 25°C. Within 24 hours the agar had changed colour from pink to clear indicating that there was no O_2 present in the growth medium. The plates were left until enough growth was seen to carry out streaking of colonies on fresh agar plates.

Agar plates and slopes (30 ml sterile tubes rather than petri dishes) were prepared for streaking. However, instead of using a sample from the microcosms, single, distinct colonies were picked off the spread plates (Section 2.4.1) with sterile rods and streaked onto the newly prepared agar plates. Again, all actions were carried out around a Bunsen flame under a stream of N_2. The plates were incubated in anaerobic jars at 25°C and a change in redox conditions was evidenced by the colour change from pink to clear. Once colonies had grown sufficiently, they were picked off and streaked onto the agar slopes, which were subsequently stored in anaerobic jars. These slopes were then anaerobically transferred for microbial identification to an accredited laboratory, CABI Bioscience UK, who carried out the DNA extraction, PCR amplification and sequencing on two isolates (microcosms 2B and 3B), as described below.

2.4.2 Isolation and Identification of Phenol Degraders by DNA Sequencing

DNA extraction was carried out using a Qiamp DNA mini kit (Qiagen, Crawley, UK) according to the manufacturers instructions. DNA was eluted in a final volume of 200 µL sterile HPLC grade water for PCR studies.

PCR amplification of the 5' portion of the 16S rDNA was achieved using 'universal' bacterial primers 27F (5'-AGAGTTTGATCMTGGCTCAG-3') and 1541R (5'-AAGGAGGTGWTCCARCC-3') [Sigma Genosys Ltd., Pampisford, UK]. PCR was performed in a total volume of 50 µL, containing 0.5 µmol/L primers, 1.5 µmol/L $MgCl_2$, 5 x 10^{-3} U/µL *Tth* enzyme (HT Biotechnology, Cambridge, UK), and 200 µmol/L dNTPs (Pharmacia) in 10 x *Tth* buffer. Reaction mixtures were incubated for 40 cycles of 1 min at 95°C, 1 min at 52°C and 1 min at 72°C. PCR products were subjected to electrophoresis in a Flowgen Midi Gel Electrophoresis tank. Fragments were separated at 5 V/cm for 2 h in a 1.5% SeaKem LE agarose gel (BMA, UK) in 0.5 x TBE (Sambrook et al., 1989). In each case a single amplification product was obtained. Initial attempts were made to amplify the entire 16S rDNA for sequencing.
PCR products were purified using Wizard PCR preps DNA purification system Promega, UK) according to the manufacturers instructions and 5 µL aliquots were subjected to electrophoresis under the same conditions as above. Attempts to sequence the entire 16S rDNA were unsuccessful. Sequencing reactions were undertaken using a SequiTherm EXCEL II kit (CAMBIO, UK) according to the manufacturers instructions and IRD-700 labelled 25f primer and IRD-800 labelled 530R (5'GTATTACCGCGGCTGCTG-3';) primer were incorporated as the sequencing primer. Sequencing was undertaken with a LiCor 4200S-2 sequencer. The obtained sequence was trimmed to remove ambiguous bases and the 'clean' sequence subjected to a BLAST (**B**asic **L**ocal **A**lignment **S**earch **T**ool) search that can compared the sequence with those contained in nucleotide and protein databases by aligning the sequence with previously characterised genes and a FASTA (**Fast-A**ll) search was also done for nucleotide comparison.

2.4.3 Protein Determination by the Bradford Assay

The method for protein determination was based on the Bradford method for total protein determination. The protein assay was performed on samples taken close to the end of the experiment (731 days), following the 3rd phenol addition to give a final biomass concentration. Protein standards were freshly prepared from Bovine Serum Albumin (BSA) [Sigma-Aldrich] and calibration was linear ($r^2 > 0.99$) [Figure A1.2, Appendix A1]. The protein concentration obtained from the Bradford assay (mg/L) was converted to a molar volume by taking the formula weight of the BSA, based on the current amino acid sequence, to be 66,430 (Hirayama et al., 1990).

2.5 Method Development and Microcosm Study into Microbial Transformation of Vinyl Chloride under SO_4^{2-}-reducing conditions.

Experiments were performed to develop an effective method to carry out a relatively long-term VC degradation experiment that could be repeatedly sampled and reliably quantify VC. As the SPME and headspace methods used in this study have not been used previously in biodegradation studies and due to the potential benefit of the method to future work, it is explained in more detail in Section 5. A brief description of inocula used in the microcosms and the analytical kit used is given in this Section.VC was analysed by sampling the headspace and injecting into a Gas Chromatograph fitted with a Mass Spectrometer detector (GC-MS) or using a Solid-Phase microextraction device that automatically and directly sampled from the headspace and injected to the GCMS.

2.5.1 Inocula used for VC Microcosm Experiments

A number of VC oxidation experiments were carried out using a range of inocula: anaerobic digester sludge, enriched cultures and sub-samples from phenol degrading microcosms (Section 2.2).
Sludge samples were obtained by filling sample bottles, without headspace, directly from the outflow of an anaerobic digester plant at a sewage treatment facility in Yorkshire, UK. The sludge was subsequently stored in an anaerobic chamber until it was used to inoculate the 20 ml microcosms.

Enrichment culture technique was carried out to select for cultures capable of functioning anaerobically in the presence of VC and, perhaps, oxidising VC. A 10 ml sample was removed from all 3 of the 20 ml microcosms (Live-1, -2 and -3), looking at VC oxidation (Section 2.5.2), and added to thrice sterilised 120 ml serum vials along with 43.5 ml of sulphate-reducing medium, 0.5 ml of vitamin solution and 0.5 ml $NaHCO_3$ prepared similarly to the SG-SO_4^{2-} in Section 2.2.3. Additionally the serum vial was amended with 0.5 ml of a trace metal solution containing $ZnCl_2$ (0.1), $CuSO_4.5H_2O$ (0.1), $CoCl_2$ (0.1g), $Na_2SeO_3.5H_2O$ (0.02), $NaMoO_4.2H_2O$ (0.1), $FeSO_4.7H_2O$ (0.5) (Postgate, 1984; Edwards et al., 1992). The vials were amended with ~ 90 µg/L VC and called Enrichment 1. The enrichment procedure was repeated after 75 days using 10 ml of Enrichment 1 instead of the microcosm sample to give Enrichment 2. Enrichment 3 was carried out another 51 days later using 10 ml of Enrichment 2 as inoculum and finally Enrichment 4 was performed after another 237 days later had elapsed using 10 ml of Enrichment 3 as the inoculum.

Table 2.3 Summary of enrichment culturing carried out to select for VC oxidising bacteria. Initial inoculum was from 20 ml microcosm experiment.

Inoculum	Days elapsed since previous enrichment	Enrichment designation	VC concentration[α] (µg/L)
VC-1	0	A-1	~ 90
VC-2	0	B-1	~ 90
VC-3	0	C-1	~ 90
A-1	75	A-2	~ 210
B-1	75	B-2	~ 210
C-1	75	C-2	~ 210
A-2	51	A-3	~ 70
B-2	51	B-3	~ 115
C-2	51	C-3	~ 70
A-3	237	A-4	1577[α]
B-3	237	B-4	1051[α]
C-3	237	C-4	1010[α]

[α] VC quantification was possible at enrichment 3 as the analytical procedure had been developed. VC concentrations prior to this are estimated from additions made, as a suitable analytical method was not yet available to quantify VC.

A 10 ml aliquot from the phenol degrading microcosms (Section 2.2) was also used to inoculate a range of 120 ml microcosms (Section 2.5.3).

2.5.2 Investigating Direct Oxidation of Vinyl Chloride under Sulphate-reducing Conditions in 20 ml Microcosms Using SPME in Conjunction with GC-MS.

Various microcosm set-ups were used to study VC oxidation. Initial experiments were carried out in 20 ml serum vials and subsequent experiments were in 120 ml serum vials.

The 20 ml microcosms were inoculated with anaerobic digester sludge whereas the 120 ml vials were inoculated with either an aliquot taken from the phenol degrading microcosms (Section 2.2), or enrichment cultures attempting to select for VC oxidisers (Table 2.3). The microcosm set-up for the 20 ml mirocosms is shown in Table 2.4.

Table 2.4 Summary of 20 ml microcosms prepared to investigate VC oxidation under sulphate-reducing conditions. Killed controls (KC) and live microcosms (VC) were prepared in triplicate.

Microcosm	Conditions	Inoculum	Initial VC (μg/L)
KC-1	Sulphate-reducing	Killed control	0.35
KC-2	Sulphate-reducing	Killed control	0.35
KC-3	Sulphate-reducing	Killed control	0.32
VC-1	Sulphate-reducing	Anaerobic sludge	0.23
VC-2	Sulphate-reducing	Anaerobic sludge	0.22
VC-3	Sulphate-reducing	Anaerobic sludge	0.23

2.5.3 Direct Oxidation of Vinyl Chloride under SO_4^{2-}-reducing Conditions in 120 ml Microcosms Inoculated with Anaerobic Enrichment Cultures

Subsequent VC oxidation experiments were carried out in 120 ml serum vials prepared using the procedures above but with some modifications. They contained 30 g of clean sediment, 58.2 ml of the SG-SO_4^{2-} and 0.6 ml each of the vitamin, trace metal and $NaHCO_3$ solutions. VC addition was from a high purity gas stock (≥ 99.5%, Fluka) and sterile, killed controls were prepared in triplicate. Calibration standards, AQC's and microcosms to determine the partitioning ratio (headspace concentration/aqueous phase concentration) were prepared in exactly the same way as experimental microcosms to minimise matrix effects. The microcosm set-up is shown in Table 2.5

Table 2.5 Summary of 120 ml microcosms prepared to investigate VC oxidation under sulphate-reducing conditions.

Microcosm designation	Inoculum	Initial headspace VC concentration (μg/L)
Control-1	Killed control	631
Control-2	Killed control	864
Control-3	Killed control	697
Live-B2-1	Enrichment B-2	760
Live-B2-2	Enrichment B-2	656
Live-B2-3	Enrichment B-2	647
Live-A3-1	Enrichment A-3	699
Live-A3-2	Enrichment A-3	743
Live-A3-3	Enrichment A-3	755
Live-C3-1	Enrichment C-3	740
Live-C3-2	Enrichment C-3	756
Live-C3-3	Enrichment C-3	715

2.5.4 Microcosms Investigating Cometabolic Degradation of Vinyl Chloride under Sulphate-reducing Conditions, Utilising Phenol as the Primary Carbon Source.

A total of 9 microcosms, 3 killed controls and 6 live, were prepared in 120 ml serum vials in a similar fashion to the microcosms in section 2.5.3. However, the inoculum in this case was a 10ml sub-sample of microcosm 2A or 3B from the phenol degradation experiment (Section 2.2). The 6 live microcosms consisted of 3 at high initial concentrations of VC and another 3 with low or zero concentrations of VC. The microcosms were amended with VC and fluorobenzene as well as phenol, which provided an alternative carbon source for the microorganisms (Table 2.6).

Table 2.6 Summary of 120 ml microcosms prepared to investigate cometabolic oxidation of VC under sulphate-reducing conditions, using phenol as the primary substrate.

Microcosm designation	Inoculum	Initial VC (μg/L)	Initial phenol (mg/L)
Con-1	Killed control	821	107.9
Con-2	Killed control	837	97.0
Con-3	Killed control	987	100.6
Live-1	Phenol degrading microcosm 2A	240	100.0
Live-2	Phenol degrading microcosm 2A	628	84.7
Live-3	Phenol degrading microcosm 2A	1018	127.0
Live-4	Phenol degrading microcosm 3B	76	165.7[α]
Live-5	Phenol degrading microcosm 3B	107	167.8[α]
Live-6	Phenol degrading microcosm 3B	0	167.8[α]

[α] **Estimated from additions to microcosms as samples not available for analysis**

2.5.5 Determination of VC by Gas Chromatography with Mass Spectrometry (GCMS).

GCMS combines chromatography and spectrometry to provide both quantitative and qualitative data of known and, in many cases, unknown compounds. The GC component is responsible for the separation of the sample components and the MS carries out a combination of ionisation, fragmentation and separation processes to provide a mass spectra, which can subsequently be used for detection.
The 20 ml microcosms were analysed by GCMS with solid phase micro-extraction (SPME) used to sample the headspace. VC concentration in the 120 ml microcosms was determined by direct sampling of the headspace and injection into the GCMS. Full explanations of these methods are given in Section 5.

3. RESULTS AND DISCUSSION - IDENTIFICATION OF TOXICITY THRESHOLDS FOR PHENOL BIODEGRADATION PROCESSES UNDER SULPHATE-REDUCING CONDITIONS AT A FIELD SITE HEAVILY CONTAMINATED WITH PHENOLICS

3.1 Biodegradation of Phenol Under Sulphate-reducing Conditions Following Initial Phenol Addition

Phenol degradation took place in all live microcosms, following an initial acclimation phase of 19 days for all microcosms. Following this lag phase and the commencement of biodegradation the redox indicator, resazurin, changed colour from pink to clear in the live microcosms, indicating reducing conditions (Figure 3.1).

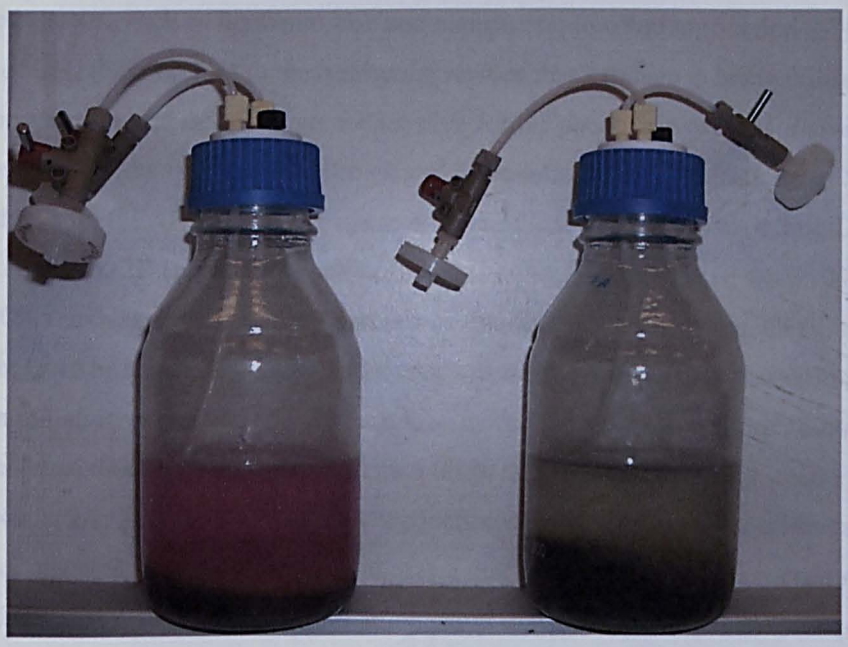

Figure 3.1 Killed control (left) and live microcosm. The colour of the redox indicator, resazurin, has changed from pink to clear in the live microcosm, following the initial lag phase, indicating reducing conditions.

The degradation of phenol was accompanied by sulphate-reduction in all of the live microcosms as shown in Figures 3.2 to 3.4. The increase from the initial concentrations

is most likely due to insufficient mixing following inoculation but there was also a distinct improvement in the HPLC methodology subsequent to day 19 which may also have had a bearing. No phenol degradation or sulphate-reduction was seen in sterile control 1B throughout the experiment or in control 1A until day 246, at which point 1A was contaminated with air during sampling and subsequently led to complete phenol degradation (Figure 3.5). A change in the redox indicator colour to dark pink/purple coupled with the fact that there was no sulphate loss indicates aerobic degradation. This shows the sensitivity of the microcosms to contamination by air and the importance of maintaining a positive pressure as well as using the 0.2μ filters. The lag phase of 19 days is relatively short but compares well with Mort and Dean-Ross (1994) who report lag phases of 15 to 20 days in acclimated sulphate-reducing bacterial cultures degrading phenol. The short lag phase is most probably due to previous exposure of the microbial consortia to phenolics, including phenol, in the field and transfer of the field sediment to the phenol amended batch reactor upon arrival in the laboratory (Section 2.2.2). Degradation of phenol proceeds rapidly following the lag phase and sulphate loss occurs simultaneously. This combined with the strong smell of H_2S gas during sampling, the onset of reducing conditions as evidenced by the redox indicator, the absence of other reduced species, such as dissolved iron and manganese, in solution (Section 3.7), and < 3 μM of CH_4 (Section 3.4) in the headspace verifies that sulphate is being utilised as the electron acceptor and that SRB are responsible for the phenol removal. Moreover, the fact that SO_4^{2-}-reduction pauses when phenol degradation ceases, indicates that SO_4^{2-}-reduction is the TEAP. The phenol concentration falls to zero (taken as < 5mg/L) in microcosms 2A, 2B (Figure 3.2) and to 13 mg/L in 3A [Figure 3.3 (i)] within 125 days but 100% removal occurs later in microcosms 3B, 4A, and 4B [Figures 3.3 (ii) and 3.4]. This seems to be dependent on the initial concentrations added to the microcosms. Those with an initial concentration of ~ 200 mg/L or more take longer to achieve 100% removal, even though the initial acclimation times are the same. Once the phenol in microcosms 2A, 2B was depleted, SO_4^{2-}-reduction ceased and the colour of the redox indicator changed from clear to pink indicating that conditions in the microcosms were less reducing. However, phenol degradation slows down or ceases in microcosms 3A, 3B, 4A and 4B before the phenol concentrations fall to zero. This coincides with SO_4^{2-} concentrations falling below 100 mg/L in these microcosms indicating that, perhaps, the production of H_2S has affected the activity of the SRB (Bolliger et al., 2001; Cunningham et al., 2001) or that there is a critical level of SO_4^{2-} required to for these microorganisms to maintain phenol biodegradation capability. This has already been documented in groundwater bacteria by other studies looking at SO_4^{2-}-reduction in contaminated aquifers (Chapelle et al., 1996; Ulrich et al., 2003; Vroblesky et al., 1996).

As the headspace was purged just prior to the 2nd SO_4^{2-} addition, it is difficult to discern whether biodegradation is inhibited due to the H_2S or because it fell below a critical threshold but a clearer picture develops following the 2nd addition of phenol.

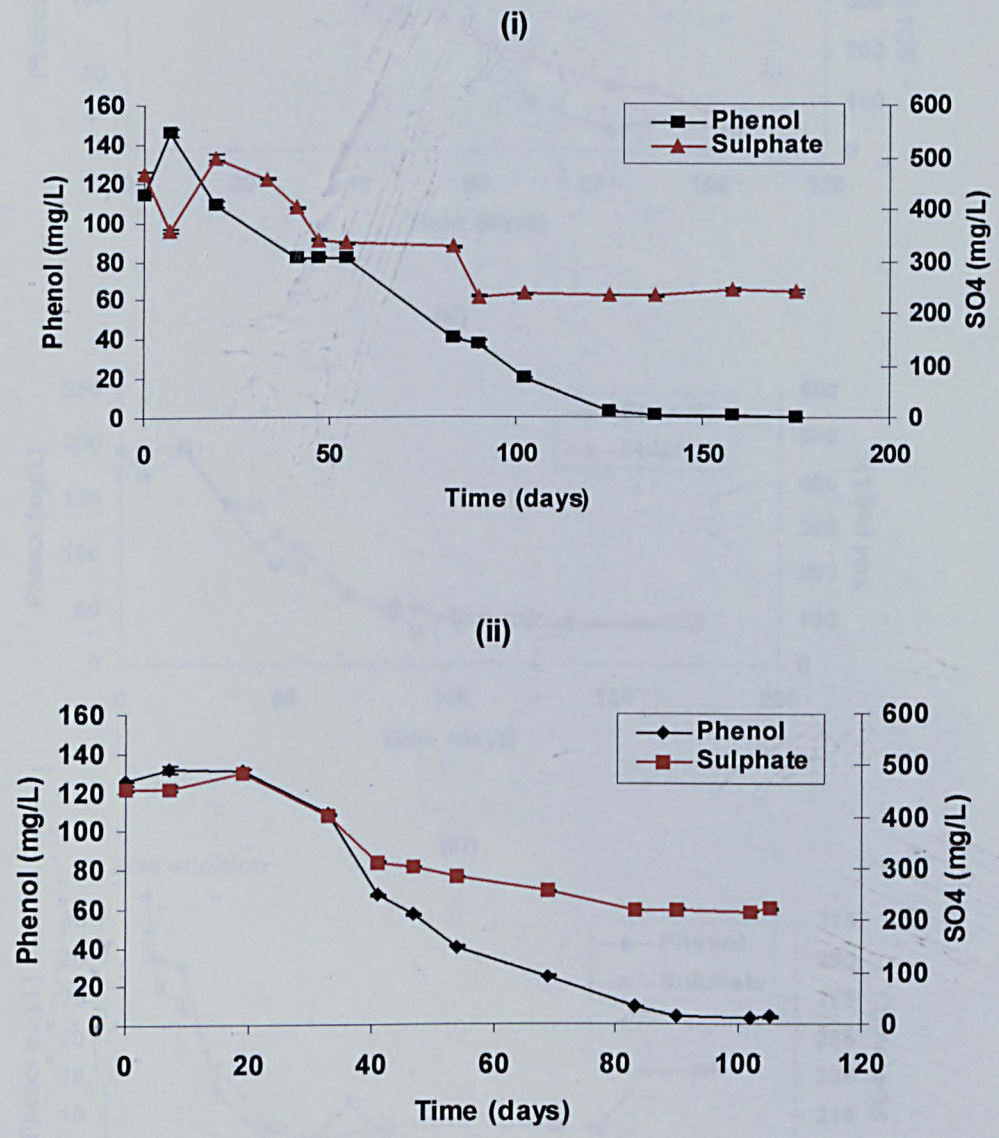

Figure 3.2 Phenol degradation and sulphate concentrations in microcosms 2A (i) and 2B (ii), following initial phenol addition. Error bars represent the % relative standard deviation of the mean of at least triplicate analytical quality controls.

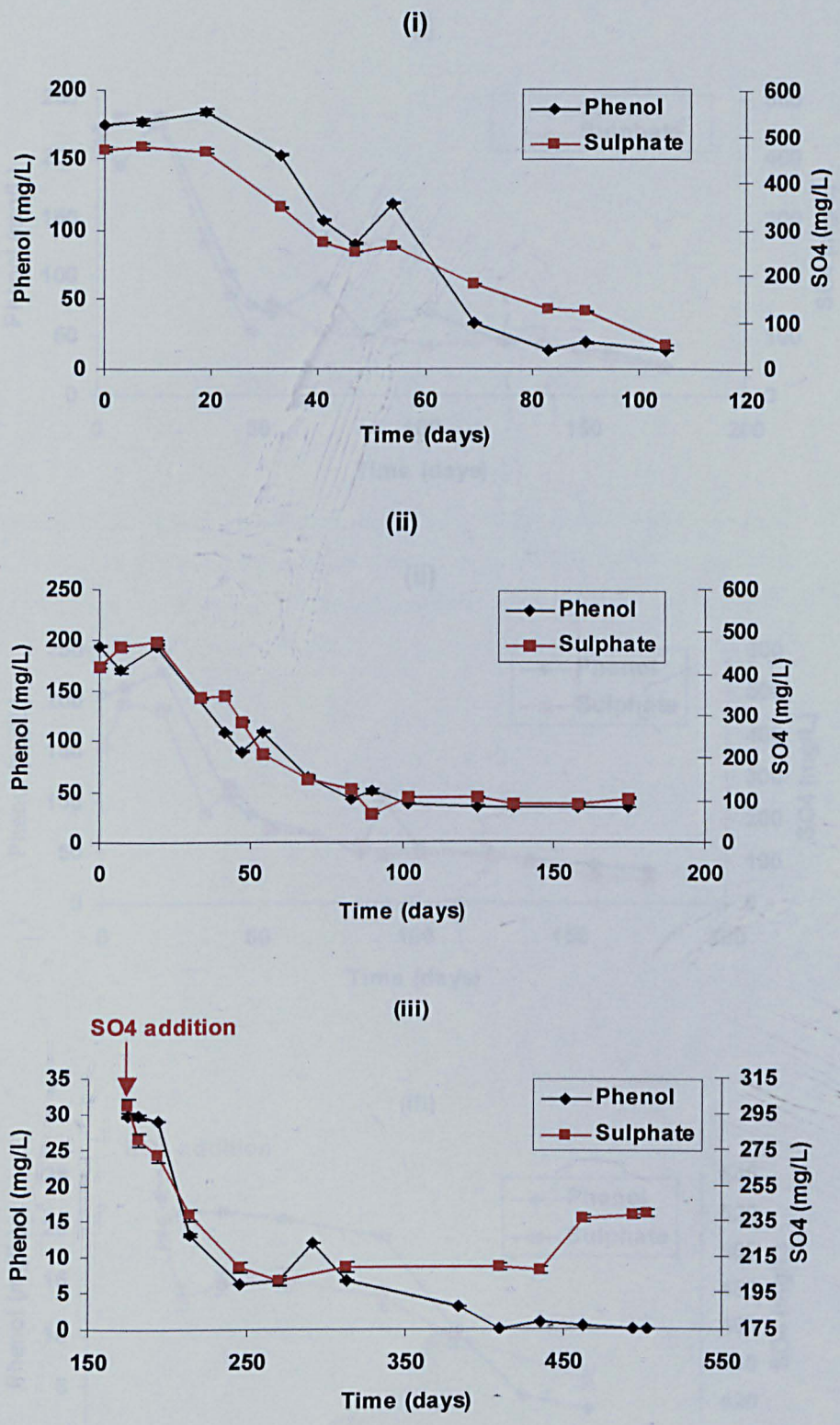

Figure 3.3 Phenol degradation and sulphate concentrations in microcosms 3A (i) and 3B (ii), following initial phenol addition. Degradation recommences in 3B following the second SO_4^{2-} addition as shown in (iii). Error bars represent the % relative standard deviation of the mean of at least triplicate analytical quality controls.

(i)

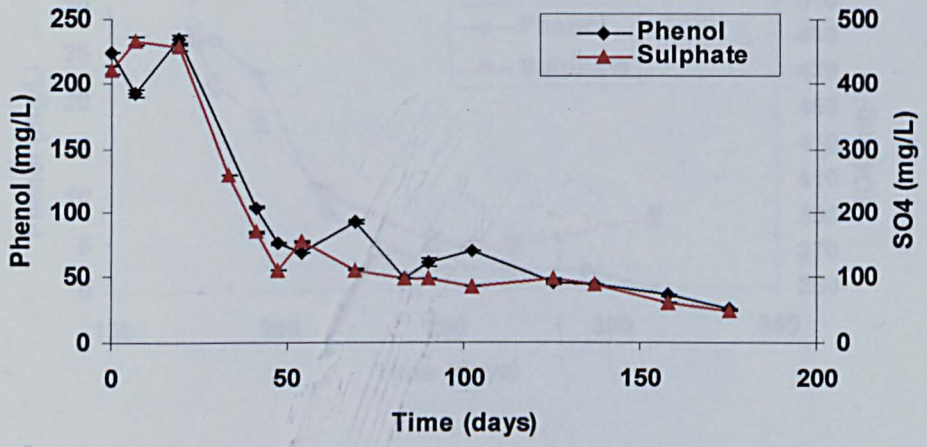
Phenol
Sulphate
Phenol (mg/L)
SO4 (mg/L)
Time (days)
0
50
100
150
200
250
300
400
500

(ii)

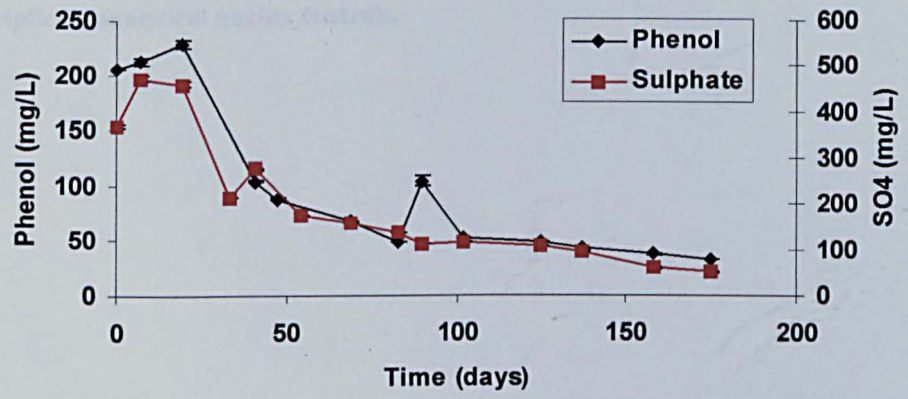
Phenol
Sulphate
Phenol (mg/L)
SO4 (mg/L)
Time (days)
0
50
100
150
200
250
300
400
500
600

(iii)

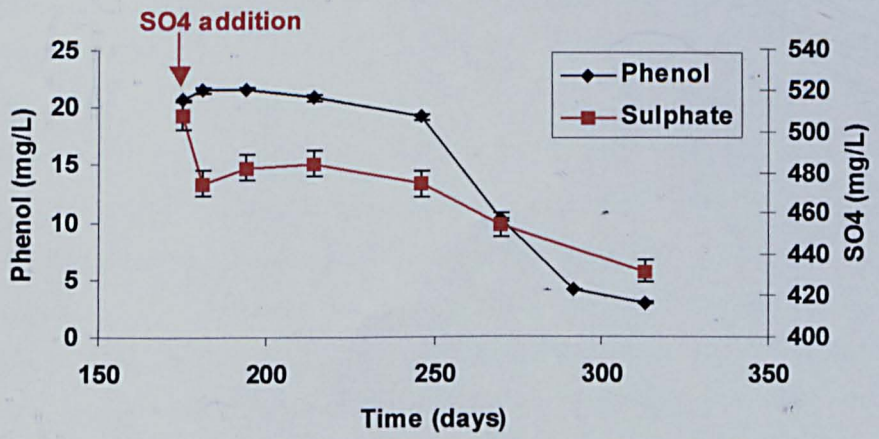
SO4 addition
Phenol
Sulphate
Phenol (mg/L)
SO4 (mg/L)
Time (days)
0
5
10
15
20
25
150
200
250
300
350
400
420
440
460
480
500
520
540

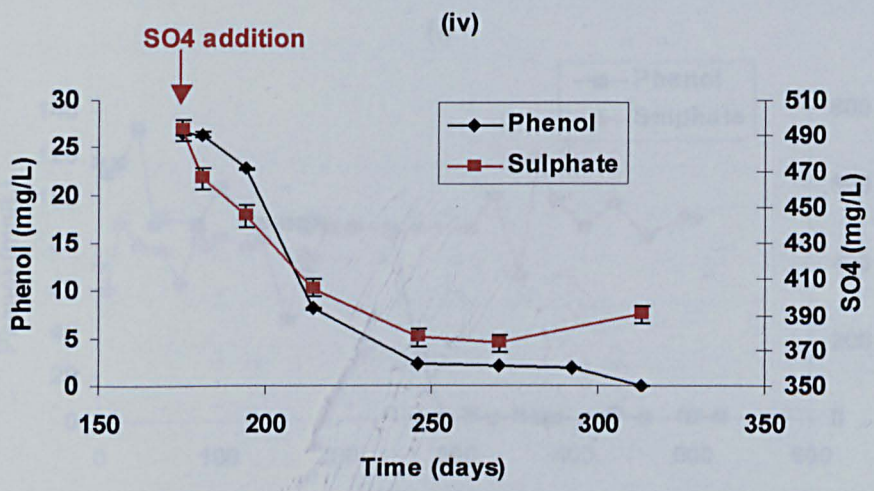

Figure 3.4 Phenol degradation and sulphate-reduction in microcosms 4A (i) and 4B (ii), following initial phenol addition and subsequent to 2nd SO_4^{2-} addition (at day 175) to 4A (iii) and 4B (iv). Error bars represent the % relative standard deviation of the mean of at least triplicate analytical quality controls.

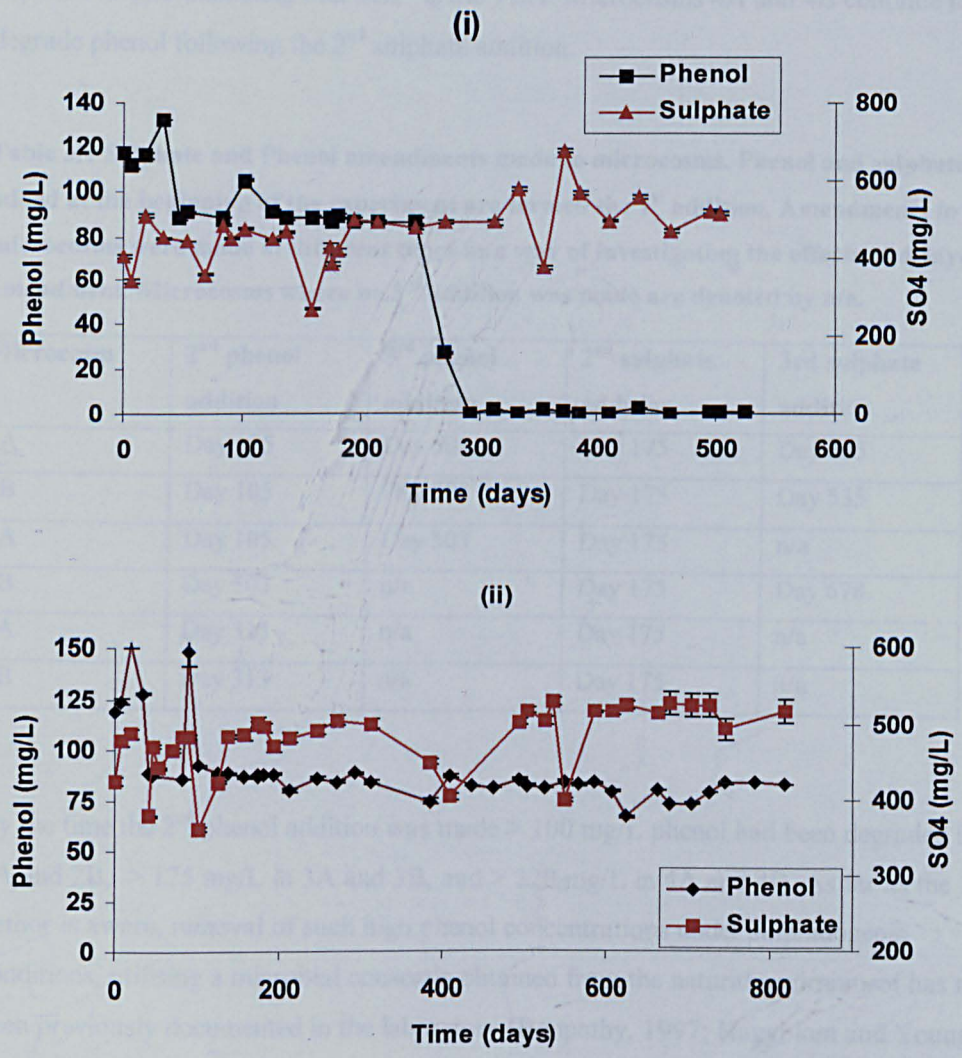

Figure 3.5 Phenol and sulphate concentrations in killed controls 1A (i) and 1B (ii). Contamination of 1A, and subsequent phenol degradation, occurred at day 246. Error bars represent the % relative standard deviation of the mean of at least triplicate analytical quality controls.

Table 3.1 shows the phenol and sulphate amendments made to the microcosms. The 2nd sulphate addition was made to all microcosms at day 175 as sulphate concentrations had fallen to below 100 mg/L in all microcosms except 2A. This happened to be before the 2nd phenol addition to microcosms 3B, 4A and 4B and their phenol degradation curves subsequent to SO_4^{2-} enrichment are shown in Figures 3.3 (iii), 3.4 (iii) and 3.4 (iv), respectively. Degradation stops in microcosm 3B but recommences following addition of excess SO_4^{2-} at day 175 and SO_4^{2-}-reduction ceases once phenol is

depleted further indicating that SO_4^{2-} is the TEA. Microcosms 4A and 4B continue to degrade phenol following the 2nd sulphate addition.

Table 3.1 Sulphate and Phenol amendments made to microcosms. Phenol and sulphate added at the beginning of the experiment are termed the 1st addition. Amendments to some microcosms were made at different times as a way of investigating the effects of delayed amendment. Microcosms where no 3rd addition was made are denoted by n/a.

Microcosm	2nd phenol addition	3rd phenol addition	2nd sulphate addition	3rd sulphate addition
2A	Day 175	Day 503	Day 175	Day 535
2B	Day 105	Day 503	Day 175	Day 535
3A	Day 105	Day 503	Day 175	n/a
3B	Day 503	n/a	Day 175	Day 678
4A	Day 313	n/a	Day 175	n/a
4B	Day 313	n/a	Day 175	n/a

By the time the 2nd phenol addition was made > 100 mg/L phenol had been degraded in 2A and 2B, > 175 mg/L in 3A and 3B, and > 220 mg/L in 4A and 4B. As far as the author is aware, removal of such high phenol concentrations under sulphidogenic conditions, utilising a microbial consortia obtained from the natural environment has not been previously documented in the laboratory (Boopathy, 1997; Haggblom and Young, 1995; Londry et al., 1997; Monserrate and Haggblom, 1997; Mort and Deanross, 1994; Suflita et al., 1989). Haggblom and Young (1995) report 120μM (11.3 mg/L) of phenol degradation by a SO_4^{2-}-reducing consortia enriched from an estuarine sediment, Mort and Dean-Ross (1994) document degradation of up to 10 mg/L, Monserrate and Haggblom (1997) have shown removal of 1mM (94 mg/L) phenol, coupled to SO_4^{2-}-reduction, Suflita *et al.* (1989) demonstrate degradation of 82μM (7.7 mg/L) of phenol and Londry *et al.* (1997) have shown degradation of 500μM (47 mg/L) by a pure sulphate-reducing bacterium culture known to grow in both freshwater and saltwater conditions. These literature values are summarised in Table 3.2.

Table 3.2 Literature values of phenol biodegradation by sulphate-reducing bacteria from natural environments. In some cases molar concentrations have been converted to mg/L.

Phenol degraded (mg/L)	Degradation rate (mg/L/day)	Source of inoculum	Reference
11.3	~ 1.6	Estuarine sediment	Haggblom and Young, 1995
47	~ 3.0	Pure culture	Londry et al., 1997
94	~ 0.5	Marine sediment	Monserrate and Haggblom, 1997
10	~ 0.3	River sediment	Mort and Deanross, 1994
7.7	~ 0.17	Shallow aquifer	Suflita et al., 1989
	~ 0.58	Sandstone aquifer	Wu, 2002

The degradation rates for the microcosms are presented in Tables 3.3 and 3.4. The average degradation rates were calculated between the commencement of biodegradation at the end of the lag phase until the point where biodegradation ceased or all of the phenol was oxidised. The maximum degradation rate occurred within 25 days of the end of the lag phase in all microcosms save 2A, where the maximum rate was recorded soon after the pause in degradation between days 41 and 54.

Table 3.3 Maximum and average phenol degradation rates in microcosms following the initial phenol and SO_4^{2-} additions and the onset of biodegradation under sulphate-reducing conditions. Rates are calculated during periods of biodegradation activity and do not include intervals where biodegradation had ceased.

Microcosm	Phenol degraded[α] (mg/L)	No of days[α]	Maximum degradation rate[α] (mg/L/day)	Average degradation rate[α] (mg/L/day)
2A	105.80	106	1.41	0.77
2B	127.54	83	5.20	1.72
3A	170.81	64	5.77	2.96
3B	156.93	83	3.94	2.00
4A	208.46	156	5.89	1.69
4B	197.22	156	5.65	1.33

[α] not including lag phase

Table 3.4 Maximum and average phenol degradation rates in microcosms following a Na_2SO_4 supplement to those microcosms depleted in SO_4^{2-}. Rates are calculated during periods of biodegradation activity and do not include intervals where biodegradation had ceased.

	Phenol degraded[α] (mg/L)	No of days[α]	Maximum degradation rate[α] (mg/L/day)	Average degradation rate[α] (mg/L/day)
3B	22.85	52	0.79	0.51
4A	16.12	46	0.37	0.23
4B	24.5	111	0.73	0.24

[α] not including lag phase

The high degradation rates following the onset of biodegradation are probably due to rapid growth of the microbial consortia subsequent to the acclimation phase. Average degradation rates from previous phenol degradation studies with SRB (Table 3.1) range from 0.17 mg/L/day to 3.0 mg/L/day (Boopathy, 1997; Haggblom and Young, 1995; Londry et al., 1997; Monserrate and Haggblom, 1997; Mort and Deanross, 1994; Suflita et al., 1989; Wu, 2002). The average degradation rate in each microcosm is within this range but generally the rates are higher than seen in previous publications. For example, Wu reports an average phenol degradation rate, under SO_4^{2-}-reducing conditions, of 6.2 μM/day (0.58 mg/L/day) in anaerobic microcosms. The fast average degradation rates, relative to previous studies, are probably due to the microbial consortia's history of exposure to phenolic compounds. They had already encountered phenolic compounds in the field and had been efficiently degrading phenol, albeit at a lower concentration, whilst in the batch reactor during preparation (Section 2.2.2). In all live microcosms, the rate is high to begin (fast biomass growth) and then falls as the phenol concentration decreases (Figure 3.6). This behaviour is consistent with a monod kinetic model for biodegradation (Broholm and Arvin, 2001; Broholm and Arvin, 2000; Broholm et al.,

2000)

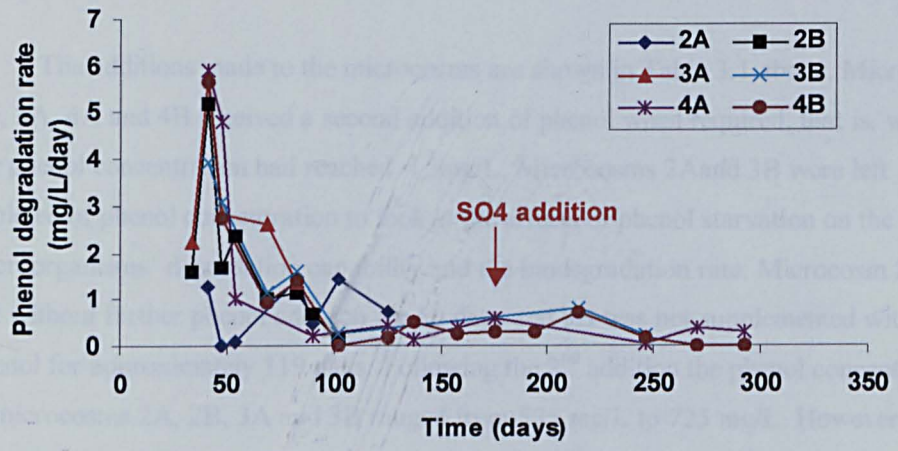

Figure 3.6 Phenol degradation rate in live microcosms following initial phenol addition, subsequent to the lag-phase. Arrow signifies sulphate addition made to microcosms 3B, 4A and 4B.

3.2 Biodegradation of Phenol under Sulphate-reducing Conditions following the 2nd Phenol Addition.

The additions made to the microcosms are shown in Table 3.1 above. Microcosms 2B, 3A, 4A and 4B received a second addition of phenol when required, that is, when the phenol concentration had reached < 5mg/L. Microcosms 2Aand 3B were left depleted of phenol concentration to look at the effects of phenol starvation on the microorganisms' degradation capability and the biodegradation rate. Microcosm 2A was left without further phenol addition for 50 days and 3B was not supplemented with phenol for approximately 119 days. Following the 2nd addition the phenol concentration in microcosms 2A, 2B, 3A and 3B ranged from 575 mg/L to 725 mg/L. However, 4A and 4B received almost double the phenol dose (~ 1330 mg/L) to test the ability of the microbial consortia to cope with this higher concentration and to help with identification of a phenol toxicity threshold. Phenol and sulphate concentrations following the 2nd phenol addition are shown in Figures 3.7 to 3.9.

Microcosms 2A [Figure 3.7 (i)] and 2B [Figure 3.7 (ii)] continued to degrade phenol with simultaneous sulphate loss at phenol concentrations of 624 mg/L and 574 mg/L, respectively. Microcosms 3A [Figure 3.8 (i)] and 3B [Figure 3.8 (ii)] also continued degrade phenol, with simultaneous SO_4^{2-}-reduction, at concentrations of 575 mg/L and 725 mg/L, respectively. There was no lag phase in microcosms 2A, 2B, 3A or 3B indicating that no adaptation was required to cope with the higher phenol. This is expected as, apart from the phenol/SO_4^{2-} additions, no changes were made to the microcosm conditions. At the 1st addition the SG composition was altered slightly from that in the batch reactor used to grow the microorganisms (Section 2.2.2), hence the lag phase.

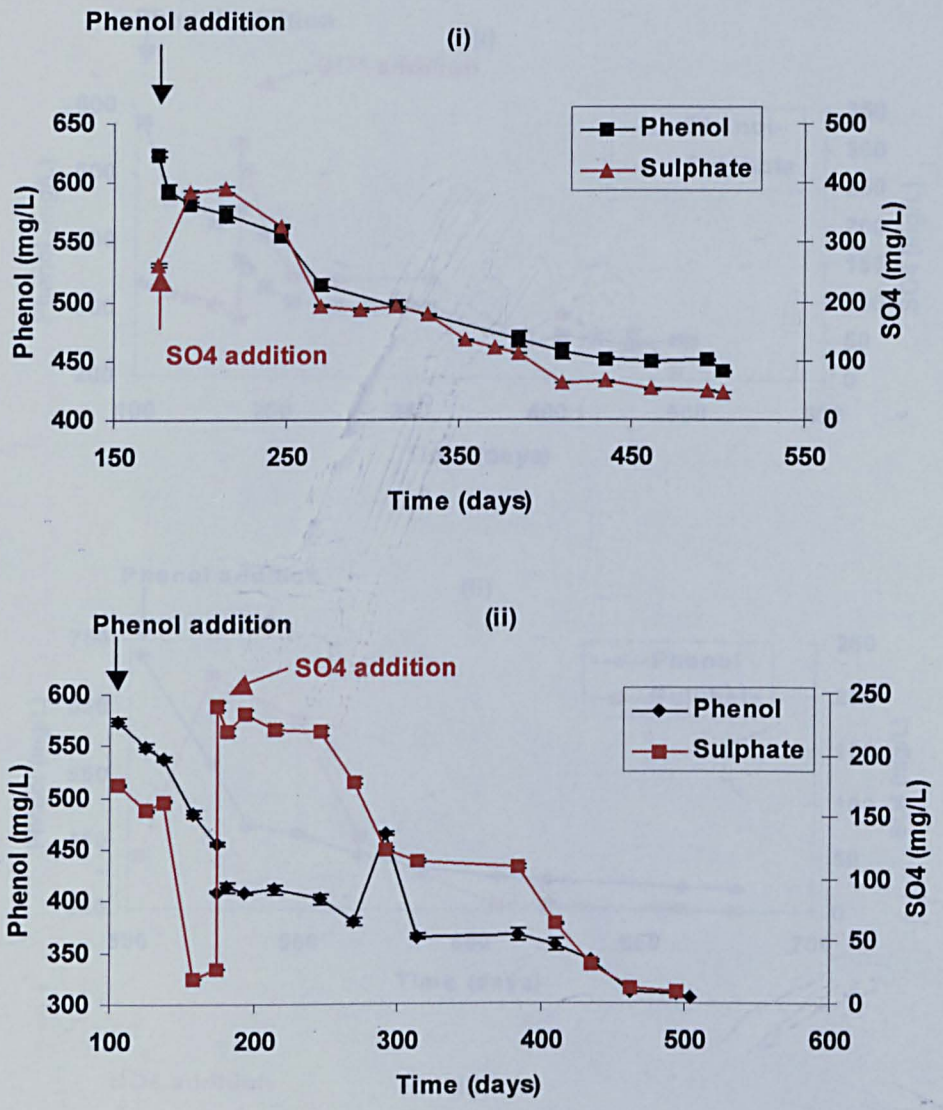

Figure 3.7 Phenol and sulphate concentrations in microcosms 2A (i) and 2B (ii) following the 2nd phenol addition at day 175 and 105, respectively. The 2nd addition of SO_4^{2-} was made to both microcosms at day 175. Error bars represent the % relative standard deviation of the mean of at least triplicate analytical quality controls.

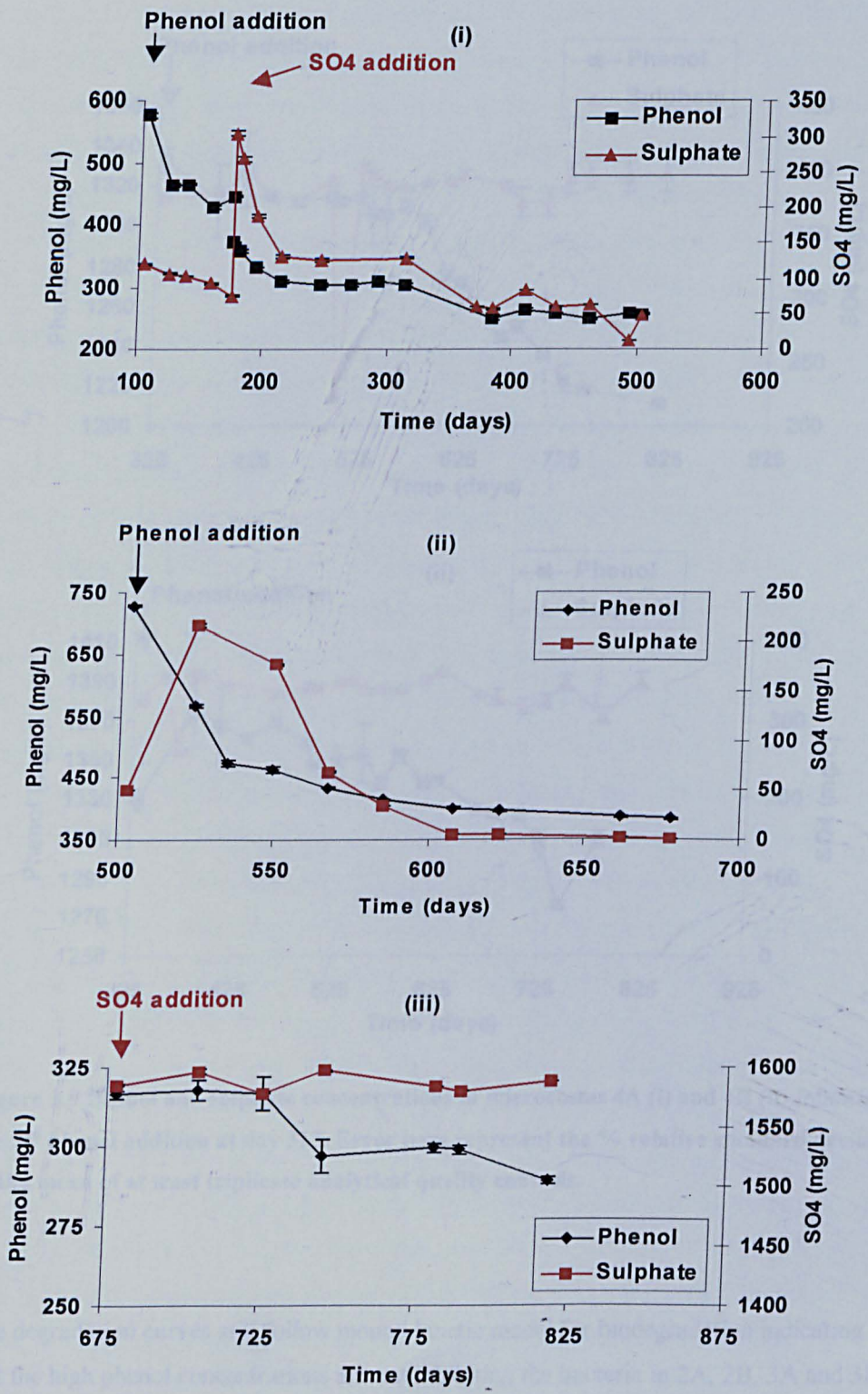

Figure 3.8 Phenol and sulphate concentrations in microcosms 3A (i) and 3B (ii) following the 2nd phenol addition at day 105 and 503, respectively. SO_4^{2-} was added to 3A at day 175 (2nd addition) and to 3B at day 678 (3rd addition). The effects of introducing extremely high SO_4^{2-} concentrations to 3B are shown in (iii). Error bars represent the % relative standard deviation of the mean of at least triplicate analytical quality controls.

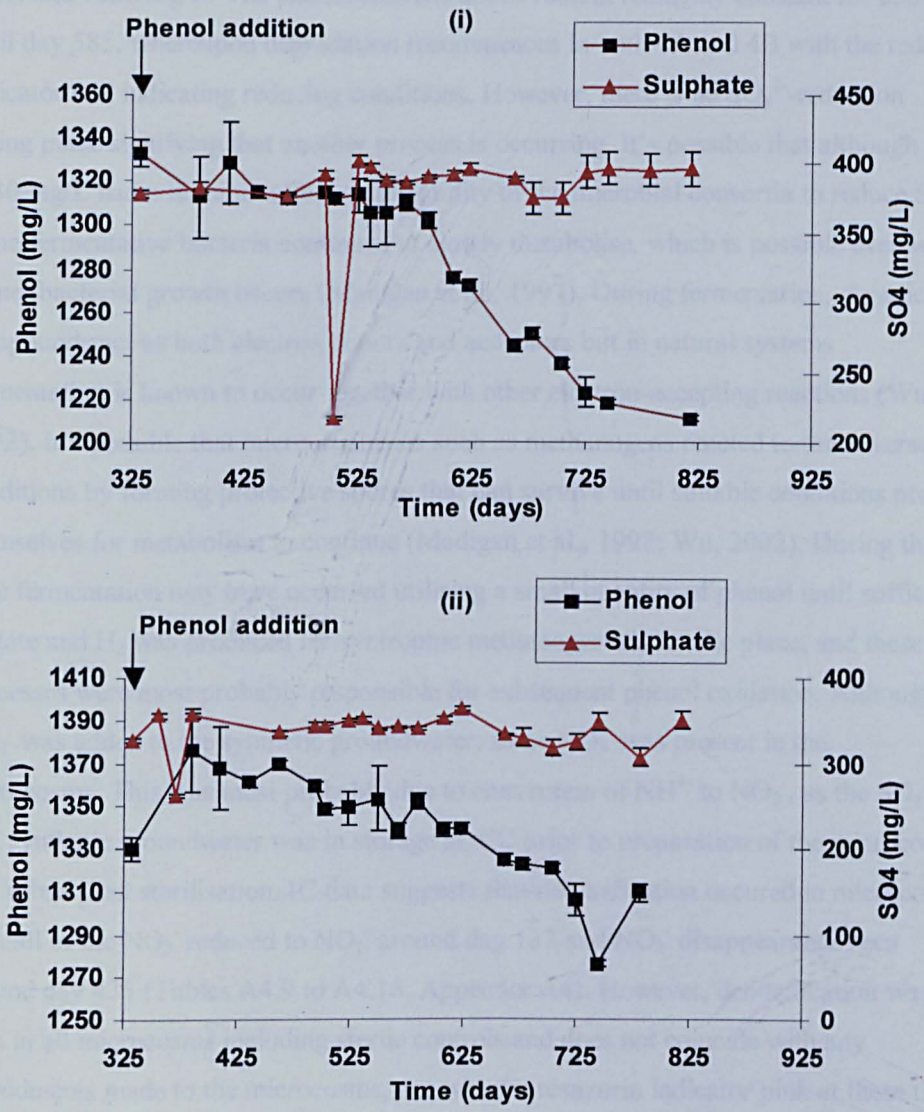

Figure 3.9 Phenol and sulphate concentrations in microcosms 4A (i) and 4B (ii) following the 2nd phenol addition at day 313. Error bars represent the % relative standard deviation of the mean of at least triplicate analytical quality controls.

The degradation curves still follow monod kinetic model for biodegradation indicating that the high phenol concentrations are not inhibiting the bacteria in 2A, 2B, 3A and 3B. However, a different trend was seen in 4A [Figure 3.9 (i)] and 4B [(Figure 3.9 (ii)]. In both 4A and 4B phenol biodegradation virtually stops following the 2nd addition of phenol at ~ 1330 mg/L. The sulphate concentration also becomes constant signifying that sulphate-reduction is no longer suggests inhibitory effects due to phenol toxicity. As phenol biodegradation still occurs in all other live microcosms, it can be assumed that the threshold at which phenol has a toxic effect on the SRB is somewhere between 725

mg/L and 1330 mg/L. The phenol concentrations remain relatively constant for 253 days until day 585, whereupon degradation recommences in both 4A and 4B with the redox indicator still indicating reducing conditions. However, there is no SO_4^{2-}-reduction taking place signifying that another process is occurring. It's possible that although ~ 1330 mg/L had a terminal effect on the ability of the microbial consortia to reduce SO_4^{2-}, some fermentative bacteria continued to slowly metabolise, which is possible even when no net bacterial growth occurs (Madigan et al., 1997). During fermentation, organic compounds act as both electron donors and acceptors but in natural systems fermentation is known to occur together with other electron-accepting reactions (Wu, 2002). It's possible that microorganisms such as methanogens reacted to the adverse conditions by forming protective spores that can survive until suitable conditions present themselves for metabolism to continue (Madigan et al., 1997; Wu, 2002). During this time fermentation may have occurred utilising a small quantity of phenol until sufficient acetate and H_2 was produced for syntrophic methanogenesis to take place, and these processes were most probably responsible for subsequent phenol oxidation. Although no NO_3^- was added to the synthetic groundwater, some NO_3^- was present in the microcosms. This was most probably due to conversion of NH^{4+} to NO_3^-, as the SO_4^{2-}-rich synthetic groundwater was in storage at 4°C prior to preparation of the microcosms, and subsequent sterilisation. IC data suggests that denitrification occured in microcosms with all of the NO_3^- reduced to NO_2^- around day 137 and NO_2^- disappearance seen around day 435 (Tables A4.9 to A4.16, Appendix A4). However, denitrification was seen in all microcosms including sterile controls and does not coincide with any amendments made to the microcosms, nor was the resazurin indicator pink at these times which would indicate less-reducing conditions. Moreover, no degradation of phenol was seen at day 137 in controls 1A and 1B or live microcosms 2A and 3B. Degradation did occur in 2B, 4A and 4B, at day 137 but the amount of SO_4^{2-} loss in these microcosms represented 75%, 95% and 100% of the theoretical stoichiometric values expected from phenol oxidation under SO_4^{2-}-reducing conditions (Table 1.2, Section 1). Therefore, it is more likely that there was a problem with the analytical procedure as NO_3^--reduction and NO_2^- loss had occurred in calibrations standards on more than one occasion. However, if it is assumed that some denitrification did occur, the maximum concentration of NO_3^- was 51 mg/L and if all of this had been converted to N_2, calculation of the stoichiometry of phenol oxidation (Section 3.6) under denitrifying conditions (Table 1.2, Section 1) shows that 51 mg/L NO_3^- could only account for removal of a maximum of 13.8 mg/L phenol. Moreover, the redox indicator remained clear indicating anaerobiosis, further suggesting that fermentation and/or

methanogenesis were the processes responsible for degradation of phenol in the absence of SO_4^{2-}-reduction in microcosms 4A and 4B.

Biodegradation stops in microcosm 3B when SO_4^{2-} is depleted, again indicating that SO_4^{2-}-reduction is the TEAP. Thus far, the SO_4^{2-} concentration in the microcosms had not exceeded 650 mg/L so an addition of ~ 1600 mg/L SO_4^{2-} was made to microcosm 3B, upon SO_4^{2-} depletion, to test what effect elevated SO_4^{2-} concentrations had on phenol degradation. As Figure 3.9 (iii) shows it seems that an almost 3-fold increase in SO_4^{2-} arrested phenol degradation and when degradation recommences after 47 days, there is no simultaneous SO_4^{2-}-reduction indicating that another process was occurring. As the conditions were still reducing, as shown by the redox indicator, again it is likely that methanogenesis and/or fermentation took place. Although only tested in one microcosm, indications are that a sudden increase in SO_4^{2-} was detrimental to the functionality of the microbial consortia suggesting that a steady increase would be more conducive to maintaining SO_4^{2-}-reducing activity. However, it is also possible that there is an optimum concentration range of SO_4^{2-} that the microbial consortia can utilise and going beyond the upper limit of this optimum inhibits the SRB. Concentrations of 1200 mg/L SO_4^{2-} have been shown to inhibit SRB (Hao et al., 1996). It is also worth considering that since the headspaces were only flushed when additions were made to the microcosms, there is a possibility that H_2S concentrations had accumulated to inhibitory levels prior to flushes. Inhibitory effects of sulphide on SRB's anaerobic biodegradative capability have been shown to occur at ~ 3.4 to 5.4 mM (Hao et al., 1996) and has also been documented at 1-3 mM for toluene degradation (Cunningham et al., 2001), although toluene degradation by *D. Toluolica* was only impeded at concentration of > 12 mM (Bolliger et al., 2001). Inhibition has also been shown to occur at 250 mg/L S^{2-} in batch cultures although the SO_4^{2-}-reducers recovered from the high sulphide concentrations (Okabe et al., 1995). Complete inhibition on SRB growing on lactate has been reported at ~ 515 mg/L S^{2-} (Reis et al., 1992). Due to purging of the headspace prior to additions, it's unlikely that S^{2-} concentrations reached completely inhibitory levels. Maximum possible concentrations of S^{2-} for the amount of SO_4^{2-}-reduced, based on the stoichiometric equation (Table 1.2, Section 1), would have been < 150 mg/L S^{2-} in all microcosms. Therefore, it's possible that sulphide may have suppressed the SRB but it is clear from the recommencement of degradation following phenol/SO_4^{2-} addition and headspace purge that the SRB were not irreversibly damaged.

The maximum degradation rate is seen immediately after the 2nd phenol addition in microcosms 2A, 3A and 3B and within 55 days in 2B (Table3.5, Table 3.6 shows

degradation rates in microcosms amended with SO_4^{2-}) indicating that the microbial consortia commences degradation immediately and there is increased activity to cope with the shock increased loading in phenol. It is possible that trace levels of O_2, present in the aqueous sampling tubes, were transferred during the phenol addition to microcosm 3B and this may have contributed to a little phenol degradation immediately after the addition. However, the redox indicator changed from pink to clear within hours of the addition and, due to the presence of sulphide in the microcosms, any trace concentrations of O_2 would have been rapidly consumed (Coates et al., 1996a; Lovley et al., 1995). Therefore, the contribution of O_2 to degradation was probably minimal and insignificant subsequent to the initial measurement. Moreover, assuming that O_2 contamination did occur, addition of 2 ml of air (which is greater than the aqueous sample tube volume), would only have contributed 0.6 mg of O_2 to the microcosm (taking air to contain 21 % O_2 and taking into consideration the molar volume of a gas, 22.4 L). Using the stoichiometric equation for aerobic oxidation of phenol (Table 1.2, Section 1), it can be shown that this would only account for a total of 0.5 mg of phenol loss, which is negligible. The maximum rate is not seen in 4A and 4B until after the onset of biodegradation at day 585. When the maximum rate of degradation following the initial phenol addition (Table 3.2) is compared with that following the 2nd phenol addition (Table 3.5) we can see that it falls in microcosms 2B, 3A, 4A and 4B, but increases in 2A and 3B

Table 3.5 Maximum and average phenol degradation rates in microcosms following the 2nd phenol addition and the onset of biodegradation. Rates are calculated during periods of biodegradation activity and do not include intervals where biodegradation had ceased.

Microcosm	Phenol degraded[α] (mg/L)	No of days[α]	Maximum degradation rate[α] (mg/L/day)	Average degradation rate[α] (mg/L/day)
2A	183.51	328	5.20	0.95
2B	117.49	70	2.56	1.59
3A	131.5	70	5.68	2.06
3B	345.29	175	8.44	2.33
4A	121.8	486	1.14	0.32
4B	66.31	397	1.51	0.37

[α] Prior to addition of SO_4^{2-}

Table 3.6 Maximum and average phenol degradation rates in microcosms following a Na_2SO_4 supplement to those microcosms depleted in SO_4^{2-}. Rates are calculated during periods of biodegradation activity and do not include intervals where biodegradation had ceased.

Microcosm	Phenol degraded (mg/L)	No of days	Maximum degradation rate (mg/L/day)	Average degradation rate (mg/L/day)
2B	107.18	322	1.08	0.41
3A	114.0	328	2.05	0.61
3B	28.5	114	0.97	0.29

Only microcosms 2A and 3B were starved of phenol but rather than losing phenol biodegradation capability, the microorganisms degraded phenol more readily. This could be due to the depletion of degradation intermediates during phenol starvation, which were probably still available to 2B and 3A. Thus, the microbial consortia (or a larger percentage of the microbial population) in 2A and 3B may have proceeded to immediately utilise phenol as the electron donor, in the absence of the simpler organic compounds. It is possible that due to the low level or absence of a suitable carbon source, the consortia had reached a stationary phase where they either lay dormant or underwent cryptic growth that is no net increase or decrease in cell numbers or perhaps spore formation occurred so that, cell functions, including energy metabolism still occurred (Madigan et al., 1997) until the 2nd addition of phenol was made. The average rate of degradation also falls following the 2nd phenol addition in all microcosms save 2A and 3B. Upon addition of phenol, the microorganisms immediately began to degrade phenol faster than previously seen in 2A and 3B or microcosms that had been immediately fed with phenol. Although the average rate falls in all but 2A and 3B, the rate is still relatively high in both 2B and 3A at 1.59 mg/L/day and 2.06 mg/L/day, respectively. Moreover, as with the initial phenol addition, the degradation rates are high in comparison to previous publications (Table 3.1) indicating that the increase in phenol concentration has not inhibited phenol degradation coupled to SO_4^{2-}-reduction. Degradation following the initial addition of phenol was already higher than previously published values for phenol degradation under SO_4^{2-}-reducing conditions. However, the 2nd addition of phenol is at concentrations which previous microcosm studies have shown to be inhibitory and toxic not only to SRB, but also to bacteria which utilise other electron acceptors under anaerobic conditions (Bandyopadhyay et al., 1998; Broholm

and Arvin, 2001; Broholm and Arvin, 2000; Broholm et al., 2000; Genthner et al., 1991; Harrison et al., 2001; Tschech and Fuchs, 1987). Tschech and Fuchs report complete cessation of degradation by denitrifiers at 470 mg/L, Broholm and Arvin show that no phenol degradation occurs under NO_3^--reducing conditions at ~ 600 mg/L phenol and Harrison *et al.* report inhibition of the anaerobic consortia between 200 and 250 mg/L total phenols. The observation of phenol degradation with simultaneous SO_4^{2-}-reduction with similar or, in the case of 2A and 3B, higher degradation rates following the 2nd phenol addition between 575 mg/L and 725 mg/L is, as far as the author is aware, unique to this study. Degradation at these concentrations by SRB have only been documented at waste-processing plants or in bioreactors (Lin and Lee, 2001; Thomas et al., 2002). Relatively fast degradation at these concentrations is most likely down to the microbial consortia's previous history of exposure to phenolics. It would seem that the microorganisms have adapted to cope and utilise concentrations of phenol previously considered toxic to SRB. Stoichiometric calculations (Section 3.6) of phenol degradation coupled to SO_4^{2-}-reduction support the phenol and SO_4^{2-} data confirming that degradation following both the initial and 2nd addition of phenol was carried out by SRB. Degradation of up to 725 mg/L phenol by SRB provides an interesting insight, under optimal conditions, into the potential of SRB to successfully contribute to bioremediation of contaminated groundwater and soil. Half-lives were calculated based on initial phenol concentrations and the average degradation rate as these can give indications of the timescales involved in plume remediation. Half-lives at initial phenol concentrations of 110 mg/L to 235 mg/L, were calculated to be between 43 and 120 days. At initial concentrations of 575 mg/L to 775 mg/L the half-life increased to between 455 days and 990 days, respectively, and at concentrations of 1000 mg/L and 1375 mg/L the half-life was between 1917 days and 2887 days, respectively. These results suggest that concentrations of up to 575 mg/L may be remediated within 3 years, if environmental conditions were suitable. However, laboratory degradation rates are often higher than those seen in the field, as is probably the case with these microcosms as they were run at 20°C. The groundwater temperature at the four-ashes site was recorded at between 7°C and 10°C (Thornton et al., 2001a) and since, in general, the rate of reaction doubles for each 10°C rise in temperature (Sawyer et al., 1994) it is probably more likely that remediation would take twice as long as the results suggest. Therefore 6 years is a better estimate of the timescale to bioremediate 575 mg/L phenol.

The results from these microcosms could have implications for enhanced in-situ bioremediation at contaminated sites where the electron acceptor supply is low. The

introduction of additional electron acceptors such a SO_4^{2-} and NO_3^- has already been demonstrated to successfully enhance bioremediation of BTEX contaminated groundwater (Cunningham et al., 2001).

3.3 Biodegradation of Phenol under Sulphate-reducing Conditions Following the 3rd Phenol Addition.

The phenol and SO_4^{2-} additions are summarised in Table 3.1 above. The 3rd phenol addition was only made to microcosms 2A, 2B and 3A. Phenol degradation and SO_4^{2-}-reduction continues in 2A [Figure 3.10 (i)] and 3A [Figure 3.10 (iii)] which is at 916 mg/L phenol, but the rate of SO_4^{2-} loss is not as high as it was prior to the phenol addition. Very little phenol degradation and SO_4^{2-}-reduction takes place in 2B indicating that ~ 1000mg/L phenol has had an inhibitory effect on the SRB whereas degradation and SO_4^{2-}-reduction continues in 3A until the SO_4^{2-} is depleted, demonstrating that 770 mg/L phenol does not inhibit reduction of SO_4^{2-} by the microbial consortia. Although SO_4^{2-}-reduction still occurs, values for SO_4^{2-} reduced, as a percentage of the expected stoichiometric theoretical requirement (Section 3.6), fall following the 3rd phenol addition. Although degradation of phenol and SO_4^{2-}-reduction still occurs in microcosm 2A, the fall in SO_4^{2-} loss and the straight degradation curve suggest that, although concentrations are not toxic, there may be some inhibitory effects on the SRB. However, in microcosm 3A the fall in SO_4^{2-} and phenol degradation rates are probably due to the low concentration of SO_4^{2-} rather than any inhibition. It can be concluded following the 3rd addition that the toxicity threshold for these groundwater-based SO_4^{2-}-reducers is somewhere between 996 mg/L (microcosm 2B) and ~ 1330 mg/L phenol (microcosms 4A and 4B following 2nd addition) which is much higher (Section 3.2) than previously documented.

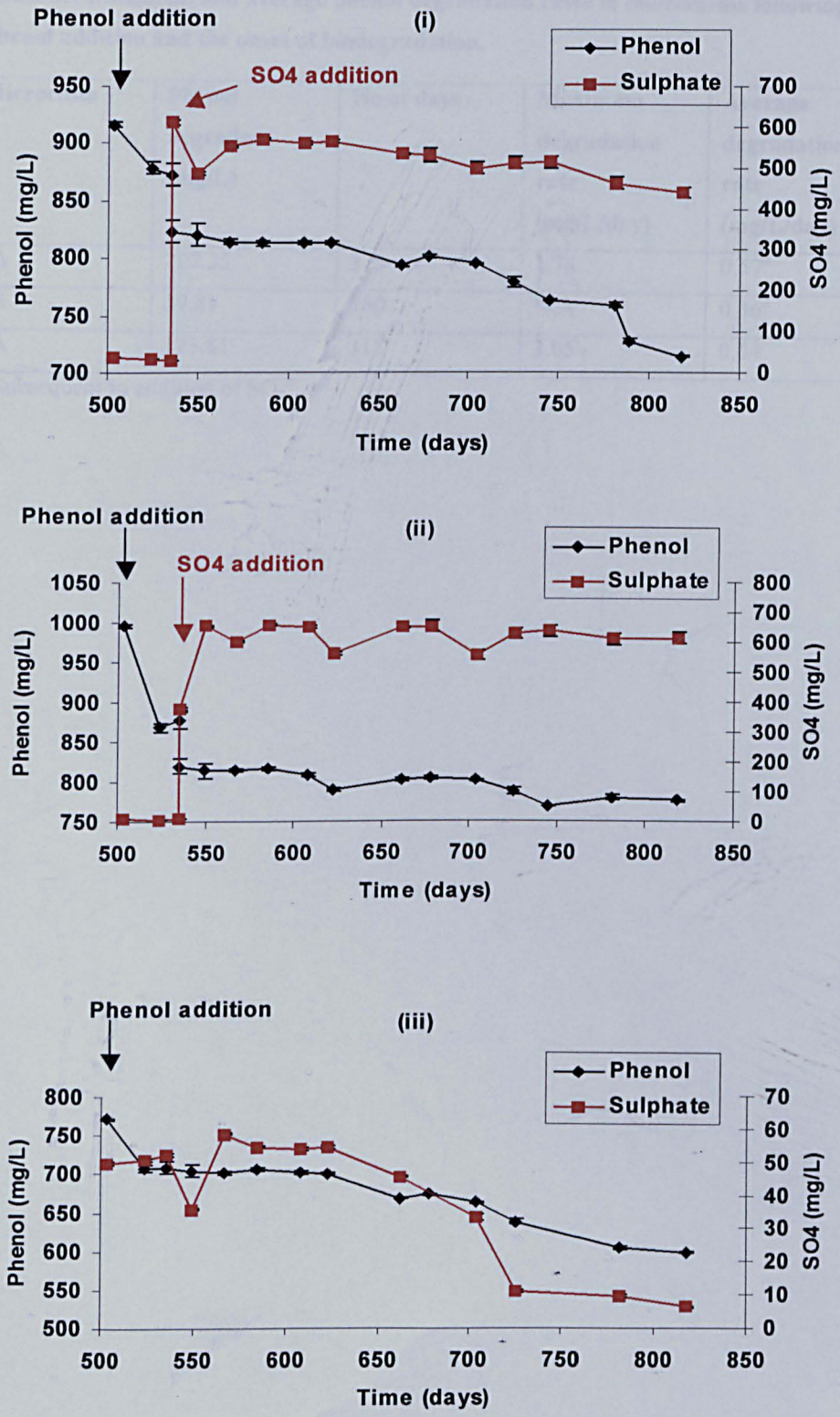

Figure 3.10 Phenol and SO_4^{2-} concentration in microcosms 2A (i), 2B (ii) and 3A (iii) following the 3rd addition of phenol at day 503. SO_4^{2-} was added to both 2A and 2B at day 535 (3rd addition). Error bars represent the % relative standard deviation of the mean of at least triplicate analytical quality controls.

Table 3.7 Maximum and average phenol degradation rates in microcosms following the 3rd phenol addition and the onset of biodegradation.

Microcosm	Phenol degraded (mg/L)	No of days	Maximum degradation rate (mg/L/day)	Average degradation rate (mg/L/day)
2A	202.35	315	1.78	0.57[α]
2B	39.81	160	N/A	0.36[α]
3A	173.81	315	3.05	0.54

[α] Subsequent to addition of SO_4^{2-}

3.4 Biogenic Gases and pH

Headspace analysis for CO_2 substantiates the phenol and SO_4^{2-} data (Figure 3.6) confirming that phenol degradation to CO_2 is occurring. The microcosm headspace was purged regularly, generally coinciding with a phenol or SO_4^{2-} addition. This was done to try and prevent H_2S concentrations reaching toxic or inhibitory levels (Bolliger et al., 2001). In the absence of Total Inorganic Carbon (TIC) measurements, it was intended to calculate TIC, and therefore carry out mass balance calculations, using data from CO_2 and pH analyses. However, this proved difficult due to the initial addition of hydrochloric acid to adjust the microcosms' pH. The acid affected the dissolved CO_2 concentration by forcing CO_2 into the headspace. Moreover, purging of the headspace via the aqueous phase to remove H_2S also affected the TIC determination. Therefore the CO_2 data is presented as an indicator of complete biodegradation of phenol to CO_2.

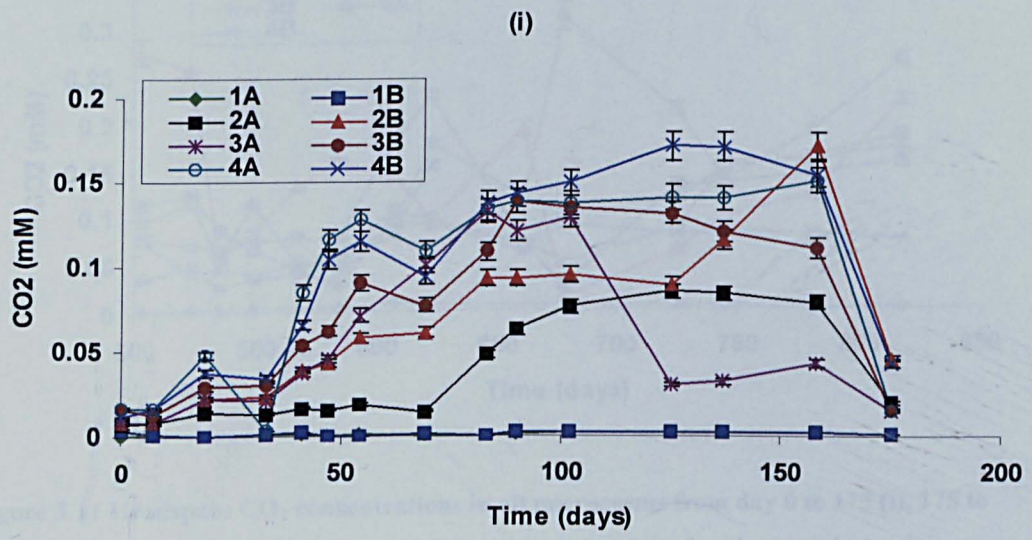

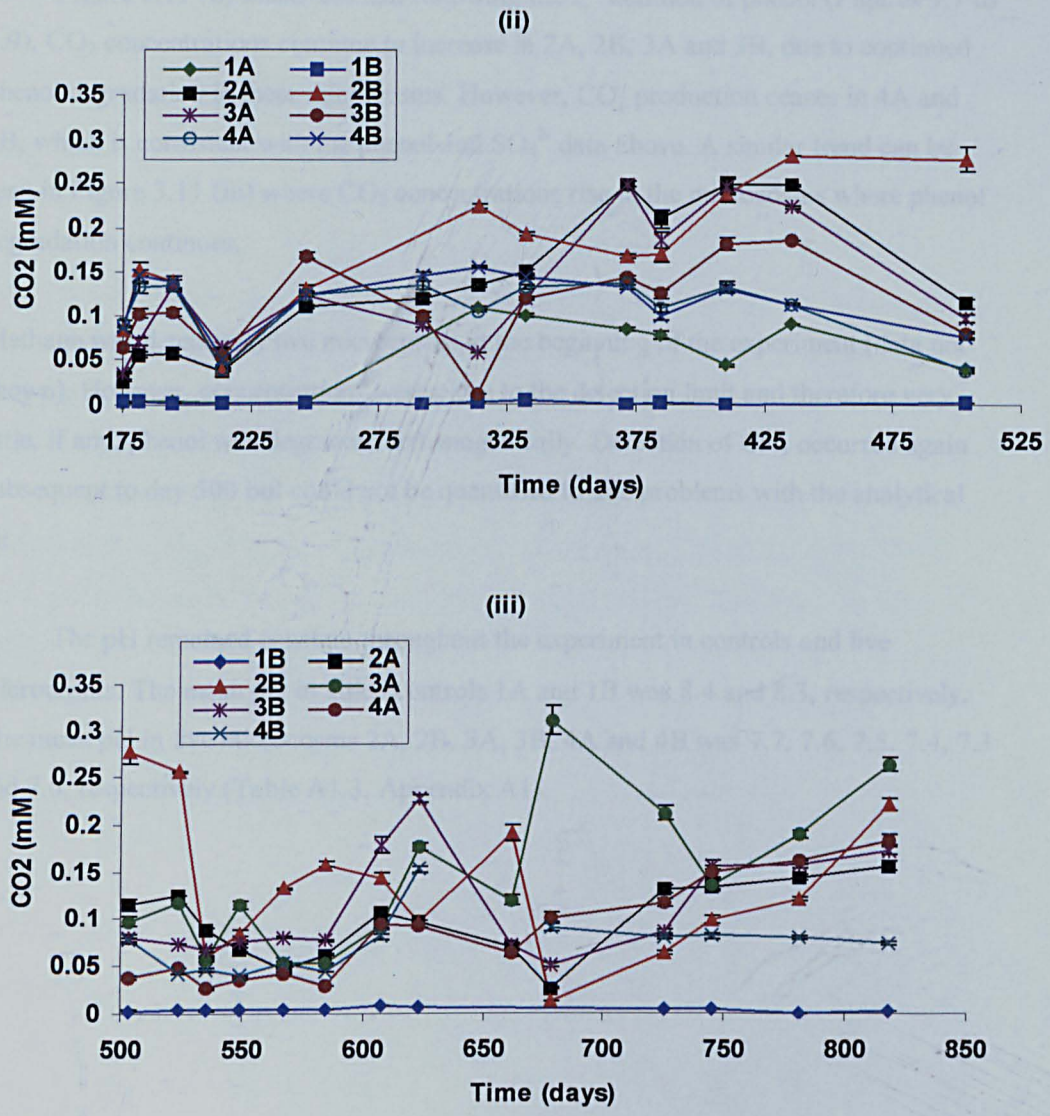

Figure 3.11 Headspace CO_2 concentrations in all microcosms from day 0 to 175 (i), 175 to 503 (ii) and 503 to end (iii). The drop in CO_2 at the last point of each graph is due to headspace purge to remove H_2S. Error bars represent the % relative standard deviation of the mean of triplicate analytical quality controls.

There is no CO_2 formation in sterile control 1B throughout the experiment and only in control 1A subsequent to contamination at day 246. As expected, following the initial addition, CO_2 concentrations are higher [Figure 3.11 (i)] in microcosms where more phenol has been degraded (Figures 3.2 to 3.4). A comparison with phenol and SO_4^{2-} graphs above shows that CO_2 concentrations level off when phenol has been consumed confirming production of CO_2 is directly linked to phenol biodegradation.

Figure 3.11 (ii) illustrates that following the 2nd addition of phenol (Figures 3.7 to 3.9), CO_2 concentrations continue to increase in 2A, 2B, 3A and 3B, due to continued phenol degradation in these microcosms. However, CO_2 production ceases in 4A and 4B, which is consistent with the phenol and SO_4^{2-} data above. A similar trend can be seen in Figure 3.11 (iii) where CO_2 concentrations rise in the microcosms where phenol degradation continues.

Methane was detected in live microcosms at the beginning of the experiment (data not shown). However, concentrations were close to the detection limit and therefore very little, if any, phenol was degraded methanogenically. Detection of CH_4 occurred again subsequent to day 500 but could not be quantified to due problems with the analytical kit.

The pH remained constant throughout the experiment in controls and live microcosms. The mean pH in killed controls 1A and 1B was 8.4 and 8.3, respectively. The mean pH in live microcosms 2A, 2B, 3A, 3B, 4A and 4B was 7.7, 7.6, 7.5, 7.4, 7.3 and 7.6, respectively (Table A1.3, Appendix A1).

3.5 H_2 Concentrations as Indicators of Electron Accepting Processes

Hydrogen measurements in live microcosms are shown in Figure 3.12. H_2 concentrations in sterile controls were at least a magnitude of order higher (19 to 192 nm) throughout the experiment (Table A3.5, Appendix A3).

Previous studies have shown that H_2 measurements can be used to determine the redox conditions of groundwater systems because differences in the free energy yield and physiology enables some microorganisms to utilise H_2 more efficiently than others and, therefore, enables competitive exclusion of less efficient TEAP's (Chapelle et al., 1996; Jakobsen et al., 1998; Lovley and Goodwin, 1988; Lovley and Phillips, 1988a; Lovley and Phillips, 1988b; Vroblesky et al., 1996). As a result of this, different H_2 concentrations can be related to specific TEAP's and previous investigations have demonstrated that H_2 concentrations of 0.2-0.8 nM are characteristic of Fe (III)-reduction, 1-4 nM are typical of SO_4^{2-}-reduction and 5-25 nM are characteristic of methanogenesis. (Chapelle, 2001; Chapelle et al., 1996; Vroblesky et al., 1996; Vroblesky and Chapelle, 1994).

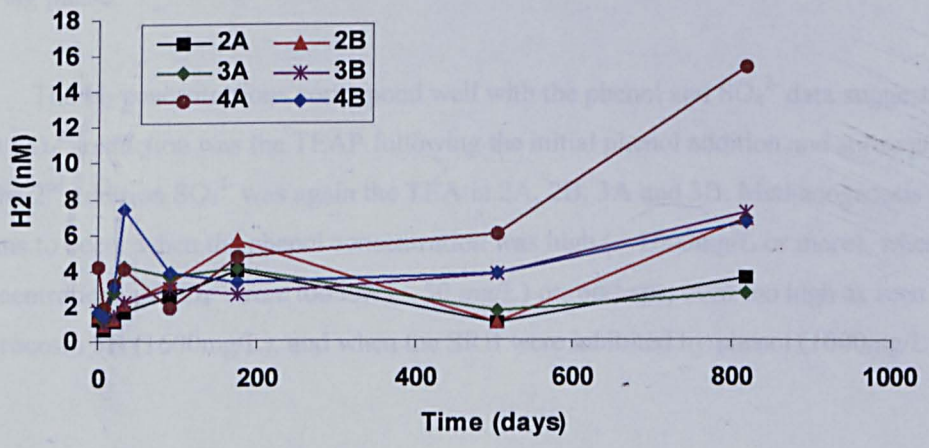

Figure 3.12 H_2 concentrations in live microcosms.

H_2 concentrations in microcosm 2A throughout the experiment, subsequent to the lag phase, range between 1.02 and 4.02 nM. These concentrations are within the range described for SO_4^{2-}-reduction above. Concentrations in 2B range between 1.03 and 3.34

nM indicating SO_4^{2-}-reduction. However, the H_2 levels are at 5.63 nM around day 175 before returning to 1.03 nM indicating that perhaps some methanogenesis took place. This is most likely due to the low SO_4^{2-} concentrations of < 30 mg/L just prior to day 175 as and methanogenesis is known out-compete SO_4^{2-}-reduction at low SO_4^{2-} concentrations (Chapelle et al., 1996; Vroblesky et al., 1996). The H_2 concentration was at 6.82 nM at the end of the experiment indicating that subsequent to the 3rd addition of phenol, where very little SO_4^{2-} was reduced, methanogenesis may have occurred. The H_2 concentration in 3A ranges between 1.61 and 4.24 nM throughout the experiment indicating that SO_4^{2-}-reduction was the TEAP. Concentrations of H_2 in 3B were between 2.25 nM and 3.73 nM throughout the experiment but were at 7.3 nM at the end. This is consistent with data shown in Figure 3.8 (iii) above, where phenol degradation occurred without concurrent SO_4^{2-}-reduction, following the SO_4^{2-} addition at day 678. H_2 in 4B ranges between 1.92 nM and 4.74 nM until day 175 but rises to 5.91 at day 503 and is at 15.35 nM at day 818 indicating that methanogenesis was the TEAP in the latter stages. This trend is consistent with the phenol and SO_4^{2-} data as phenol degradation continues whilst SO_4^{2-}-reduction stops following the 2nd phenol addition as shown in Figure 3.9 (i). Microcosm 4B has a H_2 concentration of 7.45 nM immediately after the lag phase but then ranges between 3.37 and 3.81 until the end where it as at 6.60. This points to SO_4^{2-}-reduction as the TEAP until the 2nd addition of phenol where SO_4^{2-}-reduction ceases [Figure 3.9(ii)], although some methanogenesis may have taken place immediately after the lag phase.

The H_2 concentrations correspond well with the phenol and SO_4^{2-} data suggesting that SO_4^{2-}-reduction was the TEAP following the initial phenol addition and subsequent to the 2nd addition SO_4^{2-} was again the TEA in 2A, 2B, 3A and 3B. Methanogenesis only seems to occur when the phenol concentration was high (~ 1000mg/L or more), when concentrations of SO_4^{2-} were too low (< 50 mg/L) or, perhaps, even too high as seen in microcosm 3B (1600mg/L), and when the SRB were inhibited by phenol (1000mg/L).

3.6 Stoichiometry

Stoichiometric calculations for phenol oxidation coupled to SO_4^{2-}-reduction were carried out using the reaction presented in Table 1.2, Section 1. The concentrations of phenol oxidised, SO_4^{2-} reduced and the amount of electron acceptor consumed as a percentage of the expected theoretical value are shown for the initial, 2nd and 3rd phenol additions in Tables 3.8, 3.9 and 3.10, respectively. As with the reaction rates, stoichiometric calculations did not include the lag phase. The overall stoichiometry (in bold type and identified by $^{\alpha}$ in the tables) represents the period following the onset of biodegradation until it ceased and includes some points where no biodegradation took place and, therefore, these values are generally lower than those seen at specific time periods during the course of the experiment. These overall periods were also broken down to determine SO_4^{2-}-reducing activity at specific time intervals.

The overall percentage of SO_4^{2-} reduced, following the initial phenol addition, is less than 100% of the expected theoretical value in all of the microcosms, except 2A (Table 3.8). However, percentages for the other 5 live microcosms range between 56% and 70% of the expected concentration. These values compare well with previous laboratory studies on phenol biodegradation and SO_4^{2-}-reduction (Broholm and Arvin, 2001; Broholm and Arvin, 2000; Broholm et al., 2000; Edwards et al., 1992b; Haggblom et al., 1993a; Haggblom et al., 1993b; Haggblom and Young, 1995; Londry et al., 1997; Lovley et al., 1995; Monserrate and Haggblom, 1997; Ramanand and Suflita, 1991; Suflita et al., 1989). Lower stoichiometric values could be in part due to utilisation of SO_4^{2-} for cell synthesis during bacterial growth (Bolliger et al., 2001; Haggblom and Young, 1995; Phelps et al., 1996).

Table 3.8 Phenol oxidised and SO_4^{2-} consumed in microcosms following initial phenol addition. Percentage of expected electron acceptor utilised is based on the expected theoretical concentration from the SO_4^{2-}-reduction reaction shown in Table 1.2, Section 1.

Microcosm	Time period	Figure reference	Phenol oxidised (mg/L)	SO_4^{2-} reduced (mg/L)	As percentage of theoretical requirement
2A	**Day 19 to 90**	**Figure 3.2 (i)**	**72.11**	**268.26**	**104[α]**
2A	Day 19 to 41	Figure 3.2 (i)	28.03	97.30	97
2A	Day 41 to 90	Figure 3.2 (i)	44.08	170.96	109
2B	**Day 19 to 83**	**Figure 3.2 (ii)**	**121.39**	**265.9**	**61[α]**
2B	Day 19 to 33	Figure 3.2 (ii)	22.15	83.84	106
3A	**Day 19 to 83**	**Figure 3.3 (i)**	**170.81**	**339.9**	**56[α]**
3A	Day 19 to 33	Figure 3.3 (i)	31.08	118.66	106
3A	Day 19 to 41	Figure 3.3 (i)	72.25	194.29	70
3A	Day 69 to 83	Figure 3.3 (i)	18.64	54.98	83
3B	**Day 19 to 246**	**Figures 3.3 (ii) and (iii)**	**184.09**	**462.83**	**70[α]**
3B	Day 41 to 47	Figure 3.3 (ii)	18.60	62.42	94
3B	Day 69 to 83	Figure 3.3 (ii)	22.26	58.33	74
3B	Day 214 to 246	Figure 3.3 (iii)	6.99	29.55	118[β]
4A	**Day 19 to 313**	**Figure 3.4 (i) and (iii)**	**226.18**	**483.14**	**60[α]**
4A	Day 19 to 41	Figure 3.4 (i)	29.66	286.84	62
4A	Day 270 to 313	Figure 3.4 (ii)	7.26	22.79	88[β]
4B	**Day 19 to 246**	**Figure 3.4 (ii) and (iv)**	**221.44**	**525.43**	**66[α]**
4B	Day 41 to 69	Figure 3.4 (ii)	37.2	118.3	89
4B	Day 69 to 158	Figure 3.4 (ii)	30.53	100.52	92
4B	Day 181 to 246	Figure 3.4 (iv)	24.13	88.77	103[β]

[α] Overall stoichiometric percentage for that particular time-period.

[β] Subsequent to SO_4^{2-} addition.

SO_4^{2-}-reduction seen in the microcosms generally corresponds well with the expected stoichiometric value for SO_4^{2-}. For example in microcosm 2A from day 19 to 41, the SO_4^{2-} reduced corresponds to 97% of the stoichiometric value. SO_4^{2-} consumption percentages in 3A from day 19 to 33 and 69 to 83 are 106% and 83% of the expected values, respectively. Percentages documented in microcosm 3B range between 74% and 118%, in 4A they are between 62% and 88% and in 4B they are in the range 89% to

103% confirming that SO_4^{2-}-reduction is the TEAP and that most, if not all, of the phenol is oxidised by SRB. The percentages are lower at times where microcosms depleted in SO_4^{2-} and increase following SO_4^{2-} addition (signified by $^{\beta}$ in tables), suggesting that SO_4^{2-}-reduction ceases and, perhaps, other processes occur if SO_4^{2-} concentrations fall below 100 mg/L.

Percentage SO_4^{2-} reduced ranges between 48% and 92% of the theoretical prediction, in microcosm 2A, demonstrating that SO_4^{2-}-reduction continues to be the TEAP following the 2nd phenol addition (Table 3.9). However, the lower value between days 435 and 503 was documented when SO_4^{2-} concentrations fell to < 100 mg/L, suggesting that, perhaps, there may be a critical SO_4^{2-} concentration below which other TEAP's become dominant. This trend can be seen in microcosms 2B and 3A prior to the 2nd SO_4^{2-} addition at day 175 and in 3A the percentage falls again subsequent to day 313 which happens to be where the SO_4^{2-} concentration decreases to < 100 mg/L. This also occurs in microcosm 3B subsequent to day 567. Moreover, the percentage does not increase in 2A following the 2nd SO_4^{2-} addition as SO_4^{2-} concentrations were still well above 100 mg/L prior to the amendment. Stoichiometric percentages in 2B range between 75% and 105%, in 3A they are between 47% and 87% and in 3B they are in the range 54% to 101%. As the lower values in each microcosm were documented when SO_4^{2-} concentrations fell below 100 mg/L, it is clear that SO_4^{2-}-reduction is the TEAP when SO_4^{2-} is not limiting.

Table 3.9 Phenol oxidised and SO_4^{2-} consumed in microcosms following 2nd phenol addition. Percentage of expected electron acceptor utilised is based on the expected theoretical concentration from the SO_4^{2-}-reduction reaction shown in Table 1.2, Section 1. Microcosms 4A and 4B are not shown as very little, if any, SO_4^{2-}-reduction took place following the 2nd phenol addition.

Microcosm	Time period	Figure reference	Phenol oxidised (mg/L)	SO_4^{2-} reduced (mg/L)	As percentage of theoretical requirement
2A	**Day 194 to 503**	**Figure 3.7 (i)**	**142.14**	**337.79**	**67[α]**
2A	Day 214 to 270	Figure 3.7 (i)	59.89	196.51	92[β]
2A	Day 313 to 384	Figure 3.7 (i)	29.06	78.79	76
2A	Day 384 to 435	Figure 3.7 (i)	15.48	46.94	85
2A	Day 435 to 503	Figure 3.7 (i)	10.95	18.90	48
2B	**Day 125 to 503**	**Figure 3.7 (ii)**	**195.82**	**358.62**	**51[α]**
2B	Day 137 to 158	Figure 3.7 (ii)	53.82	143.07	75
2B	Day 270 to 313	Figure 3.7 (ii)	14.93	53.51	100[β]
2B	Day 410 to 435	Figure 3.7 (ii)	15.42	46.30	84
2B	Day 462 to 503	Figure 3.7 (ii)	5.79	21.71	105
3A	**Day 125 to 503**	**Figure 3.8 (i)**	**131.97**	**286.57**	**61[α]**
3A	Day 125 to 175	Figure 3.8 (i)	17.97	31.69	49
3A	Day 175 to 194	Figure 3.8 (i)	37.36	115.92	87[β]
3A	Day 313 to 503	Figure 3.8 (i)	48.07	80.27	47
3B	**Day 524 to 608**	**Figure 3.8 (ii)**	**166.34**	**210.79**	**35[α]**
3B	Day 549 to 567	Figure 3.8 (ii)	30.15	108.61	101
3B	Day 567 to 608	Figure 3.8 (ii)	32.63	63.14	54

[α] Overall stoichiometric percentage for that particular time-period.

[β] Subsequent to SO_4^{2-} addition.

Values for SO_4^{2-} reduced, as a percentage of the expected theoretical requirement, fall following the 3rd phenol addition (Table3.10). The overall percentage in microcosm 2A is at 43%. Only 17% of the expected SO_4^{2-} is reduced between days 524 to 535 but the SO_4^{2-} concentration is below 100 mg/L during this time period and the percentage increase to 104% of the expected concentration subsequent to the 3rd SO_4^{2-} addition at day 535. However, the percentage falls again subsequent to day 678 indicating that the phenol concentration of > 900 mg/L may have had an inhibitory effect on SO_4^{2-}-reduction. The deficit in electron acceptor utilisation may be accounted for by methanogenesis or fermentationas the methanogens/fermenters may have a higher tolerance to phenol than the SRB.

Table 3.10 Phenol oxidised and SO_4^{2-} consumed in microcosms following 3rd phenol addition. Percentage of expected electron acceptor utilised is based on the expected theoretical concentration from the SO_4^{2-}-reduction reaction shown in Table 1.2, Section 1.

Microcosm	Time period	Figure reference	Phenol oxidised (mg/L)	SO_4^{2-} reduced (mg/L)	As percentage of theoretical requirement
2A	**Day 524 to 818**	**Figure 3.10 (i)**	**115.61**	**179.15**	**43$^{\alpha}$**
2A	Day 524 to 535	Figure 3.10 (i)	6.08	3.6	17
2A	Day 535 to 678	Figure 3.10 (i)	21.47	79.89	104$^{\beta}$
2A	Day 678 to 818	Figure 3.10 (i)	88.06	91.79	29
2B	**Day 535 to 818**	Figure 3.10 (ii)	**42.23**	**41.43**	**27$^{\alpha\beta}$**
2B	Day 608 to 818	Figure 3.10 (ii)	31.34	35.89	32
3A	**Day 524 to 818**	**Figure 3.10 (iii)**	**109.78**	**44.52**	**11$^{\alpha}$**
3A	Day 662 to 781	Figure 3.10 (iii)	62.96	35.97	16

$^{\alpha}$ Overall stoichiometric percentage for that particular time-period.

$^{\beta}$ Subsequent to SO_4^{2-} addition.

In comparison to 2A less phenol degradation was seen in microcosm 2B subsequent to the 3rd phenol addition. The overall stoichiometric percentage was at 27%, therefore another process such as methanogenesis was probably responsible for some of the phenol degradation. Overall, only 11% of the stoichiometric requirement was seen in microcosm 3A. This is most likely because SO_4^{2-} concentrations were well below 100 mg/L in this microcosm but the remaining SO_4^{2-} continued to be reduced and it is possible that SO_4^{2-}-reduction would have continued to be the TEAP had a further addition of SO_4^{2-} been made.

3.7 Total S and Fe(II) by ICP-AES.

Results from the ICP-AES analysis are presented in Figures 3.13 to 3.15. There is good correlation between Total S measured by ICP-AES and SO_4^{2-}-S measured by IC. Total S concentrations are slightly higher as expected (e.g. due to dissolved H_2S, organic sulphur compounds). Sulphur concentrations in killed controls remain relatively constant throughout (Figure 3.13). Total S provides another line of evidence for SO_4^{2-}-reduction in the microcosms by SRB

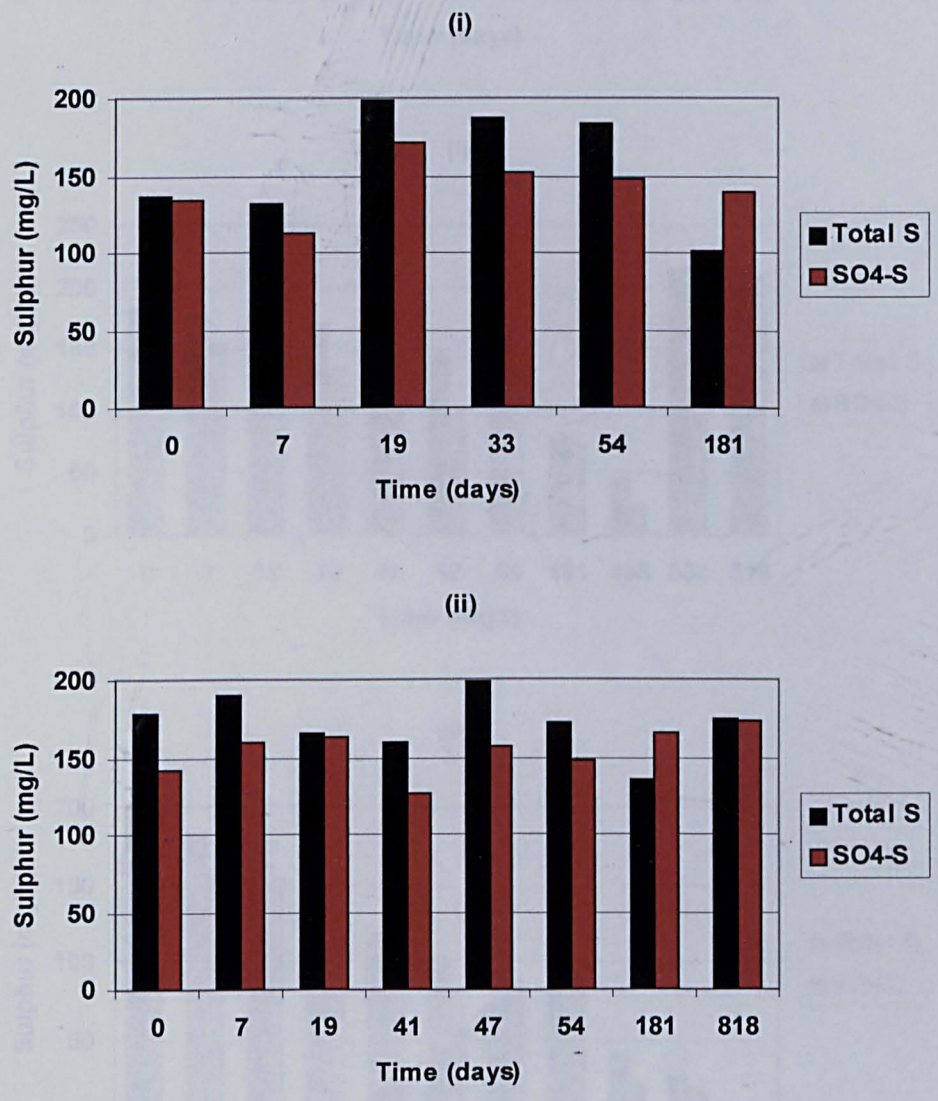

Figure 3.13 Total Sulphur by ICP-AES and SO_4^{2-} sulphur by IC in Killed controls 1A (i) and 1B (i).

(i)

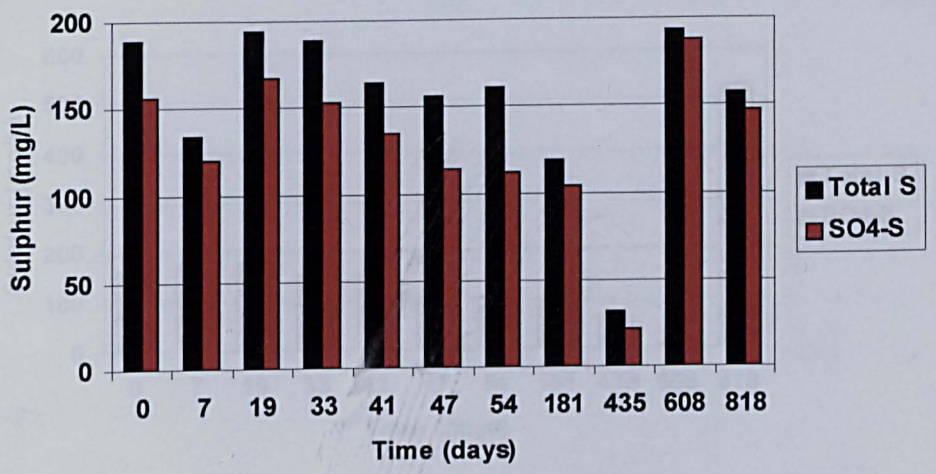
Sulphur (mg/L)
200
150
100
50
0
0 7 19 33 41 47 54 181 435 608 818
Time (days)
Total S
SO4-S

(ii)

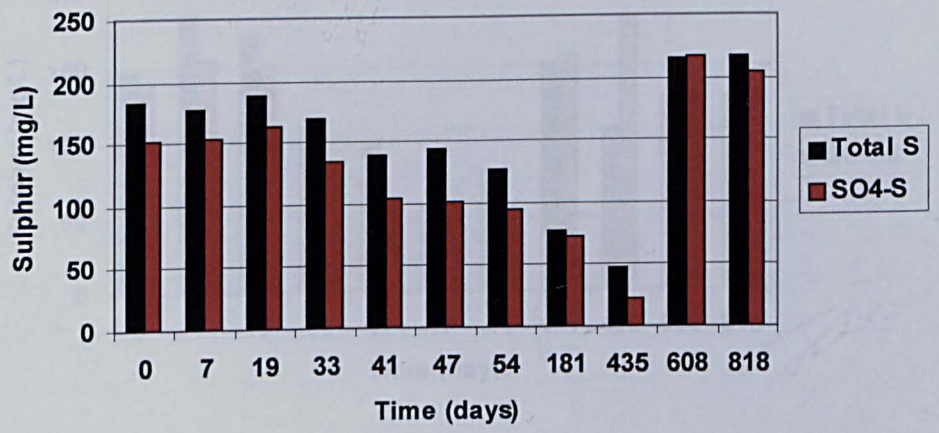
Sulphur (mg/L)
250
200
150
100
50
0
0 7 19 33 41 47 54 181 435 608 818
Time (days)
Total S
SO4-S

(iii)

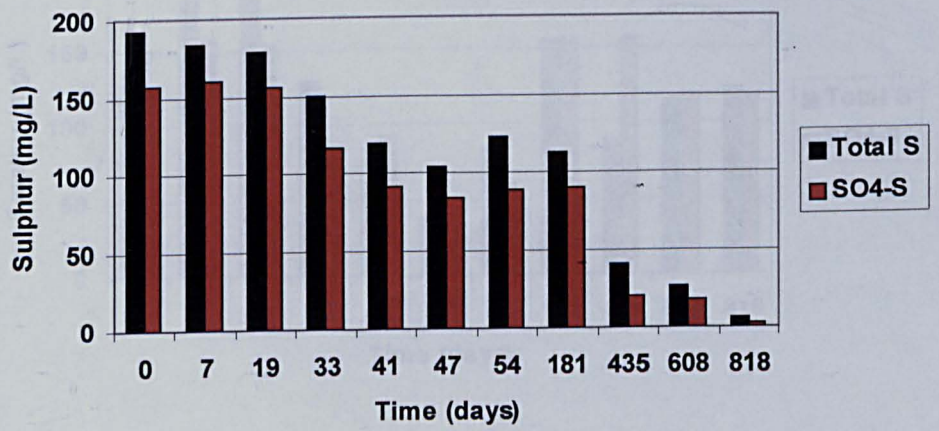
Sulphur (mg/L)
200
150
100
50
0
0 7 19 33 41 47 54 181 435 608 818
Time (days)
Total S
SO4-S

(iv)

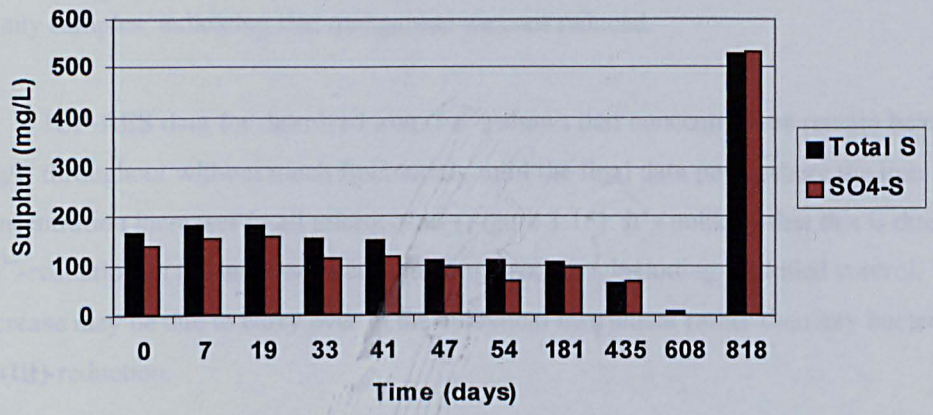

(v)

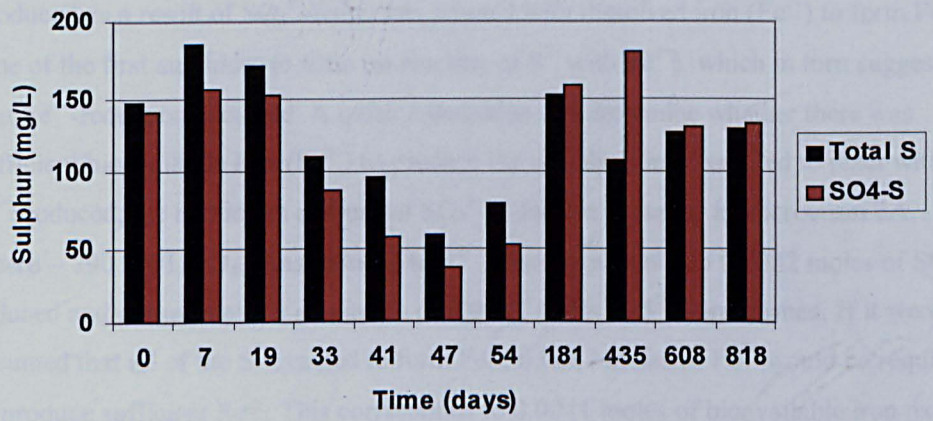

(vi)

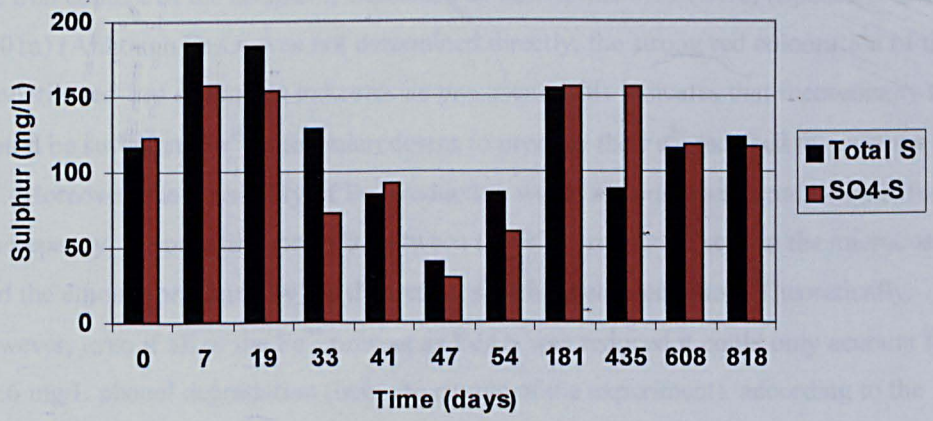

Figure 3.14 Total Sulphur by ICP-AES and SO_4^{2-} sulphur by IC in live microcosms 2A (i), 2B (ii), 3A (iii), 3B (iv), 4A (v) and 4B (iv). Points of SO_4^{2-} addition are illustrated in Table 2.2, Section 2 and in Figures 3.3 to 3.10 above.

as concentrations in live microcosms follow the same trends as SO_4^{2-} in that Total S falls as SO_4^{2-} is reduced and increases following SO_4^{2-} addition. Manganese was not detected in any samples, indicating that manganese was not reduced.

ICP-AES data for dissolved iron (Fe^{2+}) shows that concentrations remain below 1 mg/L throughout without much fluctuation, until the final data point where the iron concentration increases in all microcosms (Figure 3.15). It's unlikely that this is due to Fe^{3+}-reduction as the increase occurs in all microcosms including the killed control. The increase may be due to carry over in the analytical instrument rather than any bacterial Fe(III)-reduction.

During phenol degradation the accumulation of a black precipitate was noted on the sediment, indicating the presence of FeS (iron sulphide). This suggests that S^{2-} produced as a result of SO_4^{2-}-reduction, reacted with dissolved iron (Fe^{2+}) to form FeS (one of the first sulphides to form on reaction of S^{2-} with Fe^{2+}), which in turn suggests that Fe^{3+}-reduction occurred. A quick calculation can determine whether there was sufficient bioavailable iron (Fe^{3+}) to produce the dissolved iron required to react with the S^{2-} produced; the maximum amount of SO_4^{2-}-reduction occurred in microcosm 2A, where ~ 790 mg/L SO_4^{2-} was reduced to S^{2-}. This corresponds to 0.0082 moles of SO_4^{2-} reduced and consequently a maximum of 0.0082 moles of S^{2-} were formed. If it were assumed that all of the S^{2-} reacted to form FeS, 0.0082 moles of Fe^{3+} would be required to produce sufficient Fe^{2+}. This corresponds to 0.0041 moles of bioavailable iron oxide (Fe_2O_3), which is 0.66 g or 0.66 (wt%) as 100 g of sediment was added to each microcosm. XRF (X-Ray Fluorescence) analysis on 6 aquifer core samples showed that the iron content of the sediment, expressed as Fe_2O_3, was 0.79 (wt%) (Spence et al., 2001a) (Although Fe_2O_3 was not determined directly, the strong red colouration of the fluviatile red-bed sediments indicates its presence). This indicates that theoretically there would be sufficient Fe^{3+} in the microcosms to produce the Fe^{2+} required to consume the S^{2-}. Moreover, the possibility of Fe^{3+}-reduction would account to a certain degree for the discrepancy, at some time periods, between the SO_4^{2-}-reduction seen in the microcosms and the amount predicted by the theoretical stoichiometric equation. Theoretically, however, even if all of the Fe^{3+} present as Fe_2O_3 was reduced it could only account for 27.6 mg/L phenol degradation (over the course of the experiment), according to the theoretical stoichiometric equation (Table 1.2, Section 1).

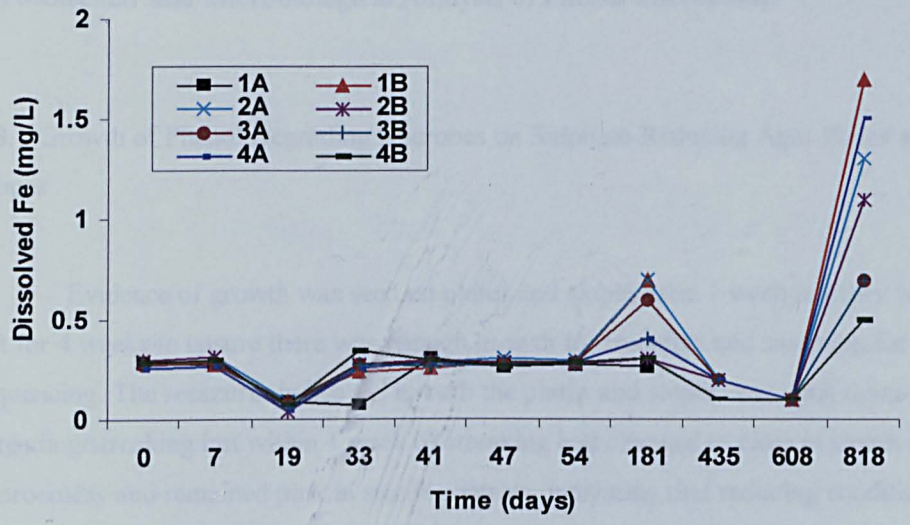

Figure 3.15 Dissolved Iron (Fe^{2+}) by ICP-AES.

3.8 Molecular and Microbiological Analysis of Phenol Microcosms

3.8.1 Growth of Phenol Degrading Microbes on Sulphate-Reducing Agar Plates and Slopes

Evidence of growth was seen on plates and slopes after 1 week but they were left for 4 weeks to ensure there was enough growth for transfers and sampling for sequencing. The resazurin indicator, in both the plates and slopes, was pink upon spreading/streaking but within 1 week of streaking had changed to clear in slopes of live microcosms and remained pink in sterile controls, indicating that reducing conditions had been achieved upon growth (Figure 3.16). Moreover, bacterial growth was only seen on live slope and not on controls. Only 1 distinct colony was seen to grow on most of the initial agar plates although 2 colony types were seen on a few plates. The second set of streaked plates followed a similar trend with 1 colony type seen on plates.

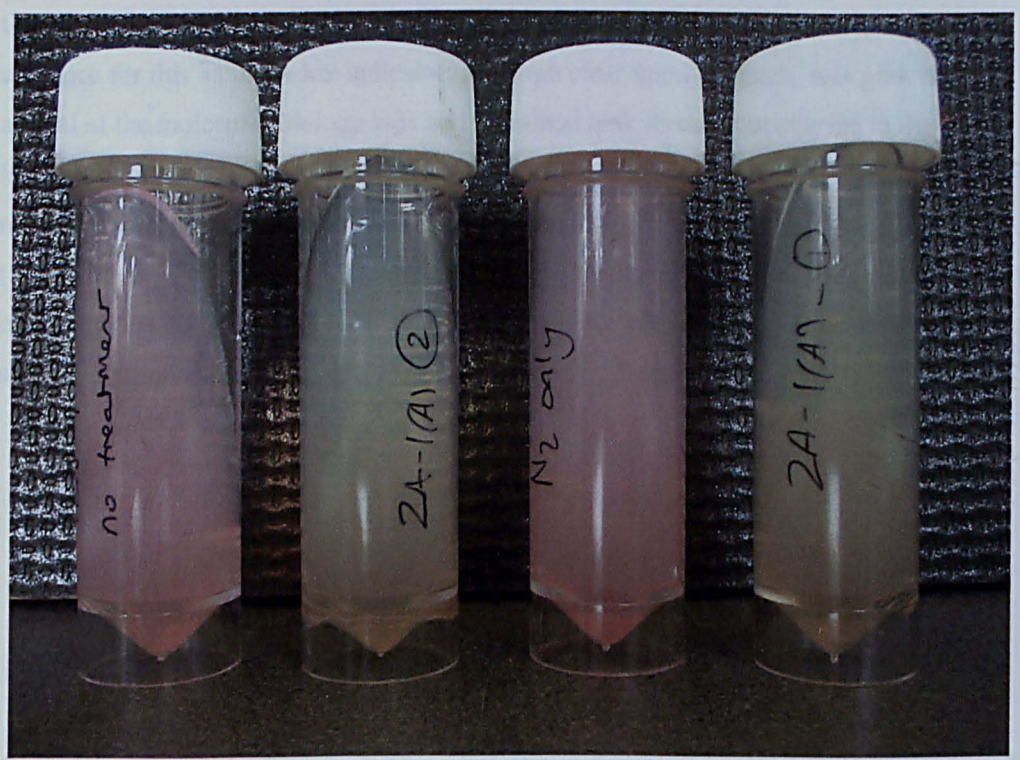

Figure 3.16 Agar slopes prepared with SO_4^{2-}-reducing agar. The redox indicator remained pink in sterile controls (1st and 3rd from left) but changed colour to clear in live slopes indicating reducing conditions. Bacterial growth was only seen on live (clear) slopes.

There was sufficient growth for transfer to slopes after around 4 weeks. The agar slopes remained clear throughout incubation in the anaerobic jars and sufficient growth of 1 colony type was seen before transport for isolation and sequencing.

3.8.2 Isolation and Identification of Phenol Degraders by DNA Sequencing

Gram negative rod-shaped bacteria were observed following gram staining and examination under the microscope. DNA was successfully extracted from the isolates and a single fragment was obtained from 16S amplification. The closest match for both isolates was to *Pseudomonas Stutzeri* with > 99% homology for the isolate from microcosm 3B and > 98% homology for the isolate from microcosm 2B (Appendix A5). *Pseudomonas Stutzeri* (Lehmann and Neumann, 1896) is a noted for being especially heterogeneous in nutritional properties and has been described previously (Sijderius, 1946). It is a denitrifier commonly found in soil and water environments (Gruntzig et al., 2001). It seems that *Pseudomonas Stutzeri* out-competed the SRB on the agar slopes and therefore the sulphate-reducers could not be isolated and identified. There is some evidence for this as the redox indicator, although clear upon dispatch, was pink on arrival at the molecular biology labs and remained pink throughout storage in the laboratory at 4°C. It is possible that the denitrifying culture remained part of the microbial consortia throughout and may have become active upon addition of NO_3^-. (Suflita et al., 1989). The NO_3^- may have been inadvertently provided during preparation of the agar as conversion of NH^{4+} to NO_3^- would have been possible as the SO_4^{2-}-rich synthetic groundwater was in storage at 4°C prior to autoclaving.

4. RESULTS AND DISCUSSION – SPREADSHEET MODELLING OF HIGH CONCENTRATION PHENOL BIODEGRADATION IN SULPHATE-REDUCING BATCH REACTORS

4.1 Biodegradation Modelling

Kinetic modelling of biodegradation processes can provide valuable information with regard to the main biological reactions occurring within contaminant plumes. The kinetic data obtained from field or batch studies allows estimates to be made of the potential of natural attenuation or biodegradation to remediate contaminated field sites, and can often influence the costing and duration estimates of remediation projects (Alvarez-Cohen and Speitel, 2001). A number of models have been used to describe biodegradation, one of the most recognized being the Monod model that can be used to describe the effect of a growth limiting substrate on the growth rate (Bekins et al., 1998; Tchobanoglous and Burton, 1991):

$$\frac{dS}{dt} = -k_{max} X \frac{S}{K_S + S} \qquad \textbf{(4.1)}$$

$\frac{dS}{dt}$ = rate of substrate utilisation (mass/unit volume . time)

$-k_{max}$ = the maximum substrate utilisation rate ($time^{-1}$)

X = the biomass concentration (mass/unit volume)

S = concentration of substrate in solution (mass/unit volume)

K_S = is the Monod half-saturation constant, substrate concentration at half the maximum utilisation rate (mass/unit volume)

The first-order approximation of the Monod model is often used with data obtained from field-scale experimentation. However, the first-order decay process is often erroneously applied as it depends on the assumption that the half-saturation constant (K_S) is much greater than the maximum concentration of the rate limiting substrate (Bekins et al., 1998; Schirmer et al., 2000). To ascertain K_S of a system requires fitting of field or laboratory data to a Monod kinetic model (Bekins et al., 1998). Previous laboratory studies have formulated kinetic models of phenol biodegradation based on the Monod function described in equation 4.1 (Acuna-Arguelles et al., 2003; Peyton et al., 2002; Wang et al., 1996; Watson et al., 2003). Although batch laboratory microcosms cannot fully represent field-based systems they can provide valuable information on biodegradation processes including substrate biodegradation potential/rates, TEA consumption, microbial population dynamics and the kinetic parameters, k_{max} and K_S. To best predict the natural attenuation or biodegradation processes in groundwater environments requires a combined approach utilising laboratory and field-based data. The benefits of a combined approach to obtain kinetic parameters in contaminated aquifers has been shown previously (Chapelle et al., 1996; Schirmer et al., 2000).

4.2 Monod Kinetic Model and Assumptions Applied to Fit Phenol Biodegradation Microcosm Data

4.2.1 Biodegradation Data Set and Dual Monod Model

The modelling was carried out, using Microsoft ® Excel 2000, on phenol and SO_4^{2-} data obtained from microcosms 2A and 2B of the phenol biodegradation experiment (Section 3). Microcosms 4A and 4B were also modelled following the 2nd, inhibitory, phenol addition at > 1300 mg/L. The material and methods used in the microcosm experiment are described in Sections 2.1-2.4. Both electron donor (phenol) and electron acceptor (SO_4^{2-}) data were used in the model; consequently the general Monod equation was modified to incorporate dual substrate utilisation as shown in equation 4.2:

$$\frac{dP}{dt} = -k_{max} X \left(\frac{S_P}{K_P + S_P} \right) \left(\frac{S_{SO4}}{K_{SO4} + S_{SO4}} \right) \quad \textbf{(4.2)}$$

$\frac{dP}{dt}$ = rate of phenol utilisation (mol/L/s)

$-k_{max}$ = the maximum substrate utilisation rate (1/s)

X = the biomass concentration (mol/L)

S_P = concentration of phenol in solution (mol/L)

S_{SO4} = concentration of SO_4^{2-} in solution (mol/L)

K_P = the Monod half-saturation constant with respect to phenol (mol/L)

K_{SO4} = the Monod half-saturation constant with respect to SO_4^{2-} (mol/L)

The dual Monod equation is appropriate as degradation were shown to vary with both the phenol (electron donor) and SO_4^{2-} (electron acceptor) concentrations (Figures 3.9 and 3.4 (i)). For clarity, the data is presented, as in Sections 3.1 to 3.3, following each phenol addition. The relevant phenol and SO_4^{2-} additions are shown in Table 4.1. Appropriate dilution calculations were carried out on biomass concentrations following each substrate addition.

Table 4.1 Sulphate and Phenol amendments made to microcosms. Phenol and sulphate added at the beginning of the experiment (time zero) are termed the 1st addition. Microcosms where no 3rd addition was made are denoted by n/a.

Microcosm	2nd phenol addition	3rd phenol addition	2nd sulphate addition	3rd sulphate addition
2A	Day 175	Day 503	Day 175	Day 535
2B	Day 105	Day 503	Day 175	Day 535
4A	Day 313	n/a	Day 175	n/a
4B	Day 313	n/a	Day 175	n/a

4.2.2 Assumptions Applied to the Model

The 19-day lag phase seen in all microcosms at the beginning of the experiment is assumed to be a period of acclimation. Therefore, the initial concentrations in the model are taken following the end of the lag phase. The final data point modelled was just prior to the depletion of substrate (electron donor), that is when the concentration of phenol reached zero (taken as < 5 mg/L based on HPLC detection limit). The initial biomass was calculated as follows:

1. The number of microbial cells in the four-ashes inoculum was estimated at 10^7 cells/ml inoculum. Ghiorse and Wilson (1988) presented an extensive summary of subsurface microbial numbers in contaminated and pristine sites. Microbial numbers in groundwater at contaminated sites ranged from 10 (sewarage sites) to 10^7 (mixed organic site) cells/ml of groundwater. Microbial numbers in solid samples obtained from 2 creosote waste sites were found to be 10^6 to 10^7 cells/g of aquifer material, therefore an estimate of 10^7 cells/ml is reasonable.

2. The mass of one cell was taken to be 1.4×10^{-13} g (Pedersen and Ekendahl, 1990). This in conjunction with the number of cells (6.06×10^6 cells/ml) and the volume of inoculum (30 ml) gave an initial biomass concentration of 8.4×10^{-1} mg/L.

3. This was converted to a molar volume (2.8×10^{-5} mol/L) by considering biomass to be stoichiometrically equivalent to hydrated carbon (CH_2O) (Watson et al., 2003).

The biomass yield coefficient (mol of biomass produced/mol of substrate consumed) was estimated at 0.1 (10% yield). This was based on 2 considerations. Firstly, Watson *et al.* use the hydrated carbon term to obtain a value of 5% biomass yield for acetate degradation coupled to SO_4^{2-}-reduction and 20% for phenol fermentation to acetate. Secondly, the protein assay (Section 2.4.3) was performed close to the end of the experiment (781 days). The protein concentration obtained by the Bradford assay (mg/L) was converted to a molar volume by taking the formula weight of the Bovine Serum Albumin (BSA), based on the current amino acid sequence, to be 66,430 (Hirayama et al., 1990). Furthermore, taking the protein content of a bacterial cell to be 55% (Madigan et al., 1997), the final biomass concentration (mol/L), at day 781, was calculated. The measured biomass concentration compared well with that predicted by the model (Table 4.3), reinforcing the 10% biomass yield assumption. Biomasss concentrations were assumed to be constant when the electron donor concentration was at zero or when electron donor consumption ceased.

4.3 Modelling Results and Discussion

Following the initial phenol addition, phenol biodegradation coupled to SO_4^{2-}-reduction occurred in microcosms 2A and 2B following a 19-day lag phase (Figure 3.2, Section 3.1). Figure 4.1 shows the experimental phenol biodegradation data and the predicted degradation curve obtained from the model, for both microcosms 2A and 2B. Figures 4.2 and 4.3 show the experimental and predicted curves for phenol biodegradation following the 2nd and 3rd phenol additions, respectively.

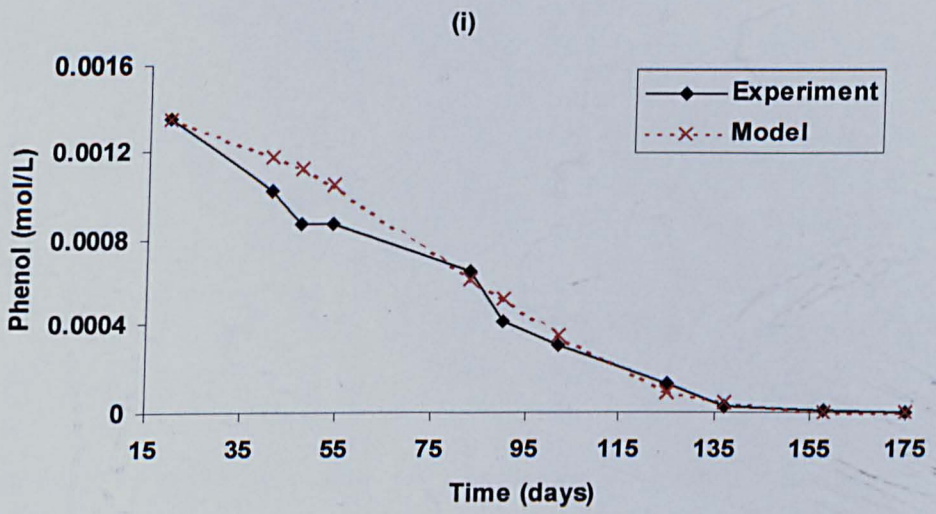

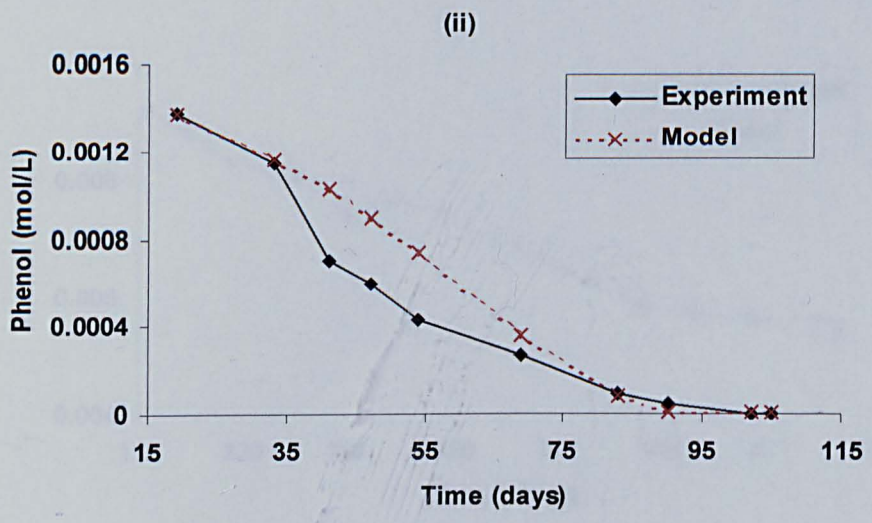

Figure 4.1 Model predictions (×) and experimental data (♦) of phenol biodegradation coupled to SO_4^{2-}-reduction in microcosms 2A (i) and 2B (ii) following the initial phenol addition.

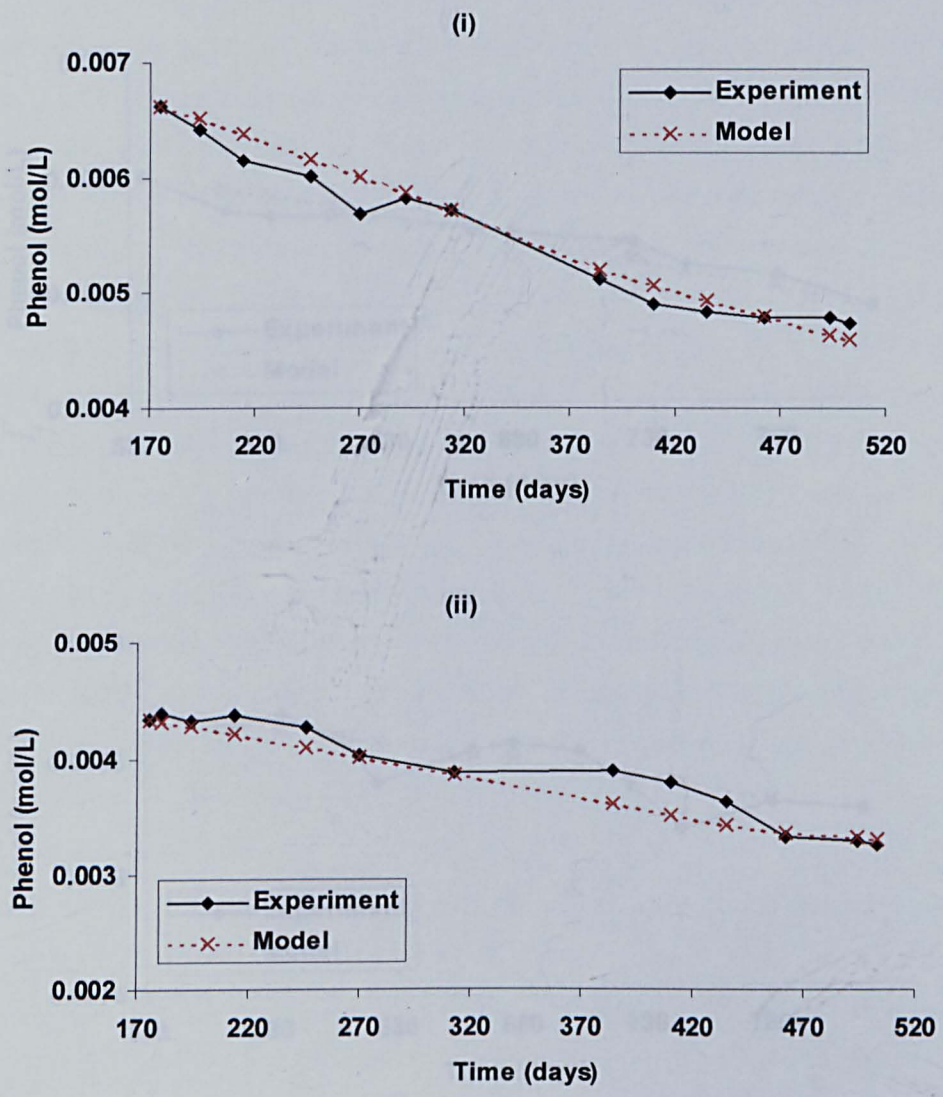

Figure 4.2 Model predictions (×) and experimental data (♦) of phenol biodegradation coupled to SO_4^{2-}-reduction in microcosms 2A (i) and 2B (ii) following the 2nd phenol addition at day 175.

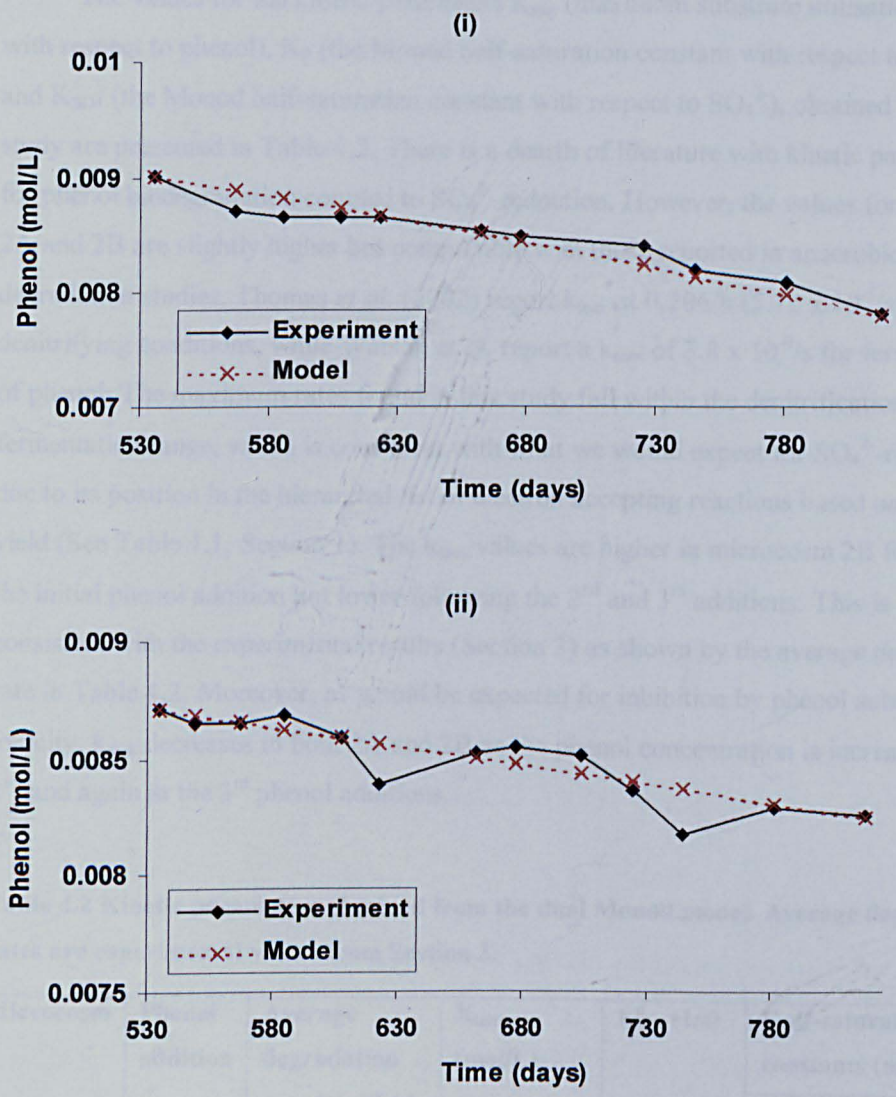

Figure 4.3 Model predictions (×) and experimental data (♦) of phenol biodegradation coupled to SO_4^{2-}-reduction in microcosms 2A (i) and 2B (ii) following the 3rd phenol addition. Data is shown subsequent to the 2nd SO_4^{2-} addition at day 535.

The curve predicted by the model in Figure 4.1 correlates well with the experimental data, with a slightly better fit obtained for microcosm 2A than 2B. Predicted values compare well with the experimental data set following the 2nd and 3rd phenol additions as shown by Figures 4.2 and 4.3, respectively.

The values for the kinetic parameters k_{max} (maximum substrate utilisation rate with respect to phenol), K_P (the Monod half-saturation constant with respect to phenol) and K_{SO4} (the Monod half-saturation constant with respect to SO_4^{2-}), obtained in this study are presented in Table 4.2. There is a dearth of literature with kinetic parameters for phenol biodegradation coupled to SO_4^{2-}-reduction. However, the values for k_{max} for 2A and 2B are slightly higher but comparable with those reported in anaerobic phenol degradation studies. Thomas *et al.* (2002) report k_{max} at 0.206/h (5.72×10^{-5}/s) under denitrifying conditions, while Watson *et al.* report a k_{max} of 3.8×10^{-8}/s for fermentation of phenol. The maximum rates found in this study fall within the denitrification and fermentation range, which is consistent with what we would expect for SO_4^{2-}-reduction, due to its position in the hierarchal list of electron accepting reactions based on energy yield (See Table 1.1, Section 1). The k_{max} values are higher in microcosm 2B following the initial phenol addition but lower following the 2nd and 3rd additions. This is consistent with the experimental results (Section 3) as shown by the average degradation rate in Table 4.2. Moreover, as would be expected for inhibition by phenol substrate toxicity, k_{max} decreases in both 2A and 2B as the phenol concentration is increased at the 2nd and again at the 3rd phenol additions.

Table 4.2 Kinetic parameters obtained from the dual Monod model. Average degradation rates are experimental values from Section 3.

Microcosm	Phenol addition	Average degradation rate (mol/L/s)	$X_{initial}$ (mol/L)	k_{max} (1/s)	Half-saturation constants (mol/L)	
					K_P	K_{SO4}
2A	Initial	$9.47 \times 10^{-11\alpha}$	2.80×10^{-5}	3.74×10^{-6}	2.00×10^{-4}	3.70×10^{-4}
2B	Initial	$2.12 \times 10^{-10\alpha}$	2.80×10^{-5}	5.35×10^{-6}	2.00×10^{-4}	3.70×10^{-4}
2A	2nd	$1.17 \times 10^{-10\beta}$	$1.30 \times 10^{-4\varepsilon}$	6.67×10^{-7}	2.00×10^{-4}	3.70×10^{-4}
2B	2nd	$5.04 \times 10^{-11\chi}$	$2.45 \times 10^{-4\varepsilon}$	1.85×10^{-7}	2.00×10^{-4}	3.70×10^{-4}
2A	3rd	$7.01 \times 10^{-11\delta}$	$2.86 \times 10^{-4\varepsilon}$	1.80×10^{-7}	2.00×10^{-4}	3.70×10^{-4}
2B	3rd	$4.43 \times 10^{-11\delta}$	$3.91 \times 10^{-4\varepsilon}$	4.90×10^{-8}	2.00×10^{-4}	3.70×10^{-4}

$^{\alpha}$ Taken from Table 3.3, Section 3.1, $^{\beta}$ Table 3.5, Section 3.2, $^{\chi}$ Table 3.6, Section 3.2 and $^{\delta}$ Table 3.7, Section 3.3.

$^{\varepsilon}$ Adjusted with dilution factor from substrate addition

The half-saturation constants (Table 4.2), K_P and K_{SO4}, were unchanged in the model throughout the experiment indicating that the microbial population's affinity for the substrate was not affected by the increased phenol concentrations, either at high phenol concentrations or low SO_4^{2-} concentrations. Values for K_P and K_{SO4} from phenol degradation with SO_4^{2-}-reduction in an anaerobic biofilm reactor were found to be 4.09 x 10^{-5} mol/L and 1.11 x 10^{-4} mol/L, respectively (Lin and Lee, 2001). Half-saturation constants for biodegradation of phenolic compounds, including phenol, coupled to SO_4^{2-}-reduction have been documented at 1.1 x 10^{-4} mol/L and 1.6 x 10^{-4} mol/L for K_P and K_{SO4}, respectively (Mayer et al., 2001). The values from this study are higher, which is consistent with the experimental results from Section 3.1, which showed that the phenol biodegradation capability and the rate at which phenol is degraded is higher than previously documented in the literature.

The measured biomass concentrations (calculated from the protein assay, see Section 4.2.2 above) at the end of the experiment for microcosms 2A and 2B were 3.07 x 10^{-4} mol/L and 3.15 x 10^{-4} mol/L, respectively (Table 4.3). Concentrations for 2A and 2B predicted by the model are slightly higher at 3.85 x 10^{-4}mol/L and 4.30 x 10^{-4} mol/L, respectively.

Table 4.3 Biomass concentrations measured in the laboratory and predicted by Monod model at the end of the experiment (day 781).

Microcosm	Biomass measured (mol/L)	Biomass predicted by model (mol/L)
2A	3.07 x 10^{-4}	3.85 x 10^{-4}
2B	3.15 x 10^{-4}	4.30 x 10^{-4}

Although the 3rd phenol addition did not inhibit degradation completely, there was a reduction in the biodegradation rate especially in microcosm 2B (Section 3.3), indicating that the high concentrations of phenol exerted some inhibitory effects on the microbial consortia, most probably leading to slower growth, if not a decline, in the microbial populations. Therefore, incorporation of an inhibition or slow-growth term in the Monod function (Equation 4.2) would, perhaps, compensate for this extra growth seen in the model and give an improved correlation with the measured value.

4.4 Summary

Phenol biodegradation curves obtained from the model correlate well with the experimental data, as do predicted biomass concentrations at the conclusion of the experiment. Values for k_{max} (maximum phenol utilisation rate) are between 4.90 x 10^{-8}/s and 3.74 x 10^{-6}/s. They fall within the range expected of phenol biodegradation coupled to SO_4^{2-}-reduction based on literature values (Thomas et al., 2002; Watson et al., 2003). The values for k_{max} fall, as expected, as the phenol concentrations are increased (2nd addition) from the initial 1.4 x 10^{-3} mol/L to 6.6 x 10^{-3} mol/L in 2A and 4.4 x 10^{-3} mol/L in 2B. The same trend is seen when the concentrations in 2A and 2B are increased (3rd addition) to 9.0 x 10^{-3} mol/L and 8.7 x 10^{-3} mol/L, respectively. Half-saturation constants K_P (phenol) and K_{SO4} (sulphate) were determined to be 2.0 x 10^{-4} mol/L and 3.7 x 10^{-4}, respectively. These values are of the same order of magnitude but higher than those reported in the literature (Lin and Lee, 2001; Mayer et al., 2001). This is consistent with the results of Section 3, where the microbial consortia's phenol biodegradation capability and the rate at which they oxidised phenol are higher than previously documented.

5. RESULTS AND DISCUSSION – METHOD DEVELOPMENT AND MICROCOSM STUDIES INTO MICROBIAL OXIDATION OF VINYL CHLORIDE IN GROUNDWATER

Additional methodological information related to this section (e.g. enrichment preparation) can be found in Section 2.5.

5.1 SPME Analytical Background

Analysis and handling of VC in biodegradation experiments can be problematic due to its high volatility and toxicity. Detection of VC in bioremediation studies has traditionally been carried out using headspace and or purge and trap sampling followed by Gas Chromatography (GC) FID (Flame Ionisation Detector) (Ballapragada et al., 1997; CRC, 2002; Davis et al., 2002; Deng et al., 1999; Distefano, 1999; Hartmans and Debont, 1992; He et al., 2002; Hunkeler et al., 2002; Keppler et al., 2002; Kleikemper et al., 2002; Koziollek et al., 1999; Mahapatra et al., 2002; Martinez et al., 2002; Maymo-Gatell et al., 2001; Ndon et al., 2000; Peyton et al., 2002; Suthersan, 2002; Thomas et al., 2002; Verce et al., 2000; Wu, 2002; Zeng and Noblet, 2002). Detection by GC-PID (Photo Ionisation Detector) (Rosner et al., 1997), scintillation counting (Bradley and Chapelle, 1998c; Davis and Carpenter, 1990; Klecka et al., 1990) and, more recently, GC-MS (Mass Spectrometry) (Keppler et al., 2002) has also been successfully carried out. However, purge and trap involves a time-consuming and often costly sample preparation stage. Solid-phase Microextraction (SPME) is a sample extraction technique developed over a decade ago (Arthur and Pawliszyn, 1990) that has been used in environmental analysis of water samples (Achten and Puttman, 2000) The SPME device consists of a 1 cm long fused silica fibre, coated with a polymer. An autosampler exposes the fibre to the headspace or aqueous phase of the sample vial [Figure 5.1].

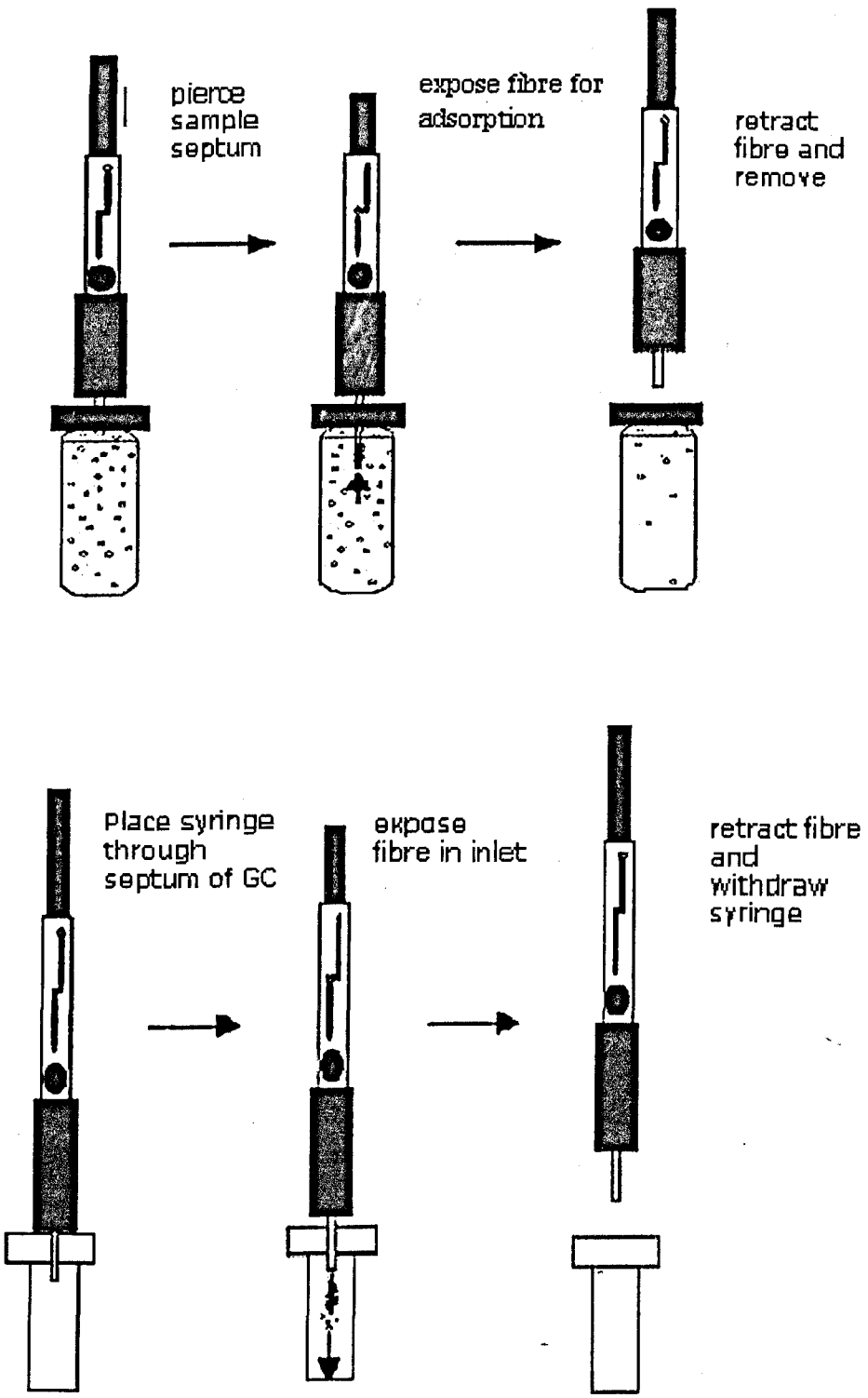

Figure 5.1 Schematic showing Solid-Phase microextraction (SPME) procedure. The injection depth of the needle/fibre can be adjusted so as to sample from the headspace alone (Courtesy of Sigma-Aldrich).

After a short period of time a three-phase (liquid, gas and fibre) equilibrium is reached and the amount absorbed by the fibre (n) in headspace analysis can be expressed as:

$$n = C_0V_1V_2K_1K_2 / K_1K_2V_1 + K_2V_3 + V_2 \quad \textbf{(5.1)}$$

C_0 - is the initial analyte concentration in the aqueous phase

V_1 - volume of the coating

V_2 - volume of the aqueous phase

V_3 - volume of the headspace

K_1 - C_1/C_3 is the coating/gas partition coefficient

K_2 - C_3/C_2 is the gas/ liquid partition coefficient

C_1, C_2, and C_3 are the equilibrium concentrations of the analyte in the fibre coating, aqueous phase, and vapour phase, respectively.

The organic analyte, VC, adsorbs to the coating on the fibre before being removed and injected into the GCMS injector. The VC thermally desorbs and is transported to the GC capillary column. SPME can simultaneously extract and concentrate organic analytes in a single step, has been shown to be as sensitive as purge and trap but is relatively inexpensive, rapid, fully automated and does not require the use of organic solvents (Chai et al., 1993; Lovley et al., 1993; MacGillivray et al., 1994; Zeng and Noblet, 2002). When used in conjunction with GC-MS, SPME can provide an adaptable and practical technique for analysis of complex environmental samples.

Analysis of VC by SPME has been demonstrated in conjunction with GCMS for both aqueous and solid samples (Charvet et al., 2000). However, although SPME has been used in the analysis of common groundwater contaminants (Dewsbury et al., 2003);Achten, 2000 #361], it has not, as far as the author is aware, been utilised in a biodegradation microcosm study. SPME provides an opportunity to run microcosms looking at biodegradation of volatile organics that do not require manual extraction of samples, which often causes problems in quantification, sample loss and disruption to the microcosms.

5.2 Preparation of Standards, Quality Controls and Determination of the Partition Coefficient

In order to minimise any matrix effects or variation in VC partitioning between the gaseous and aqueous phase, serum vials used for the calibration standards were prepared similarly, in triplicate, to the experimental microcosms with SO_4^{2-} rich synthetic groundwater (SG-SO_4^{2-}) compensating for the volume of inocula. An independent check showed the effect of using SG-SO_4^{2-} instead of inocula to be negligible (data not shown). Independent analytical quality controls (AQC) were prepared in the same way. VC addition to the standards was from 100µg/ml in UHQ water diluted from 2000µg VC/ml methanol stock solution (Supelco).

Independent experiments were carried out to determine the partitioning of VC between the headspace and the aqueous phase. Henry's coefficients, H_c (concentration in gas phase/concentration in aqueous phase), were initially obtained for serum vials with UHQ water to compare and confirm with published values and subsequently with serum vials prepared identically to the experimental microcosms. H_c for VC in UHQ water vials was determined to be 1.07, which corresponds well with published values of 1.08 (CRC, 2002; Suthersan, 2002) and 1.06 (Schafer et al., 1998). However, H_c was found to be 2.41 in experimental microcosms. The higher value for the coefficient is not unexpected as the synthetic groundwater contains a variety of salts and increased ionic strength is known to reduce the aqueous solubility of volatile organics, thereby increasing the concentration of volatile compounds in the headspace relative to the aqueous phase (salting-out effect) (Achten and Puttman, 2000; Dewsbury et al., 2003; MacGillivray et al., 1994; Zhang and Pawliszyn, 1996)].

The following sections describe the microcosm experiments investigating direct microbial transformation of VC under SO_4^{2-}-reducing conditions and cometabolic mineralisation of VC by SRB using phenol as the primary growth substrate.

5.3 Experimental Design and Construction of 20 ml Microcosms Investigating VC Oxidation under Anaerobic Conditions

The 20 ml microcosms were prepared in triplicate by addition of 5.0 g clean sediment, 7.2 ml of the SG-SO_4^{2-} and 0.1 ml of the trace metals solution. These were flushed with N_2 and any remaining gases were removed by applying a vacuum (29 in.Hg [73.7 cm], 1.0 Torr) in an evacuation chamber before sealing magnetic, Teflon-lined silicone rubber septa (Jones, UK), in an anaerobic glove-box. The microcosms were autoclaved 3 times (cooled between cycles) at 121°C for 30 minutes in autoclave bags and then allowed to cool in a clean room fitted with a high efficiency, particulate air filter, which constantly removed air from the room and replaced it with purified air. Here, 0.1 ml of vitamin solution and 0.1 ml of $NaHCO_3$ solution were added to the reactors around a Bunsen flame to ensure sterile conditions. The microcosms were inoculated with 2.5 ml anaerobic digester sludge. After a 16-24 hour acclimation period microcosms were amended with ~ 0.3 µg/l VC (99.9% purity as 1 ml ampoules with 2000 µgVC/ml methanol, Supelco Inc., Bellefonte, PA) and mixed thoroughly. Triplicate killed controls, inoculated before sterilisation, were also prepared simultaneously. The microcosm set-up is shown in Table 5.1.

Table 5.1 Summary of 20 ml microcosms prepared to investigate VC oxidation under sulphate-reducing conditions. Killed controls (KC) and live microcosms (VC) were prepared in triplicate.

Microcosm	Conditions	Inoculum	Initial VC (µg/L)
KC-1	Sulphate-reducing	Killed control	0.35
KC-2	Sulphate-reducing	Killed control	0.35
KC-3	Sulphate-reducing	Killed control	0.32
VC-1	Sulphate-reducing	Anaerobic sludge	0.23
VC-2	Sulphate-reducing	Anaerobic sludge	0.22
VC-3	Sulphate-reducing	Anaerobic sludge	0.23

The headspace of standards and samples was sampled using a CombiPAL auto-sampler (CTC Analytics) incorporating an SPME fibre, with a 75µm Carboxen-PDMS (polydimethylsiloxane) polymer coating (Supelco), which was conditioned according to the manufacturers instructions prior to analysis. Following a 10 min sample extraction, the fibre was inserted into a 1079 GC injector at 280°C, with a split ratio of 5:1, to allow

thermal desorption of the extracted analytes. Desorption time was set at 7 min which also allowed the fibre to condition between samples. The Varian 3800 GC, utilising Helium as carrier gas (1ml/min), was equipped with a 30m x 0.25mm, 1.4μm thick film, CP Select-624 fused silica column (Varian Chrompack) and the following temperature programme was employed: column temperature held at 60°C for 5 min, increased to 250°C at a rate of 20°C/min where it was held for 5.5 min. Peak detection and identification was by MS (Varian, Saturn 2000) using a scan range 40-650 m/z, optimised at 40-70 m/z.

5.4 Experimental Design and Construction of 120 ml microcosms Investigating VC Oxidation under SO_4^{2-}-reducing Conditions

5.4.1 Investigation of VC Oxidation under SO_4^{2-}-reducing Conditions in Microcosms Sampled Directly from the Headspace and Analysed by GC-MS

Microcosms were prepared in 120 ml serum vials using the procedure described in Section 5.3 above but with the following modifications; microcosms contained 30 g of clean sediment, 58.2 ml of the SG-SO_4^{2-} and 0.6 ml each of the vitamin, trace metal and $NaHCO_3$ solutions. VC addition was from a high purity gas stock (≥ 99.5%, Fluka) through a gastight syringe, the initial VC concentrations added are shown in Table 5.2.

A total of 18 microcosms were initially prepared, including triplicate killed controls, in 120 ml serum vials and inoculated with enrichments cultured from VC1, VC2, and VC3 from the 20 ml SPME experiment (See Section 2.5.1 for enrichment procedure). Standards were prepared and analysed just prior to analysis of the experimental microcosms. Headspace samples of 200 μL were taken directly from standards and samples using a gas-tight syringe with a luer-lock fitting (Hamilton). The samples were immediately injected into the 1177 GC injector, of a Varian 3800 GC, at 250°C, with a split ratio of 10:1, to allow thermal desorption of the extracted analytes. The GC utilised Helium as carrier gas (1ml/min), was equipped with a 30m x 0.25mm, 1.4μm thick film, CP Select-624 fused silica column (Varian Chrompack) and the following temperature programme was employed: column temperature held at 40°C for 5 min, increased to 230°C at a rate of 25°C/min. Peak detection and identification was by MS (Varian, Saturn 2000) using a scan range 40-650 m/z, optimised at 40-70 m/z.

Headspace samples of 200 µL were also taken, less frequently, for CO_2, CH_4 and C_2H_4 analysis. These were analysed by GC as described in Section 2.3.3.

The redox indicator in the 15 live microcosms changed colour from pink to clear indicating reducing conditions, whilst the killed controls remained pink. However, VC analysis proved problematic, as there was considerable fluctuation in the VC concentrations in both killed controls and live microcosms (data not shown). The variation was most likely due to the volatility of VC that resulted in small but significant losses from the headspace during sampling. Numerous attempts were made to overcome the problem including the use of different syringe types and a range of septa for the serum vials but the experiments were unsuccessful as satisfactory calibration curves and reliable data could not be attained. Therefore, it was decided that an internal calibration standard method would be employed, the justification and description of which is given in Section 5.4.2.

5.4.2 Investigation of VC Oxidation under SO_4^{2-}-reducing Conditions in 120 ml Microcosms Amended with an Internal Standard to Correct for Extraction Losses. Direct Headspace Sampling and Analysis by GC-MS.

The inability to successfully calibrate and analyse VC by direct headspace sampling in 5.4.1 led to incorporation of an internal standard into the methodology. The precision and accuracy of analysis can be improved by the use of internal calibration standards, with similar physico-chemical properties to the compound of interest. Internal calibration standards are known to improve the analytical quality control and precision of analytical methods by minimising extraction errors and accounting for matrix effects (Dewsbury et al., 2003). Fluorobenzene was chosen as the internal standard as it has similar properties to VC and is recommended by the USEPA in method 502.2 for volatile organic compounds analysis and has been used in other studies as an internal standard for analysis of volatiles, including VC (Achten and Puttman, 2000; Martinez et al., 2002). Moreover, fluorobenzene is highly recalcitrant to anaerobic biodegradation: aerobic degradation has only been documented twice previously; by a *Pseudomonas putida* strain growing on a fructose-containing medium and by a consortium of 3 bacterial strains using fluorobenzene as the sole carbon source (Carvalho et al., 2002).

Microcosms were constructed as described in 5.4.1. A total of 12 microcosms (3 killed controls and 9 live) were prepared and inoculated with enrichments cultured from VC1, VC2, and VC3 from the 20 ml SPME experiment (Table 5.1). High purity fluorobenzene (> 99%, Aldrich) was used to prepare a 3333.3 mg/L internal standard stock solution in UHQ. Once prepared each standard, analytical quality control and experimental microcosm received a 10 µL addition of the internal standard with a calibrated gas-tight syringe and were mixed thoroughly. In between sampling, experimental microcosms were stored inverted, in the dark a 20°C. Calibrations were carried out on the morning of the analysis and were found to be linear ($r^2 > 0.99$) [Figure C1.2, Appendix C1]. Headspace samples of 200 µL were taken directly from standards and samples using a gas-tight syringe with a luer-lock fitting (Hamilton). The samples were immediately injected into the 1177 GC injector using the GC-MS conditions described in 5.4.1 above with the internal standard correction function enabled. Headspace samples (200 µL) for CO_2, CH_4 and C_2H_4 analysis, and aqueous sampling (2 ml) for SO_4^{2-} analysis was also carried out, although less frequently. The microcosm set-up for the experiment is shown in Table 5.2.

Table 5.2 Summary of 120 ml microcosms prepared to investigate VC oxidation under sulphate-reducing conditions.

Microcosm designation	Inoculum	Initial headspace VC concentration (µg/L)
Control-1	Killed control	631
Control-2	Killed control	864
Control-3	Killed control	697
Live-B2-1	Enrichment B-2	760
Live-B2-2	Enrichment B-2	656
Live-B2-3	Enrichment B-2	647
Live-A3-1	Enrichment A-3	699
Live-A3-2	Enrichment A-3	743
Live-A3-3	Enrichment A-3	755
Live-C3-1	Enrichment C-3	740
Live-C3-2	Enrichment C-3	756
Live-C3-3	Enrichment C-3	715

5.5 Use of Solid-Phase Micro-extraction (SPME) in Conjunction with GC-MS to Determine VC in a Microcosm Experiment Investigating Direct Microbial Transformation of VC under SO_4^{2-}-reducing Conditions.

Calibrations were linear ($r^2 > 0.99$) (Figure C1.1, Appendix C1) and VC was successfully detected at 1 ppb demonstrating the sensitivity of the method. The redox indicator, resazurin, changed colour from pink to clear indicating reducing and, therefore, anaerobic conditions. Initial experimental microcosms, inoculated with anaerobic digester sludge, showed VC degradation, as shown in Figure 5.2 (ii), whereas there was no VC loss in killed controls after 51 days [(Figure 5.2(i)]. At the final sampling point after 51 days, VC concentrations in live microcosms 1, 2 and 3 had fallen by 77.01%, 78.27% and 91.9%, of the initial concentration, respectively. This contrasted with a maximum of 14.7% loss from killed controls.

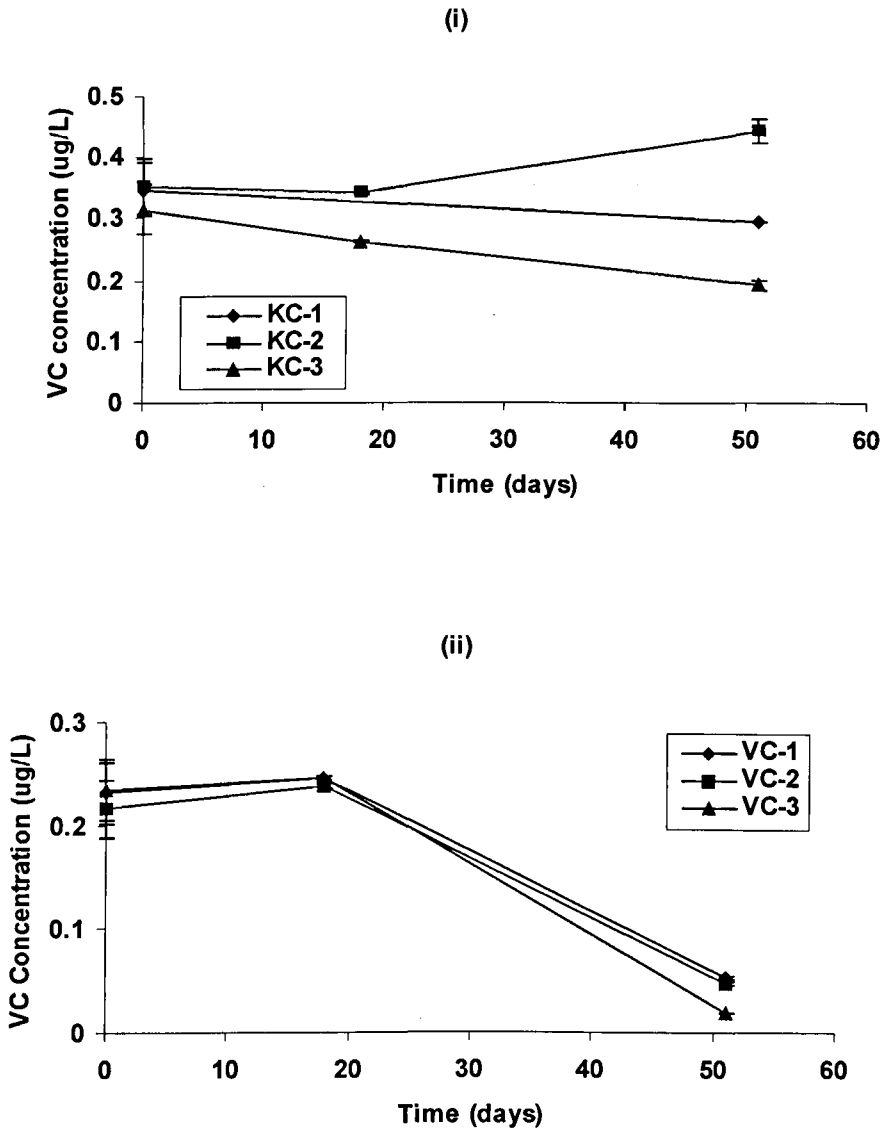

Figure 5.2 Headspace VC concentrations in (i) killed controls (KC) and (ii) 20 ml microcosms inoculated with anaerobic digester sludge . Error bars represent the % relative standard deviation of the mean, of triplicate analytical quality controls.

The redox dye indicated that anaerobic conditions were maintained throughout the experiment. As the synthetic groundwater was rich in SO_4^{2-} (~ 500 mg/L), it's likely that degradation was coupled to SO_4^{2-}-reduction because methanogenesis was unlikely to have occurred at such high dissolved SO_4^{2-} concentrations. It's possible that Fe^{3+}-reduction occurred as the sediment material contains iron oxides at 0.8 wt.% (Spence et al., 2001a) that may have been reduced to Fe^{2+}. The results suggest that VC oxidation may have taken place under anaerobic conditions, which has been previously documented (Bradley and Chapelle, 1996; Bradley and Chapelle, 1998a; Bradley and

Chapelle, 1998b; Bradley and Chapelle, 1998c; Bradley et al., 1998a; Bradley et al., 1998b; Bradley et al., 1998c; Chapelle et al., 1996; Landmeyer et al., 1998; Vroblesky et al., 1996).

Utilisation of the SPME method was successful in this biodegradation experiment, however the experiment had the following limitations:

- The microcosm volume of 20 ml was too small to enable sampling of the aqueous phase for analysis of electron acceptors (e.g. Fe^{3+}, SO_4^{2-}) and the gas phase for biogenic gases

- The SPME fibre removes some of the volatile organic compound each time a sample is taken, which eventually leads to depletion of the analyte. However, a higher initial concentration and shorter extraction time can counter this effect to enable longer-term experiments.

- The SPME auto-sampler did not have sampling trays suitable to analyse the 120 ml microcosms although this limitation could have been overcome with time.

Due to the above limitations it was decided to carry out further experiments in larger, 120 ml, microcosms as these would allow scope for more sampling and analysis of reactants and products such as electron acceptors and biogenic gases. Due to the auto-sampler limitations VC was determined by direct headspace sampling and injection into the GC-MS, as described in 5.4.2.

5.6 Microcosm Study, using 120 ml Microcosms, Investigating Direct Microbial Transformation of VC under SO_4^{2-}-reducing Conditions, Inoculated with Anaerobic Digester Sludge Enrichments.

Within 1 week of inoculation the redox indicator changed colour from pink to clear in microcosms Live-A3-1, -2 and -3 indicating reducing conditions, whereas the other 6 live microcosms changed colour 15 days later. The killed controls remained pink throughout the course of the experiment. The VC data from the GC-MS analysis is shown in Figures 5.3 to 5.5 below. No VC degradation was seen in killed controls [Figure 5.3 (i)], or any of the live microcosms [Figures 5.3 (ii), 5.4 and 5.5] over a

period of 169 days. No ethene or methane was detected in the microcosms (Data not shown).

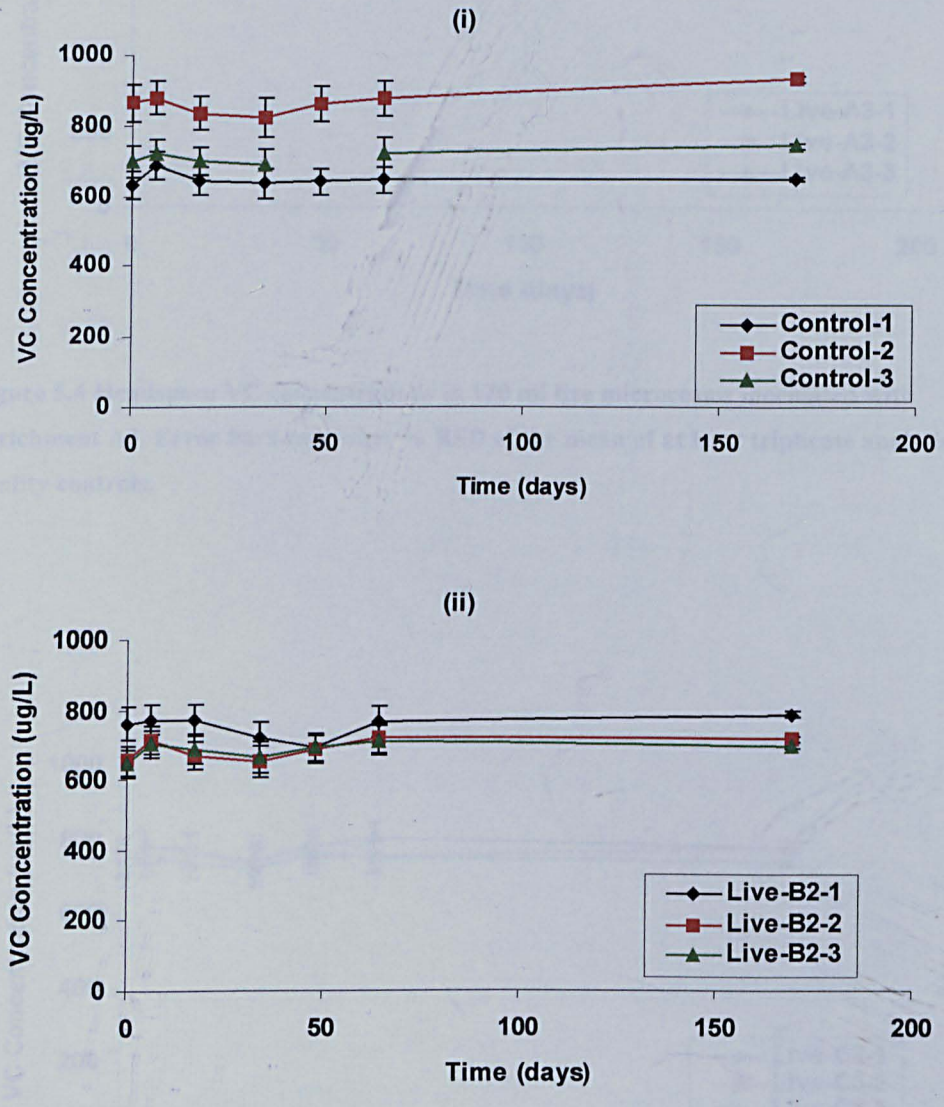

Figure 5.3 Direct VC oxidation experiment in 120 ml microcosms. Headspace VC concentrations determined by GC-MS in killed controls (i) and live microcosms inoculated with enrichment B-2 (ii). Error bars represent % RSD of the mean of at least triplicate analytical quality controls.

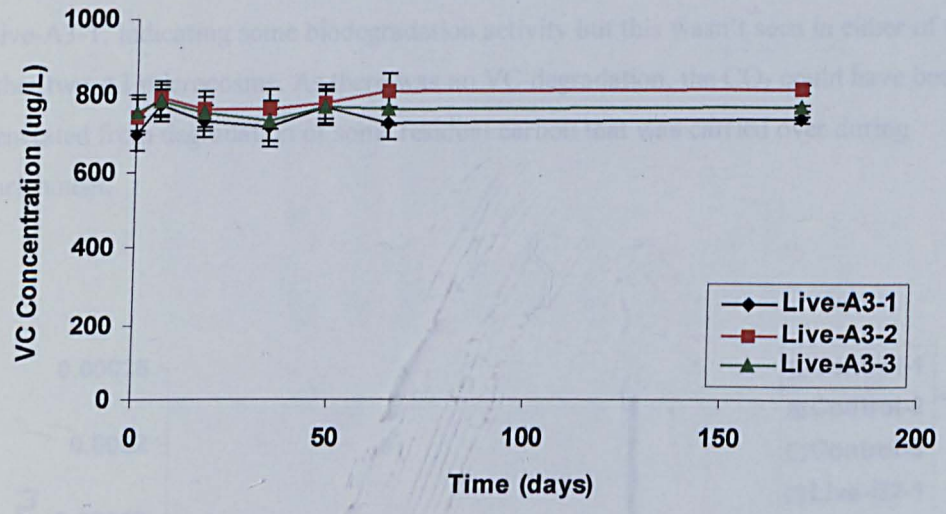

Figure 5.4 Headspace VC concentrations in 120 ml live microcosms inoculated with enrichment A3. Error bars represent % RSD of the mean of at least triplicate analytical quality controls.

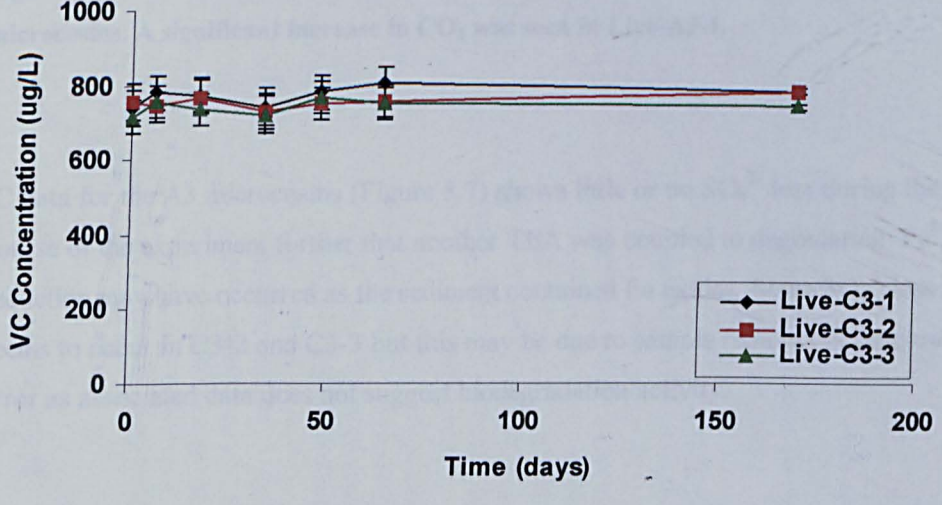

Figure 5.5 Headspace VC concentrations in 120 ml live microcosms inoculated with enrichment C3. Error bars represent % RSD of the mean of at least triplicate analytical quality controls.

Concentrations of CO_2 are shown in Figure 5.6. There was a CO_2 increase in microcosm Live-A3-1, indicating some biodegradation activity but this wasn't seen in either of the other two A3 microcosms. As there was no VC degradation, the CO_2 could have been generated from degradation of some residual carbon that was carried over during enrichment.

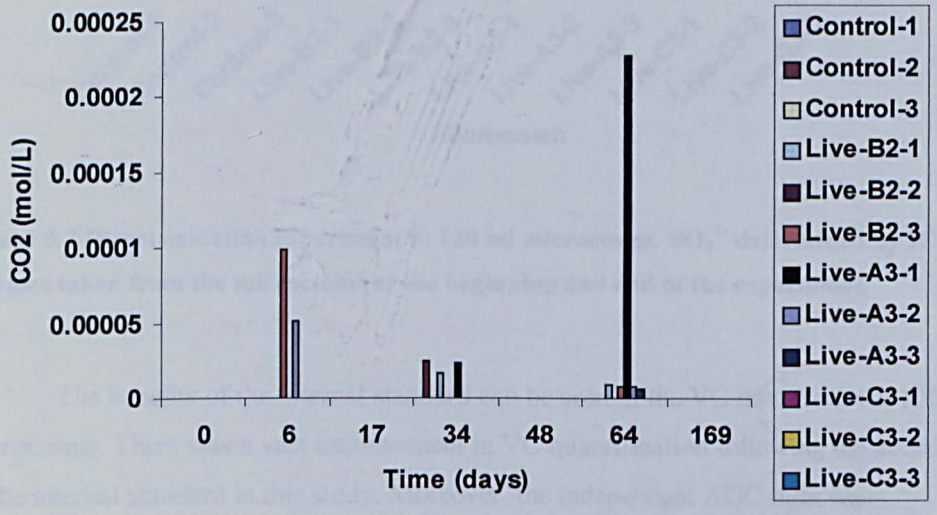

Figure 5.6 CO_2 concentrations by GC in direct oxidation experiment utilising 120 ml microcosms. A significant increase in CO_2 was seen in Live-A3-1.

IC data for the A3 microcosms (Figure 5.7) shows little or no SO_4^{2-} loss during the course of the experiment further that another TEA was coupled to degradation. Fe^{3+}-reduction may have occurred as the sediment contained Fe oxides. Some SO_4^{2-} loss seems to occur in C3-2 and C3-3 but this may be due to sample removal or preparation error as associated data does not suggest biodegradation activity.

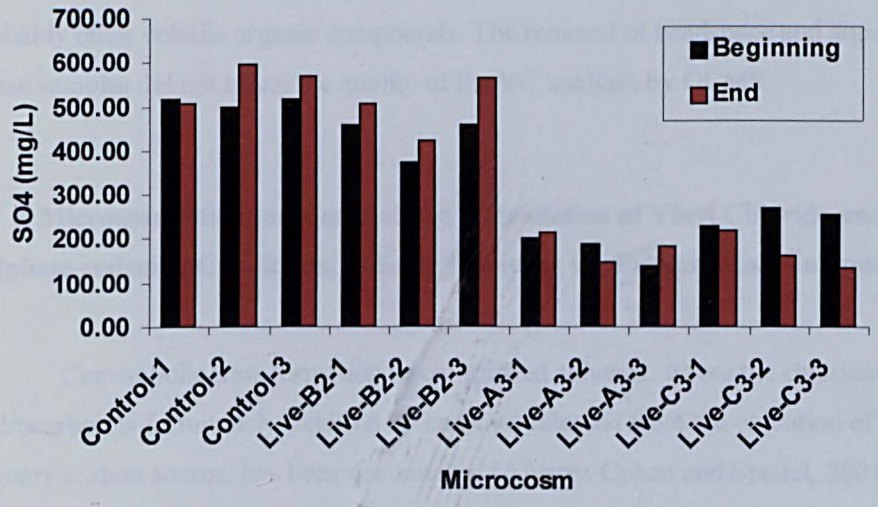

Figure 5.7 Direct oxidation experiment in 120 ml microcosms. SO_4^{2-} determined by IC from samples taken from the microcosms at the beginning and end of the experiment.

The benefits of the internal standard can be seen in the VC data from the 120 ml microcosms. There was a vast improvement in VC quantification following the addition of the internal standard in this study. Moreover, the independent AQC data was consistently accurate over the course of the169 day experiment (Figure 5.8). In fact, the %RSD of the 25, 295 µg/L AQC's run throughout the experiment was only 5.8%.

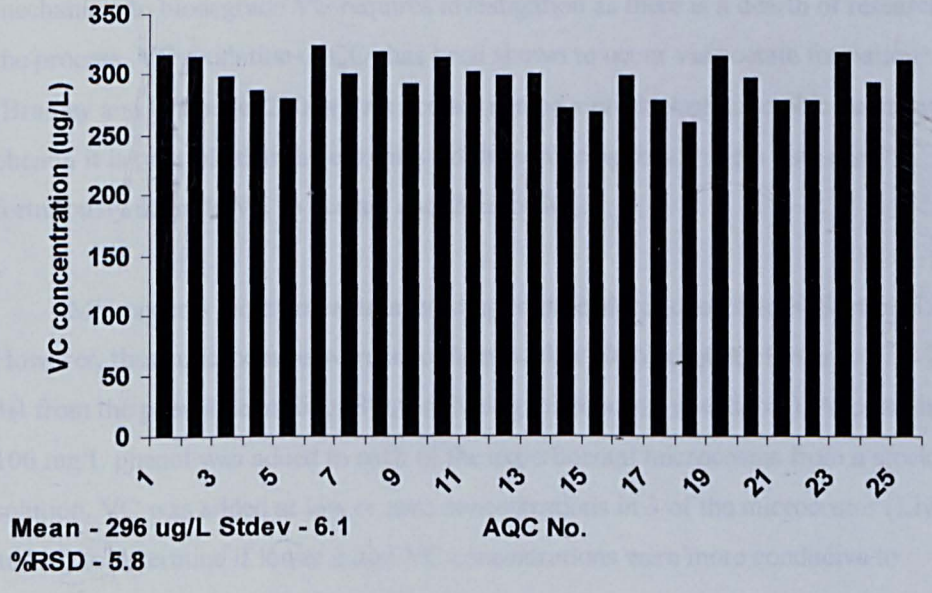

Figure 5.8 VC concentration in 25 analytical quality controls (AQC's) analysed by GC-MS over the course of the 169 day, direct oxidation, 120 ml microcosm experiment.

The method is suitable to run long-term experiments on VC biodegradation and most probably other volatile organic compounds. The removal of headspace and aqueous phase samples did not affect the quality of the VC analysis by GCMS.

5.7 A Microcosm Study on Cometabolic Degradation of Vinyl Chloride under Sulphate-reducing Conditions, utilising Phenol as the Primary Carbon Source.

Cometabolic transformation of chlorinated solvents, where the chlorinated hydrocarbon is fortuitously oxidised by enzymes released from the oxidation of another primary carbon source, has been documented (Alvarez-Cohen and Speitel, 2001; Chang and AlvarezCohen, 1997; Gao and Skeen, 1999; Hopkins et al., 1993a; Landmeyer et al., 1998; Lee et al., 2000; Lerner et al., 2000; Mousavi and Sarlack, 1997; Semprini et al., 1992). The process has mainly been documented under aerobic conditions, although cometabolic degradation could take place anaerobically (Wiedemeier et al., 1998). Anaerobic co-metabolism has previously been documented in biodegradation studies, including under SO_4^{2-}-reducing conditions (Annweiler et al., 2001; Daun et al., 1998). The rate of cometabolic activity increases as the degree of dechlorination decreases (McCarty and Semprini, 1994; Vogel, 1994), therefore VC would potentially be more susceptible to cometabolic biodegradation than its parent compounds. McCarty and Semprini (1994) suggest that VC has some potential to undergo anaerobic cometabolism with production of CO_2 via acetic acid. The possibility of anaerobic cometabolism as a mechanism to biodegrade VC requires investigation as there is a dearth of research into the process. VC oxidation to CO_2 has been shown to occur via acetate formation (Bradley and Chapelle, 2000a). As acetate can be a product of anaerobic degradation of phenol, it is possible that the enzymes produced during this process may also fortuitously degrade VC to acetate and then to CO_2.

Microcosms were prepared according to procedures described in Section 5.4.2. However, these microcosms were inoculated with a 10 ml aliquot of microcosms 2A and 3B from the phenol degrading, SO_4^{2-}-reducing microcosms (Section 3). Approximately 100 mg/L phenol was added to each of the experimental microcosms from a stock solution. VC was added at low or zero concentrations in 3 of the microcosms (Live-4, -5 and -6) to determine if lower initial VC concentrations were more conducive to cometabolic biodegradation. The internal standard method was employed with 10 µL of the fluorobenzene stock added to experimental microcosm, standards and AQC's. The experimental set-up is shown in Table 5.3.

Table 5.3 Summary of 120 ml microcosms prepared to investigate cometabolic oxidation of VC under sulphate-reducing conditions, using phenol as the primary substrate.

Microcosm designation	Inoculum	Initial VC (μg/L)	Initial phenol (mg/L)
Con-1	Killed control	821	107.9
Con-2	Killed control	837	97.0
Con-3	Killed control	987	100.6
Live-1	Phenol degrading microcosm 2A	240	100.0
Live-2	Phenol degrading microcosm 2A	628	84.7
Live-3	Phenol degrading microcosm 2A	1018	127.0
Live-4	Phenol degrading microcosm 3B	76	165.7[α]
Live-5	Phenol degrading microcosm 3B	107	167.8[α]
Live-6	Phenol degrading microcosm 3B	0	167.8[α]

[α] **Estimated from additions to microcosms as samples not available for analysis**

Headspace samples of 200 μL were taken directly from standards and samples using a gas-tight syringe with a luer-lock fitting (Hamilton). The samples were immediately injected into the 1177 GC injector using the GC-MS conditions described in Section 5.4.1 above. Less frequent headspace sampling (200 μL) for CO_2, CH_4 and C_2H_4 analysis, and aqueous sampling (2 ml) for SO_4^{2-} analysis was also carried out.

The redox indicator changed colour from pink to clear in all live microcosms within 1 week of preparation indicating reducing conditions. The controls remained pink. VC concentrations for live microcosms and controls are shown in Figure 5.9.

(i)

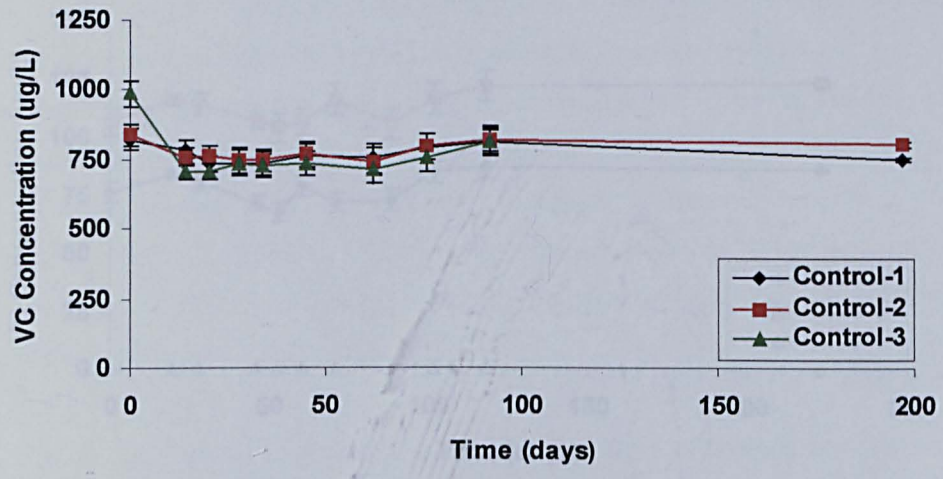
1250
1000
750
500
250
0
VC Concentration (ug/L)
0
50
100
150
200
Time (days)
Control-1
Control-2
Control-3

(ii)

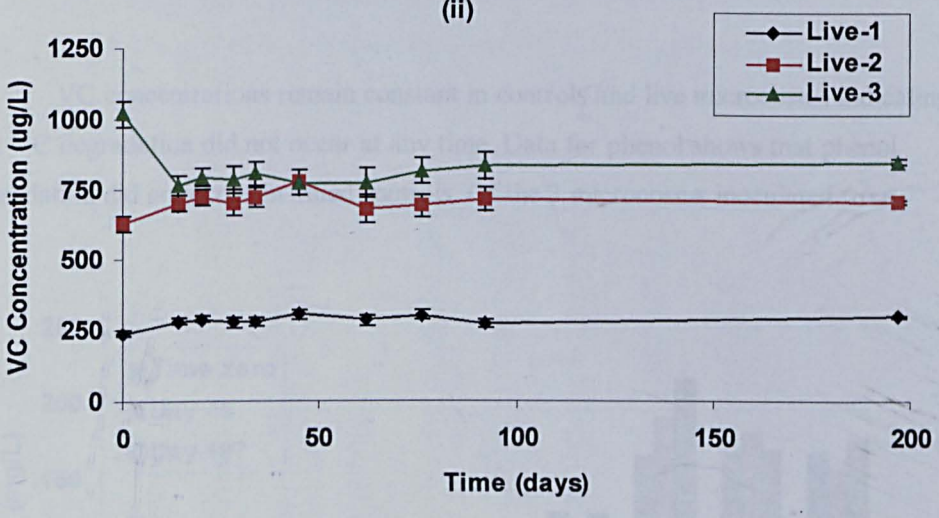
1250
1000
750
500
250
0
VC Concentration (ug/L)
0
50
100
150
200
Time (days)
Live-1
Live-2
Live-3

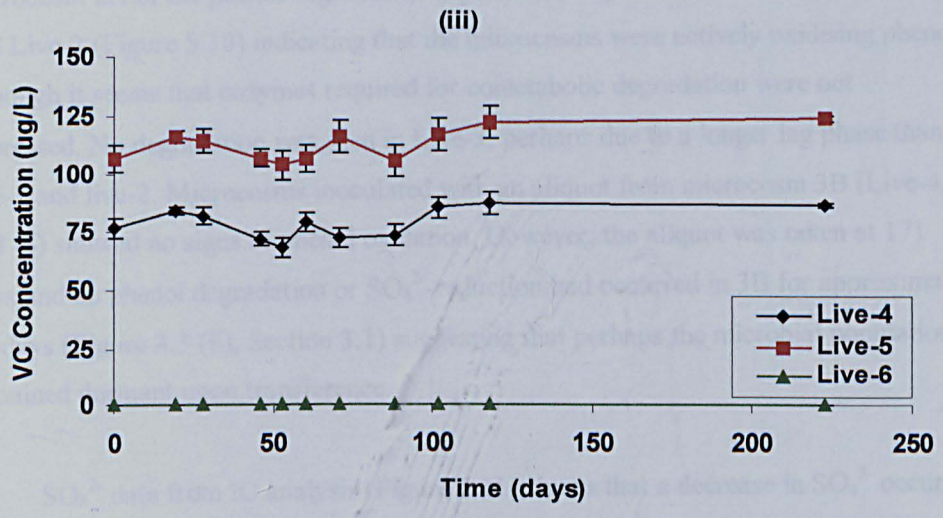

Figure 5.9 Phenol co-metabolism experiment. VC concentrations by GC-MS in killed controls (i), live microcosms at high initial VC inoculated with 2A from phenol experiment (ii), and live microcosms at low or zero initial VC inoculated with 3B from phenol experiment (iii). Error bars represent % RSD of the mean of at least triplicate analytical quality controls.

VC concentrations remain constant in controls and live microcosms indicating that VC degradation did not occur at any time. Data for phenol shows that phenol degradation did not occur in killed controls. Of the 3 microcosms inoculated from

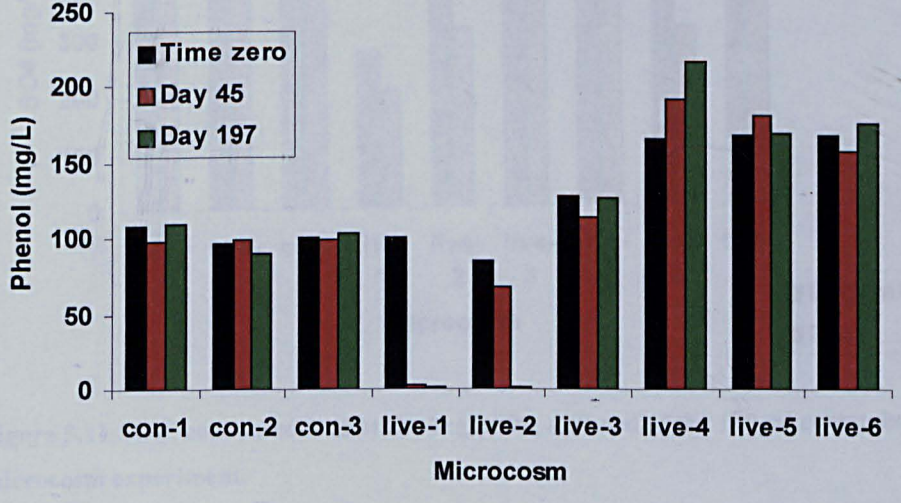

Figure 5.10 Phenol concentrations in 120 ml cometabolic microcosms. Phenol degradation occurs in microcosms live-1 and live-2.

microcosm 2A of the phenol degradation experiment, degradation occurred in Live-1 and Live-2 (Figure 5.10) indicating that the microcosms were actively oxidising phenol although it seems that enzymes required for cometabolic degradation were not expressed. No degradation was seen in Live-3, perhaps due to a longer lag phase than live-1 and live-2. Microcosms inoculated with an aliquot from microcosm 3B (Live-4, -5 and -6) showed no signs of phenol oxidation. However, the aliquot was taken at 171 days and no phenol degradation or SO_4^{2-}-reduction had occurred in 3B for approximately 70 days (Figure 3.3 (ii), Section 3.1) suggesting that perhaps the microbial population remained dormant upon transference.

SO_4^{2-} data from IC analysis (Figure 5.11) shows that a decrease in SO_4^{2-} occurs in microcosms Live-1, Live-2, and Live-5 indicating that perhaps phenol degradation is coupled to SO_4^{2-}-reduction. For microcosm live-1 the concentration of SO_4^{2-} degraded is only 19% of the amount of predicted by the theoretical stochiometric equation for phenol oxidation (Table 1.2, Section 1), indicating that perhaps Fe(III)-reduction occurred as Fe oxides were present in the sediment (See section3.7). However, the decrease of SO_4^{2-} in live-2 is 77% of the expected theoretical concentration, suggesting that SO_4^{2-}-reduction is the TEAP and is coupled to phenol oxidation in this microcosm.

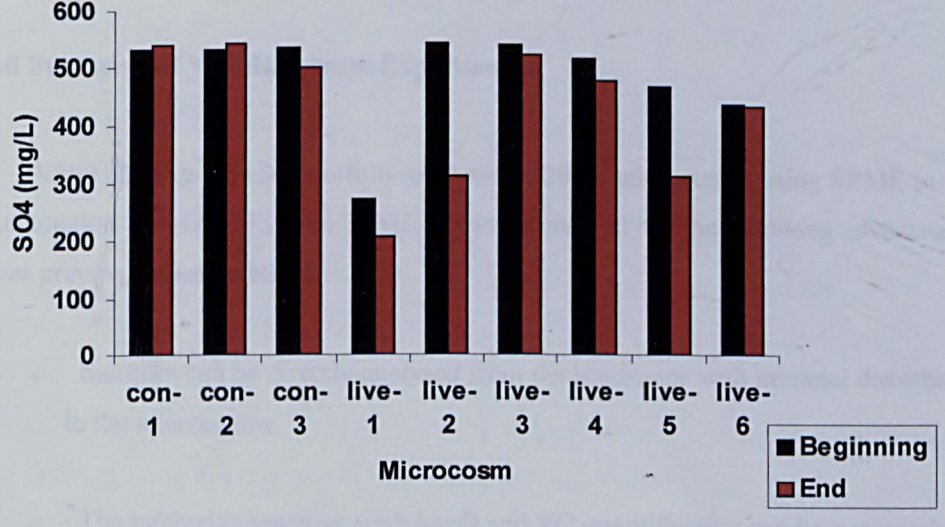

Figure 5.11 SO_4^{2-} concentrations at the beginning and end of the 120 ml cometabolic microcosm experiment.

The SO_4^{2-} loss in live-5 may be due to analytical error as the CO_2 data shows that significant CO_2 was only produced in microcosms Live-1 and Live-2 (Figure 5.12). The

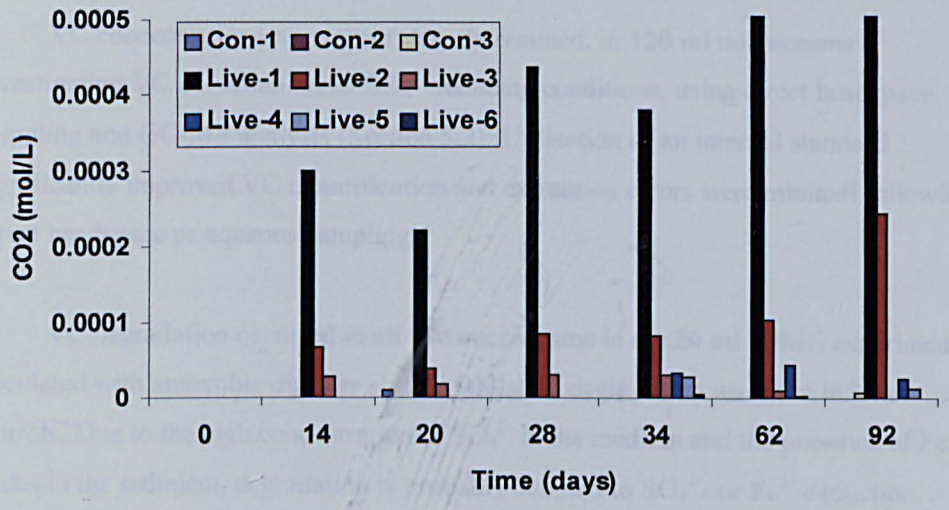

Figure 5.12 CO_2 concentrations in 120 ml cometabolic microcosms. CO_2 production only occurs in microcosms Live-1 and Live-2.

CO_2 data confirms the trends seen in Figures 5.10 and 5.11, that phenol oxidation only occurs in microcosms live-1 and live-2 which were inoculated with microcosm 2A of the phenol degradation experiment. Phenol was utilised as the primary substrate in microcosms Live-1 and Live-2, but VC was not cometabolically degraded.

5.8 Summary of VC Microcosm Experiments

Vinyl chloride was successfully analysed in 20 ml microcosms using SPME in conjunction with GC-MS. The SPME analytical method has the following advantages over previously used methods:

- Samples can be directly analysed from the headspace with minimal disturbance to the microcosms.
- The method is sensitive (ppb level) and VC quantification can be accurately, and precisely carried out by SPME with only very small extraction errors
- Utilisation of an internal standard, such as fluorobenzene, would reduce extraction errors and provide the opportunity to run long-term microcosms that could be frequently sampled for additional reactants (e.g. Fe^{3+} and SO_4^{2-}) and products (H_2)

VC concentrations were accurately determined, in 120 ml microcosms investigating VC oxidation under SO_4^{2-}-reducing conditions, using direct headspace sampling and GC-MS analysis (Section 5.2). Utilisation of an internal standard significantly improved VC quantification and extraction errors were minimal following direct headspace or aqueous sampling.

VC degradation occurred in all live microcosms in the 20 ml SPME experiment inoculated with anaerobic digester sludge, whilst no degradation was seen in killed controls. Due to the high concentration of SO_4^{2-} in the medium and the presence of Fe oxides in the sediment, degradation is probably coupled to SO_4^{2-}- or Fe^{3+}-reduction. However, further studies in the form of 120 ml microcosms were carried to confirm these results.

VC degradation was not seen in any of the microcosms inoculated with the enrichment cultures indicating that the microbial consortia had no capability to degrade VC under the conditions in these microcosms. This suggests that either the results from the 20 ml microcosm were erroneous or that the VC degrading culture was not grown successfully during the enrichment process. It's possible that during sub-culturing, a cofactor present in the digester sludge was diluted so that the organisms could not grow or perhaps there was some oxygen contamination during sub-culturing which adversely affected growth. Absolute confirmation of degradation would have been more likely had an internal standard, such as fluorobenzene, been utilised in the 20 ml microcosms, as any extraction errors would have been minimised.

VC was successfully analysed in cometabolic microcosms inoculated with microbes from the phenol degradation experiment (Section 5.3). Although phenol degradation and SO_4^{2-}-reduction was seen in microcosms Live-1 and Live-2, cometabolic VC degradation did not occur indicating that VC degradation could not be stimulated by products of phenol oxidation or perhaps the enzymes required were not expressed. Although no VC degradation was seen in either of the 120 ml microcosm experiments, direct VC oxidation under SO_4^{2-}-reducing conditions has been reported once previously with inocula from stream-bed sediments contaminated with chlorinated solvents (Bradley and Chapelle, 1998a; Bradley and Chapelle, 1998b; Bradley and Chapelle, 1998c; Bradley et al., 1998a; Bradley et al., 1998b; Bradley et al., 1998c; Landmeyer et al., 1998). The absence of anaerobic degradation in microcosms inoculated with anaerobic digester sludge enrichments or phenol degrading SO_4^{2-}-

reducers from a phenolics contaminated site suggests that, perhaps, the potential to degrade VC is limited to SO_4^{2-}-reducers that have had a history of exposure to VC in the natural environment or that specific environmental conditions are required.

This work has shown the difficulties inherent in analysing for volatile reactive organic compounds, such as VC. As mentioned in Section 5.1, previous studies documenting degradation have sampled microcosms by purge and trap techniques and used radiolabeled VC (Bradley and Chapelle, 1998a; Bradley and Chapelle, 1998b; Bradley and Chapelle, 1998c; Bradley et al., 1998a; Bradley et al., 1998b; Bradley et al., 1998c; Davis and Carpenter, 1990; Klecka et al., 1990; Landmeyer et al., 1998). Other than sampling difficulties, these methods have other disadvantages including accidental purging of VC with CO_2 during sampling, introduction of water into the GC, peak broadening due to inefficient sample transfer and impurities in the radio-labeled VC. The methodology in the experiments presented removes some of the problems associated with previous microcosm techniques and have shown that this methodology is suitable for long-term microcosm experiments, and forms a sound basis for future studies of VC degradation under various electron-accepting conditions.

Further experiments are needed to study direct VC oxidation under a range of electron accepting conditions to quantify its capability to remediate VC contamination and gain insights into the metabolic pathways involved. Research is also required to improve our understanding of the microbial processes and organisms involved, in terms of the VC oxidation capability and whether it is inherent in specific types of microorganisms or in a consortium. The possibility of anaerobic cometabolic oxidation of VC requires further investigation, as there is a dearth of research into this process. Although there is potential for cometabolic degradation of VC, a better understanding of the enymatic pathways involved in direct VC oxidation would allow a better assessment of suitable primary cometabolic substrates. The internal standard method is suitable to quantify reactants and products including VC, electron acceptors, biodegradation products and biomass as both gaseous and aqueous samples can be removed. Therefore, it can be utilised in future studies into VC biodegradation.

6. CONCLUSIONS

6.1 Phenol Biodegradation Capability of SRB from a Highly Contaminated Field Site.

Biodegradation of phenol coupled to SO_4^{2-}-reduction occurred in all live microcosms inoculated with bacteria from the four-ashes field site. Phenol degraded readily at initial concentrations of ≤ 235 mg/L, with concurrent SO_4^{2-}-reduction and a lag phase of 19 days in all live microcosms. Phenol biodegradation continued until concentrations of phenol were close to zero. However, degradation ceased when sulphate concentrations fell below ~ 100mg/L, and resumed upon addition of sulphate indicating that there was a critical minimum sulphate requirement for degradation coupled to SO_4^{2-}-reduction to occur. This effect also confirmed that reduction of sulphate was the TEAP following the initial phenol addition.

Biodegradation coupled to SO_4^{2-}-reduction continued in microcosms amended with between 575 mg/L and 770 mg/L phenol with no lag phase. Degradation proceeds at these phenol concentrations until it is limited by low concentrations of sulphate. High sulphate (~ 1590 mg/L) also seemed to limit phenol degradation and sulphate loss indicating that there may have been an inhibitory effect due to the sulphate toxicity. This may have been less significant had the sulphate concentrations been increased gradually. Oxidation of phenol concentrations of up to 770 mg/L under sulphidogenic conditions has not been reported in bacteria from sediment or groundwater systems. Previous studies have shown phenol to be inhibitory or toxic at concentrations between 200 mg/L and 600 mg/L, not only to sulphate-reducing bacteria but also to bacteria utilising alternative electron acceptors under anaerobic conditions. The degradative capability of the bacteria may be due to adaptation following previous exposure to phenolic compounds at the contaminated field site. Phenol degradation with reduction of sulphate was also observed at concentrations of ~ 900 mg/L, although alternative electron accepting processes such as methanogenesis and fermentation may also contributed to phenol oxidation.

Inhibition of phenol degradation and SO_4^{2-}-reduction occurred in microcosms amended with phenol between ~ 1000 mg/L and ~ 1330 mg/L indicating that ~ 1000

mg/L is the toxicity threshold for the sulphate-reducing bacteria. Phenol oxidation recommenced after 253 days in microcosms with ~ 1330 mg/L phenol, but no sulphate loss was seen indicating that another electron acceptor was utilised. As the microcosms were still anaerobic as evidenced by the clear colour of the redox indicator, it is likely that methanogenesis and/or fermentation was occurring.

Average degradation rates were relatively high in comparison to published values following the initial phenol addition (≤ 235 mg/L). In all microcosms, the rate was high to begin with and then fell as the phenol concentration decreased which is consistent with the Monod kinetic model for biodegradation. Average degradation rates fell following amendment with phenol between 575 mg/L and 770 mg/L except in microcosms starved of phenol for 50 to 119 days, indicating that the microorganisms are fairly resilient, and perhaps lay dormant or utilised intermediate products until the microcosms were amended with additional phenol. Average degradation rates were lowest following amendment with ~ 1000 mg/L to ~ 1330 mg/L phenol which is consistent with inhibition of the sulphate-reducing bacteria.

Results from stoichiometric calculations, based on the theoretical equation for phenol oxidation under sulphate-reducing conditions, correlated well with the experimental data. Following the initial phenol addition (≤ 235 mg/L), the experimental sulphate loss often corresponded to between 80% and 100% of the expected theoretical value for the amount of phenol oxidised emphasising that SO_4^{2-}-reduction was the TEAP. The calculated values for SO_4^{2-}-reduction again correlate well with experimental data at concentrations of 575 mg/L and 770 mg/L phenol but the percentage falls or is zero at concentrations of ~ 1000 mg/L and ~ 1330 mg/L, respectively and so does not account for the phenol oxidised at the higher concentrations. The redox indicator remained clear indicating anaerobiosis, therefore conditions did not become aerobic. Although iron-reduction occurred, it could only contribute to a maximum of ~ 30 mg/L phenol loss, therefore it is highly likely that fermentation and/or methanogenesis occurred following cessation or inhibition of SO_4^{2-}-reduction. This is confirmed by the H_2 analysis as concentrations are in the range for SO_4^{2-}-reduction (1-4 nM) throughout the experiment until phenol concentrations are extremely high (≥ 1000 mg/L), sulphate concentrations are low (< 50 mg/L) or too high (~ 1590 mg/L), and at these times the H_2 concentrations reflect those found under methanogenic conditions (5-25 nM).

Microbial growth and evidence of anaerobiosis was seen on the SO_4^{2-}-reducing agar slopes. DNA was successfully extracted from the isolates and a single fragment was obtained from 16S amplification. The closest match for both isolates was to *Pseudomonas Stutzeri* which is a denitrifier commonly found in soil and water environments. It seems that *Pseudomonas Stutzeri* out-competed the SRB on the agar slopes and therefore the sulphate-reducers could not be isolated and identified. This may have occurred during transportation of the samples, as the redox indicator had turned pink upon arrival for sequencing.

6.2 Monod Kinetic Modelling of Phenol Biodegradation Data

Phenol biodegradation curves obtained from the model correlate well with the experimental data, as do predicted biomass concentrations at the conclusion of the experiment. Values for k_{max} (maximum phenol utilisation rate) are between 4.90×10^{-8}/s and 3.74×10^{-6}/s. They fall within the range expected of phenol biodegradation coupled to SO_4^{2-}-reduction based on literature values. The values for k_{max} fall, as expected, as the phenol concentrations are increased (2nd addition) from the initial 1.4×10^{-3} mol/L to 6.6×10^{-3} mol/L in 2A, and 4.4×10^{-3} mol/L in 2B. The same trend is seen when the concentrations in 2A and 2B are increased (3rd addition) to 9.0×10^{-3} mol/L and 8.7×10^{-3} mol/L, respectively. Half-saturation constants K_P (phenol) and K_{SO4} (sulphate) were determined to be 2.0×10^{-4} mol/L and 3.7×10^{-4}, respectively. These values are of the same order of magnitude but higher than those reported in the literature. This is consistent with the results of Section 3, where the microbial consortia's phenol biodegradation capability and the rate at which they oxidised phenol are higher than previously documented. The kinetic parameters obtained can contribute towards predictions of in situ bioremediation of phenol in conjunction with an effective modelling approach that incorporates scaling-up methods and the biological reactions involved.

6.3 Methodology and Microcosms Investigating Oxidative Microbial Transformation of Vinyl Chloride

Vinyl chloride was successfully analysed in 20 ml microcosms using SPME in conjunction with GC-MS. The SPME analytical method allowed direct analysis of VC from the headspace with no sample preparation and minimal disturbance to the microcosms. The method was sensitive (ppb level) and VC quantification was with only very small extraction errors

VC concentrations were accurately determined, in 120 ml microcosms investigating VC oxidation under SO_4^{2-}-reducing conditions, using direct headspace sampling and GC-MS analysis. Utilisation of an internal standard significantly improved VC quantification and extraction errors were minimal following direct headspace or aqueous sampling.

VC degradation occurred in all live microcosms in the 20 ml SPME experiment inoculated with anaerobic digester sludge, whilst no degradation was seen in killed controls. Due to the high concentration of SO_4^{2-} in the medium and the presence of Fe oxides in the sediment, any degradation was probably coupled to SO_4^{2-}- or Fe^{3+}-reduction. Subsequent experiments on 120 ml microcosms were not able to confirm the results of this experiment, perhaps due to problems in sub-culturing the microorganisms.

VC degradation was not seen in any of the microcosms inoculated with the enrichment cultures indicating that the microbial consortia had no capability to degrade VC under the conditions in these microcosms. This suggests that either the results from the 20 ml microcosm were erroneous or that the VC degrading culture was not grown successfully during the enrichment process. It's possible that during sub-culturing, a cofactor present in the digester sludge was diluted so that the organisms could not grow or perhaps there was some oxygen contamination that adversely affected growth. Absolute confirmation of degradation would have been more likely had an internal standard, such as fluorobenzene, been utilised in the 20 ml microcosms, as any extraction errors would have been minimised.

VC was successfully analysed in cometabolic microcosms inoculated with microbes from the phenol degradation experiment. Although phenol degradation and SO_4^{2-}-reduction was seen in microcosms live-1 and live-2, cometabolic VC degradation

did not occur indicating that VC degradation could not be stimulated by products of phenol oxidation or perhaps the enzymes required were not expressed. As direct VC oxidation under SO_4^{2-}-reducing conditions has only been reported once previously with inocula from stream-bed sediments contaminated with chlorinated solvents, perhaps, the potential to degrade VC is limited to SO_4^{2-}-reducers that have had a history of exposure to VC in the natural environment, or that specific environmental conditions are required.

This work has shown the difficulties inherent in analysing for volatile reactive organic compounds, such as VC. The methodology presented in these experiments removes some of the problems associated with previous microcosm techniques such as purge and trap and forms a sound basis for future long term studies of VC degradation under various electron-accepting conditions.

6.4 Implications for MNA and Enhanced In Situ Bioremediation

The results from these microcosms could have implications for enhanced in-situ bioremediation of phenol contaminated sites. The results show that indigenous microbial populations have the capability to degrade higher concentrations of phenol than previously documented. In particular, sulphate-reduction could contribute considerably to phenol bioremediation. Half-life calculations on phenol biodegradation results suggest that concentrations of up to 575 mg/L may be remediated within 6 years, if environmental conditions were suitable (e.g. in terms of bacterial numbers, electron acceptor concentration). In the presence of an active sulphate-reducing bacterial population, biodegradation would eventually be limited by low sulphate concentrations either because of low background concentrations or depletion due to use as an electron acceptor. Therefore, additional sulphate would need to be supplied to bioremediate high concentrations of phenol in groundwater. The introduction of additional electron acceptors such a SO_4^{2-} and NO_3^- has already been demonstrated to successfully enhance bioremediation of BTEX contaminated groundwater and can also be used at phenol contaminated sites.

6.5 Further Work

It would be interesting to identify the phenol degrading, sulphate-reducing microorganism to determine whether specific microorganisms perform degradation of high phenol concentrations. Identification of the bacteria would allow comparisons with existing data on microorganisms from sediment and groundwater environments and provide information for future phenol bioremediation studies.

The SPME method requires further investigation as it could be a useful tool in laboratory microcosm studies. Utilisation of an internal standard, such as fluorobenzene, would reduce extraction errors and provide the opportunity to run long-term microcosms that could be frequently sampled for additional reactants and products.

Additional experimentation is required into direct oxidation of VC under various electron-accepting conditions. Information is required on the microbes responsible, biological processes and biochemical reactions occurring. Further laboratory based microcosm studies can contribute to our understanding of these processes, their biological potential and how we may enhance degradation of VC at contaminated sites.

The possibility of anaerobic cometabolism as a mechanism to biodegrade VC requires investigation as there is a dearth of research on this subject. Moreover the pathways, in terms of enzymes and co-factors involved are poorly understood and elucidation of these could open up a number of possibilities for further research.

Further microcosm investigations studies, on both phenol and VC, in tandem with field based studies can improve our understanding of the factors that control phenol and VC degradation.

7. REFERENCES

Achten, C. and Puttman, W., 2000. Determination of Methyl *tert*-Butyl Ether in Surface Water by use of Solid-Phase Microextraction. Environmental Science & Technology, 34(7): 1359-1364.

Acuna-Arguelles, M.E., Olguin-Lora, P. and Razo-Flores, E., 2003. Toxicity and kinetic parameters of the aerobic biodegradation of the phenol and alkylphenols by a mixed culture. Biotechnology Letters, 25(7): 559-564.

Albrechtsen, H.J. and Christensen, T.H., 1994. Evidence For Microbial Iron Reduction in a Landfill Leachate-Polluted Aquifer (Vejen, Denmark). Applied and Environmental Microbiology, 60(11): 3920-3925.

Alvarez-Cohen, L. and Speitel, G.E., 2001. Kinetics of aerobic cometabolism of chlorinated solvents. Biodegradation, 12(2): 105-126.

Ambujom, S. and Manilal, V.B., 1995. Phenol Degradation by a Stable Aerobic Consortium and Its Bacterial Isolates. Biotechnology Letters, 17(4): 443-448.

Annweiler, E., Michaelis, W. and Meckenstock, R.U., 2001. Anaerobic cometabolic conversion of benzothiophene by a sulfate-reducing enrichment culture and in a tar-oil- contaminated aquifer. Applied and Environmental Microbiology, 67(11): 5077-5083.

Appelo, C.A.J. and Postma, D., 1999. Geochemistry, groundwater and pollution. A.A. Balkema, Rotterdam.

Arthur, C.L. and Pawliszyn, J., 1990. Solid phase microextraction with thermal desorption using fused silica optical fibres. Journal of Analytical Chemistry, 62: 2145-2148.

ATSDR, 1990. Case Studies in Environmental Medicine: Vinyl Chloride Toxicity, Agency for Toxic Substances and Disease Registry, US Public Health Service, US Department of Health and Human Services, Atlanta, Georgia.

ATSDR, 1993. Toxicological Profile for Vinyl Chloride, Agency for Toxic Substances and Disease Registry, US Public Health Service, US Department of Health and Human Services, Atlanta, Georgia.

Ballapragada, B.S., Stensel, H.D., Puhakka, J.A. and Ferguson, J.F., 1997. Effect of hydrogen on reductive dechlorination of chlorinated ethenes. Environmental Science & Technology, 31(6): 1728-1734.

Bandyopadhyay, K., Das, D. and Maiti, B.R., 1998. Kinetics of phenol degradation using Pseudomonas putida MTCC 1194. Bioprocess Engineering, 18(5): 373-377.

Bekins, B.A., Warren, E. and Godsy, E.M., 1998. A comparison of zero-order, first-order, and Monod biotransformation models. Ground Water, 36(2): 261-268.

Beller, H.R., Grbic Galic, D. and Reinhard, M., 1992a. Microbial degradation of toluene under sulfate-reducing conditions and the influence of iron on the process. APPLIED AND ENVIRONMENTAL MICROBIOLOGY, 58(3): 786-793.

Beller, H.R., Grbicgalic, D. and Reinhard, M., 1992b. Microbial-Degradation of Toluene Under Sulfate-Reducing Conditions and the Influence of Iron On the Process. Applied and Environmental Microbiology, 58(3): 786-793.

Bolliger, C., Schroth, M.H., Bernasconi, S.M., Kleikemper, J. and Zeyer, J., 2001. Sulfur isotope fractionation during microbial sulfate reduction by toluene-degrading bacteria. Geochimica Et Cosmochimica Acta, 65(19): 3289-3298.

Bone, T.L. and Balkwill, D.L., 1988. Morphological and Cultural Comparison of Microorganisms in Surface Soil and Subsurface Sediments at a Pristine Study Site in Oklahoma. Microbial Ecology, 16(1): 49-64.

Boopathy, R., 1997. Anaerobic phenol degradation by microorganisms of swine manure. Current Microbiology, 35(1): 64-67.

Boopathy, R., Kulpa, C.F. and Manning, J., 1998. Anaerobic biodegradation of explosives and related compounds by sulfate-reducing and methanogenic bacteria: a review. Bioresource Technology, 63(1): 81-89.

Borch, T., Ambus, P., Laturnus, F., Svensmark, B. and Gron, C., 2003. Biodegradation of chlorinated solvents in a water unsaturated topsoil. Chemosphere, 51(2): 143-152.

Bradley, P.M., 2000. Microbial degradation of chloroethenes in groundwater systems. Hydrogeology Journal, 8(1): 104-111.

Bradley, P.M. and Chapelle, F.H., 1996. Anaerobic mineralization of vinyl chloride in Fe(III)-reducing, aquifer sediments. Environmental Science & Technology, 30(6): 2084-2086.

Bradley, P.M. and Chapelle, F.H., 1997. Kinetics of DCE and VC mineralization under methanogenic and Fe(III)-reducing conditions. Environmental Science & Technology, 31(9): 2692-2696.

Bradley, P.M. and Chapelle, F.H., 1998a. Effect of contaminant concentration on aerobic microbial mineralization of DCE and VC in stream-bed sediments. Environmental Science & Technology, 32(5): 553-557.

Bradley, P.M. and Chapelle, F.H., 1998b. Microbial mineralization of VC and DCE under different terminal electron accepting conditions. Anaerobe, 4(2): 81-87.

Bradley, P.M. and Chapelle, F.H., 1998c. Microbial mineralization of VC and DCE under different terminal electron accepting conditions [Full text delivery]. Anaerobe, 4(2): 81-87.

Bradley, P.M. and Chapelle, F.H., 2000a. Acetogenic microbial degradation of vinyl chloride. Environmental Science & Technology, 34(13): 2761-2763.

Bradley, P.M. and Chapelle, F.H., 2000b. Aerobic microbial mineralization of dichloroethene as sole carbon substrate. Environmental Science & Technology, 34(1): 221-223.

Bradley, P.M., Chapelle, F.H. and Lovley, D.R., 1998a. Humic acids as electron acceptors for anaerobic microbial oxidation of vinyl chloride and dichloroethene. Applied and Environmental Microbiology, 64(8): 3102-3105.

Bradley, P.M., Chapelle, F.H. and Wilson, J.T., 1998b. Field and laboratory evidence for intrinsic biodegradation of vinyl chloride contamination in a Fe(III)-reducing aquifer. Journal of Contaminant Hydrology, 31(1-2): 111-127.

Bradley, P.M., Landmeyer, J.E. and Dinicola, R.S., 1998c. Anaerobic oxidation of 1,2-C-14 dichloroethene under Mn(IV)- reducing conditions. Applied and Environmental Microbiology, 64(4): 1560-1562.

Broholm, K. and Arvin, E., 2001. Biodegradation of creosote compounds: Comparison of experiments at different scales. Ground Water Monitoring and Remediation, 21(4): 101-108.

Broholm, M.M. and Arvin, E., 2000. Biodegradation of phenols in a sandstone aquifer under aerobic conditions and mixed nitrate and iron reducing conditions. Journal of Contaminant Hydrology, 44(3-4): 239-273.

Broholm, M.M., Crouzet, C., Arvin, E. and Mouvet, C., 2000. Concurrent nitrate and Fe(III) reduction during anaerobic biodegradation of phenols in a sandstone aquifer. Journal of Contaminant Hydrology, 44(3-4): 275-300.

Calabrese, E.J. and Kenyon, E.M., 1991. Air Toxics and Risk Assessment. Lewis Publishers, Chelsea, Michigan.

Caldwell, M.E., Garrett, R.M., Prince, R.C. and Suflita, J.M., 1998. Anaerobic biodegradation of long-chain n-alkanes under sulfate- reducing conditions. Environmental Science and Technology, 32(14): 2191-2195.

Carey, M.A., Finnamore, J.R., Morrey, M.J. and Marsland, P.A., 2000. Guidance on the assessment and monitoring of natural attenuation of contaminants in groundwater, Environment Agency R&D Publication 95, Environment Agency.

Carvalho, M.F., Alves, C.C.T., Ferreira, M.I.M., De Marco, P. and Castro, P.M.L., 2002. Isolation and Initial Characterization of a Bacterial Consortium Able to

Mineralize Fluorobenzene. Applied and Environmental Microbiology, 68(1): 102-105.

Chai, M., Arthur, C.L., Pawliszyn, J., Belardi, R.P. and Pratt, K.F., 1993. Determination of Volatile Chlorinated Hydrocarbons in Air and Water With Solid-phase Microextraction. Analyst, 118: 1501-1505.

Chang, H.L. and AlvarezCohen, L., 1997. Two-stage methanotrophic bioreactor for the treatment of chlorinated organic wastewater. Water Research, 31(8): 2026-2036.

Chapelle, F.H., 2000. The significance of microbial processes in hydrogeology and geochemistry. Hydrogeology Journal, 8(1): 41-46.

Chapelle, F.H., 2001. Groundwater Microbiology and Geochemistry. John Wiley & Sons Inc., New York.

Chapelle, F.H., Bradley, P.M., Lovley, D.R. and Vroblesky, D.A., 1996. Measuring Rates of Biodegradation in a Contaminated Aquifer Using Field and Laboratory Methods. Ground Water, 34(4): 691-698.

Charvet, R., Cun, C. and Leroy, P., 2000. Vinyl Chloride analysis with Solid Phase Microextraction (SPME)/GC/MS applied to analysis in materials and aqueous samples. Analusis, 29: 980-987.

Coates, J.D., Anderson, R.T. and Lovley, D.R., 1996a. Oxidation of polycyclic aromatic hydrocarbons under sulfate-reducing conditions. Applied and Environmental Microbiology, 62(3): 1099-1101.

Coates, J.D., Anderson, R.T., Woodward, J.C., Phillips, E.J.P. and Lovley, D.R., 1996b. Anaerobic Hydrocarbon Degradation in Petroleum-Contaminated Harbor Sediments Under Sulfate-Reducing and Artificially Imposed Iron- Reducing Conditions. Environmental Science & Technology, 30(9): 2784-2789.

CRC, 2002. Handbook of Chemistry and Physics. CRC Press LLC, Boca Raton.

Cunningham, J.A., Rahme, H., Hopkins, G.D., Lebron, C. and Reinhard, M., 2001. Enhanced In Situ Bioremediation of BTEX-Contaminated Groundwater by Combined Injection of Nitrate and Sulfate. Environmental Science & Technology, 35(8): 1663-1670.

Daun, G., Lenke, H., Reuss, M. and Knackmuss, H.J., 1998. Biological treatment of TNT-contaminated soil. 1. Anaerobic cometabolic reduction and interaction of TNT and metabolites with soil components. Environmental Science & Technology, 32(13): 1956-1963.

Davis, G.B. et al., 1999. The variability and intrinsic remediation of a BTEX plume in anaerobic sulphate-rich groundwater. Journal of Contaminant Hydrology, 36(3-4): 265-290.

Davis, J.W. and Carpenter, C.L., 1990. Aerobic Biodegradation of Vinyl-Chloride in Groundwater Samples. Applied and Environmental Microbiology, 56(12): 3878-3880.

Davis, J.W. et al., 2002. Natural attenuation of chlorinated solvents at Area 6, Dover Air Force Base: characterization of microbial community structure. Journal of Contaminant Hydrology, 57(1-2): 41-59.

Deng, B.L., Burris, D.R. and Campbell, T.J., 1999. Reduction of vinyl chloride in metallic iron-water systems. Environmental Science & Technology, 33(15): 2651-2656.

Devlin, J.F. and Muller, D., 1999. Field and laboratory studies of carbon tetrachloride transformation in a sandy aquifer under sulfate reducing conditions. Environmental Science & Technology, 33(7): 1021-1027.

Dewsbury, P., Thornton, S.F. and Lerner, D.N., 2003. Improved analysis of MTBE, TAME, and TBA in petroleum fuel-contaminated groundwater by SPME using deuterated internal standards with GC-MS. Environmental Science & Technology, 37(7): 1392-1397.

Distefano, T.D., 1999. The effect of tetrachloroethene on biological dechlorination of vinyl chloride: Potential implication for natural bioattenuation. Water Research, 33(7): 1688-1694.

ECVM, 1999. Vinyl Chloride Monomer (VCM), European Council of Vinyl Manufactureres (ECVM), Available from: ECVM, Ave E Van Nieuwenhuyse 4, Box 4, B-1160, Brussels, Belgium.

Edwards, E.A., Wills, L.E., Reinhard, M. and Grbic Galic, D., 1992a. Anaerobic degradation of toluene and xylene by aquifer microorganisms under sulfate-reducing conditions. APPLIED AND ENVIRONMENTAL MICROBIOLOGY, 58(3): 794-800.

Edwards, E.A., Wills, L.E., Reinhard, M. and Grbicgalic, D., 1992b. Anaerobic Degradation of Toluene and Xylene By Aquifer Microorganisms Under Sulfate-Reducing Conditions. Applied and Environmental Microbiology, 58(3): 794-800.

EEC, 1988. EUROPEAN COMMUNITIES (QUALITY OF WATER INTENDED FOR HUMAN CONSUMPTION) REGULATIONS (No. 80/778/EEC)(1).

Ehrlich, G.G., Godsy, E.M., Goerlitz, D.F. and Hult, M.F., 1983. Microbial Ecology of a Creosote-Contaminated Aquifer At St-Louis Park, Minnesota. Developments in Industrial Microbiology, 24: 235-245.

Ellis, L., 2000. Tetrachloroethene Pathway Map (Anaerobic). University of Minnesota Biocatalysis/Biodegradation Database.

Eweis, J.B., Ergas, S.J., Chang, D.P.Y. and Schroeder, E.D., 1998. Bioremediation Principles. WCB/McGraw Hill, Malaysia.

Fauque, G.D., 1995. Ecology of Sulfate-Reducing Bacteria. In: L.L. Barton (Editor), Sulfate-Reducing Bacteria. Biotechnology Handbooks. Plenum Press, New York, pp. 217-241.

Fetter, C.W., 1994. Applied Hydrogeology. Prentice-Hall, Inc., New Jersey.

Fetter, C.W., 1999. Contaminant Hydrogeology. Prentice-Hall Inc., New Jersey.

Flyvbjerg, J., Arvin, E., Jensen, B.K. and Olsen, S.K., 1993. Microbial-Degradation of Phenols and Aromatic-Hydrocarbons in Creosote-Contaminated Groundwater Under Nitrate-Reducing Conditions. Journal of Contaminant Hydrology, 12(1-2): 133-150.

Gao, J.W. and Skeen, R.S., 1999. Glucose-induced biodegradation of cis-dichloroethylene under aerobic conditions. Water Research, 33(12): 2789-2796.

Genthner, B.R.S., Townsend, G.T. and Chapman, P.J., 1991. Para-Hydroxybenzoate As an Intermediate in the Anaerobic Transformation of Phenol to Benzoate. Fems Microbiology Letters, 78(2-3): 265-270.

Gerritse, J., Renard, V., Visser, J. and Gottschal, J.C., 1995. Complete Degradation of Tetrachloroethene by Combining Anaerobic Dechlorinating and Aerobic Methanotrophic Enrichment Cultures. Applied Microbiology and Biotechnology, 43(5): 920-928.

Ghiorse, W.C. and Wilson, J.T., 1988. Microbial Ecology of the Terrestrial Subsurface. Advances in Applied Microbiology, 33: 107-172.

Godsy, E.M., Goerlitz, D.F. and Ehrlich, G.G., 1983. Methanogenesis of Phenolic-Compounds By a Bacterial Consortium From a Contaminated Aquifer in St-Louis Park, Minnesota. Bulletin of Environmental Contamination and Toxicology, 30(3): 261-268.

Gruntzig, V., Nold, S.C., Zhou, J. and Tiedje, J.M., 2001. *Pseudomonas Stutzeri* Nitrite Reductase Gene Abundance in Environmental Samples Measured by Real-Time PCR. Applied and Environmental Microbiology, 67(2): 760-768.

Haggblom, M.M., Rivera, M.D. and Young, L.Y., 1993a. Effects of Auxiliary Carbon-Sources and Electron-Acceptors On Methanogenic Degradation of Chlorinated Phenols. Environmental Toxicology and Chemistry, 12(8): 1395-1403.

Haggblom, M.M., Rivera, M.D. and Young, L.Y., 1993b. Influence of Alternative Electron Acceptors on the Anaerobic Biodegradability of Chlorinated Phenols and Benzoic Acids. Applied and Environmental Microbiology, 59(4): 1162-1167.

Haggblom, M.M. and Young, L.Y., 1995. Anaerobic Degradation of Halogenated Phenols by Sulfate- Reducing Consortia. Applied and Environmental Microbiology, 61(4): 1546-1550.

Hao, O.J., Chen, J.M., Huang, L. and Buglass, R.L., 1996. Sulfate-reducing bacteria. Critical Reviews in Environmental Science and Technology, 26(2): 155-187.

Harrison, I. et al., 2001. Microcosm studies of microbial degradation in a coal tar distillate plume. Journal of Contaminant Hydrology, 53(3-4): 319-340.

Hartmans, S. and Debont, J.A.M., 1992. Aerobic Vinyl-Chloride Metabolism in Mycobacterium-Aurum L1. Applied and Environmental Microbiology, 58(4): 1220-1226.

Hartmans, S., Debont, J.A.M., Tramper, J. and Luyben, K., 1985. Bacterial-Degradation of Vinyl-Chloride. Biotechnology Letters, 7(6): 383-388.

He, J.Z. et al., 2002. Acetate versus hydrogen as direct electron donors to stimulate the microbial reductive dechlorination process at chloroethene- contaminated sites. Environmental Science & Technology, 36(18): 3945-3952.

Higgo, J.J.W., Nielsen, P.H., Bannon, M.P., Harrison, I. and Christensen, T.H., 1996. Effect of geochemical conditions on fate of organic compounds in groundwater. Environmental Geology, 27(4): 335-346.

Hirayama, K., Akashi, S., Furuya, M. and Fukuhara, K., 1990. Rapid Confirmation and Revision of the Primary Structure of Bovine Serum-Albumin by Esims and Frit-Fab Lc Ms. Biochemical and Biophysical Research Communications, 173(2): 639-646.

Hopkins, G.D., Munakata, J., Semprini, L. and McCarty, P.L., 1993a. Trichloroethylene Concentration Effects On Pilot Field-Scale in-Situ Groundwater Bioremediation By Phenol-Oxidizing Microorganisms. Environmental Science & Technology, 27(12): 2542-2547.

Hopkins, G.D., Semprini, L. and McCarty, P.L., 1993b. Microcosm and in-Situ Field Studies of Enhanced Biotransformation of Trichloroethylene By Phenol-Utilizing Microorganisms. Applied and Environmental Microbiology, 59(7): 2277-2285.

Hunkeler, D., Aravena, R. and Cox, E., 2002. Carbon isotopes as a tool to evaluate the origin and fate of vinyl chloride: Laboratory experiments and modeling of isotope evolution. Environmental Science & Technology, 36(15): 3378-3384.

Jakobsen, R. et al., 1998. H-2 concentrations in a landfill leachate plume (Grindsted, Denmark): In situ energetics of terminal electron acceptor processes. Environmental Science & Technology, 32(14): 2142-2148.

Kazumi, J., Haggblom, M.M. and Young, L.Y., 1995. Degradation of Monochlorinated and Nonchlorinated Aromatic-Compounds Under Iron-Reducing Conditions. Applied and Environmental Microbiology, 61(11): 4069-4073.

Kennedy, L.G., Everett, J.W., Dewers, T., Pickins, W. and Edwards, D., 1999. Application of mineral iron and sulfide analysis to evaluate natural attenuation at fuel contaminated site. Journal of Environmental Engineering-Asce, 125(1): 47-56.

Keppler, F., Borchers, R., Pracht, J., Rheinberger, S. and Scholer, H.F., 2002. Natural formation of vinyl chloride in the terrestrial environment. Environmental Science & Technology, 36(11): 2479-2483.

Klecka, G.M., Davis, J.W., Gray, D.R. and Madsen, S.S., 1990. Natural bioremediation of organic contaminants in ground water. Cliffs-dow superfund site. Ground Water, 28(4): 534-543.

Kleikemper, J. et al., 2002. Activity and diversity of sulfate-reducing bacteria in a petroleum hydrocarbon-contaminated aquifer. Applied and Environmental Microbiology, 68(4): 1516-1523.

Koziollek, P., Bryniok, D. and Knackmuss, H.J., 1999. Ethene as an auxiliary substrate for the cooxidation of cis- 1,2-dichloroethene and vinyl chloride. Archives of Microbiology, 172(4): 240-246.

Kuhlmann, B. and Schottler, U., 1996. Influence of different redox conditions on the biodegradation of the pesticide metabolites phenol and chlorophenols. International Journal of Environmental Analytical Chemistry, 65(1-4): 289-295.

Landmeyer, J.E., Chapelle, F.H., Petkewich, M.D. and Bradley, P.M., 1998. Assessment of natural attenuation of aromatic hydrocarbons in groundwater near a former manufactured-gas plant, South Carolina, USA. Environmental Geology, 34(4): 279-292.

Lay, J.J. and Cheng, S.S., 1998. Influence of hydraulic loading rate on UASB reactor treating phenolic wastewater. Journal of Environmental Engineering-Asce, 124(9): 829-837.

Lee, S.B., Strand, S.E. and Stensel, H.D., 2000. Sustained degradation of trichloroethylene in a suspended growth gas treatment reactor by an actinomycetes enrichment. Environmental Science & Technology, 34(15): 3261-3268.

LeGall, J. and Xavier, A.V., 1996. Anaerobes response to oxygen: The sulfate-reducing bacteria. Anaerobe, 2(1): 1-9.

Lehmann, K.B. and Neumann, R., 1896. Atlas und Grunriss der Bakteriologie und Lehrbuch der Speciellen Bakteriologischen Diagnostik. J.F. Lehmann, Munchen.

Lerner, D.N. et al., 2000. Ineffective natural attenuation of degradable organic compounds in a phenol-contaminated aquifer. Ground Water, 38(6): 922-928.

Lin, Y.H. and Lee, K.K., 2001. Verification of anaerobic biofilm model for phenol degradation with sulfate reduction. Journal of Environmental Engineering-Asce, 127(2): 119-125.

Londry, K.L., Fedorak, P.M. and Suflita, J.M., 1997. Anaerobic degradation of m-cresol by a sulfate-reducing bacterium. Applied and Environmental Microbiology, 63(8): 3170-3175.

Lovley, D.R., Coates, J.D., Woodward, J.C. and Phillips, E.J.P., 1995. Benzene Oxidation Coupled to Sulfate Reduction. Applied and Environmental Microbiology, 61(3): 953-958.

Lovley, D.R. et al., 1998. Humic substances as a mediator for microbially catalyzed metal reduction. Acta Hydrochimica Et Hydrobiologica, 26(3): 152-157.

Lovley, D.R. et al., 1993. Geobacter-Metallireducens Gen-Nov Sp-Nov, a Microorganism Capable of Coupling the Complete Oxidation of Organic-Compounds to the Reduction of Iron and Other Metals. Archives of Microbiology, 159(4): 336-344.

Lovley, D.R. and Goodwin, S., 1988. Hydrogen Concentrations as an Indicator of the Predominant Terminal Electron-Accepting Reactions in Aquatic Sediments. Geochimica Et Cosmochimica Acta, 52(12): 2993-3003.

Lovley, D.R. and Lonergan, D.J., 1990. Anaerobic Oxidation of Toluene, Phenol, and Para-Cresol By the Dissimilatory Iron-Reducing Organism, Gs-15. Applied and Environmental Microbiology, 56(6): 1858-1864.

Lovley, D.R. and Phillips, E.J.P., 1988a. Manganese Inhibition of Microbial Iron Reduction in Anaerobic Sediments. Geomicrobiology Journal, 6(3-4): 145-155.

Lovley, D.R. and Phillips, E.J.P., 1988b. Novel Mode of Microbial Energy-Metabolism - Organic-Carbon Oxidation Coupled to Dissimilatory Reduction of Iron or Manganese. Applied and Environmental Microbiology, 54(6): 1472-1480.

Ludvigsen, L., Albrechtsen, H.J., Heron, G., Bjerg, P.L. and Christensen, T.H., 1998. Anaerobic microbial redox processes in a landfill leachate contaminated aquifer (Grindsted, Denmark). Journal of Contaminant Hydrology, 33(3-4): 273-291.

MacGillivray, B., Pawliszyn, J., Fowlie, P. and Sagara, C., 1994. Headspace Solid-Phase Microextraction versus Purge and Trap for the Determination of Substituted Benzene Compounds in Water. Journal of Chromatographic Science, 32: 317-322.

Madigan, M.T., Martinko, J.M. and Parker, J., 1997. Brock Biology of Microorganisms. Prentice-Hall, Inc., New Jersey.

Mahapatra, S., Mahapatra, M. and Mondal, B., 2002. Phenol - an indicator of groundwater pollution by industrial effluents in Durgapur, West Bengal. Journal of the Geological Society of India, 59(3): 259-263.

Martinez, E., Lacorte, S., Llobet, I., Viana, P. and Barcelo, D., 2002. Multicomponent analysis of volatile organic compounds in water by automated purge and trap coupled to gas chromatography-mass spectrometry. Journal of Chromatography A, 959(1-2): 181-190.

Mayer, K.U., Benner, S.G., Frind, E.O., Thornton, S.F. and Lerner, D.N., 2001. Reactive transport modeling of processes controlling the distribution and natural attenuation of phenolic compounds in a deep sandstone aquifer. Journal of Contaminant Hydrology, 53(3-4): 341-368.

Maymo-Gatell, X., Anguish, T. and Zinder, S.H., 1999. Reductive dechlorination of chlorinated ethenes and 1,2- dichloroethane by "Dehalococcoides ethenogenes" 195. Applied and Environmental Microbiology, 65(7): 3108-3113.

Maymo-Gatell, X., Nijenhuis, I. and Zinder, S.H., 2001. Reductive dechlorination of cis-1,2-dichloroethene and vinyl chloride by "Dehalococcoides ethenogenes". Environmental Science & Technology, 35(3): 516-521.

McCarty, P.L. and Semprini, L., 1994. Ground-water Treatment for Chlorinated Solvents. In: R.D. Norris et al. (Editors), Handbook of Bioremediation. Lewis Publishers, Boca Raton, Florida.

Monserrate, E. and Haggblom, M.M., 1997. Dehalogenation and biodegradation of brominated phenols and benzoic acids under iron-reducing, sulfidogenic, and methanogenic conditions. Applied and Environmental Microbiology, 63(10): 3911-3915.

Mort, S.L. and Deanross, D., 1994. Biodegradation of Phenolic-Compounds by Sulfate-Reducing Bacteria from Contaminated Sediments. Microbial Ecology, 28(1): 67-77.

Mousavi, M.F. and Sarlack, N., 1997. Spectrophotometric determination of trace amounts of sulfide ion based on its catalytic reduction reaction with Methylene Blue in the presence of Te(IV). Analytical Letters, 30(8): 1567-1578.

Ndon, U.J., Randall, A.A. and Khouri, T.Z., 2000. Reductive dechlorination of tetrachloroethylene by soil sulfate-reducing microbes under various electron donor conditions. Environmental Monitoring and Assessment, 60(3): 329-336.

Okabe, S., Nielsen, P.H., Jones, W.L. and Characklis, W.G., 1995. Sulfide Product Inhibition of Desulfovibrio-Desulfuricans in Batch and Continuous Cultures. Water Research, 29(2): 571-578.

Parker, S.P., 1980. McGraw-Hill Encyclopedia of Environmental Science. McGraw-Hill Inc.

Pedersen, K. and Ekendahl, S., 1990. Distribution and Activity of Bacteria in Deep Granitic Groundwaters of Southeastern Sweden. Microbial Ecology, 20(1): 37-52.

Peyton, B.M., Wilson, T. and Yonge, D.R., 2002. Kinetics of phenol biodegradation in high salt solutions. Water Research, 36(19): 4811-4820.

Phelps, C.D., Kazumi, J. and Young, L.Y., 1996. Anaerobic degradation of benzene in BTX mixtures dependent on sulfate reduction. Fems Microbiology Letters, 145(3): 433-437.

Postgate, J.R., 1984. The sulphate-reducing bacteria. Cambridge University Press, Cambridge.

Price, M., 1996. Introducing Groundwater. Chapman & Hall, UK.

Ramanand, K. and Suflita, J.M., 1991. Anaerobic Degradation of Meta-Cresol in Anoxic Aquifer Slurries - Carboxylation Reactions in a Sulfate-Reducing Bacterial Enrichment. Applied and Environmental Microbiology, 57(6): 1689-1695.

Reis, M.A.M., Almeida, J.S., Lemos, P.C. and Carrondo, M.J.T., 1992. Effect of Hydrogen-Sulfide on Growth of Sulfate Reducing Bacteria. Biotechnology and Bioengineering, 40(5): 593-600.

Rosner, B.M., McCarty, P.L. and Spormann, A.M., 1997. In vitro studies on reductive vinyl chloride dehalogenation by an anaerobic mixed culture. Applied and Environmental Microbiology, 63(11): 4139-4144.

Salanitro, J.P., Wisniewski, H.L., Byers, D.L., Neaville, C.C. and Schroder, R.A., 1997. Use of aerobic and anaerobic microcosms to assess BTEX biodegradation in aquifers. Ground Water Monitoring and Remediation, 17(3): 210-221.

Sambrook, J., Fritsch, E.F. and Maniatis, T., 1989. Molecular Cloning: A Laboratory Manual. Cold Spring Harbour Laboratory Press, New York.

Sawyer, C.N., McCarty, P.L. and Parkin, G.F., 1994. Chemistry for Environmental Engineering. McGraw-Hill Inc., Singapore.

Schafer, D., Schafer, W. and Kinzelbach, W., 1998. Simulation of reactive processes related to biodegradation in aquifers - 2. Model application to a column study on organic carbon degradation. Journal of Contaminant Hydrology, 31(1-2): 187-209.

Schirmer, M., Molson, J.W., Frind, E.O. and Barker, J.F., 2000. Biodegradation modelling of a dissolved gasoline plume applying independent laboratory and field parameters. Journal of Contaminant Hydrology, 46(3-4): 339-374.

Schwarzenbach, R.P., Gschwend, P.M. and Imboden, D.M., 2003. Environmental Organic Chemistry. John Wiley & Sons, Inc., New Jersey.

Semprini, L., Hopkins, G.D., Roberts, P.V. and McCarty, P.L., 1992. Pilot Scale Field Studies of Insitu Bioremediation of Chlorinated Solvents. Journal of Hazardous Materials, 32(2-3): 145-162.

Shah, N.W., 1999. Natural attenuation of organic pollutants in groundwater: anaerobic biodegradation of phenol under sulphate-reducing conditions. M.Sc. (Research) Thesis, University of Sheffield, Sheffield.

Sijderius, R., 1946. Heterotrophe bacterien, die thiosulfaat oxydeeren, University of Amsterdam, Amsterdam, 146 pp.

Spence, M.J., 2001. Isotopic Fractionation as a Diagnostic Tool for In-Situ Biodegradation. PhD Thesis, University of Leeds, Leeds.

Spence, M.J., Bottrell, S.H., Higgo, J.J.W., Harrison, I. and Fallick, A.E., 2001a. Denitrification and phenol degradation in a contaminated aquifer. Journal of Contaminant Hydrology, 53(3-4): 305-318.

Spence, M.J., Bottrell, S.H., Thornton, S.F. and Lerner, D.N., 2001b. Isotopic modelling of the significance of bacterial sulphate reduction for phenol attenuation in a contaminated aquifer. Journal of Contaminant Hydrology, 53(3-4): 285-304.

Suflita, J.M., Liang, L.N. and Saxena, A., 1989. The anaerobic biodegradation of o-, m- and p-cresol by sulfate-reducing bacterial enrichment cultures obtained from a shallow anoxic aquifer. Journal Of Industrial Microbiology, 4(4): 255-266.

Suthersan, S.S., 1997. Remediation Engineering Design Concepts. CRC Press, USA.

Suthersan, S.S., 2002. Natural and Enhanced Remediation Systems. CRC Press LLC, Boca Raton, Florida.

Tchobanoglous, G. and Burton, F.L., 1991. Wastewater engineering : treatment, disposal, and reuse. McGraw-Hill, Singapore.

Thomas, S., Sarfaraz, S., Mishra, L.C. and Iyengar, L., 2002. Degradation of phenol and phenolic compounds by a defined denitrifying bacterial culture. World Journal of Microbiology & Biotechnology, 18(1): 57-63.

Thornton, S.F., Lerner, D.N. and Banwart, S.A., 2001a. Assessing the natural attenuation of organic contaminants in aquifers using plume-scale electron and carbon balances: model development with analysis of uncertainty and parameter sensitivity. Journal of Contaminant Hydrology, 53(3-4): 199-232.

Thornton, S.F. et al., 2001b. Processes controlling the distribution and natural attenuation of dissolved phenolic compounds in a deep sandstone aquifer. Journal of Contaminant Hydrology, 53(3-4): 233-267.

Trauth, R. and Xanthopoulos, C., 1997. Non-point pollution of groundwater in urban areas. Water Research, 31(11): 2711-2718.

Tschech, A. and Fuchs, G., 1987. Anaerobic degradation of phenol by pure cultures of newly isolated dentrifying pseudomonads. Archives of Microbiology, 148: 213-217.

U.S. Department of Health and Human Services, P.H.S., Centers for Disease Control and Prevention., 1997. Pocket Guide to Chemical Hazards., National Institute for Occupational Safety and Health (NIOSH). Cincinnati, Ohio.

Ulrich, G.A., Breit, G.N., Cozzarelli, I.M. and Suflita, J.M., 2003. Sources of sulfate supporting anaerobic metabolism in a contaminated aquifer. Environmental Science & Technology, 37(6): 1093-1099.

USEPA, 1993. Health Effects Assessment Summary Tables, Environmental Criteria and Assessment Office, Office of Research and Development, United States Environmental Protection Agency, Cincinnati, Ohio.

Verce, M.F., Ulrich, R.L. and Freedman, D.L., 2000. Characterization of an isolate that uses vinyl chloride as a growth substrate under aerobic conditions. Applied and Environmental Microbiology, 66(8): 3535-3542.

Vogel, T.M., 1994. Natural Bioremediation of Chlorinated Solvents. In: R.D. Norris et al. (Editors), Handbook of Bioremediation. Lewis Publishers, Boca Raton, Florida.

Vroblesky, D.A., Bradley, P.M. and Chapelle, F.H., 1996. Influence of Electron Donor on the Minimum Sulfate Concentration Required for Sulfate Reduction in a Petroleum Hydrocarbon-Contaminated Aquifer. Environmental Science & Technology, 30(4): 1377-1381.

Vroblesky, D.A., Bradley, P.M. and Chapelle, F.H., 1997. Lack of correlation between organic acid concentrations and predominant electron-accepting processes in a contaminated aquifer. Environmental Science & Technology, 31(5): 1416-1418.

Vroblesky, D.A. and Chapelle, F.H., 1994. Temporal and Spatial Changes of Terminal Electron-Accepting Processes in a Petroleum Hydrocarbon-Contaminated Aquifer and the Significance For Contaminant Biodegradation. Water Resources Research, 30(5): 1561-1570.

Wang, K.W., Baltzis, B.C. and Lewandowski, G.A., 1996. Kinetics of phenol biodegradation in the presence of glucose. Biotechnology and Bioengineering, 51(1): 87-94.

Watson, I.A., Oswald, S.E., Mayer, K.U., Wu, Y.X. and Banwart, S.A., 2003. Modeling kinetic processes controlling hydrogen and acetate concentrations in an aquifer-derived microcosm. Environmental Science & Technology, 37(17): 3910-3919.

Wiedemeier, T.H., Rifai, H.S., Newell, C.J. and Wilson, J.T., 1999. Natural Attenuation of fuels and chlorinated solvents in the subsurface. John Wiley & Sons, Inc., USA.

Wiedemeier, T.H. et al., 1998. Technical Protocol for Evaluating Natural Attenuation of Chlorinated Solvents in Groundwater, National Risk Management Research Laboratory, Office of Research and Development, USEPA, Cincinnati, Ohio.

Wilson, B.H., Wilson, J.T., Kampbell, D.H., Bledsoe, B.E. and Armstrong, J.M., 1990. Biotransformation of Monoaromatic and Chlorinated Hydrocarbons at an Aviation Gasoline Spill Site. Geomicrobiology Journal, 8(3-4): 225-240.

Wu, Y., 2002. Assessing the role of fermentation in intrinsic biodegradation of organic pollutants in groundwater. PhD Thesis Thesis, University of Sheffield, Sheffield.

Yang, R.D. and Humphrey, A.E., 1975. Dynamic and steady state studies of phenol biodegradation in pure and mixed cultures. Biotechnol-Bioeng. 1975 Aug;, 17(8): 1211-35.

Zeng, E.Y. and Noblet, J.A., 2002. Theoretical Considerations on the Use of Solid-Phase Microextraction with Complex Environmental Samples. Environmental Science & Technology, 36(15): 3385-3392.

Zhang, Z. and Pawliszyn, J., 1996. Sampling Volatile Organic Compounds using a Modified Solid Phase Microextraction Device. Journal of High Resolution Chromatography, 19: 155-160.

APPENDICES

APPENDIX A – PHENOL BIODEGRADATION MICROCOSMS: DATA AND ASSOCIATED INFORMATION

A1. Synthetic Groundwater Composition, Pressure Transducer and Protein Determination Calibration Curves, and pH

A2. HPLC Analysis of Microcosm Samples

A3. Headspace CO_2 and H_2 data

A4 Dissolved Ion Concentrations by Ion Chromatography

A4.1 Anions

A 4.2 Cations

A4.5 Data from Total Elemental Analysis by Inductively Coupled Plasma Atomic Emission Spectroscopy (ICP-AES).

A5 Results of DNA Sequencing of Phenol Degraders. Taxonomy Report and Results of BLAST (Basic Local Alignment Search Tool) and FASTA (Fast-All) Searches

APPENDIX B – KINETIC MODELLING DATA

B1 Biodegradation Modelling – Measured and Predicted Data

APPENDIX C – VC OXIDATION MICROCOSMS: DATA AND CALIBRATION

C1. Calibration Curves for SPME/GC-MS Method and Manual Injection/GC-MS Method with Fluorobenzene Internal Standard

C2. Direct Oxidation of VC in 20 ml Microcosms Inoculated with Anaerobic Digester Sludge.

C3. Direct Oxidation of VC in 120 ml Microcosms Inoculated with Anaerobic Digester Sludge Enrichment Cultures.

C4. Data from Study on Cometabolic Degradation of Vinyl Chloride under Sulphate-reducing Conditions, utilising Phenol as the Primary Carbon Source.

APPENDIX A – PHENOL BIODEGRADATION MICROCOSMS: DATA AND ASSOCIATED INFORMATION

A1. Synthetic Groundwater Composition, Pressure Transducer and Protein Determination Calibration Curves, and pH

Table A1.1 Synthetic groundwater prepared for growth of field inoculum and subsequent microcosm study on phenol biodegradation.

Salt[α]	Composition for inoculum, SG (mg/L of UHQ water)	Composition for microcosms, SG-SO_4^{2-} (mg/L of UHQ water)
NaH_2PO_4	60	527.9
$(NH_4)_2SO_4/NH_4Cl$	47.6	1498
KH_2PO4/KCl	22	96.9
$CaCl_2.6H_2O$	126.8	149
$MgCl_2.6H_2O$	Not added	99.6
$MgSO_4.7H_2O$	170	101.1
$MnCl_2.4H_2O$	0.6	4.95
Na_2SO_4	2900	1611
$NaHCO_3$	1950	2520
NaCl	10.3	99.4
$Na_2MoO_4.2H_2O$	Not added	0.97
Resazurin indicator	1000	1000

[α] **Alternative salts used in SG (inoculum) are marked in red**

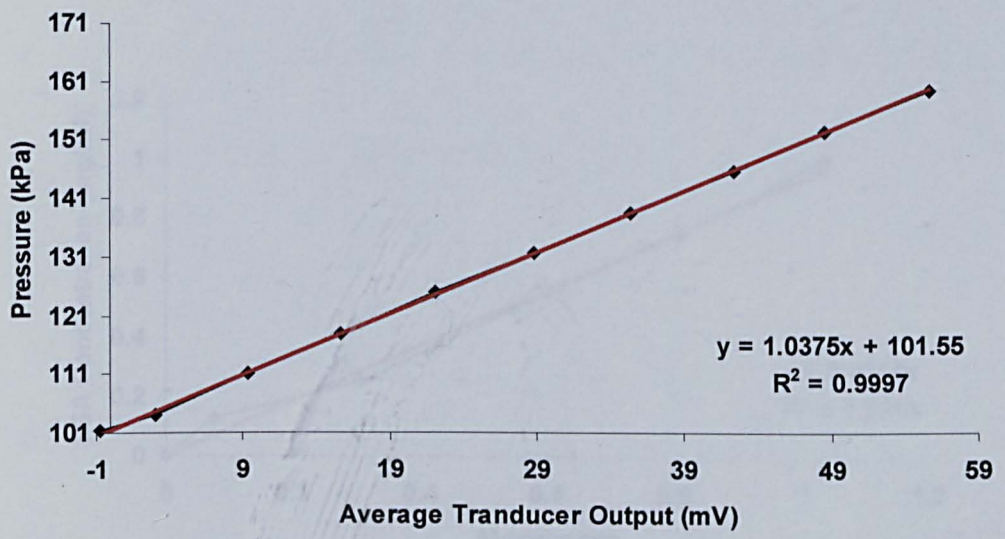

Figure A1.1 Pressure transducer calibration. Linear regression (red line) and r^2 values are shown.

Table A1.2 Pressure transducer calibration data

Transducer Output (mV)	Transducer Output Average (mV)	Pressure (psi)	Pressure (kPa)
-0.70 -0.70 -0.70	-0.70	14.72	101.33
3.00 3.20 3.10	3.10	16.72	104.10
9.50 9.50 9.10	9.37	17.72	110.98
15.60 15.70 15.60	15.63	18.72	117.86
22.10 22.20 22.00	22.10	19.72	124.75
29.10 28.50 29.00	28.87	20.72	131.63
34.90 35.60 35.90	35.47	21.72	138.51
42.30 42.50 42.60	42.47	22.72	145.40
48.50 48.40 49.00	48.63	23.72	152.28
55.70 55.90 55.90	55.83	24.72	159.16

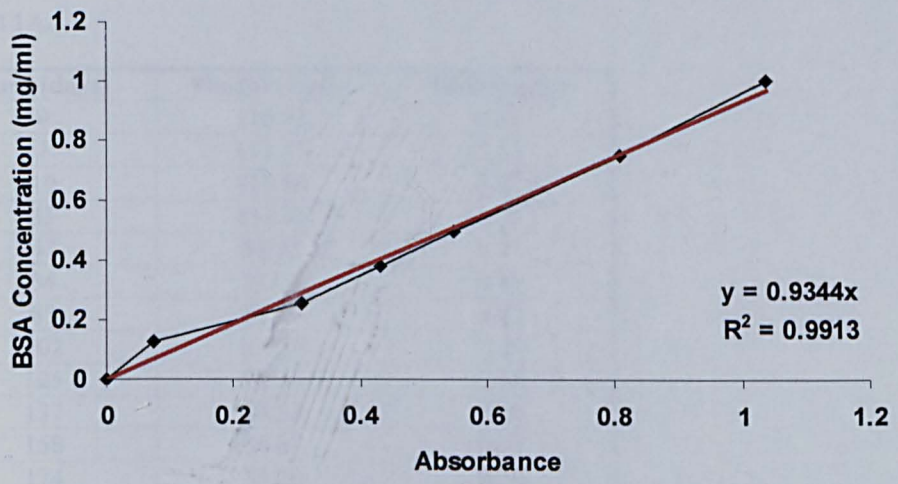

Figure A1.2 Protein determination calibration curve (Bradford Assay). Standards prepared from Bovine Serum Albumin (BSA). Linear regression (red line) and r^2 values are shown.

Table A1.3 pH measurements taken over the course of the experiment

Day measured	pH - 1A	pH - 1B	pH - 2A	pH - 2B
0	8.4	7.9	7.9	7.5
54	8.5	8.6	8.2	7.9
102	8.5	8.4	7.6	7.6
246	8.4	8.4	7.5	7.6
410	8.3	8.1	7.7	7.6
503	8.4	8.3	7.4	7.8
623	8.4	8.2	7.4	7.5
818	8.3	8.3	7.5	7.5
Mean	**8.4**	**8.3**	**7.7**	**7.6**
Day measured	**pH - 3A**	**pH - 3B**	**pH - 4A**	**pH - 4B**
0	7.4	7.3	7.2	7.2
54	7.9	7.9	7.7	7.7
102	7.6	7.6	7.6	7.5
246	7.4	7.1	7.1	7.6
410	7.4	7.2	7.4	7.7
503	7.6	7.4	7.2	7.6
623	7.5	7.3	7.3	7.7
818	7.4	7.5	7.3	7.6
Mean	**7.5**	**7.4**	**7.3**	**7.6**

2. HPLC Analysis of Microcosm Samples

Table A2.1 Phenol analysis and relative standard deviations (RSD) of AQC's, in killed control 1A.

Time (days)	Phenol (mg/L)	RSD (mg/L)
0	116.92	0.05
7	111.73	1.62
19	115.66	1.67
33	131.97	0.33
47	88.22	0.71
54	91.04	0.44
83	88.76	0.03
102	104.88	0.39
125	91.11	0.68
137	88.38	0.30
158	88.87	0.66
174	88.90	0.38
175	87.19	0.37
181	89.62	0.95
194	86.61	0.25
214	87.10	1.01
246	87.21	1.01
270	27.05	0.26
292	0.00	0.00
313	1.44	0.01
332	0.00	0.00
354	1.63	0.01
371	0.99	0.00
384	0.00	0.00
410	0.31	0.00
435	2.26	0.00
462	0.34	0.00
494	0.67	0.00
503	0.98	0.00
524	0.84	0.00

Table A2.2 Phenol analysis and relative standard deviations (RSD) of AQC's, in killed control 1B.

Time (days)	Phenol (mg/L)	RSD (mg/L)
0	118.72	0.05
7	124.22	1.80
19	151.84	2.20
33	128.21	0.32
41	87.90	0.22
47	86.98	0.70
83	84.71	0.02
90	148.25	7.03
102	91.79	0.34
125	87.71	0.66
137	87.81	0.29
158	85.97	0.63
174	87.04	0.37
175	86.58	0.37
181	86.87	0.92
194	87.55	0.26
214	79.19	0.92
246	85.13	0.99
270	83.60	0.79
292	87.91	0.33
313	83.16	0.79
384	73.96	1.05
410	86.02	1.22
435	81.26	0.15
462	80.15	0.15
494	84.53	0.16
503	81.74	0.15
524	80.31	0.46
549	83.63	0.94
567	81.90	0.22
585	82.81	0.22
608	78.82	0.17
623	66.37	0.14
662	79.08	0.17
678	72.63	0.11
704	73.03	0.11
725	78.36	0.44
745	82.75	0.73
781	83.11	0.26
818	82.62	0.11

Table A2.3 Phenol analysis and relative standard deviations (RSD) of AQC's, in live microcosm 2A.

Time (days)	Phenol (mg/L)	RSD (mg/L)
0	113.32	0.05
7	146.24	2.12
19	109.11	1.58
41	81.08	0.20
47	81.91	0.66
54	81.25	0.39
83	40.22	0.01
90	37.00	1.76
102	20.03	0.07
125	3.31	0.02
137	1.09	0.00
158	1.40	0.01
175	0.00	0.00
175	624.20	2.68
181	593.00	6.28
194	582.83	1.71
214	574.05	6.64
246	557.00	6.45
270	514.16	4.87
313	496.18	4.70
384	467.12	6.61
410	457.42	6.47
435	451.64	0.85
462	449.64	0.85
494	451.18	0.85
503	440.69	0.80
503	916.16	1.65
524	878.84	5.07
535	872.76	9.84
535	823.36	9.28
549	820.50	9.25
567	814.51	2.18
585	813.66	2.18
608	813.90	1.73
623	813.70	1.73
662	794.12	1.69
678	801.89	1.23
704	795.24	1.22
725	778.91	4.33
745	763.57	0.77
781	758.67	2.34
789	727.26	2.24
818	713.81	0.98

Table A2.4 Phenol analysis and relative standard deviations (RSD) of AQC's in live microcosm 2B.

Time (days)	Phenol (mg/L)	RSD (mg/L)
0	125.28	0.05
7	131.49	1.90
19	130.13	1.88
33	107.98	0.27
41	66.40	0.17
47	56.29	0.46
54	39.81	0.19
69	24.73	0.45
83	8.74	0.00
90	3.89	0.18
102	2.59	0.01
105	3.55	0.03
105	573.55	4.29
125	549.07	4.10
137	537.39	1.80
158	483.57	3.57
175	456.06	1.96
175	409.12	1.75
181	413.49	4.38
194	407.32	1.19
214	412.00	4.77
246	401.80	4.65
270	380.35	3.61
292	465.75	1.74
313	365.42	3.46
384	366.77	5.19
410	356.80	5.05
435	341.38	0.64
462	312.10	0.59
494	309.36	0.58
503	306.31	0.55
503	995.51	1.80
524	867.88	5.00
535	876.58	9.88
535	819.24	9.23
549	813.86	9.17
567	813.97	2.18
585	816.82	2.19
608	808.35	1.72
623	789.48	1.68
662	802.08	1.70
678	804.29	1.24
704	801.39	1.23
725	786.86	4.37
745	769.01	0.77
781	779.97	2.40
818	777.01	1.06

Table A2.5 Phenol analysis and relative standard deviations (RSD) of AQC's, in live microcosm 3A.

Time (days)	Phenol (mg/L)	RSD (mg/L)
0	174.65	0.07
7	176.57	2.55
19	184.37	2.67
33	153.29	0.39
41	107.12	0.27
47	90.16	0.73
54	118.87	0.58
69	32.20	0.58
83	13.56	0.00
90	19.05	0.90
105	13.41	0.05
105	576.97	4.31
125	463.44	3.46
137	464.44	1.55
158	428.48	3.16
175	445.47	1.91
175	370.83	1.59
181	358.53	3.80
194	333.47	0.98
214	311.59	3.61
246	306.03	3.54
270	306.48	2.90
292	311.13	1.16
313	304.90	2.89
384	250.65	3.55
410	263.76	3.73
435	258.42	0.49
462	248.67	0.47
494	258.61	0.49
503	256.83	0.46
503	771.42	1.39
524	707.39	4.08
535	707.69	7.98
549	703.27	7.93
567	701.28	1.88
585	705.68	1.89
608	700.75	1.49
623	698.97	1.48
662	666.74	1.42
678	672.34	1.04
704	661.38	1.02
725	636.68	3.54
781	603.78	1.86
818	597.61	0.82

Table A2.6 Phenol analysis and relative standard deviations (RSD) of AQC's, in live microcosm 3B.

Time (days)	Phenol (mg/L)	RSD (mg/L)
0	194.83	0.08
7	170.63	2.47
19	194.58	2.81
41	107.98	0.27
47	89.38	0.72
54	109.12	0.53
69	64.52	1.17
83	42.26	0.01
90	50.45	2.39
102	37.65	0.14
125	35.33	0.26
137	35.16	0.12
158	35.15	0.26
175	33.96	0.15
175	29.66	0.13
181	29.67	0.31
194	29.04	0.09
214	13.18	0.15
246	6.19	0.07
270	6.81	0.06
292	11.98	0.04
313	6.65	0.06
384	3.17	0.04
410	0.00	0.00
435	0.85	0.00
462	0.54	0.00
494	0.00	0.00
503	0.00	0.00
503	727.72	1.31
524	566.65	3.27
535	473.79	5.34
549	463.09	5.22
567	432.94	1.16
585	414.10	1.11
608	400.31	0.85
623	395.41	0.84
662	385.10	0.82
678	382.43	0.59
678	316.47	0.49
704	317.63	0.49
725	316.41	1.76
745	296.93	0.30
781	299.43	0.92
789	298.89	0.92
818	289.13	0.40

Table A2.7 Phenol analysis and relative standard deviations (RSD) of AQC's, in live microcosm 4A.

Time (days)	Phenol (mg/L)	RSD (mg/L)
0	223.65	0.09
7	191.91	2.78
19	234.06	3.39
41	104.40	0.26
47	75.60	0.61
54	68.38	0.33
69	93.34	1.69
83	48.65	0.01
90	60.53	2.87
102	70.13	0.26
125	45.25	0.34
137	43.79	0.15
158	35.84	0.26
175	25.60	0.11
175	20.70	0.09
181	21.52	0.23
194	21.66	0.06
214	20.82	0.24
246	19.10	0.22
270	10.24	0.10
292	4.17	0.02
313	2.98	0.03
332	1332.98	6.19
384	1312.72	18.57
410	1328.26	18.79
435	1314.54	2.47
462	1311.75	2.47
494	1314.60	2.47
503	1311.71	2.37
524	1313.49	7.57
535	1305.49	14.71
549	1305.89	14.72
567	1310.55	3.51
585	1302.45	3.49
608	1276.15	2.71
623	1272.66	2.70
662	1244.00	2.64
678	1250.12	1.92
704	1236.51	1.90
725	1222.96	6.80
745	1218.25	1.23
818	1211.18	1.66

Table A2.8 Phenol analysis and relative standard deviations (RSD) of AQC's, in live microcosm 4B.

Time (days)	Phenol (mg/L)	RSD (mg/L)
0	206.04	0.08
7	212.86	3.08
19	228.72	3.31
41	104.40	0.26
47	88.05	0.71
69	67.20	1.21
83	47.76	0.01
90	104.35	4.95
102	52.02	0.19
125	48.11	0.36
137	42.17	0.14
158	36.67	0.27
175	31.50	0.14
175	26.48	0.11
181	26.39	0.28
194	22.77	0.07
214	8.18	0.09
246	2.26	0.03
270	2.01	0.02
292	1.89	0.01
313	0.00	0.00
332	1330.00	5.62
384	1375.81	19.46
410	1367.58	19.35
435	1360.93	2.56
462	1369.14	2.58
494	1359.10	2.56
503	1348.13	2.43
524	1349.09	7.78
549	1353.20	15.25
567	1338.30	3.59
585	1351.71	3.62
608	1338.79	2.84
623	1339.04	2.84
662	1324.25	2.81
678	1322.31	2.04
704	1320.62	2.03
725	1306.34	7.26
745	1276.13	1.28
781	1309.50	4.04

A3. Headspace CO_2 and H_2 data

Table A3.1 Headspace CO_2 concentrations and relative standard deviations (RSD) of AQC's, in killed controls 1A and 1B. Calculated as described in Section 2.3.3. (ND - No data)

Time (days)	1A - CO2 (mol/L)	1A - RSD (mol/L)	Time (days)	1B - CO2 (mol/L)	1B - RSD (mol/L)
0	5.355E-04	2.677E-05	0	4.063E-03	2.031E-04
7	7.582E-04	3.791E-05	7	9.180E-04	4.590E-05
19	ND	ND	19	3.133E-04	1.567E-05
33	1.538E-03	7.691E-05	33	1.586E-03	7.932E-05
41	1.371E-03	6.855E-05	41	1.810E-03	9.050E-05
47	4.263E-04	2.132E-05	47	3.733E-04	1.866E-05
54	1.146E-03	5.729E-05	54	4.237E-04	2.118E-05
69	1.531E-04	7.653E-06	69	1.101E-03	5.506E-05
83	2.358E-04	1.179E-05	83	5.526E-04	2.763E-05
90	1.552E-03	7.759E-05	90	1.861E-03	9.306E-05
102	1.844E-03	9.218E-05	102	2.008E-03	1.004E-04
125	2.090E-03	1.045E-04	125	2.090E-03	1.045E-04
137	2.139E-03	1.069E-04	137	2.098E-03	1.049E-04
158	2.247E-03	1.123E-04	158	2.207E-03	1.103E-04
175	1.455E-03	7.277E-05	175	1.346E-03	6.729E-05
175	2.836E-03	1.418E-04	175	4.160E-03	2.080E-04
181	3.562E-03	1.781E-04	181	4.933E-03	2.466E-04
194	3.443E-03	1.721E-04	194	3.228E-03	1.614E-04
214	2.457E-03	1.769E-05	214	2.621E-03	1.887E-05
246	2.555E-03	4.513E-05	246	2.682E-03	4.737E-05
313	1.090E-01	1.143E-03	292	4.331E-04	1.653E-05
332	9.982E-02	1.361E-03	313	3.010E-03	3.156E-05
371	8.423E-02	1.163E-03	332	4.607E-03	6.282E-05
384	7.748E-02	3.609E-03	371	1.369E-04	1.890E-06
410	4.327E-02	1.527E-03	384	1.827E-03	8.508E-05
435	9.156E-02	1.767E-04	410	5.986E-04	2.112E-05
503	4.014E-02	2.007E-03	503	3.086E-03	1.543E-04
524	ND	ND	524	3.899E-03	1.106E-05
535	ND	ND	535	3.137E-03	1.244E-04
549	ND	ND	549	4.514E-03	1.485E-04
567	ND	ND	567	3.439E-03	3.752E-05
585	ND	ND	585	4.480E-03	6.811E-05
608	ND	ND	608	8.691E-03	3.807E-04
623	ND	ND	623	5.732E-03	1.109E-04
725	ND	ND	725	3.969E-03	1.374E-04
745	ND	ND	745	3.360E-03	1.256E-04
781	ND	ND	781	5.919E-04	1.225E-05
818	ND	ND	818	2.999E-03	8.238E-05

Table A3.2 Headspace CO_2 concentrations and relative standard deviations (RSD) of AQC's, in live microcosms 2A and 2B. Calculated as described in Section 2.3.3.

Time (days)	2A - CO2 (mol/L)	2A - RSD (mol/L)	2B - CO2 (mol/L)	2B - RSD (mol/L)
0	7.115E-03	3.557E-04	8.529E-03	4.265E-04
7	7.941E-03	3.971E-04	8.493E-03	4.246E-04
19	1.408E-02	7.039E-04	2.263E-02	1.131E-03
33	1.295E-02	6.474E-04	2.312E-02	1.156E-03
41	1.665E-02	8.323E-04	3.864E-02	1.932E-03
47	1.535E-02	7.677E-04	4.295E-02	2.148E-03
54	1.829E-02	9.143E-04	5.757E-02	2.879E-03
69	1.412E-02	7.059E-04	6.070E-02	3.035E-03
83	4.747E-02	2.374E-03	9.339E-02	4.670E-03
90	6.248E-02	3.124E-03	9.306E-02	4.653E-03
102	7.634E-02	3.817E-03	9.564E-02	4.782E-03
125	8.568E-02	4.284E-03	9.002E-02	4.501E-03
137	8.461E-02	4.231E-03	1.163E-01	5.817E-03
158	7.933E-02	3.967E-03	1.720E-01	8.602E-03
175	2.003E-02	1.002E-03	4.590E-02	2.295E-03
175	2.722E-02	1.361E-03	8.422E-02	4.211E-03
181	5.594E-02	2.797E-03	1.538E-01	7.692E-03
194	5.835E-02	2.917E-03	1.385E-01	6.924E-03
214	3.793E-02	2.731E-04	4.076E-02	2.935E-04
246	1.102E-01	1.946E-03	1.317E-01	2.326E-03
292	1.201E-01	4.584E-03	2.230E-01	2.338E-03
313	1.343E-01	1.408E-03	1.923E-01	2.622E-03
332	1.502E-01	2.048E-03	1.690E-01	2.334E-03
371	2.489E-01	3.437E-03	1.703E-01	7.930E-03
384	2.100E-01	9.780E-03	2.362E-01	8.336E-03
410	2.473E-01	8.728E-03	2.814E-01	5.429E-04
435	2.473E-01	4.772E-04	2.778E-01	1.389E-02
503	1.145E-01	5.725E-03	2.778E-01	1.389E-02
524	1.246E-01	3.534E-04	2.552E-01	7.239E-04
535	8.667E-02	3.437E-03	5.853E-02	2.321E-03
549	6.747E-02	2.220E-03	8.401E-02	2.764E-03
567	4.676E-02	5.103E-04	1.325E-01	1.446E-03
585	6.079E-02	9.242E-04	1.593E-01	2.422E-03
608	1.065E-01	4.665E-03	1.435E-01	6.288E-03
623	9.540E-02	1.846E-03	9.520E-02	1.843E-03
662	6.835E-02	2.936E-03	1.913E-01	8.216E-03
678	2.567E-02	1.277E-03	1.285E-02	6.397E-04
725	1.308E-01	4.527E-03	6.241E-02	2.160E-03
745	1.342E-01	5.015E-03	9.814E-02	3.667E-03
781	1.445E-01	2.990E-03	1.202E-01	2.488E-03
818	1.572E-01	4.319E-03	2.200E-01	6.043E-03

Table A3.3 Headspace CO_2 concentrations and relative standard deviations (RSD) of AQC's, in live microcosms 3A and 3B. Calculated as described in Section 2.3.3.

Time (days)	3A - CO2 (mol/L)	3A - RSD (mol/L)	3B - CO2 (mol/L)	3B - RSD (mol/L)
0	8.220E-03	4.110E-04	1.643E-02	8.214E-04
7	8.684E-03	4.342E-04	1.231E-02	6.155E-04
19	2.244E-02	1.122E-03	2.860E-02	1.430E-03
33	2.131E-02	1.066E-03	3.027E-02	1.514E-03
41	3.685E-02	1.843E-03	5.332E-02	2.666E-03
47	4.560E-02	2.280E-03	6.210E-02	3.105E-03
54	7.143E-02	3.572E-03	9.100E-02	4.550E-03
69	1.012E-01	5.061E-03	7.706E-02	3.853E-03
83	1.328E-01	6.639E-03	1.090E-01	5.449E-03
90	1.211E-01	6.053E-03	1.381E-01	6.903E-03
102	1.293E-01	6.467E-03	1.352E-01	6.758E-03
125	3.034E-02	1.517E-03	1.317E-01	6.585E-03
137	3.199E-02	1.599E-03	1.206E-01	6.032E-03
158	4.268E-02	2.134E-03	1.114E-01	5.570E-03
175	1.534E-02	7.668E-04	1.456E-02	7.279E-04
175	3.619E-02	1.810E-03	6.344E-02	3.172E-03
181	7.099E-02	3.549E-03	1.025E-01	5.125E-03
194	1.346E-01	6.728E-03	1.039E-01	5.194E-03
214	6.335E-02	4.561E-04	5.390E-02	3.881E-04
246	1.239E-01	2.189E-03	1.688E-01	2.982E-03
292	8.918E-02	3.404E-03	1.006E-01	3.840E-03
313	5.770E-02	6.051E-04	1.032E-02	1.082E-04
332	1.203E-01	1.640E-03	1.197E-01	1.633E-03
371	2.489E-01	3.437E-03	1.431E-01	1.977E-03
384	1.865E-01	8.685E-03	1.252E-01	5.833E-03
410	2.459E-01	8.678E-03	1.809E-01	6.385E-03
435	2.228E-01	4.299E-04	1.858E-01	3.585E-04
503	9.683E-02	4.842E-03	7.866E-02	3.933E-03
503	9.683E-02	4.842E-03	7.866E-02	3.933E-03
524	1.170E-01	3.318E-04	7.275E-02	2.063E-04
535	5.572E-02	2.210E-03	6.644E-02	2.635E-03
549	1.143E-01	3.762E-03	7.527E-02	2.477E-03
567	5.288E-02	5.770E-04	7.946E-02	8.670E-04
585	5.148E-02	7.826E-04	7.616E-02	1.158E-03
608	9.109E-02	3.991E-03	1.789E-01	7.838E-03
623	1.769E-01	3.423E-03	2.275E-01	4.404E-03
662	1.193E-01	5.124E-03	7.006E-02	3.009E-03
678	3.112E-01	1.549E-02	4.998E-02	2.488E-03
725	2.114E-01	7.320E-03	8.555E-02	2.962E-03
745	1.358E-01	5.076E-03	1.571E-01	5.870E-03
781	1.888E-01	3.908E-03	1.582E-01	3.275E-03
818	2.629E-01	7.221E-03	1.727E-01	4.743E-03

Table A3.4 Headspace CO_2 concentrations and relative standard deviations (RSD) of AQC's, in live microcosms 4A and 4B. Calculated as described in Section 2.3.3. (ND - No data)

Time (days)	4A - CO2 (mol/L)	4A - RSD (mol/L)	4B - CO2 (mol/L)	4B - RSD (mol/L)
0	1.588E-02	7.938E-04	1.139E-02	5.695E-04
7	1.666E-02	8.330E-04	1.611E-02	8.053E-04
19	4.773E-02	2.386E-03	3.719E-02	1.859E-03
33	3.422E-03	1.711E-04	3.430E-02	1.715E-03
41	8.493E-02	4.247E-03	6.566E-02	3.283E-03
47	1.159E-01	5.797E-03	1.042E-01	5.209E-03
54	1.276E-01	6.378E-03	1.148E-01	5.742E-03
69	1.097E-01	5.486E-03	9.399E-02	4.699E-03
83	1.332E-01	6.660E-03	1.372E-01	6.861E-03
90	1.384E-01	6.919E-03	1.426E-01	7.128E-03
102	1.370E-01	6.851E-03	1.496E-01	7.481E-03
125	1.413E-01	7.063E-03	1.719E-01	8.596E-03
137	1.411E-01	7.055E-03	1.713E-01	8.563E-03
158	1.516E-01	7.581E-03	1.550E-01	7.751E-03
175	1.490E-02	7.448E-04	4.328E-02	2.164E-03
175	9.009E-02	4.504E-03	8.538E-02	4.269E-03
181	1.334E-01	6.671E-03	1.455E-01	7.276E-03
194	1.341E-01	6.706E-03	1.397E-01	6.985E-03
214	3.890E-02	2.801E-04	5.199E-02	3.743E-04
246	1.235E-01	2.181E-03	1.246E-01	2.200E-03
292	1.355E-01	5.172E-03	1.453E-01	5.545E-03
313	1.048E-01	1.099E-03	1.558E-01	1.634E-03
332	1.328E-01	1.811E-03	1.435E-01	1.957E-03
371	1.369E-01	1.891E-03	1.325E-01	1.830E-03
384	1.083E-01	5.047E-03	9.906E-02	4.614E-03
410	1.339E-01	4.726E-03	1.312E-01	4.629E-03
435	1.132E-01	2.185E-04	1.141E-01	2.201E-04
503	3.776E-02	1.888E-03	7.638E-02	3.819E-03
503	3.776E-02	1.888E-03	7.638E-02	3.819E-03
524	4.823E-02	1.368E-04	4.230E-02	1.200E-04
535	2.658E-02	1.054E-03	4.647E-02	1.843E-03
549	3.600E-02	1.184E-03	3.923E-02	1.291E-03
567	4.254E-02	4.641E-04	5.109E-02	5.575E-04
585	2.946E-02	4.479E-04	4.402E-02	6.691E-04
608	9.423E-02	4.128E-03	8.052E-02	3.528E-03
623	9.232E-02	1.787E-03	1.540E-01	2.981E-03
662	6.165E-02	2.648E-03	ND	ND
678	1.005E-01	5.004E-03	8.952E-02	4.455E-03
725	1.172E-01	4.056E-03	7.878E-02	2.727E-03
745	1.500E-01	5.606E-03	8.077E-02	3.018E-03
781	1.615E-01	3.343E-03	7.891E-02	1.633E-03
818	1.842E-01	5.059E-03	7.321E-02	2.011E-03

Table A3.5 Headspace H_2 concentrations in killed controls and live microcosms. Calculated as described in Section 2.3.3. (N/A - Not Applicable)

Time (days)	1A - H2 (nM)	1B - H2 (nM)	2A - H2 (nM)	2B - H2 (nM)
0	20.55	18.87	1.25	1.42
7	58.09	20.63	0.71	0.89
19	94.13	29.21	1.10	1.26
33	153.88	18.63	1.60	2.11
90	226.28	41.85	2.59	3.34
175	353.86	192.49	4.02	5.63
503	N/A	112.93	1.02	1.03
818	N/A	49.32	3.50	6.82
Time (days)	**3A - H2 (nM)**	**3B - H2 (nM)**	**4A - H2 (nM)**	**4B - H2 (nM)**
0	1.59	1.80	4.19	1.61
7	1.10	0.96	1.90	1.40
19	2.81	1.49	3.23	3.07
33	4.24	2.25	4.06	7.45
90	3.65	3.01	1.92	3.81
175	4.08	2.67	4.74	3.37
503	1.61	3.73	5.91	3.73
818	2.60	7.23	15.35	6.60

A4 Dissolved Ion Concentrations by Ion Chromatography

A4.1 Anions

Table A4.1 Sulphate concentrations with relative standard deviations (RSD) of AQC's in killed control 1A.

Time (days)	Sulphate (mg/L	RSD (mg/L)
0	403.51	5.27
7	338.57	4.42
19	511.92	6.69
33	453.21	1.55
54	444.72	1.52
69	356.77	1.83
83	487.67	2.50
90	452.86	2.33
102	477.62	2.45
125	449.82	2.31
137	469.82	2.41
158	265.35	3.43
174	432.63	5.60
175	382.48	4.95
181	417.87	5.41
194	499.51	6.47
214	496.41	6.43
246	481.67	6.24
270	495.93	6.42
313	494.34	6.40
332	577.17	6.40
354	373.93	6.40
371	674.37	6.40
384	565.23	4.95
410	498.56	4.36
435	555.63	4.86
462	472.38	4.16
494	522.32	4.60
503	517.00	4.55

Table A4.2 Sulphate concentrations with relative standard deviations (RSD) of AQC's in killed control 1B.

Time (days)	Sulphate (mg/L)	RSD (mg/L)
0	424.31	5.55
7	477.97	6.25
19	488.33	6.38
33	N/A	0.00
41	380.26	1.30
47	471.03	1.61
54	441.55	1.51
69	466.02	2.39
83	483.90	2.48
90	483.85	2.48
102	362.62	1.86
125	422.88	2.17
137	484.56	2.49
158	485.45	6.28
174	502.67	6.51
175	498.19	6.45
181	496.27	6.42
194	470.14	6.09
214	481.91	6.24
246	492.79	6.38
270	505.61	6.55
313	499.71	6.47
384	447.87	3.92
410	403.52	3.53
494	503.07	4.43
503	518.29	4.56
524	504.61	4.44
535	530.08	4.67
549	398.96	2.12
585	516.17	2.53
608	517.85	4.45
623	525.08	4.52
662	514.50	2.52
678	528.05	16.01
704	525.98	15.95
725	525.90	15.95
745	493.30	14.96
818	517.75	15.70

Table A4.3 Sulphate concentrations with relative standard deviations (RSD) of AQC's in live microcosm 2A.

Time (days)	Sulphate (mg/L)	RSD (mg/L)
0	467.09	6.10
7	357.96	4.68
19	499.92	6.53
33	458.23	1.56
41	402.62	1.37
47	340.37	1.16
54	334.63	1.14
83	327.86	1.68
90	231.66	1.19
102	236.37	1.21
125	233.81	1.20
137	233.11	1.20
158	244.43	3.16
175	241.13	3.12
175	262.11	3.39
194	384.01	4.97
214	389.65	5.04
246	328.30	4.25
270	193.14	2.50
292	185.33	2.40
313	190.85	2.47
332	178.40	1.56
354	135.17	1.18
371	122.73	1.07
384	112.06	0.98
410	61.88	0.54
435	65.12	0.57
462	51.74	0.46
494	49.04	0.43
503	46.22	0.41
503	37.84	0.33
524	33.97	0.30
535	30.37	0.27
535	611.00	5.38
549	486.69	2.58
567	551.64	2.70
585	571.65	2.80
608	561.64	4.83
623	564.85	4.86
662	535.11	2.62
678	531.11	16.10
704	500.17	15.17
725	512.51	15.54
745	514.37	15.60
781	461.96	14.01
818	439.32	13.32

Table A4.4 Sulphate concentrations with relative standard deviations (RSD) of AQC's in live microcosm 2B.

Time (days)	Sulphate (mg/L)	RSD (mg/L)
0	456.10	5.96
7	457.59	5.98
19	486.04	6.35
33	402.20	1.37
41	312.88	1.07
47	303.57	1.04
54	285.69	0.97
69	257.23	1.32
83	220.14	1.13
90	221.11	1.14
102	215.77	1.11
105	222.91	1.14
105	176.50	0.91
125	156.25	0.80
137	163.63	0.84
158	20.56	0.27
175	28.63	0.37
175	241.14	3.12
181	219.63	2.84
194	234.31	3.03
214	221.88	2.87
246	220.00	2.85
270	179.10	2.32
313	125.59	1.63
384	115.41	1.01
410	110.63	0.97
435	64.33	0.56
462	31.85	0.28
494	12.50	0.11
503	10.14	0.09
503	9.26	0.08
524	7.33	0.06
535	8.45	0.07
535	377.67	3.32
549	653.68	3.47
567	601.71	2.95
585	656.35	3.22
608	648.14	5.58
623	559.98	4.82
662	648.69	3.18
678	652.38	19.78
704	556.48	16.87
725	627.81	19.04
745	636.98	19.32
781	608.93	18.46
818	612.25	18.57

Table A4.5 Sulphate concentrations with relative standard deviations (RSD) of AQC's in live microcosm 3A.

Time (days)	Sulphate (mg/L)	RSD (mg/L)
0	470.62	6.15
7	475.92	6.22
19	466.75	6.10
33	348.09	1.19
41	272.46	0.93
47	250.78	0.86
54	264.05	0.90
69	181.83	0.93
83	126.85	0.65
90	122.01	0.63
102	51.56	0.26
105	120.47	0.62
125	107.96	0.55
137	104.62	0.54
158	94.17	1.22
175	76.27	0.99
175	304.14	3.94
181	269.41	3.49
194	188.22	2.44
214	131.41	1.70
246	126.59	1.64
313	129.53	1.68
371	61.19	0.54
384	57.22	0.50
410	85.22	0.75
435	60.57	0.53
462	63.43	0.56
494	12.52	0.11
503	49.26	0.43
503	49.82	0.44
524	50.99	0.45
535	52.35	0.46
549	35.99	0.19
567	58.65	0.29
585	54.63	0.27
608	54.08	0.47
623	54.19	0.47
662	45.52	0.22
704	33.35	1.01
725	11.15	0.34
781	9.55	0.29
818	6.47	0.20

Table A4.6 Sulphate concentrations with relative standard deviations (RSD) of AQC's in live microcosm 3B.

Time (days)	Sulphate (mg/L)	RSD (mg/L)
0	420.05	5.49
7	465.20	6.08
19	476.29	6.22
33	341.59	1.16
41	348.08	1.19
47	285.66	0.97
54	208.88	0.71
69	150.55	0.77
83	125.26	0.64
90	67.21	0.35
102	106.24	0.55
125	106.53	0.55
137	90.99	0.47
158	91.78	1.19
175	104.16	1.35
175	300.06	3.88
181	280.59	3.63
194	271.39	3.51
214	238.91	3.09
246	209.36	2.71
270	202.02	2.62
313	209.49	2.71
410	209.80	1.84
435	207.73	1.82
462	236.09	2.08
494	238.75	2.10
503	239.38	2.11
503	50.32	0.44
524	215.95	1.89
549	176.91	0.94
567	68.30	0.33
585	33.92	0.17
608	5.16	0.04
623	4.33	0.04
662	1.44	0.01
678	0.41	0.01
678	1585.00	48.06
704	1596.14	48.40
725	1578.00	47.85
745	1596.65	48.42
781	1582.91	48.00
789	1578.85	47.88
818	1587.88	48.15

Table A4.7 Sulphate concentrations with relative standard deviations (RSD) of AQC's in live microcosm 4A.

Time (days)	Sulphate (mg/L)	RSD (mg/L)
0	420.88	5.50
7	466.50	6.10
19	456.58	5.97
33	259.78	0.89
41	169.74	0.58
47	110.22	0.38
54	154.13	0.53
69	110.90	0.57
83	97.11	0.50
90	96.67	0.50
102	84.92	0.44
125	96.27	0.49
137	88.41	0.45
158	61.48	0.80
175	49.85	0.65
175	508.46	6.58
181	474.89	6.15
194	482.69	6.25
214	484.43	6.27
246	474.48	6.14
270	454.84	5.89
313	432.05	5.59
332	378.07	3.31
384	382.56	3.35
462	376.14	3.31
494	392.14	3.45
503	216.81	1.91
524	402.56	3.54
535	397.70	3.50
549	388.38	2.06
567	386.24	1.89
585	390.80	1.91
608	391.87	3.37
623	396.56	3.41
662	389.36	1.91
678	375.43	11.38
704	375.72	11.39
725	393.99	11.95
745	396.56	12.03
781	395.48	11.99
818	396.32	12.02

Table A4.8 Sulphate concentrations with relative standard deviations (RSD) of AQC's in live microcosm 4B.

Time (days)	Sulphate (mg/L)	RSD (mg/L)
0	367.47	4.80
7	471.79	6.17
19	459.18	6.00
33	214.54	0.73
41	277.27	0.95
54	176.53	0.60
69	158.97	0.82
83	137.59	0.71
90	111.40	0.57
102	117.19	0.60
125	108.19	0.56
137	96.24	0.49
158	58.45	0.76
175	49.79	0.64
175	493.11	6.38
181	465.84	6.03
194	445.00	5.76
214	405.12	5.24
246	377.07	4.88
270	374.01	4.84
313	390.30	5.05
332	326.31	2.86
354	355.92	3.12
371	262.94	2.30
384	355.41	3.11
462	334.97	2.95
494	343.10	3.02
503	343.59	3.02
524	349.60	3.08
535	351.13	3.09
549	339.24	1.80
567	341.97	1.68
585	340.31	1.67
608	351.00	3.02
623	363.08	3.12
662	332.67	1.63
678	329.81	10.00
704	317.76	9.64
725	324.35	9.84
745	347.73	10.54
781	306.88	9.31
818	350.07	10.62

Table A4.9 Anions by IC in killed control 1A (n.d. - not detected).

Time (days)	Nitrite (mg/L)	Nitrate (mg/L)	Phosphate (mg/L)	Chloride (mg/L)
0	0.20	49.77	10.54	1003.33
7	n.d.	49.52	10.25	1171.91
19	n.d.	50.00	11.13	1620.34
33	n.d.	7.77	9.24	1404.93
41	n.d.	1.71	9.20	634.65
47	n.d.	2.20	9.29	553.38
54	n.d.	1.94	9.77	836.88
69	n.d.	39.12	n.d.	1399.98
83	n.d.	36.92	n.d.	1540.65
90	n.d.	36.55	6.14	1345.14
102	n.d.	36.50	1.06	1411.54
125	n.d.	36.32	n.d.	1406.77
137	n.d.	36.12	n.d.	1272.34
158	21.92	1.21	8.32	840.60
175	32.61	n.d.	8.77	1348.85
175	24.18	n.d.	17.19	861.22
181	24.82	n.d.	n.d.	937.60
194	39.23	n.d.	2.71	1580.18
214	37.79	n.d.	21.69	1550.00
246	n.d.	n.d.	4.06	1588.12
270	41.88	n.d.	11.00	1575.62
313	n.d.	15.32	4.98	1649.93
384	51.40	n.d.	13.40	1537.89
410	44.02	n.d.	32.37	1338.57
435	49.13	n.d.	24.72	1376.29
462	n.d.	2.21	17.43	1205.76
494	n.d.	0.37	17.05	1308.72
503	n.d.	0.59	n.d.	1325.50

Table A4.10 Anions by IC in killed control 1B (n.d. - not detected).

Time (days)	Nitrite (mg/L)	Nitrate (mg/L)	Phosphate (mg/L)	Chloride (mg/L)
0	n.d.	49.30	8.33	1074.53
7	n.d.	50.02	8.62	1083.70
19	n.d.	50.33	7.51	1618.32
33	n.d.	37.31	9.13	n.d.
41	n.d.	2.70	5.82	1340.23
47	n.d.	3.31	3.75	1606.74
54	n.d.	2.58	n.d.	1041.78
69	n.d.	35.20	n.d.	1480.97
83	n.d.	36.86	n.d.	1589.10
90	n.d.	36.29	n.d.	1561.01
102	n.d.	37.85	n.d.	872.70
125	n.d.	37.20	n.d.	873.04
137	n.d.	38.61	n.d.	1571.92
158	33.71	0.26	n.d.	1521.87
175	42.14	2.97	5.28	1619.42
175	39.75	1.23	7.41	1486.11
181	35.08	n.d.	11.18	1267.77
194	41.38	n.d.	1.97	1527.55
214	36.48	n.d.	n.d.	1311.74
246	42.75	n.d.	5.58	1630.27
270	n.d.	n.d.	n.d.	1609.77
313	31.75	n.d.	8.48	1312.48
332	47.87	n.d.	7.56	1375.57
354	27.33	n.d.	5.20	861.71
371	58.97	1.50	8.66	1672.01
384	32.81	n.d.	7.24	1032.15
410	40.50	n.d.	6.54	1168.67
435	56.88	0.69	6.35	1572.84
462	n.d.	5.65	15.88	717.91
494	n.d.	0.85	n.d.	1200.45
503	n.d.	0.68	5.22	1346.29
524	n.d.	0.69	n.d.	1289.83
535	n.d.	1.10	11.18	1377.87
549	15.88	2.09	4.32	1059.90
567	n.d.	8.74	45.70	n.d.
585	n.d.	1.02	4.63	1338.93
608	n.d.	1.43	n.d.	1336.50
623	n.d.	1.02	3.00	1363.86
662	n.d.	1.56	1.93	1345.82
678	n.d.	0.48	0.99	1312.92
704	3.61	0.60	n.d.	1274.30
725	5.11	1.22	n.d.	1274.83
745	n.d.	n.d.	n.d.	1191.56
818	3.66	n.d.	n.d.	1264.64

Table A4.11 Anions by IC in live microcosm 2A (n.d. - not detected).

Time (days)	Nitrite (mg/L)	Nitrate (mg/L)	Phosphate (mg/L)	Chloride (mg/L)
0	n.d.	48.84	60.21	1004.66
7	n.d.	48.88	56.51	716.48
19	n.d.	49.20	67.55	1448.81
33	n.d.	2.68	62.07	924.13
41	n.d.	2.17	49.37	1225.51
47	n.d.	1.82	49.39	1039.56
54	n.d.	n.d.	45.41	1126.79
69	n.d.	34.26	45.90	971.93
83	n.d.	38.84	65.90	1359.26
90	n.d.	35.39	54.05	1009.41
102	n.d.	35.01	68.82	1339.01
125	n.d.	35.01	68.82	1339.01
137	n.d.	35.74	49.21	1353.08
158	42.68	n.d.	62.94	1421.11
175	38.23	n.d.	70.66	1429.46
175	20.63	n.d.	40.34	722.47
181	16.64	n.d.	52.14	578.38
194	31.54	n.d.	39.30	996.70
214	25.12	n.d.	59.66	842.65
246	25.34	n.d.	48.03	999.81
270	22.29	n.d.	65.96	903.41
292	25.17	n.d.	47.03	984.13
313	17.05	n.d.	60.13	561.67
332	21.85	n.d.	58.20	686.92
354	25.25	n.d.	40.38	784.86
371	34.41	n.d.	39.19	957.21
384	42.53	n.d.	76.03	1300.33
410	29.04	n.d.	53.75	901.96
435	28.46	n.d.	80.66	858.65
462	n.d.	0.62	41.29	746.41
494	n.d.	2.52	58.32	889.40
503	n.d.	0.38	56.05	892.41
503	n.d.	n.d.	55.64	801.63
524	n.d.	1.10	44.65	806.35
535	n.d.	n.d.	39.18	807.87
535	n.d.	0.36	68.32	830.98
549	n.d.	n.d.	65.11	641.65
567	n.d.	n.d.	76.17	823.36
585	n.d.	n.d.	68.54	834.73
608	n.d.	n.d.	50.32	828.48
623	n.d.	n.d.	64.51	840.45
662	n.d.	n.d.	63.13	834.72
678	n.d.	n.d.	60.18	773.38
704	0.41	0.66	56.00	790.52
725	0.25	n.d.	59.80	830.17
745	2.63	1.29	57.35	853.35
781	3.47	n.d.	62.06	810.28
818	n.d.	n.d.	53.88	818.92

Table A4.12 Anions by IC in live microcosm 2B (n.d. - not detected).

Time (days)	Nitrite (mg/L)	Nitrate (mg/L)	Phosphate (mg/L)	Chloride (mg/L)
0	n.d.	48.72	64.91	1065.83
7	n.d.	49.17	87.39	1303.57
19	n.d.	48.87	78.26	1433.48
33	n.d.	2.25	69.31	1061.98
41	n.d.	2.05	63.31	957.75
47	n.d.	1.67	54.56	1200.66
54	n.d.	2.21	51.79	1249.16
69	n.d.	35.36	70.14	1332.35
83	n.d.	35.06	59.66	1221.49
90	n.d.	36.46	68.52	1328.52
102	n.d.	35.01	59.49	1363.75
105	n.d.	36.77	68.88	1329.49
105	n.d.	36.02	55.21	1040.15
125	n.d.	36.39	48.68	955.77
137	n.d.	35.68	67.88	1175.28
158	22.15	n.d.	44.57	743.59
175	33.91	n.d.	83.79	1232.76
175	22.91	n.d.	81.79	1009.68
181	23.22	n.d.	58.75	844.49
194	27.53	n.d.	79.20	1016.92
214	22.86	n.d.	72.00	916.19
246	0.22	n.d.	75.48	870.15
270	n.d.	n.d.	65.60	1046.12
313	22.97	n.d.	49.12	1010.60
332	25.46	n.d.	60.90	761.95
354	30.56	n.d.	43.62	1006.90
371	31.55	n.d.	38.11	962.34
384	24.59	n.d.	42.17	780.57
410	45.80	n.d.	52.25	1326.61
435	27.07	n.d.	70.07	782.40
462	n.d.	n.d.	64.20	918.74
494	n.d.	n.d.	70.05	915.50
503	n.d.	n.d.	58.22	925.15
503	n.d.	n.d.	50.40	789.79
524	n.d.	n.d.	50.88	811.39
535	n.d.	n.d.	52.27	799.14
535	n.d.	n.d.	65.60	469.45
549	n.d.	n.d.	82.37	823.11
567	n.d.	n.d.	77.76	767.82
585	n.d.	2.55	80.70	844.38
608	n.d.	n.d.	58.64	829.97
623	n.d.	0.22	55.90	841.40
662	n.d.	0.80	75.97	838.92
678	n.d.	n.d.	70.34	835.84
678	n.d.	n.d.	29.72	437.41
704	4.77	n.d.	60.99	656.15
725	0.82	n.d.	54.95	804.66
745	0.23	0.54	59.37	821.58
781	n.d.	n.d.	51.90	807.46
818	6.13	n.d.	53.71	847.18

Table A4.13 Anions by IC in live microcosm 3A (n.d. - not detected).

Time (days)	Nitrite (mg/L)	Nitrate (mg/L)	Phosphate (mg/L)	Chloride (mg/L)
0	n.d.	49.84	50.92	983.27
7	n.d.	50.02	48.33	1191.92
19	n.d.	49.51	46.61	1378.24
33	n.d.	1.57	32.88	1395.04
41	n.d.	1.87	31.81	1017.62
47	n.d.	2.12	36.57	863.37
54	n.d.	1.38	41.92	1305.38
69	n.d.	35.19	n.d.	1354.01
83	n.d.	35.44	45.84	1361.16
90	n.d.	36.80	45.38	1323.49
102	n.d.	35.56	35.24	565.41
105	n.d.	36.00	n.d.	1395.06
125	n.d.	36.05	46.82	1209.29
137	n.d.	36.49	37.88	1189.52
158	29.89	n.d.	43.57	1262.20
175	30.08	n.d.	38.22	1274.07
175	24.72	n.d.	35.67	1032.08
181	21.76	n.d.	43.23	1017.29
194	24.11	n.d.	43.11	1046.02
214	26.95	n.d.	41.82	1031.55
246	n.d.	n.d.	43.63	1051.05
270	10.43	n.d.	25.55	296.22
313	22.54	n.d.	32.96	1029.77
332	30.58	n.d.	51.06	927.91
354	29.58	n.d.	35.95	924.69
371	32.48	n.d.	22.72	970.94
384	27.87	n.d.	27.65	843.14
410	40.80	n.d.	42.37	1229.44
435	30.56	n.d.	63.25	911.34
462	n.d.	n.d.	54.10	927.40
494	n.d.	1.77	18.54	268.37
503	n.d.	2.94	56.14	735.07
503	n.d.	n.d.	39.48	820.94
524	n.d.	n.d.	36.57	831.58
535	n.d.	n.d.	44.21	836.47
549	n.d.	n.d.	10.62	50.05
567	n.d.	40.40	49.58	830.52
585	n.d.	n.d.	47.71	833.05
608	n.d.	0.35	25.38	835.14
623	n.d.	0.71	37.32	840.49
662	n.d.	n.d.	41.27	831.90
704	1.35	1.10	38.40	816.18
725	n.d.	n.d.	40.52	449.11
745	0.90	n.d.	25.40	825.02
781	0.83	0.32	30.97	806.14
789	n.d.	n.d.	54.97	807.50
818	n.d.	n.d.	23.10	807.00

Table A4.14 Anions by IC in live microcosm 3B (n.d. - not detected).

Time (days)	Nitrite (mg/L)	Nitrate (mg/L)	Phosphate (mg/L)	Chloride (mg/L)
0	n.d.	49.25	73.90	830.36
7	n.d.	49.55	76.60	1041.18
19	n.d.	49.09	85.04	1421.21
33	n.d.	1.91	62.95	1249.06
41	n.d.	1.85	68.76	1374.62
47	n.d.	2.34	72.50	1209.31
54	n.d.	1.06	63.72	1207.58
69	n.d.	34.61	74.33	1306.00
83	n.d.	37.28	83.30	1338.12
90	n.d.	35.55	66.34	689.05
102	n.d.	36.12	74.69	1304.82
125	n.d.	35.43	68.72	1194.53
137	n.d.	35.86	74.51	990.60
158	30.53	n.d.	52.73	1229.15
175	27.06	n.d.	106.37	1060.83
175	33.03	n.d.	95.92	1192.49
181	29.70	n.d.	77.32	1151.10
194	32.32	n.d.	57.58	1207.86
214	34.99	n.d.	76.24	1187.58
246	n.d.	n.d.	79.70	1232.97
270	26.02	n.d.	65.33	1162.16
313	28.55	21.84	79.30	1190.45
332	27.25	n.d.	74.40	846.05
354	35.34	n.d.	61.90	1023.56
371	37.90	0.25	69.84	1151.70
384	43.52	n.d.	84.95	1275.25
410	32.22	n.d.	60.61	996.98
435	29.06	n.d.	63.20	933.20
462	n.d.	n.d.	84.59	1044.17
494	n.d.	n.d.	77.44	1044.88
503	n.d.	n.d.	86.11	1050.33
503	n.d.	0.44	39.63	829.19
524	n.d.	n.d.	74.51	1014.87
535	n.d.	588.89	15.39	433.42
549	n.d.	n.d.	69.55	938.59
567	n.d.	n.d.	54.05	692.83
585	n.d.	n.d.	81.23	948.54
608	n.d.	n.d.	49.08	939.72
623	n.d.	n.d.	59.64	956.15
662	n.d.	n.d.	63.48	854.05
678	n.d.	0.45	70.11	895.16
678	0.29	n.d.	59.77	590.90
678	n.d.	n.d.	120.33	960.72
704	n.d.	n.d.	110.24	954.63
725	n.d.	0.32	110.78	946.13
745	0.51	n.d.	96.68	953.99
781	0.64	n.d.	111.28	942.37
789	n.d.	n.d.	113.24	948.51
818	9.40	0.26	108.98	942.49

Table A4.15 Anions by IC in live microcosm 4A (n.d. - not detected).

Time (days)	Nitrite (mg/L)	Nitrate (mg/L)	Phosphate (mg/L)	Chloride (mg/L)
0	n.d.	48.64	83.85	908.23
7	n.d.	49.56	77.76	1240.49
19	n.d.	49.75	85.99	1374.33
33	n.d.	1.14	71.80	1074.83
41	n.d.	1.03	58.56	975.56
47	n.d.	1.83	71.44	1135.65
54	n.d.	2.18	88.22	n.d.
69	n.d.	34.47	77.31	1262.27
83	n.d.	34.62	59.52	1291.34
90	n.d.	35.72	62.33	1259.39
102	n.d.	36.29	71.10	1206.49
125	n.d.	36.68	63.69	1290.74
137	n.d.	35.95	76.65	1226.92
158	29.30	n.d.	62.98	1119.14
175	35.46	n.d.	126.93	1358.09
175	29.07	n.d.	76.86	1072.77
181	26.04	n.d.	72.26	1091.25
194	28.78	n.d.	103.24	1122.85
214	n.d.	n.d.	87.82	1052.33
246	n.d.	n.d.	68.09	1141.64
270	n.d.	n.d.	80.69	1102.11
313	21.33	n.d.	81.49	1121.66
332	20.94	n.d.	90.91	658.73
354	35.14	n.d.	82.69	1028.49
371	19.64	n.d.	44.88	545.79
384	26.17	n.d.	83.07	852.08
410	39.77	n.d.	93.21	1183.22
435	n.d.	n.d.	87.75	1140.46
462	n.d.	n.d.	79.42	825.03
494	n.d.	n.d.	71.43	849.74
503	n.d.	1.24	54.52	446.37
524	n.d.	n.d.	67.58	876.44
535	n.d.	n.d.	68.67	870.23
549	n.d.	n.d.	59.93	850.95
567	n.d.	n.d.	47.25	851.61
585	n.d.	n.d.	50.27	855.68
608	n.d.	n.d.	36.41	858.50
623	n.d.	0.56	45.01	858.10
662	n.d.	n.d.	56.03	856.03
678	n.d.	0.23	55.83	761.81
704	0.98	n.d.	48.17	813.70
725	n.d.	n.d.	47.59	827.71
745	0.21	n.d.	34.77	827.52
781	n.d.	n.d.	38.10	n.d.
818	0.74	n.d.	24.61	819.14

Table A4.16 Anions by IC in live microcosm 4B (n.d. - not detected).

Time (days)	Nitrite (mg/L)	Nitrate (mg/L)	Phosphate (mg/L)	Chloride (mg/L)
0	n.d.	49.10	48.69	1010.03
7	n.d.	49.31	54.94	1345.30
19	n.d.	49.48	63.86	1396.18
33	n.d.	1.95	45.95	728.22
41	n.d.	1.70	54.53	1325.37
47	n.d.	n.d.	55.43	499.05
54	n.d.	1.23	48.51	n.d.
69	n.d.	36.12	41.97	1275.85
83	n.d.	36.01	41.15	1301.10
90	n.d.	35.69	56.83	1062.05
102	n.d.	36.84	40.07	1243.18
125	n.d.	36.58	46.15	1307.26
137	n.d.	36.30	49.64	1265.27
158	31.08	n.d.	68.67	1155.09
175	33.07	1.29	79.16	1211.92
175	27.17	n.d.	78.93	1117.37
181	29.49	n.d.	66.00	1164.70
194	29.28	n.d.	47.22	1165.40
214	28.90	n.d.	76.80	1154.34
246	n.d.	n.d.	48.83	1169.36
270	n.d.	6.93	40.66	1115.74
313	27.38	11.31	37.51	1140.65
332	19.46	n.d.	67.91	596.21
354	29.61	0.72	57.56	937.09
371	20.81	n.d.	53.21	681.47
384	31.80	n.d.	60.54	920.53
410	33.86	n.d.	75.51	1051.87
435	37.10	n.d.	72.34	1126.32
462	n.d.	n.d.	60.26	836.74
494	n.d.	n.d.	57.03	831.40
503	n.d.	n.d.	56.21	866.85
524	n.d.	n.d.	53.71	881.83
535	n.d.	n.d.	42.18	883.27
549	n.d.	n.d.	37.42	866.68
567	n.d.	n.d.	40.90	871.88
585	n.d.	n.d.	47.08	867.80
608	n.d.	n.d.	34.12	882.68
623	n.d.	n.d.	42.20	886.29
662	n.d.	0.66	41.83	850.27
678	n.d.	n.d.	40.04	791.05
704	0.43	0.25	35.87	719.90
725	0.70	n.d.	28.09	720.44
745	n.d.	n.d.	37.06	843.85
781	0.22	n.d.	36.68	785.01
818	1.24	0.32	28.39	842.90

A 4.2 Cations

Table A4.17 Cations by IC in killed control 1A (n.d. - not detected).

Time (days)	Potassium (mg/L)	Magnesium (mg/L)	Calcium (mg/L)	Sodium (mg/L)	Ammonium (mg/L)
0	27.97	6.05	23.00	472.04	206.84
7	33.76	6.07	22.34	483.39	237.06
19	45.28	7.82	21.53	672.47	313.22
33	42.82	5.67	19.14	643.73	284.05
41	19.58	4.15	18.40	302.70	189.57
47	17.47	4.51	18.72	269.86	180.90
54	29.66	5.73	19.77	505.69	195.50
69	39.90	6.25	17.47	592.45	350.57
83	43.27	6.43	18.70	695.92	388.50
90	39.47	6.83	19.73	635.42	332.80
102	40.61	7.15	19.09	694.75	286.12
125	40.40	6.89	20.14	653.56	358.62
137	36.80	7.08	20.19	628.72	351.45
158	26.77	n.d.	20.63	392.10	211.77
175	40.17	n.d.	23.47	594.08	328.44
175	30.45	n.d.	27.59	436.27	224.66
181	29.05	n.d.	26.43	480.09	247.33
194	45.11	n.d.	22.16	682.60	390.11
214	44.49	n.d.	23.19	669.59	397.89
246	44.43	n.d.	26.28	673.12	386.53
270	46.51	n.d.	34.98	686.88	399.34
313	49.18	11.87	28.94	666.77	296.03
384	68.40	14.91	37.76	887.77	381.00
410	55.07	13.24	43.71	721.71	343.02
435	46.59	14.03	48.92	758.77	347.69
462	41.49	14.06	49.23	629.33	373.24
494	46.79	16.44	55.86	712.38	426.62
503	60.37	16.33	58.50	763.80	348.58

Table A4.18 Cations by IC in killed control 1B (n.d. - not detected).

Time (days)	Potassium (mg/L)	Magnesium (mg/L)	Calcium (mg/L)	Sodium (mg/L)	Ammonium (mg/L)
0	29.69	5.26	29.78	493.98	216.31
7	30.08	5.23	30.12	518.01	221.45
19	41.28	6.63	29.14	649.63	299.68
33	35.48	5.05	24.69	519.91	203.65
41	40.87	5.73	25.12	590.24	271.08
47	54.43	7.03	29.53	716.61	316.52
54	32.74	5.05	28.65	543.53	224.48
69	39.65	6.00	29.46	657.05	346.37
83	42.47	6.60	30.36	696.57	394.92
90	42.14	6.77	29.33	695.76	387.63
102	24.07	4.60	29.64	447.92	251.01
125	24.38	4.33	29.42	484.11	235.93
137	42.58	6.67	30.26	706.76	393.71
158	41.57	n.d.	34.68	647.56	352.39
175	44.19	n.d.	31.56	676.28	382.66
175	41.79	n.d.	34.59	648.43	338.26
181	35.12	n.d.	33.89	586.31	310.77
194	41.24	n.d.	35.62	639.86	367.71
214	40.38	n.d.	25.58	606.80	330.39
246	44.41	n.d.	35.44	687.13	381.24
270	44.15	n.d.	36.22	675.91	378.72
313	50.23	7.55	30.44	694.71	314.57
332	61.41	7.68	34.15	741.87	333.94
354	25.08	4.88	26.54	448.91	249.02
371	66.04	9.54	37.88	942.18	389.53
384	29.20	7.94	30.38	541.30	324.60
410	34.48	6.08	27.28	566.68	356.38
435	59.64	9.22	35.14	873.73	380.32
462	34.70	9.82	30.85	503.85	296.66
494	37.74	8.74	42.68	647.07	377.38
503	55.47	9.61	44.95	755.42	330.57
524	54.23	9.17	41.99	720.48	333.74
535	57.99	10.21	44.02	784.97	358.56
549	32.34	7.33	37.00	526.97	318.26
567	38.00	0.76	22.68	0.60	0.68
585	53.43	9.03	40.34	742.19	331.09
608	40.88	8.77	37.89	717.49	395.24
623	43.16	9.06	39.92	767.60	430.43
662	51.57	8.21	37.02	721.23	317.10
678	37.17	10.00	47.36	718.15	451.05
704	59.78	9.63	49.33	750.03	254.83
725	63.27	10.22	48.95	757.12	261.35
745	58.04	9.23	46.64	701.69	231.96
818	65.13	10.70	50.00	763.78	264.58

Table A4.19 Cations by IC in killed control 2A (n.d. - not detected).

Time (days)	Potassium (mg/L)	Magnesium (mg/L)	Calcium (mg/L)	Sodium (mg/L)	Ammonium (mg/L)
0	52.56	10.27	21.69	510.32	228.40
7	37.39	10.70	21.04	384.56	181.20
19	72.29	11.84	21.05	636.80	301.98
33	58.27	11.86	21.50	602.76	207.23
41	74.50	8.54	21.66	599.95	259.26
47	61.52	9.95	16.50	514.52	229.11
54	64.65	9.35	18.27	515.17	325.39
69	55.59	9.11	20.98	526.65	273.35
83	74.95	11.72	21.17	687.56	275.81
90	55.13	10.93	21.22	505.33	272.66
102	74.28	13.47	22.14	636.19	341.82
125	71.69	10.12	20.37	652.43	354.89
137	72.13	9.21	20.69	665.30	361.73
158	n.d.	n.d.	23.68	653.82	263.35
175	76.93	n.d.	23.88	661.03	281.24
175	42.48	n.d.	21.14	427.61	179.01
181	31.47	n.d.	22.21	403.02	178.52
194	57.55	n.d.	24.21	592.66	244.06
214	49.00	n.d.	25.25	546.01	204.37
246	57.47	n.d.	29.52	600.47	216.68
270	52.21	n.d.	31.53	560.40	225.47
292	57.17	n.d.	31.96	597.68	241.78
313	34.63	6.52	22.51	448.72	149.83
332	42.56	10.48	23.19	484.47	182.04
354	48.75	5.57	22.22	486.87	253.18
371	61.29	5.67	19.31	653.78	236.31
384	85.07	8.96	30.14	916.41	321.58
410	56.72	5.54	26.19	587.35	235.49
435	53.15	9.76	24.94	565.20	228.31
462	48.21	10.45	32.12	505.42	190.37
494	60.97	12.88	34.52	624.97	235.79
503	61.10	14.02	35.31	637.86	239.59
503	54.31	13.84	33.50	564.74	213.07
524	57.29	11.84	33.11	580.65	215.09
535	56.46	10.42	32.85	585.08	215.60
535	57.22	12.44	34.53	858.09	226.74
549	41.22	13.22	31.98	628.17	180.37
567	70.65	11.55	42.63	780.45	206.88
585	53.94	12.43	32.01	814.06	221.33
608	55.37	8.85	32.21	836.23	235.48
623	57.05	12.03	33.66	879.77	238.31
662	52.97	11.13	32.61	806.55	209.91
678	49.92	16.97	40.44	827.69	141.86
704	56.67	15.29	42.43	804.38	142.28
725	60.12	13.41	42.37	850.09	133.86
745	62.72	14.58	42.39	874.78	127.37
781	62.36	17.72	43.76	842.90	159.23
818	65.57	16.40	44.74	848.92	168.10

Table A4.20 Cations by IC in killed control 2B (ND - No Data/n.d. - not detected).

Time (days)	Potassium (mg/L)	Magnesium (mg/L)	Calcium (mg/L)	Sodium (mg/L)	Ammonium (mg/L)
0	56.29	11.01	24.70	518.26	235.06
7	65.58	15.66	26.02	572.94	286.92
19	73.98	13.42	24.59	621.57	307.45
33	63.09	12.58	21.93	557.85	229.97
41	38.75	4.61	10.65	284.77	154.25
47	69.97	9.87	20.72	575.32	256.32
54	73.37	10.45	22.83	609.62	282.55
69	72.77	11.52	23.61	636.89	348.21
83	66.66	10.66	22.88	596.53	336.81
90	73.97	12.70	22.82	630.85	363.67
102	73.31	10.55	24.00	652.89	353.13
105	ND	ND	ND	ND	ND
105	ND	ND	ND	ND	ND
125	53.99	9.36	20.83	474.26	277.05
137	65.00	13.57	22.17	574.41	334.87
158	39.19	n.d.	28.56	399.71	223.77
175	67.69	n.d.	27.68	547.44	290.22
175	57.66	n.d.	27.14	596.02	227.19
181	50.32	n.d.	26.65	516.00	252.90
194	58.22	n.d.	27.04	579.86	281.77
214	53.51	n.d.	27.11	553.96	268.17
246	52.52	n.d.	27.74	538.91	257.65
270	59.63	n.d.	26.55	583.23	286.78
313	56.19	8.74	22.98	607.37	246.76
332	52.45	9.87	21.83	504.80	186.72
354	65.40	4.39	19.36	661.00	258.46
371	62.46	3.42	17.22	597.80	255.86
384	49.09	5.20	18.95	512.31	207.72
410	89.50	5.08	26.30	937.40	337.68
435	49.13	7.59	22.21	488.01	255.74
462	61.55	15.03	34.43	616.67	238.81
494	63.21	14.61	34.42	632.30	241.94
503	63.11	15.08	34.72	644.54	229.94
503	55.20	13.10	30.71	549.83	214.54
524	57.89	13.15	31.89	570.02	222.78
535	56.21	13.35	31.55	561.78	218.76
535	31.85	13.99	27.23	496.30	138.42
549	52.53	13.95	31.85	797.87	229.52
567	63.85	13.44	38.16	772.66	212.24
585	56.08	13.70	31.57	845.09	226.57
608	56.67	10.55	31.33	872.92	232.02
623	55.69	11.66	30.06	873.27	236.07
662	54.70	13.69	31.16	837.16	221.19
678	56.96	17.53	43.41	905.77	197.21
678	29.05	12.25	33.37	481.13	99.76
704	45.59	18.58	40.81	701.19	94.48
725	60.79	14.33	41.47	858.77	143.77
745	63.35	16.99	40.94	868.06	161.25
781	64.07	17.78	42.77	865.90	169.31
818	69.29	16.65	43.17	905.89	175.65

Table A4.21 Cations by IC in killed control 3A (ND - No data/n.d. - not detected).

Time (days)	Potassium (mg/L)	Magnesium (mg/L)	Calcium (mg/L)	Sodium (mg/L)	Ammonium (mg/L)
0	54.44	10.84	26.09	504.52	218.09
7	63.69	10.77	26.81	554.67	251.91
19	70.11	12.17	26.38	597.75	283.07
33	79.97	8.27	22.37	623.18	270.90
41	60.88	8.04	20.45	467.72	262.21
47	52.05	7.29	24.33	440.32	183.91
54	74.65	11.23	24.31	634.14	277.35
69	76.51	10.51	24.05	643.59	354.68
83	76.27	13.24	24.42	644.96	358.28
90	75.34	12.29	22.86	617.42	340.93
102	30.45	8.75	24.06	297.69	179.16
105	ND	ND	ND	ND	ND
125	67.39	11.86	20.79	593.74	323.69
137	68.39	11.40	20.26	580.21	315.82
158	70.12	n.d.	24.21	572.47	284.80
175	69.92	n.d.	25.35	590.13	233.39
175	58.66	n.d.	23.13	615.79	237.65
181	58.81	n.d.	23.85	615.03	206.29
194	59.38	n.d.	24.97	616.95	194.91
214	59.77	n.d.	26.66	615.40	231.64
246	59.84	n.d.	26.33	617.92	233.88
270	17.63	n.d.	12.09	191.56	93.46
313	44.07	6.2	26.46	613.23	242.06
332	59.98	10.55	18.45	628.67	148.49
354	59.65	4.54	19.28	604.28	172.29
371	62.63	4.13	12.48	658.21	231.74
384	53.81	4.3	17.29	560.56	204.8
410	81.1	5.84	21.81	857.21	297.06
435	58.39	7.87	19.61	621.97	228.29
462	62.87	15.04	29.64	633.44	224.87
494	63.98	16.55	30.07	650.85	236.86
503	54.76	14.15	31.80	523.27	191.84
503	58.39	12.97	28.39	590.11	211.99
524	59.55	12.02	27.99	600.53	216.68
535	60.12	14.00	28.58	613.44	216.94
549	54.44	11.09	25.35	557.43	211.52
567	62.31	16.97	31.44	578.83	205.81
585	54.77	11.46	25.75	578.88	208.69
608	57.67	7.36	25.72	610.07	212.10
623	59.50	8.38	26.97	637.21	230.20
662	54.08	11.40	24.15	572.83	199.82
704	60.62	17.47	32.50	598.12	154.78
725	23.66	20.04	33.98	286.45	152.73
745	63.35	14.98	37.53	609.22	154.54
781	63.26	16.96	35.32	603.11	164.75
789	61.78	16.27	41.49	833.21	164.80
818	64.39	17.49	34.97	604.68	172.29

Table A4.22 Cations by IC in killed control 3B (n.d. - not detected).

Time (days)	Potassium (mg/L)	Magnesium (mg/L)	Calcium (mg/L)	Sodium (mg/L)	Ammonium (mg/L)
0	44.90	11.71	25.52	440.75	212.37
7	55.10	11.84	25.22	513.43	251.13
19	72.69	12.58	24.27	614.93	318.00
33	37.21	4.00	11.19	288.80	169.49
41	83.36	9.83	24.54	658.98	307.64
47	71.21	12.31	23.95	600.31	259.70
54	70.69	10.56	22.57	556.99	361.58
69	72.89	10.55	24.32	618.19	374.84
83	72.49	11.70	25.43	612.21	359.53
90	36.91	11.65	24.39	348.05	230.74
102	71.13	10.81	23.84	612.72	369.75
125	65.81	10.67	23.79	570.05	352.36
137	51.54	11.45	23.65	488.44	311.63
158	68.63	n.d.	26.86	544.47	341.59
175	67.68	n.d.	32.79	498.01	274.13
175	67.43	n.d.	27.43	637.63	334.50
181	65.69	n.d.	26.04	632.80	333.86
194	67.37	n.d.	25.20	654.85	284.44
214	67.68	n.d.	29.08	639.74	329.50
246	67.52	n.d.	26.52	657.81	270.90
270	66.93	n.d.	26.16	647.98	255.61
313	65.56	7.25	28.40	664.57	344.05
332	59.51	10.32	20.83	528.1	290.13
354	66.11	5.51	20.44	604.58	228.3
371	78.39	6.45	19.96	749.36	305.86
384	85.04	6.92	20.78	823.54	351.29
410	63.74	6.35	18.53	582.66	336.97
435	59.76	7.12	19.01	540.96	323.7
462	71.67	17.65	33.42	678.20	298.90
494	73.46	16.53	33.79	695.07	295.12
503	74.00	18.03	34.94	706.84	308.03
503	58.89	12.67	27.98	594.33	213.55
524	72.69	15.88	31.67	676.41	273.05
535	86.98	3.48	25.95	510.50	261.66
549	60.81	12.58	28.66	594.04	266.34
567	65.75	11.40	30.57	614.94	258.80
585	61.80	12.19	27.39	618.26	261.03
608	52.59	7.65	26.35	616.80	330.61
623	68.19	10.64	28.37	658.94	333.97
662	54.15	10.61	26.62	526.96	273.99
678	58.41	15.54	38.30	629.59	202.36
678	32.16	16.28	37.15	370.68	189.19
678	61.14	18.10	41.50	1368.62	165.50
704	75.20	18.83	43.93	1350.66	169.73
725	78.50	19.37	46.10	1349.75	194.65
745	75.18	18.12	43.79	1357.85	177.51
781	79.32	19.60	48.37	1357.85	187.11
789	79.85	21.21	47.41	1359.71	195.92
818	82.12	21.53	50.36	1357.04	206.88

Table A4.23 Cations by IC in killed control 4A (n.d. - not detected).

Time (days)	Potassium (mg/L)	Magnesium (mg/L)	Calcium (mg/L)	Sodium (mg/L)	Ammonium (mg/L)
0	50.25	14.23	34.26	467.17	221.06
7	65.17	9.68	33.14	565.40	290.13
19	71.45	13.10	34.56	606.86	310.78
33	68.94	10.65	32.30	507.12	311.39
41	59.14	8.86	28.57	465.72	301.34
47	66.50	12.21	29.27	536.74	229.94
54	77.44	14.00	34.51	648.33	315.38
69	73.47	11.94	32.17	612.99	363.14
83	72.23	7.40	29.27	625.69	349.04
90	72.72	8.68	30.39	615.81	344.76
102	71.00	10.47	29.78	584.04	330.40
125	74.77	7.92	30.94	637.90	373.68
137	71.78	12.85	31.61	601.26	363.04
158	67.11	n.d.	37.50	523.47	267.85
175	77.34	n.a.	40.51	617.79	362.77
175	62.18	n.a.	32.64	749.28	218.07
181	63.68	n.a.	33.86	745.53	259.97
194	65.80	n.a.	34.61	765.59	289.43
214	61.62	n.a.	34.64	744.65	243.40
246	65.62	n.a.	32.71	763.29	247.15
270	64.67	n.a.	36.27	750.98	276.03
313	95.05	n.a.	35.56	803.80	285.70
332	44.59	9.47	24.61	585.15	184.33
354	68.93	5.59	23.76	756.62	245.29
371	79.65	3.99	17.91	470.94	145.99
384	56.43	7.03	23.53	664.17	210.21
410	81.13	4.57	29.30	981.42	322.81
435	76.20	6.94	26.50	899.22	297.06
462	57.54	14.13	35.43	655.59	197.88
494	62.19	14.68	33.70	696.81	251.99
503	27.34	13.19	31.03	370.33	177.15
524	65.19	14.91	34.65	732.50	260.97
535	67.90	13.87	34.32	721.70	248.24
549	56.97	12.53	31.15	656.31	246.62
567	60.40	9.83	30.47	673.08	239.42
585	59.17	11.73	28.91	688.88	245.13
608	62.68	7.34	31.64	730.28	234.71
623	65.80	9.25	33.66	759.84	263.28
662	58.87	12.40	29.57	682.41	240.22
678	52.87	19.82	42.03	666.62	151.89
704	60.46	16.61	39.96	653.66	166.13
725	66.03	19.61	39.15	696.43	167.55
745	69.08	16.68	36.04	709.38	191.92
781	67.77	16.23	41.24	708.15	179.24
818	68.94	13.55	45.10	708.02	195.61

Table A4.24 Cations by IC in killed control 4B (n.d. - not detected).

Time (days)	Potassium (mg/L)	Magnesium (mg/L)	Calcium (mg/L)	Sodium (mg/L)	Ammonium (mg/L)
0	55.59	9.26	35.36	465.33	236.34
7	69.54	10.08	35.09	590.78	301.54
19	72.26	12.14	35.24	607.55	311.22
33	47.98	9.39	31.26	371.91	241.43
41	80.15	10.17	33.62	646.16	296.96
47	27.33	10.84	29.29	247.28	182.98
54	75.07	9.61	32.54	607.33	266.61
69	70.92	7.46	33.20	610.55	368.55
83	74.72	7.77	32.70	619.94	369.13
90	59.13	11.68	31.65	492.80	306.37
102	68.10	6.70	25.45	579.55	349.19
125	73.43	8.41	32.55	618.11	364.78
137	70.87	9.98	33.85	609.59	363.29
158	67.95	n.d.	40.09	500.15	306.05
175	73.32	n.d.	40.32	527.88	287.80
175	65.76	n.d.	36.46	750.10	240.98
181	66.32	n.d.	37.45	746.15	267.19
194	66.92	n.d.	34.19	746.72	282.31
214	66.56	n.d.	36.78	751.98	290.77
246	66.15	n.d.	37.79	748.83	272.94
270	n.d.	n.d.	32.06	731.40	277.21
313	222.23	n.d.	36.17	954.65	283.43
332	37.77	8.52	25.18	544.96	162.85
354	62.14	5.11	22.32	683.21	255.63
371	44.00	4.36	24.22	493.74	173.42
384	60.83	5.48	24.38	674.58	260.66
410	71.13	8.07	28.25	787.17	296.50
435	75.55	6.93	31.28	855.49	313.96
462	59.23	13.21	36.68	650.73	239.43
494	63.52	13.90	36.86	685.67	242.49
503	63.94	13.94	34.59	687.38	260.01
524	65.38	13.06	37.82	706.32	253.93
535	64.91	9.29	37.66	703.61	255.41
549	58.40	9.63	34.45	644.59	250.63
567	61.40	8.35	34.96	673.88	244.92
585	58.85	11.49	32.58	670.43	247.54
608	63.90	7.50	33.78	726.73	227.87
623	66.83	9.72	35.38	753.45	267.11
662	57.95	9.99	32.91	645.08	236.07
678	54.79	15.92	42.55	664.21	158.26
704	55.09	15.74	39.76	597.19	144.58
725	56.44	15.13	40.77	599.31	155.27
745	70.04	15.17	40.80	696.78	192.82
781	62.76	15.70	42.24	636.73	171.32
818	69.63	13.94	45.75	697.51	200.37

A4.5 Data from Total Elemental Analysis by Inductively Coupled Plasma Atomic Emission Spectroscopy (ICP-AES).

Table A4.25 Total Sulphur concentrations, in killed controls and live microcosms, by ICP-AES (ND - No data, N/A – Not Applicable)

Time (days)	1A Total S (mg/L)	1B Total S (mg/L)	2A Total S (mg/L)	2B Total S (mg/L)
0	136.694	178.098	189.010	183.572
7	131.747	189.341	133.067	177.938
19	198.156	166.400	194.783	187.705
33	187.701	ND	189.241	170.002
41	ND	159.550	164.174	139.426
47	ND	198.160	155.999	143.215
54	183.442	171.521	160.883	127.353
181	100.670	135.300	118.100	78.100
435	N/A	ND	31.400	48.200
608	N/A	ND	193.600	215.600
818	N/A	174.600	156.500	216.200
Time (days)	**3A Total S (mg/L)**	**3B Total S (mg/L)**	**4A Total S (mg/L)**	**4B Total S (mg/L)**
0	192.149	166.524	146.564	116.556
7	183.154	183.779	184.830	185.865
19	178.531	182.159	170.730	183.599
33	149.951	155.232	109.529	127.761
41	119.257	152.806	96.303	85.406
47	103.399	110.259	58.058	39.017
54	122.608	111.853	78.085	86.110
181	113.100	104.500	152.300	154.700
435	39.900	63.800	108.000	88.700
608	27.000	8.100	127.200	114.700
818	6.100	526.400	129.600	123.100

Table A4.26 Total dissolved Iron (Fe^{2+}) concentrations, in killed controls and live microcosms, by ICP-AES (ND - No data, N/A – Not Applicable).

Time (days)	1A Fe(II) (mg/L)	1B Fe(II) (mg/L)	2A Fe(II) (mg/L)	2B Fe(II) (mg/L)
0	0.281	0.294	0.296	0.296
7	0.270	0.278	0.311	0.311
19	0.089	0.091	0.088	0.037
33	0.065	0.240	0.267	0.278
41	0.300	0.254	0.285	0.297
47	0.269	0.281	0.305	0.288
54	0.275	0.288	0.296	0.279
181	2.600	0.700	0.700	0.300
435	N/A	ND	0.200	0.200
608	N/A	0.100	0.100	0.100
818	N/A	1.700	1.300	1.100
Time (days)	**3A Fe(II) (mg/L)**	**3B Fe(II) (mg/L)**	**4A Fe(II) (mg/L)**	**4B Fe(II) (mg/L)**
0	0.272	0.288	0.251	0.284
7	0.287	0.296	0.267	0.298
19	0.078	0.062	0.044	0.065
33	0.273	0.272	0.259	0.343
41	0.282	0.264	0.283	0.297
47	0.272	0.270	0.267	0.268
54	0.287	0.284	0.282	0.288
181	0.600	0.400	0.400	0.300
435	0.200	0.200	0.200	0.100
608	0.100	0.100	0.100	0.100
818	0.700	0.700	1.500	0.500

A5 Results of DNA Sequencing of Phenol Degraders. Taxonomy Report and Results of BLAST (Basic Local Alignment Search Tool) and FASTA (Fast-All) Searches

BLASTN 2.2.6 [Apr-09-2003]

Results for **IMI** 390582

Sequences producing significant alignments:	Score (bits)	E Value
gi|31074757|emb|AJ312163.1|PST312163 Pseudomonas stutzeri p...	814	0.0
gi|15919407|gb|AF406655.1| Pseudomonas alcaligenes strain A...	802	0.0
gi|31074756|emb|AJ312162.1|PST312162 Pseudomonas stutzeri p...	802	0.0
gi|3172546|gb|AF067960.1|AF067960 Pseudomonas stutzeri KC 1...	798	0.0
gi|3139129|gb|AF063219.1|AF063219 Pseudomonas stutzeri 16S ...	798	0.0
gi|14572057|gb|AF390747.1|AF390747 Pseudomonas alcaligenes ...	794	0.0
gi|31074761|emb|AJ312167.1|PST312167 Pseudomonas stutzeri p...	794	0.0
gi|31074760|emb|AJ312166.1|PST312166 Pseudomonas stutzeri p...	794	0.0
gi|31074759|emb|AJ312165.1|PST312165 Pseudomonas stutzeri p...	794	0.0
gi|31338424|emb|AJ319662.1|PST319662 Pseudomonas stutzeri p...	794	0.0
gi|12055465|emb|AJ295682.1|PST295682 Pseudomonas stutzeri p...	790	0.0
gi|12055464|emb|AJ295681.1|PST295681 Pseudomonas stutzeri p...	790	0.0
gi|22004061|dbj|AB079094.1| Pseudomonas putida gene for 16S...	790	0.0
gi|1718243|gb|U65012.1|PSU65012 Pseudomonas stutzeri 16S rR...	790	0.0
gi|1142678|gb|U25431.1|PSU25431 Pseudomonas stutzeri 16S ri...	790	0.0
gi|15919408|gb|AF406656.1| Pseudomonas putida strain A4 16S...	788	0.0
gi|31075561|gb|AY269255.1| Pseudomonas alcaligenes strain T...	786	0.0
gi|31075501|gb|AY269195.1| Pseudomonas alcaligenes strain T...	786	0.0
gi|15637545|gb|AF408938.1|AF408938 Pseudomonas sp. C25B 16S...	786	0.0
gi|15637538|gb|AF408931.1|AF408931 Pseudomonas sp. C35B 16S...	786	0.0
gi|15637515|gb|AF408908.1|AF408908 Pseudomonas sp. C86C 16S...	786	0.0
gi|30038534|dbj|AB108691.1| Pseudomonas putida gene for 16S...	786	0.0
gi|31074758|emb|AJ312164.1|PST312164 Pseudomonas stutzeri p...	786	0.0
gi|20385334|gb|AF368760.1| Pseudomonas sp. OPS1 16S ribosom...	782	0.0
gi|7243300|gb|AF065166.1|AF065166 Pseudomonas sp. PH1 16S r...	782	0.0
gi|16116685|emb|AJ270451.1|PST270451 Pseudomonas stutzeri p...	782	0.0
gi|1142694|gb|U26420.1|PSU26420 Pseudomonas stutzeri strain...	782	0.0
gi|1142686|gb|U26261.1|PSU26261 Pseudomonas stutzeri ATCC 1...	782	0.0
gi|4433342|dbj|D84022.1|PSEIAM21 Pseudomonas nitroreducens ...	782	0.0
gi|27529617|emb|AJ514431.1|UBA514431 Uncultured bacterium p...	780	0.0
gi|3021612|dbj|D85998.1| Pseudomonas putida 16S ribosomal R...	780	0.0
gi|25992136|gb|AF509331.1| Pseudomonas putida strain DSM 36...	778	0.0
gi|30060242|gb|AY254572.1| Pseudomonas sp. B2 16S ribosomal...	778	0.0
gi|26557036|gb|AE016791.1| Pseudomonas putida KT2440 sectio...	778	0.0
gi|26557026|gb|AE016782.1| Pseudomonas putida KT2440 sectio...	778	0.0
gi|26557021|gb|AE016778.1| Pseudomonas putida KT2440 sectio...	778	0.0
gi|26557018|gb|AE016775.1| Pseudomonas putida KT2440 sectio...	778	0.0
gi|26557017|gb|AE016774.1| Pseudomonas putida KT2440 sectio...	778	0.0
gi|24527329|gb|AY144260.1| Uncultured gamma proteobacterium...	778	0.0
gi|21898829|gb|AY121982.1| Pseudomonas putida strain RA16 1...	778	0.0
gi|21898828|gb|AY121981.1| Pseudomonas putida strain RA9 16...	778	0.0
gi|4107385|emb|AJ009491.1|UEAJ9491 uncultured bacterium SJA...	778	0.0
gi|2832450|emb|AJ002805.1|PSPAJ2805 Pseudomonas sp. 16S rRN...	778	0.0
gi|6723841|emb|AJ271219.1|PPU271219 Pseudomonas putida 16S ...	778	0.0
gi|10954024|gb|AF307872.1| Pseudomonas sp. 8IDINH 16S ribos...	778	0.0
gi|10954019|gb|AF307867.1| Pseudomonas putida- PR1MN1 16S ri...	778	0.0
gi|10954018|gb|AF307866.1| Pseudomonas putida 3IA2NH 16S ri...	778	0.0
gi|10954017|gb|AF307865.1| Pseudomonas putida 3IIIA2NH 16S ...	778	0.0
gi|10954016|gb|AF307864.1| Pseudomonas putida 5IIIASal 16S ...	778	0.0
gi|17298555|gb|AF447394.1|AF447394 Pseudomonas putida 16S r...	778	0.0
gi|15637547|gb|AF408940.1|AF408940 Pseudomonas sp. C16C 16S...	778	0.0
gi|15637546|gb|AF408939.1|AF408939 Pseudomonas sp. C22B 16S...	778	0.0
gi|15637541|gb|AF408934.1|AF408934 Pseudomonas sp. C30E 16S...	778	0.0
gi|15637525|gb|AF408918.1|AF408918 Pseudomonas sp. C75D 16S...	778	0.0
gi|15637517|gb|AF408910.1|AF408910 Pseudomonas sp. C86A 16S...	778	0.0

gi|15637516|gb|AF408909.1|AF408909 Pseudomonas sp. C86B 16S...	778	0.0
gi|15637481|gb|AF408874.1|AF408874 Pseudomonas sp. NZCB7 16...	778	0.0
gi|14718773|gb|AY040872.1| Pseudomonas sp. WBC-3 16S riboso...	778	0.0
gi|10732840|gb|AF309079.1|AF309079 Pseudomonas sp. MB1 16S ...	778	0.0
gi|10567517|gb|AF094746.1|AF094746 Pseudomonas putida strai...	778	0.0
gi|10567512|gb|AF094741.1|AF094741 Pseudomonas putida strai...	778	0.0
gi|10567508|gb|AF094737.1|AF094737 Pseudomonas putida strai...	778	0.0
gi|31074762|emb|AJ312168.1|PST312168 Pseudomonas stutzeri p...	778	0.0
gi|31074755|emb|AJ312161.1|PST312161 Pseudomonas stutzeri p...	778	0.0
gi|4928633|gb|AF135269.1|AF135269 Pseudomonas sp. SF1 16S r...	778	0.0
gi|33329788|gb|AF532866.1| Pseudomonas sp. K2 16S ribosomal...	778	0.0
gi|3142687|gb|AF064458.1|AF064458 Pseudomonas monteilii 16S...	778	0.0
gi|1142693|gb|U26419.1|PSU26419 Pseudomonas stutzeri strain...	778	0.0
gi|1142654|gb|U22426.1|PSU22426 Pseudomonas stutzeri strain...	778	0.0
gi|3021604|dbj|D83788.1| Pseudomonas putida 16S ribosomal R...	778	0.0
gi|531254|dbj|D37924.1|PSEGYRB2 Pseudomonas putida (strain ...	778	0.0
gi|3021605|dbj|D85991.1| Pseudomonas putida 16S ribosomal R...	778	0.0
gi|7415644|dbj|AB029257.1| Pseudomonas putida gene for 16S ...	778	0.0
gi|4165415|dbj|AB021409.1| Pseudomonas monteilii DNA for 16...	778	0.0
gi|453512|gb|L28676.1|PSE16SRNAB Pseudomonas putida 16S rib...	778	0.0
gi|5881244|gb|AF180146.1|AF180146 Pseudomonas putida 16S ri...	776	0.0
gi|30527211|gb|AY275482.1| Pseudomonas sp. MSB2071 16S ribo...	774	0.0
gi|30527210|gb|AY275481.1| Pseudomonas sp. MSB2084 16S ribo...	774	0.0
gi|28194116|gb|AF468450.1| Pseudomonas sp. Ps 3-10 16S ribo...	774	0.0
gi|22218221|gb|AF529342.1| Uncultured gamma proteobacterium...	774	0.0
gi|1841469|emb|Y11150.1|PGY11150 Pseudomonas graminis 16S r...	774	0.0
gi|15778357|gb|AF411854.1|AF411854 Pseudomonas sp. 5A 16S r...	774	0.0
gi|15625313|gb|AF326381.1|AF326381 Pseudomonas sp. PCP 16S ...	774	0.0
gi|15625309|gb|AF326377.1|AF326377 Pseudomonas sp. ISO6 16S...	774	0.0
gi|10567514|gb|AF094743.1|AF094743 Pseudomonas putida strai...	774	0.0
gi|27530750|dbj|AB074631.1| Uncultured gamma proteobacteriu...	774	0.0
gi|23821285|dbj|AB008001.1| Pseudomonas putida gene for 16S...	774	0.0
gi|32263436|gb|AY312988.1| Pseudomonas sp. FA1 16S ribosoma...	774	0.0
gi|3021607|dbj|D85993.1| Pseudomonas putida 16S ribosomal R...	774	0.0
gi|14275941|dbj|AB051698.1| Pseudomonas sp. LAB-21 gene for...	774	0.0
gi|14275940|dbj|AB051697.1| Pseudomonas sp. LAB-20 gene for...	774	0.0
gi|21898827|gb|AY121980.1| Pseudomonas putida strain RA2 16...	772	0.0
gi|3169022|emb|AJ005167.1|PSAJ5167 Pseudomonas stutzeri 16S...	772	0.0
gi|14190212|gb|AF378011.1|AF378011 Pseudomonas sp. ML2 16S ...	772	0.0
gi|7804928|gb|AF251336.1|AF251336 Pseudomonas sp. SV16 16S ...	772	0.0
gi|32351738|gb|AY308050.1| Pseudomonas putida 16S ribosomal...	772	0.0
gi|13236289|gb|AF321028.1| Pseudomonas sp. GOBB3-105 16S ri...	770	0.0
gi|25992135|gb|AF509330.1| Pseudomonas putida strain DSM 36...	770	0.0
gi|18542495|gb|AF469258.1| Uncultured gamma proteobacterium...	770	0.0
gi|27501698|gb|AY170458.1| Pseudomonas putida isolate AQ22....	770	0.0

>gi|31074757|emb|AJ312163.1|PST312163 Pseudomonas stutzeri partial 16S rRNA gene, strain 28a3

Length = 1450

Score = 814 bits (410), Expect = 0.0
Identities = 429/436 (98%)
Strand = Plus / Plus

Sequence data for **IMI** 390582 compared to nearest match, *Pseudomonas stutzeri*, strain 28a3

```
390582 1    gagagcttgctctctgattcagcggcggacgggtgagtaatgcctaggaatctgcctggt 60
            ||||||||||||||||||||||||||||||||||||||||||||||||||||||||||||
28a3: 59    gagagcttgctctctgattcagcggcggacgggtgagtaatgcctaggaatctgcctggt 118
```

```
390582 61  agtgggggacaacgtttcgaaaggaacgctaataccgcatacgtcctacgggagaaagca 120
           ||||||||||||||||||||||||||||||||||||||||||||||||||||||||||||
28a3: 119 agtgggggacaacgtttcgaaaggaacgctaataccgcatacgtcctacgggagaaagca 178


390582: 121 ggggaccttcgggccttgcgctatcagatgagcctaggtcggattagctagttggtgagg 180
            ||||||||||||||||||||||||||||||||||||||||||||||||||||||||||||
28a3: 179  ggggaccttcgggccttgcgctatcagatgagcctaggtcggattagctagttggtgagg 238


390582: 181 taaaggctcaccaaggcgacgatccgtaactggtctgagaggatgatcagtcacactgga 240
            ||| ||||||||||||||||||||||||||||||||||||||||||||||||||||||||
28a3: 239  taatggctcaccaaggcgacgatccgtaactggtctgagaggatgatcagtcacactgga 298


390582: 241 actgagacacggtccagactcctacgggaggcagcagtggggaatatwagacaatgggcg 300
            ||||||||||||||||||||||||||||||||||||||||||||||||  ||||||||||||
28a3: 299  actgagacacggtccagactcctacgggaggcagcagtggggaatattggacaatgggcg 358


390582: 301 aaagctgtatccagccatgccgcgtgtgtgaagaaggtcttcggattgtaaagcacttta 360
            |||||   ||||||||||||||||||||||||||||||||||||||||||||||||||||
28a3: 359  aaagcctgatccagccatgccgcgtgtgtgaagaaggtcttcggattgtaaagcacttta 418


390582: 361 agttgggaggaagggcagtaagttaataccttgctgtttttacgttaccgacagaataag 420
            |||||||||||||||||||||||||||||||||||||||| ||||||||||||||||||
28a3: 419  agttgggaggaagggcagtaagttaataccttgctgttttgacgttaccgacagaataag 478


390582: 421 caccggctaacttcgt 436
            ||||||||||||||||
28a3: 479  caccggctaacttcgt 494
```

Taxonomy Report

```
Bacteria ..............................   101 hits   41 orgs
. Proteobacteria ......................   100 hits   40 orgs
. . Gammaproteobacteria ...............    98 hits   38 orgs
. . . Pseudomonas .....................    94 hits   37 orgs
[Pseudomonadales; Pseudomonadaceae]
. . . . Pseudomonas stutzeri ..........    21 hits    1 orgs [Pseudomonas
stutzeri group]
. . . . Pseudomonas aeruginosa group ...     5 hits    2 orgs
. . . . . Pseudomonas alcaligenes ......     4 hits    1 orgs
. . . . . Pseudomonas nitroreducens ....     1 hits    1 orgs
. . . . Pseudomonas putida group .......    37 hits    3 orgs
. . . . . Pseudomonas putida ...........    35 hits    2 orgs
. . . . . . Pseudomonas putida KT2440 ..     6 hits    1 orgs
. . . . . Pseudomonas monteilii ........     2 hits    1 orgs
. . . . Pseudomonas sp. C25B ...........     1 hits    1 orgs
. . . . Pseudomonas sp. C35B ...........     1 hits    1 orgs
. . . . Pseudomonas sp. C86C ...........     1 hits    1 orgs
. . . . Pseudomonas sp. OPS1 ...........     1 hits    1 orgs
. . . . Pseudomonas sp. PH1 ............     1 hits    1 orgs
. . . . Pseudomonas sp. B2 .............     1 hits    1 orgs
. . . . uncultured bacterium SJA-129 ...     1 hits    1 orgs [environmental
samples]
. . . . Pseudomonas sp. 8IDINH .........     1 hits    1 orgs
```

. . . . Pseudomonas sp. C16C	1 hits	1 orgs	
. . . . Pseudomonas sp. C22B	1 hits	1 orgs	
. . . . Pseudomonas sp. C30E	1 hits	1 orgs	
. . . . Pseudomonas sp. C75D	1 hits	1 orgs	
. . . . Pseudomonas sp. C86A	1 hits	1 orgs	
. . . . Pseudomonas sp. C86B	1 hits	1 orgs	
. . . . Pseudomonas sp. NZCB7	1 hits	1 orgs	
. . . . Pseudomonas sp. WBC-3	1 hits	1 orgs	
. . . . Pseudomonas sp. SF1	1 hits	1 orgs	
. . . . Pseudomonas sp. K2	1 hits	1 orgs	
. . . . Pseudomonas sp. MSB2071	1 hits	1 orgs	
. . . . Pseudomonas sp. MSB2084	1 hits	1 orgs	
. . . . Pseudomonas umsongensis	1 hits	1 orgs	
. . . . Pseudomonas graminis	1 hits	1 orgs	
. . . . Pseudomonas sp. 5A	1 hits	1 orgs	
. . . . Pseudomonas sp. PCP	1 hits	1 orgs	
. . . . Pseudomonas sp. ISO6	1 hits	1 orgs	
. . . . Pseudomonas sp. FA1	1 hits	1 orgs	
. . . . Pseudomonas sp. LAB-21	1 hits	1 orgs	
. . . . Pseudomonas sp. LAB-20	1 hits	1 orgs	
. . . . Pseudomonas sp. ML2	1 hits	1 orgs	
. . . . Pseudomonas sp. SV16	1 hits	1 orgs	
. . . . Pseudomonas sp. GOBB3-105	1 hits	1 orgs	
. . . uncultured gamma proteobacterium .	4 hits	1 orgs	[unclassified Gammaproteobacteria; environmental samples]
. . unclassified pseudomonads	2 hits	2 orgs	[unclassified Proteobacteria]
. . . Pseudomonas sp.	1 hits	1 orgs	
. . . Pseudomonas sp. MB1	1 hits	1 orgs	
. uncultured bacterium	1 hits	1 orgs	[unclassified Bacteria; environmental samples]

Results for **IMI** 390583

Sequences producing significant alignments:	Score (bits)	E Value
gi|7321257|emb|AJ288147.1|PST288147 Pseudomonas stutzeri pa...	915	0.0
gi|19550729|gb|AF482684.1| Pseudomonas sp. BU 16S ribosomal...	915	0.0
gi|22474443|emb|AJ312172.1|PST312172 Pseudomonas stutzeri p...	915	0.0
gi|15778356|gb|AF411853.1|AF411853 Pseudomonas sp. 5.1 16S ...	915	0.0
gi|3372815|gb|AF064636.1|AF064636 Pseudomonas sp. NAP-3-1 1...	915	0.0
gi|7321258|emb|AJ288148.1|PST288148 Pseudomonas stutzeri pa...	907	0.0
gi|22474447|emb|AJ312176.1|PST312176 Pseudomonas stutzeri p...	907	0.0
gi|22474446|emb|AJ312175.1|PST312175 Pseudomonas stutzeri p...	907	0.0
gi|22474445|emb|AJ312174.1|PST312174 Pseudomonas stutzeri p...	907	0.0
gi|22474438|emb|AJ312157.1|PST312157 Pseudomonas stutzeri p...	907	0.0
gi|22474437|emb|AJ312156.1|PST312156 Pseudomonas stutzeri p...	907	0.0
gi|31074754|emb|AJ312160.1|PST312160 Pseudomonas stutzeri p...	907	0.0
gi|2708833|gb|AF038653.1|AF038653 Pseudomonas stutzeri 16S ...	907	0.0
gi|32527611|gb|AY321589.1| Pseudomonas stutzeri 16S ribosom...	907	0.0
gi|1142689|gb|U26415.1|PSU26415 Pseudomonas stutzeri strain...	907	0.0
gi|1142677|gb|U25280.1|PSU25280 Pseudomonas stutzeri strain...	907	0.0
gi|1142655|gb|U22427.1|PSU22427 Pseudomonas stutzeri strain...	907	0.0
gi|18476076|gb|AY017341.1| Pseudomonas chloritidismutans 16...	901	0.0
gi|24636584|dbj|AB095005.1| Pseudomonas sp. KNA6-5 gene for...	899	0.0
gi|16116687|emb|AJ270453.1|PST270453 Pseudomonas stutzeri p...	899	0.0
gi|16116686|emb|AJ270452.1|PST270452 Pseudomonas stutzeri p...	899	0.0
gi|22474439|emb|AJ312158.1|PST312158 Pseudomonas stutzeri p...	895	0.0
gi|27464920|gb|AF548761.1| Uncultured Pseudomonas sp. clone...	891	0.0

gi|15183111|gb|AY039438.1| Soil bacterium S95M1 16S ribosom...	891	0.0
gi|25188160|dbj|AB096261.1| Pseudomonas stutzeri gene for 1...	891	0.0
gi|28881848|emb|AJ548920.1|UPS548920 uncultured Pseudomonas...	891	0.0
gi|1508844|gb|U64001.1|PSU64001 Pseudomonas sp. SCB24 16S r...	889	0.0
gi|22474444|emb|AJ312173.1|PST312173 Pseudomonas stutzeri p...	883	0.0
gi|3005684|gb|AF054933.1|AF054933 Pseudomonas stutzeri stra...	881	0.0
gi|11137579|emb|AJ391194.1|PSP391194 Pseudomonas sp. AS-33,...	873	0.0
gi|24636583|dbj|AB095004.1| Pseudomonas sp. KNA6-3 gene for...	869	0.0
gi|17220728|gb|AY014810.1| Pseudomonas sp. NZ047 16S riboso...	867	0.0
gi|15637491|gb|AF408884.1|AF408884 Pseudomonas sp. NZPN5 16...	867	0.0
gi|31074753|emb|AJ312159.1|PST312159 Pseudomonas stutzeri p...	867	0.0
gi|22217940|emb|AJ244724.1|PCF244724 Pseudomonas cf. stutze...	867	0.0
gi|14275776|emb|AJ006108.3|PST6108 Pseudomonas stutzeri 16S...	866	0.0
gi|1381185|gb|U58659.1|PSU58659 Pseudomonas stutzeri 16S rR...	864	0.0
gi|17220727|gb|AY014809.1| Pseudomonas sp. NZ043 16S riboso...	864	0.0
gi|17220730|gb|AY014812.1| Pseudomonas sp. NZ059 16S riboso...	862	0.0
gi|22267071|gb|AY043698.1| Uncultured gamma proteobacterium...	860	0.0
gi|21320120|gb|AY095404.1| Uncultured yard-trimming-compost...	860	0.0
gi|20531210|gb|AF500282.1| Pseudomonas sp. SMCC B0280 16S r...	860	0.0
gi|20453986|gb|AF500620.1| Pseudomonas sp. SMCC B0310 16S r...	860	0.0
gi|19908354|gb|AY082368.1| Uncultured Pseudomonas sp. clone...	860	0.0
gi|3172546|gb|AF067960.1|AF067960 Pseudomonas stutzeri KC 1...	860	0.0
gi|15077676|gb|AF359550.1|AF359550 Marine bacterium SCRIPPS...	860	0.0
gi|15824752|gb|AF332511.1|AF332511 Pseudomonas gingeri stra...	860	0.0
gi|15705393|gb|AF320991.1|AF320991 Pseudomonas gingeri 16S ...	860	0.0
gi|15637542|gb|AF408935.1|AF408935 Pseudomonas sp. C27D 16S...	860	0.0
gi|15637529|gb|AF408922.1|AF408922 Pseudomonas sp. C66B 16S...	860	0.0
gi|15637527|gb|AF408920.1|AF408920 Pseudomonas sp. C72A 16S...	860	0.0
gi|15637510|gb|AF408903.1|AF408903 Pseudomonas sp. C14B 16S...	860	0.0
gi|15637475|gb|AF408868.1|AF408868 Pseudomonas sp. NZWM2 16...	860	0.0
gi|15637474|gb|AF408867.1|AF408867 Pseudomonas sp. NZWM3 16...	860	0.0
gi|15625307|gb|AF326375.1|AF326375 Pseudomonas sp. GP11 16S...	860	0.0
gi|10567516|gb|AF094745.1|AF094745 Pseudomonas putida strai...	860	0.0
gi|10567507|gb|AF094736.1|AF094736 Pseudomonas putida strai...	860	0.0
gi|30519878|dbj|AB109777.1| Pseudomonas putida gene for 16S...	860	0.0
gi|30519877|dbj|AB109776.1| Pseudomonas putida gene for 16S...	860	0.0
gi|31074757|emb|AJ312163.1|PST312163 Pseudomonas stutzeri p...	860	0.0
gi|1907107|emb|Z76667.1|PPZ76667 P.putida 16S rRNA gene	860	0.0
gi|1907095|emb|Z76655.1|PAZ76655 P.asplenii 16S rRNA gene	860	0.0
gi|1907092|emb|Z76652.1|PAZ76652 P.agarici 16S rRNA gene	860	0.0
gi|3139129|gb|AF063219.1|AF063219 Pseudomonas stutzeri 16S ...	860	0.0
gi|531253|dbj|D37923.1|PSEGYRB1 Pseudomonas putida (strain ...	860	0.0
gi|3021608|dbj|D85994.1| Pseudomonas putida 16S ribosomal R...	860	0.0
gi|7384769|dbj|AB030583.1| Pseudomonas alcalophila 16S ribo...	860	0.0
gi|4165403|dbj|AB021397.1| Pseudomonas asplenii DNA for 16S...	860	0.0
gi|4165387|dbj|AB021381.1| Pseudomonas fuscovaginae DNA for...	860	0.0
gi|6165447|emb|AJ272542.1|PSP272542 Pseudomonas sp. partial...	856	0.0
gi|15637490|gb|AF408883.1|AF408883 Pseudomonas sp. NZWM7 16...	856	0.0
gi|5690462|gb|AF170358.1|AF170358 Pseudomonas sp. PK 16S ri...	856	0.0
gi|15637493|gb|AF408886.1|AF408886 Pseudomonas sp. NZPN3 16...	854	0.0
gi|2337766|dbj|AB002660.1| Unidentified gamma proteobacteri...	854	0.0
gi|21327116|gb|AF511436.1| Pseudomonas alcaligenes 16S ribo...	852	0.0
gi|20531209|gb|AF500281.1| Pseudomonas sp. SMCC B0259 16S r...	852	0.0
gi|15637535|gb|AF408928.1|AF408928 Pseudomonas sp. C54A 16S...	852	0.0
gi|17932875|emb|Z76674.1|PMZ76674 P.mendocina (strain DSM 5...	852	0.0
gi|16116692|emb|AJ270458.1|PST270458 Pseudomonas stutzeri p...	852	0.0
gi|16116691|emb|AJ270457.1|PST270457 Pseudomonas stutzeri p...	852	0.0
gi|16116690|emb|AJ270456.1|PST270456 Pseudomonas stutzeri p...	852	0.0
gi|16116689|emb|AJ270455.1|PST270455 Pseudomonas stutzeri p...	852	0.0
gi|16116688|emb|AJ270454.1|PST270454 Pseudomonas stutzeri p...	852	0.0
gi|4433323|dbj|D84005.1|PSEATCC04 Pseudomonas agarici 16S r...	852	0.0

gi|3021606|dbj|D85992.1| Pseudomonas putida 16S ribosomal R...	852	0.0
gi|28932770|gb|AY214348.1| Pseudomonas sp. A_wp02262 16S ri...	850	0.0
gi|3135065|emb|AJ006110.1|PAL6110 Pseudomonas alcaligenes 1...	850	0.0
gi|10567510|gb|AF094739.1|AF094739 Pseudomonas putida strai...	850	0.0
gi|14275936|dbj|AB051693.1| Pseudomonas sp. LAB-06 gene for...	850	0.0
gi|1907104|emb|Z76664.1|PMZ76664 P.mendocina (strain LMG 12...	848	0.0
gi|3097462|dbj|AB011762.1| unidentified gamma proteobacteri...	848	0.0
gi|21327113|gb|AF511433.1| Pseudomonas fluorescens 16S ribo...	846	0.0
gi|21070093|gb|AF506040.1| Pseudomonas fluorescens LCSA0TU1...	846	0.0
gi|19851209|gb|AF365657.1| Uncultured bacterium clone BM89D...	846	0.0
gi|17220734|gb|AY014816.1| Pseudomonas sp. NZ092 16S riboso...	846	0.0
gi|31415501|gb|AY293865.1| Pseudomonas sp. NUST03 16S ribos...	844	0.0
gi|21538848|gb|AF467303.1| Uncultured Pseudomonas sp. clone...	844	0.0
gi|20531205|gb|AF500277.1| Pseudomonas sp. SMCC B0205 16S r...	844	0.0
gi|20149126|gb|AF494091.1| Pseudomonas nitroreducens strain...	844	0.0
gi|13236452|gb|AF336311.1| Pseudomonas sp. SMCC D0715 16S r...	844	0.0

>gi|7321257|emb|AJ288147.1|PST288147 Pseudomonas stutzeri partial 16S rRNA gene, isolate BTH 922
Length = 1370

Score = 915 bits (461), Expect = 0.0
Identities = 472/475 (99%), Gaps = 1/475 (0%)
Strand = Plus / Plus

Sequence data for **IMI** 390583 compared to nearest match, *Pseudomonas stutzeri*, isolate BTH 922

```
390583: 1   ctaacacatgcaagtcgagcggatgaagagagcttgctctctgattcagcggcggacggg 60
            ||||||||||||||||||||||||||||||||||||||||||||||||||||||||||||
BTH922:37   ctaacacatgcaagtcgagcggatgaagagagcttgctctctgattcagcggcggacggg 96

390583: 61  tgagtaatgcctaggaatctgcctgatagtgggggacaacgtttcgaaaggaacgctaat 120
            ||||||||||||||||||||||||||||||||||||||||||||||||||||||||||||
BTH922:97   tgagtaatgcctaggaatctgcctgatagtgggggacaacgtttcgaaaggaacgctaat 156

390583: 121 accgcatacgtcctacgggagaaagcaggggaccttcgggccttgcgctatcagatgagc 180
            ||||||||||||||||||||||||||||||||||||||||||||||||||||||||||||
BTH922:157 accgcatacgtcctacgggagaaagcaggggaccttcgggccttgcgctatcagatgagc 216

390583: 181 ctaggtcggattagctagttggtgaggtaatggctcaccaaggcgacgatccgtaactgg 240
            ||||||||||||||||||||||||||||||||||||||||||||||||||||||||||||
BTH922:217 ctaggtcggattagctagttggtgaggtaatggctcaccaaggcgacgatccgtaactgg 276

390583: 241 tctgagaggatgatcagtcacactggaactgagacacggtccagacttctacgggaggca 300
            |||||||||||||||||||||||||||||||||||||| ||||||||||||
BTH922:277 tctgagaggatgatcagtcacactggaactgagacacggtccagactcctacgggaggca 336
```

```
390583: 301 gcagtggggaatattggacaatgggcgaaag-ctgatccagccatgccgcgtgtgtgaag 359
            ||||||||||||||||||||||||||||| ||||||||||||||||||||||||||
BTH922:337 gcagtggggaatattggacaatgggcgaaagcctgatccagccatgccgcgtgtgtgaag 396

390583: 360 aaggtcttcggattgtaaagcactttaagttgggaggaagggcattaacctaatacgtta 419
            ||||||||||||||||||||||||||||||||||||||||||||||||||||||||||
BTH922:397 aaggtcttcggattgtaaagcactttaagttgggaggaagggcattaacctaatacgtta 456

390583: 420 gtgttttgacgttaccgacagaataagcaccggctaacttcgtgccwgcagccgc 474
            |||||||||||||||||||||||||||||||||||||||||||||||| ||||||||
BTH922:457 gtgttttgacgttaccgacagaataagcaccggctaacttcgtgccagcagccgc 511
```

Taxonomy Report

Bacteria	100 hits	51 orgs
. Gammaproteobacteria	96 hits	47 orgs
[Proteobacteria]		
. . Pseudomonas	93 hits	46 orgs
[Pseudomonadales; Pseudomonadaceae]		
. . . Pseudomonas stutzeri group	32 hits	2 orgs
. . . . Pseudomonas stutzeri	31 hits	1 orgs
. . . . Pseudomonas cf. stutzeri V4.MO.16	1 hits	1 orgs
. . . Pseudomonas sp. BU	1 hits	1 orgs
. . . Pseudomonas sp. 5.1	1 hits	1 orgs
. . . Pseudomonas sp. NAP-3-1	1 hits	1 orgs
. . . Pseudomonas chloritidismutans	1 hits	1 orgs
. . . Pseudomonas sp. KNA6-5	1 hits	1 orgs
. . . uncultured Pseudomonas sp.	4 hits	1 orgs
[environmental samples]		
. . . Pseudomonas sp. SCB24	1 hits	1 orgs
. . . Pseudomonas sp. AS-33	1 hits	1 orgs
. . . Pseudomonas sp. KNA6-3	1 hits	1 orgs
. . . Pseudomonas sp. NZ047	1 hits	1 orgs
. . . Pseudomonas sp. NZPN5	1 hits	1 orgs
. . . Pseudomonas sp. NZ043	1 hits	1 orgs
. . . Pseudomonas sp. NZ059	1 hits	1 orgs
. . . Pseudomonas sp. SMCC B0280	1 hits	1 orgs
. . . Pseudomonas sp. SMCC B0310	1 hits	1 orgs
. . . Pseudomonas gingeri	2 hits	1 orgs
. . . Pseudomonas sp. C27D	1 hits	1 orgs
. . . Pseudomonas sp. C66B	1 hits	1 orgs
. . . Pseudomonas sp. C72A	1 hits	1 orgs
. . . Pseudomonas sp. C14B	1 hits	1 orgs
. . . Pseudomonas sp. NZWM2	1 hits	1 orgs
. . . Pseudomonas sp. NZWM3	1 hits	1 orgs
. . . Pseudomonas sp. GP11	1 hits	1 orgs
. . . Pseudomonas putida	9 hits	1 orgs
[Pseudomonas putida group]		
. . . Pseudomonas asplenii	2 hits	1 orgs
. . . Pseudomonas agarici	2 hits	1 orgs
. . . Pseudomonas alcaliphila	1 hits	1 orgs
. . . Pseudomonas fuscovaginae	1 hits	1 orgs
[Pseudomonas syringae group]		
. . . Pseudomonas sp. B5	1 hits	1 orgs
. . . Pseudomonas sp. NZWM7	1 hits	1 orgs
. . . Pseudomonas sp. PK	1 hits	1 orgs
. . . Pseudomonas sp. NZPN3	1 hits	1 orgs

. . . Pseudomonas aeruginosa group	5 hits	3 orgs
. . . . Pseudomonas alcaligenes	2 hits	1 orgs
. . . . Pseudomonas mendocina	2 hits	1 orgs
. . . . Pseudomonas nitroreducens	1 hits	1 orgs
. . . Pseudomonas sp. SMCC B0259	1 hits	1 orgs
. . . Pseudomonas sp. C54A	1 hits	1 orgs
. . . Pseudomonas sp. A_wp02262	1 hits	1 orgs
. . . Pseudomonas sp. LAB-06	1 hits	1 orgs
. . . Pseudomonas fluorescens	2 hits	1 orgs
[Pseudomonas fluorescens group]		
. . . Pseudomonas sp. NZ092	1 hits	1 orgs
. . . Pseudomonas sp. NUST03	1 hits	1 orgs
. . . Pseudomonas sp. SMCC B0205	1 hits	1 orgs
. . . Pseudomonas sp. SMCC D0715	1 hits	1 orgs
. . uncultured gamma proteobacterium	3 hits	1 orgs
[unclassified Gammaproteobacteria; environmental samples]		
. unclassified Bacteria	4 hits	4 orgs
. . unclassified Bacteria (miscellaneous)	2 hits	2 orgs
. . . soil bacterium S95M1	1 hits	1 orgs
. . . marine bacterium SCRIPPS_740	1 hits	1 orgs
. . environmental samples	2 hits	2 orgs
. . . uncultured yard-trimming-compost bacterium .	1 hits	1 orgs
. . . uncultured bacterium	1 hits	1 orgs

APPENDIX B – KINETIC MODELLING DATA

B1 Biodegradation Modelling – Measured and Predicted Data

Table B1.1 Microcosm 2A modelling data: phenol and sulphate measured by HPLC. Rate, biomass and phenol predicted by the dual Monod Model.

Time (days)	Measured Phenol (mol/L)	Measured Sulphate (mol/L)	Biomass, X (mol/L)	dP/dt (mol/L/s)	Predicted Phenol (mol/L)
19	1.36E-03	1.49E-03	2.80E-05	6.31E-06	1.36E-03
41	1.01E-03	1.20E-03	4.19E-05	8.63E-06	1.17E-03
47	8.66E-04	1.01E-03	4.71E-05	9.05E-06	1.11E-03
54	8.67E-04	9.95E-04	5.34E-05	1.02E-05	1.04E-03
83	6.45E-04	9.75E-04	8.30E-05	1.49E-05	6.10E-04
90	4.10E-04	6.89E-04	9.34E-05	1.32E-05	5.18E-04
102	3.03E-04	7.03E-04	1.09E-04	1.39E-05	3.50E-04
125	1.24E-04	6.95E-04	1.41E-04	1.14E-05	8.80E-05
137	2.33E-05	6.93E-04	1.55E-04	3.41E-06	4.71E-05
158	1.32E-05	7.27E-04	1.62E-04	2.15E-06	1.86E-06
175	0.00E+00	7.17E-04	1.66E-04	0.00E+00	1.86E-06
175	6.63E-03	7.80E-04	1.30E-04	4.92E-06	6.63E-03
194	6.41E-03	1.14E-03	1.39E-04	5.87E-06	6.52E-03
214	6.15E-03	1.16E-03	1.51E-04	6.38E-06	6.39E-03
246	6.01E-03	9.76E-04	1.71E-04	6.92E-06	6.17E-03
270	5.69E-03	5.74E-04	1.88E-04	6.36E-06	6.02E-03
292	5.82E-03	5.51E-04	2.02E-04	6.73E-06	5.87E-03
313	5.72E-03	5.68E-04	2.16E-04	7.28E-06	5.72E-03
384	5.12E-03	3.33E-04	2.68E-04	7.03E-06	5.22E-03
410	4.91E-03	1.84E-04	2.86E-04	5.26E-06	5.08E-03
435	4.83E-03	1.94E-04	2.99E-04	5.69E-06	4.94E-03
462	4.79E-03	1.54E-04	3.14E-04	5.11E-06	4.80E-03
494	4.79E-03	1.46E-04	3.31E-04	5.17E-06	4.64E-03
503	4.74E-03	1.37E-04	3.35E-04	5.02E-06	4.59E-03
503	9.73E-03	1.13E-04	3.02E-04	5.29E-07	9.73E-03
524	9.54E-03	1.01E-04	3.03E-04	4.78E-07	9.72E-03
535	9.31E-03	9.03E-05	3.03E-04	4.29E-07	9.72E-03
535	9.01E-03	1.82E-03	2.86E-04	3.61E-06	9.01E-03
567	8.70E-03	1.64E-03	2.97E-04	3.69E-06	8.89E-03
585	8.65E-03	1.70E-03	3.04E-04	3.80E-06	8.82E-03
608	8.65E-03	1.67E-03	3.13E-04	3.89E-06	8.73E-03
623	8.65E-03	1.68E-03	3.19E-04	3.97E-06	8.67E-03
662	8.54E-03	1.59E-03	3.34E-04	4.12E-06	8.51E-03
678	8.48E-03	1.58E-03	3.41E-04	4.19E-06	8.45E-03
725	8.40E-03	1.52E-03	3.60E-04	4.41E-06	8.24E-03
745	8.19E-03	1.53E-03	3.69E-04	4.51E-06	8.15E-03
781	8.09E-03	1.37E-03	3.85E-04	4.61E-06	7.98E-03
818	7.82E-03	1.31E-03	4.03E-04	4.76E-06	7.81E-03

Table B1.2 Microcosm 2B modelling data: phenol and sulphate measured by HPLC. Rate, biomass and phenol predicted by the dual Monod Model.

Time (days)	Measured Phenol (mol/L)	Measured Sulphate (mol/L)	Biomass, X (mol/L)	dP/dt (mol/L/s)	Predicted Phenol (mol/L)
19	1.38E-03	5.06E-03	2.80E-05	1.05E-05	1.38E-03
33	1.15E-03	4.19E-03	4.28E-05	1.55E-05	1.17E-03
41	7.05E-04	3.26E-03	5.51E-05	1.78E-05	1.02E-03
47	5.98E-04	3.16E-03	6.58E-05	2.04E-05	9.01E-04
54	4.23E-04	2.97E-03	8.01E-05	2.24E-05	7.45E-04
69	2.63E-04	2.68E-03	1.14E-04	2.62E-05	3.52E-04
83	9.28E-05	2.29E-03	1.50E-04	1.90E-05	8.60E-05
90	4.14E-05	2.30E-03	1.64E-04	1.12E-05	7.90E-06
102	0.00E+00	2.25E-03	1.64E-04	0.00E+00	7.90E-06
105	0.00E+00	2.32E-03	1.64E-04	0.00E+00	7.90E-06
105	6.09E-03	1.84E-03	1.49E-04	1.70E-05	6.09E-03
125	5.83E-03	1.63E-03	1.83E-04	2.04E-05	5.68E-03
137	5.71E-03	1.70E-03	2.08E-04	2.34E-05	5.40E-03
158	5.14E-03	2.14E-04	2.57E-04	1.28E-05	5.14E-03
175	4.85E-03	2.98E-04	2.79E-04	1.69E-05	4.85E-03
175	4.35E-03	2.51E-03	2.45E-04	3.26E-06	4.35E-03
181	4.39E-03	2.29E-03	2.47E-04	3.25E-06	4.33E-03
194	4.33E-03	2.44E-03	2.51E-04	3.33E-06	4.28E-03
214	4.38E-03	2.31E-03	2.58E-04	3.39E-06	4.22E-03
246	4.27E-03	2.29E-03	2.68E-04	3.53E-06	4.10E-03
270	4.04E-03	1.86E-03	2.77E-04	3.52E-06	4.02E-03
313	3.88E-03	1.31E-03	2.92E-04	3.46E-06	3.87E-03
384	3.90E-03	1.20E-03	3.17E-04	3.68E-06	3.61E-03
410	3.79E-03	1.15E-03	3.26E-04	3.75E-06	3.51E-03
435	3.63E-03	6.70E-04	3.36E-04	3.27E-06	3.43E-03
462	3.32E-03	3.32E-04	3.44E-04	2.45E-06	3.36E-03
494	3.29E-03	1.30E-04	3.52E-04	1.38E-06	3.32E-03
503	3.25E-03	1.06E-04	3.53E-04	1.18E-06	3.31E-03
503	1.06E-02	9.63E-05	3.12E-04	3.28E-05	1.06E-02
524	9.22E-03	7.63E-05	3.81E-04	3.31E-05	9.88E-03
535	9.31E-03	8.79E-05	4.18E-04	4.07E-05	9.43E-03
535	8.70E-03	3.93E-03	3.91E-04	1.48E-06	8.70E-03
549	8.65E-03	6.80E-03	3.93E-04	1.54E-06	8.68E-03
567	8.65E-03	6.26E-03	3.95E-04	1.55E-06	8.65E-03
585	8.68E-03	6.83E-03	3.98E-04	1.56E-06	8.63E-03
608	8.59E-03	6.75E-03	4.02E-04	1.58E-06	8.59E-03
623	8.39E-03	5.83E-03	4.04E-04	1.57E-06	8.57E-03
662	8.52E-03	6.75E-03	4.10E-04	1.61E-06	8.50E-03
678	8.55E-03	6.79E-03	4.13E-04	1.62E-06	8.48E-03
704	8.51E-03	5.79E-03	4.17E-04	1.62E-06	8.44E-03
725	8.36E-03	6.53E-03	4.21E-04	1.65E-06	8.40E-03
745	8.17E-03	6.63E-03	4.24E-04	1.66E-06	8.37E-03
781	8.29E-03	6.34E-03	4.30E-04	1.68E-06	8.31E-03
818	8.26E-03	6.37E-03	4.36E-04	1.70E-06	8.24E-03

APPENDIX C – VC OXIDATION MICROCOSMS: DATA AND CALIBRATION

C1. Calibration Curves for SPME/GC-MS Method and Manual Injection/GC-MS Method with Fluorobenzene Internal Standard

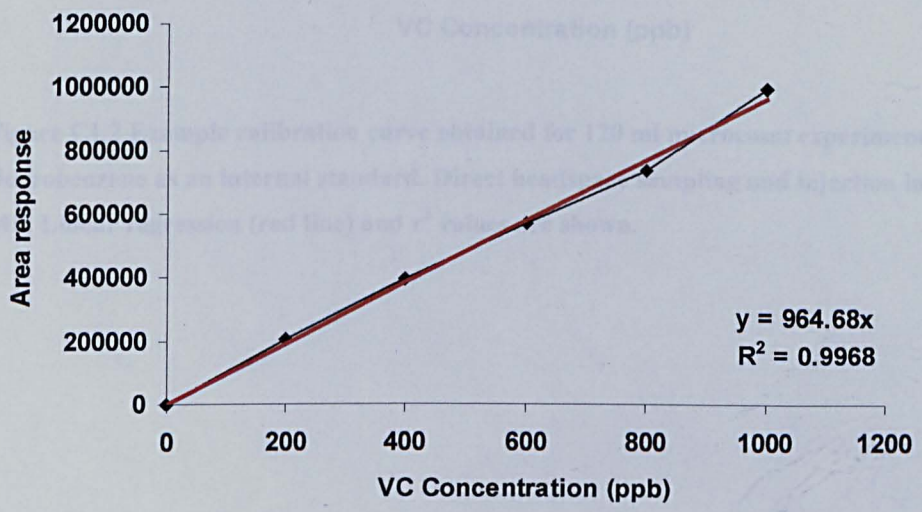

Figure C1.1 Calibration curve obtained by SPME/GC-MS for analysis of 20 ml microcosms inoculated with anaerobic digester sludge. Linear regression (red line) and r^2 values are shown.

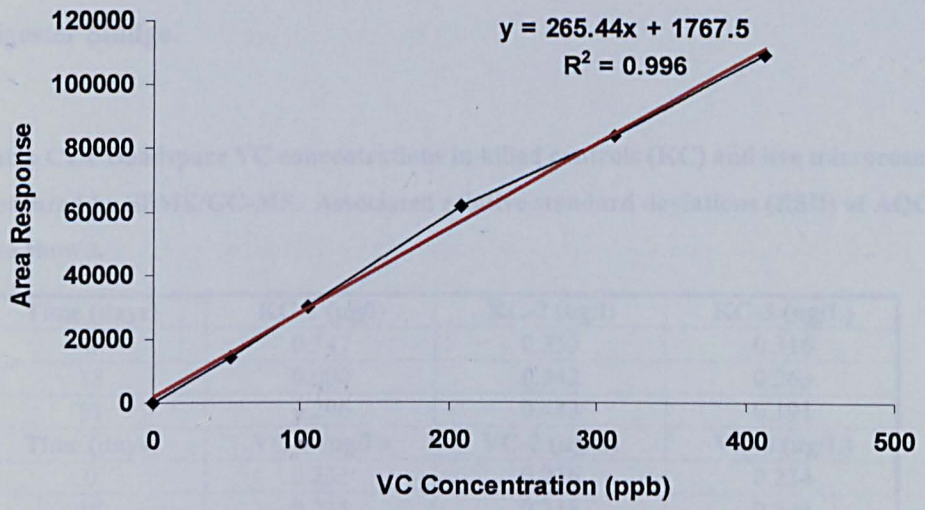

Figure C1.2 Example calibration curve obtained for 120 ml microcosm experiment utilising fluorobenzene as an internal standard. Direct headspace sampling and injection into GC-MS. Linear regression (red line) and r^2 values are shown.

C2. Direct Oxidation of VC in 20 ml Microcosms Inoculated with Anaerobic Digester Sludge.

Table C2.1 Headspace VC concentrations in killed controls (KC) and live microcosms (VC) measured by SPME/GC-MS. Associated relative standard deviations (RSD) of AQC's are also shown.

Time (days)	KC-1 (ug/l)	KC-2 (ug/l)	KC-3 (ug/L)
0	0.347	0.353	0.316
18	0.000	0.342	0.263
51	0.296	0.443	0.191
Time (days)	**VC-1 (ug/L)**	**VC-2 (ug/L)**	**VC-3 (ug/L)**
0	0.231	0.216	0.234
18	0.245	0.238	0.244
51	0.053	0.047	0.019
Time (days)	**KC-1 RSD (ug/L)**	**KC-2 RSD (ug/L)**	**KC-3 RSD (ug/L)**
0	0.044	0.045	0.040
18	0.000	0.002	0.002
51	0.013	0.020	0.009
Time (days)	**VC-1 RSD (ug/L)**	**VC-1 RSD (ug/L)**	**VC-1 RSD (ug/L)**
0	0.029	0.027	0.030
18	0.001	0.001	0.001
51	0.002	0.002	0.001

C3. Direct Oxidation of VC in 120 ml Microcosms Inoculated with Anaerobic Digester Sludge Enrichment Cultures.

Table C3.1 Headspace VC Concentrations in killed controls from 120 ml Microcosm Experiment Inoculated with Enrichment Cultures. Measured by Direct Headspace Sampling and Injection into GC-MS. Relative standard deviations (RSD) of AQC's are shown.

Time (days)	Control-1 (ug/L)	Control-2 (ug/L)	Control-3 (ug/L)
0	630.854	864.375	696.649
6	688.097	878.909	721.543
17	641.881	834.590	698.270
34	635.368	820.731	685.248
48	640.137	859.860	ND
64	645.678	879.099	722.684
169	649.129	931.228	741.283
Time (days)	Control 1-RSD (ug/L)	Control 2-RSD (ug/L)	Control 3-RSD (ug/L)
0	39.860	54.614	44.017
6	38.028	48.573	39.876
17	37.511	48.773	40.806
34	43.063	55.626	46.444
48	36.901	49.567	ND
64	36.670	49.927	41.044
169	6.999	10.041	7.993

Table C3.2 Headspace VC Concentrations in live microcosms B2 from 120 ml Microcosm Experiment Inoculated with Enrichment Cultures. Measured by Direct Headspace Sampling and Injection into GC-MS. Relative standard deviations (RSD) of AQC's are shown.

Time (days)	Live-B2-1 (ug/L)	Live-B2-2 (ug/L)	Live-B2-3 (ug/L)
0	759.562	655.717	646.942
6	770.686	714.431	704.202
17	769.766	669.283	687.670
34	717.905	650.552	662.112
48	689.819	684.110	690.734
64	765.313	717.536	709.805
169	788.496	717.059	699.216
Time (days)	Live-B2-1-RSD (ug/L)	Live-B2-2-RSD (ug/L)	Live-B2-3-RSD (ug/L)
0	47.992	41.431	40.876
6	42.592	39.483	38.918
17	44.984	39.112	40.187
34	48.657	44.092	44.876
48	39.765	39.436	39.818
64	43.465	40.751	40.312
169	8.502	7.732	7.539

Table C3.3 Headspace VC Concentrations in live microcosms A3 from 120 ml Microcosm Experiment Inoculated with Enrichment Cultures. Measured by Direct Headspace Sampling and Injection into GC-MS. Relative standard deviations (RSD) of AQC's are shown.

Time (days)	Live-A3-1 (ug/L)	Live-A3-2 (ug/L)	Live-A3-3 (ug/L)
0	699.182	743.412	754.640
6	775.661	795.678	785.773
17	735.432	765.279	754.595
34	717.642	763.906	734.587
48	768.538	782.983	771.300
64	729.526	811.498	766.783
169	737.946	818.401	768.669
Time (days)	Live-A3-1-RSD (ug/L)	Live-A3-2-RSD (ug/L)	Live-A3-3-RSD (ug/L)
0	44.177	46.971	47.681
6	42.867	43.974	43.426
17	42.978	44.722	44.098
34	48.639	51.775	49.788
48	44.303	45.136	44.462
64	41.432	46.088	43.548
169	7.957	8.825	8.288

Table C3.4 Headspace VC Concentrations in live microcosms C3 from 120 ml Microcosm Experiment Inoculated with Enrichment Cultures. Measured by Direct Headspace Sampling and Injection into GC-MS. Relative standard deviations (RSD) of AQC's are shown.

Time (days)	Live-C3-1 (ug/L)	Live-C3-2 (ug/L)	Live-C3-3 (ug/L)
0	739.520	756.390	714.545
6	779.746	743.315	753.650
17	772.706	767.397	735.474
34	740.237	729.674	719.939
48	780.921	748.142	766.317
64	800.611	753.733	747.813
169	783.756	782.796	742.081
Time (days)	Live-C3-1-RSD (ug/L)	Live-C3-2-RSD (ug/L)	Live-C3-3-RSD (ug/L)
0	46.726	47.791	45.148
6	43.093	41.080	41.651
17	45.156	44.846	42.980
34	50.171	49.455	48.795
48	45.017	43.127	44.175
64	45.469	42.807	42.471
169	8.451	8.441	8.002

Table C3.5 Headspace CO_2 concentrations in killed controls and live microcosms from 120 ml Microcosm Experiment Inoculated with Enrichment Cultures. Measured by Direct Headspace Sampling and Injection into GC. All concentrations are in mol/L.

Time (days)	Control-1	Control-2	Control-3
0	0	0	0
6	0	0	0
17	0	0	0
34	0	2.50297E-05	0
48		0	0
64	0	0	0
Time (days)	**Live-B2-1**	**Live-B2-2**	**Live-B2-3**
0	0	0	0
6	0	0	9.84038E-05
17	0	0	0
34	1.72427E-05	0	0
48	0	0	0
64	9.25948E-06	0	7.30737E-06
Time (days)	**Live-A3-1**	**Live-A3-2**	**Live-A3-3**
0	0	0	0
6	0	5.02587E-05	0
17	0	0	0
34	2.32988E-05	0	0
48	0	0	0
64	0.000227486	8.23816E-06	6.71005E-06
Time (days)	**Live-C3-1**	**Live-C3-2**	**Live-C3-3**
0	0	0	0
6	0	0	0
17	0	0	0
34	0	0	0
48	0	0	0
64	0	0	0

Table C3.6 SO_4^{2-} determined by IC from samples taken from the 120 ml microcosms inoculated with anaerobic enrichment cultures at the beginning and end of the experiment.

Sampled at	Control-1 (mg/L)	Control-2 (mg/L)	Control-3 (mg/L)
Beginning	517.15	495.91	515.81
End	506.37	595.08	571.63
	Live-B2-1 (mg/L)	**Live-B2-2 (mg/L)**	**Live-B2-3 (mg/L)**
Beginning	459.88	374.27	457.05
End	505.21	422.78	566.28
	Live-A3-1 (mg/L)	**Live-A3-2 (mg/L)**	**Live-A3-3 (mg/L)**
Beginning	202.47	188.36	139.3
End	214.75	149.25	184.13
	Live-C3-1 (mg/L)	**Live-C3-2 (mg/L)**	**Live-C3-3 (mg/L)**
Beginning	228.07	270.64	255.15
End	217.74	160.01	134.23

C4. Data from Study on Cometabolic Degradation of Vinyl Chloride under Sulphate-reducing Conditions, utilising Phenol as the Primary Carbon Source.

Table C4.1 Headspace VC concentrations in killed controls with relative standard deviations (RSD) of AQC's. Measured by direct headspace sampling and injection into GC-MS (ND - No data).

Time (days)	Control-1 (ug/L)	Control-2 (ug/L)	Control-3 (ug/L)
0	821.43	837.32	986.55
14	787.06	756.13	705.99
20	732.46	766.12	705.04
28	736.11	745.90	735.89
34	735.12	745.64	726.21
45	759.61	766.43	733.30
62	753.11	742.70	713.29
76	794.19	796.86	753.08
92	815.56	820.40	810.12
197	746.99	801.86	ND
Time (days)	Control 1-RSD (ug/L)	Control 2-RSD (ug/L)	Control 3-RSD (ug/L)
0	37.97	38.70	45.60
14	33.39	32.07	29.95
20	28.16	29.45	27.11
28	46.51	47.13	46.50
34	40.63	41.21	40.13
45	44.39	44.79	42.85
62	51.04	50.34	48.34
76	45.78	45.94	43.41
92	46.32	46.59	46.01
197	8.05	8.65	ND

Table C4.2 Headspace VC concentrations in live microcosms with relative standard deviations (RSD) of AQC's. Measured by direct headspace sampling and injection into GC-MS.

Time (days)	Live-1 (ug/L)	Live-2 (ug/L)	Live-3 (ug/L)
0	240.45	627.96	1017.82
14	281.36	699.09	760.94
20	288.26	719.33	792.12
28	276.02	700.03	779.81
34	277.28	720.73	800.43
45	305.74	773.57	769.86
62	283.17	677.79	770.61
76	303.27	688.22	812.08
92	273.22	712.89	829.95
197	298.54	707.28	847.76
Time (days)	**Live 1-RSD (ug/L)**	**Live 2-RSD (ug/L)**	**Live3-RSD (ug/L)**
0	11.11	29.03	47.05
14	11.93	29.65	32.28
20	11.08	27.66	30.45
28	17.44	44.23	49.27
34	15.32	39.83	44.24
45	17.87	45.21	44.99
62	19.19	45.94	52.23
76	17.48	39.67	46.81
92	15.52	40.49	47.14
197	3.22	7.63	9.14
Time (days)	**Live-4 (ug/L)**	**Live-5 (ug/L)**	**Live-6 (ug/L)**
0	75.99	106.96	0.00
19	84.20	116.02	0.00
28	81.76	114.45	0.00
46	71.56	107.17	0.00
53	67.83	103.93	0.00
60	78.78	106.81	0.00
71	71.94	115.99	0.00
88	73.19	105.95	0.00
102	85.26	117.25	0.00
118	87.12	122.05	0.00
223	86.19	123.37	0.00
Time (days)	**Live 4-RSD (ug/L)**	**Live 5-RSD (ug/L)**	**Live 6-RSD (ug/L)**
0	4.31	6.06	0.00
19	1.78	2.45	0.00
28	3.78	5.29	0.00
46	2.75	4.12	0.00
53	4.29	6.57	0.00
60	4.35	5.90	0.00
71	4.20	6.78	0.00
88	4.96	7.18	0.00
102	4.91	6.76	0.00
118	4.95	6.93	0.00
223	0.93	1.33	0.00

Table C4.3 Phenol concentrations determined by HPLC for cometabolic degradation experiment

Time	con-1 (mg/L)	con-2 (mg/L)	con-3 (mg/L)
Time zero	107.861	96.962	100.649
Day 45	97.985	98.781	98.836
Day 197	109.459	89.668	102.294
	live-1 (mg/L)	**live-2 (mg/L)**	**live-3 (mg/L)**
Time zero	100.007	84.661	126.994
Day 45	2.329	68.247	112.828
Day 197	1.153	1.343	126.497
	live-4 (mg/L)	**live-5 (mg/L)**	**live-6 (mg/L)**
Time zero	165.7	167.8	167.8
Day 45	190.918	181.35	158.027
Day 197	216.115	168.705	175.765

Table C4.5 Headspace CO_2 concentrations in killed controls and live microcosms from cometabolic degradation experiment. Measured by Direct Headspace Sampling and Injection into GC (ND - No data)

Time (days)	Con-1 (mol/L)	Con-2 (mol/L)	Con-3 (mol/L)
0	0.00E+00	0.00E+00	0.00E+00
14	0.00E+00	2.67E-08	3.24E-09
20	9.60E-06	0.00E+00	0.00E+00
28	4.81E-07	6.73E-07	3.92E-07
34	4.01E-07	4.29E-07	5.16E-07
62	7.13E-07	8.04E-07	5.90E-07
92			8.93E-06
Time (days)	**Live-1 (mol/L)**	**Live-2 (mol/L)**	**Live-3 (mol/L)**
0	0.00E+00	0.00E+00	0.00E+00
14	3.01E-04	6.61E-05	2.96E-05
20	2.19E-04	3.96E-05	1.70E-05
28	4.36E-04	8.60E-05	3.00E-05
34	3.78E-04	8.18E-05	3.02E-05
62	1.05E-03	1.05E-04	9.31E-06
92	5.18E-04	2.44E-04	ND
Time (days)	**Live-4 (mol/L)**	**Live-5 (mol/L)**	**Live-6 (mol/L)**
0	0.00E+00	0.00E+00	0.00E+00
19	0.00E+00	0.00E+00	0.00E+00
28	0.00E+00	0.00E+00	0.00E+00
46	0.00E+00	0.00E+00	0.00E+00
53	3.43E-05	2.93E-05	6.32E-06
60	4.50E-05	2.24E-06	0.00E+00
71	2.59E-05	1.17E-05	0.00E+00
88		1.82E-05	0.00E+00
102	ND	ND	ND
118	7.50E-06	ND	0.00E+00